Title
Investigating Dysregulated Metabolic Pathways that Drive Cancer Pathogenicity

Author
Roberts, Lindsay Shayna

Publication Date
2017

Peer reviewed|Thesis/dissertation

Investigating Dysregulated Metabolic Pathways that Drive Cancer Pathogenicity

By

Lindsay Shayna Roberts

A dissertation submitted in partial satisfaction of the

requirements for the degree of

Doctor of Philosophy

in

Metabolic Biology

in the

Graduate Division

of the

University of California, Berkeley

Committee in charge:

Professor Daniel K. Nomura, Chair
Professor James Olzmann
Professor Sarah Stanley

Spring 2017

ABSTRACT

Investigating Dysregulated Metabolic Pathways that Drive Cancer Pathogenicity

by

Lindsay Shayna Roberts

Doctor of Philosophy in Metabolic Biology

University of California, Berkeley

Professor Daniel K. Nomura, Chair

In the United States, it is estimated that over 200,000 women will be diagnosed with breast cancer and nearly 40,000 women will die of breast cancer in 2016[1]. Mortality from breast cancer is almost always attributed to metastatic spread of the disease to other organs, thus precluding resection as a treatment method.[2] Unfortunately, conventional chemotherapy fails to eradicate many aggressive breast cancers. Studies over the past decade have uncovered certain breast cancer cell-types, such as estrogen/progesterone/human epidermal growth factor receptor 2 (ER/PR/ HER2)-negative (triple-negative) breast cancers (TNBCs) that show poor prognosis and chemotherapy resistance within breast tumors.[3–5] Eliminating these breast cancer types is critical in reducing the mortality associated with breast cancer. Current therapeutic strategies for breast cancer include resection, nonspecific therapies such as radiation or chemotherapy, and targeted strategies for combating certain types of breast cancers. However, there are no targeted strategies for combating the most aggressive types of breast cancers, including TNBCs.

Cancer cells are known to possess altered metabolism that fuels their malignancy and pathogenicity. Most of what has been known about cancer cell metabolism focuses on the well-characterized central carbon pathways, however, the mapping of the human genome revealed that cellular metabolic networks extend far beyond that. In this dissertation I present some extensions of our understanding of dysregulated cancer cell metabolism in areas of lipid metabolism and membrane glycosylation. Furthermore, using drugs and drug candidates already in clinical trials or the clinic, I identify new metabolic targets that, when inhibited, contribute to or are responsible for killing TNBC cells. Increasing our understanding of cancer cell metabolism, especially in the context of small molecule inhibitors, will hopefully enable or promote the development of targeted therapeutics for these highly lethal and poorly treated cancers.

DEDICATION

Achieving this goal of earning my Ph.D. was made possible by the help and support of many important people in my life to whom I would like to dedicate this dissertation:

To all of my mentors – in science and in life.

In science

To Dr. Sharon Fleming and Mark Fitch, my first two mentors in research, for taking a chance on an excited, naïve, new freshman undergrad. Without that opportunity I would not have discovered and developed my love for research. To Dr. Marc Hellerstein, Dr. Matthew Bruss, Dr. Cyrus Khambatta, and Dr. Airlia Thompson for encouraging me, giving advice, and providing new opportunities for me to cultivate my scientific passions. To my Ph.D. advisor, Dr. Daniel Nomura, for pushing me to work harder and more thoughtfully that I knew possible. I've learned so much about research, science, and myself throughout this experience, and I thank you for giving me this opportunity.

To Dr. Mela Mulvihill for being the first to welcome me into the lab and quickly becoming my go-to person for any help I needed scientifically or personally. To Dr. Rebecca Kohnz for being my science Google and "sialyl-mate", I attribute so much of my scientific knowledge to you and your mentorship. To Dr. Leslie Bateman, thank you for being honest, direct, brilliant, and caring – your friendship and colleagueship is one of the best things to have come out of my graduate experience. To Peter Yan, my undergrad, for teaching me about mentoring and helping me learn things more thoroughly than ever before. To all the past and present members of the Nomura Research Group, I could not have done this without each of you -- you shared in my accomplishments and my struggles, you kept me going when I wanted to quit, you are why I wanted to come to work every day, and you are why I am so sad that this journey is over.

Finally, to now Dr. Sharon Louie, my counterpart throughout these past five years. I am so honored to have shared this experience with you. I feel so lucky to have had an amazing friend and colleague next to me every step of the way and I know that was a major part of my success (and sanity!). I will truly miss working with you and will always be just a text or call away for any help or advice you need – science, personal, general, fitness, food, anything. #LindsayandSharonisPhinisheD!

In life

To my parents, Joan and Peter Roberts, for investing in my education, for encouraging me and enabling me to explore my passions, for supporting me and always being proud. To my brother, Kevin Roberts, for thinking everything I do is way cooler than it actually is and for always acting interested and trying to understand what I'm talking about. To my grandfather, "PopPop", for your continued interest and excitement in my work – anytime I became jaded or bored, you kept me going. To my future in-laws,

Sharon Casey and George Littleton, thank you for your constant interest in my work, thank you for bragging for me and celebrating with me, and thank you for reminding me about how special and monumental this all is.

To my best friends Marcy and Mac Matthews, thank you for always being available to distract me from science when I needed a break or to listen to me talk about my work when I was excited. Thank you for cooking for me when I was too stressed, and toasting with me when I had accomplishments to commemorate. Thank you for bringing Owen Matthews into my life. Or maybe, more accurately, thank you for letting me help bring Owen into my life. To little Owen, this dissertation is also dedicated to you and your future. I can't wait to see your amazing accomplishments and contributions to this world, but just remember I put you in my dedication and, fair is fair, I better be in yours!

To my amazing fiancé, Dr. Casey Stark, thank you for always knowing how to help me. Thank you for pushing me when I needed a kick, thank you for catching me when I collapsed, thank you for forgiving me when I was stressed and lashed out, thank you for supporting me in every meaning of the word. And to our fur-baby, Kaia Starberts, thank you for reminding me how much more there is to life than science. Thank you for getting us outside to enjoy family time together, breathe in fresh air, and see the natural beauty of the bay area.

To my "health team" at the Recreational Sports Facility, Geoffrey Suguitan and Devin Wicks, thank you for providing classes so physically challenging that I forgot about everything else – no matter what was going on at work, I could always handle it after getting some clarity and perspective in one of your classes. Also, thank you for being my friends and allies; I will miss my exercise routine and gossiping with you guys every week.

Again, thank you to everyone in this dedication and everyone else with whom I crossed paths these past five years, you all made this work possible.

With gratitude (and relief),

Lindsay S. Roberts

Dr. Lindsay S. Roberts

TABLE OF CONTENTS

LIST OF FIGURES

LIST OF APPENDICES

LIST OF INITIALISMS

2-AG	2-arachidonylglycerol
2-HG	2-hydroxyglutarate
ABPP	activity-based protein profiling
AC	acyl carnitine
Ac_4-ManNaC	tetraacetylated N-acetylmannosamine
AdipoR1/R2	adiponectin receptor 1 or 2
AGPS	alkylglyceronephosphate synthase
AKR1B10	aldo-keto reductase family 1 member b10
AKT/PKB	protein kinase B
AMPK	adenosine monophosphate kinase
ASC	adipose stromal cells
ATGL	adipose triglyceride lipase
ATX	autotaxin
AURK	aurora kinase
BLT1	leukotriene receptor 1
C1P	ceramide-1-phosphate
cAMP	cyclic adenosine monophosphate
CD36	cluster of differentiation 36
COX-2	cyclooxygenase-2
CPT1	carnitine-palmitoyl transferase 1
CREB	cAMP-response binding element binding protein
DAG	diacylglycerol
DMP	discovery metabolite profiling
DPP9	dipeptidyl peptidase 9
EC50	50% effective concentration
ECM	extracellular matrix
EGFR	epidermal growth factor receptor
EMT	epithelial to mesenchymal transition
EP2	PGE_2 receptor

EPAC	exchange protein activated by cAMP isoform 1
ER	estrogen receptor
ERK1/2	extracellular signal-regulated kinase 1/2 (MAPK)
FASN	fatty acid synthase
FCCP	trifluoromethoxy carbonylcyanide phenylhydrazone
FFA	free fatty acid
FXR	farnesoid X receptor
GFP	green fluorescent protein
GTPase	guanosine triphosphatase
HAT	histone acetyltransferase
HDAC	histone deacetylase
HER2	human epidermal growth factor receptor 2
HIF-1α	hypoxia induced factor-1α
HRAS	harvey rat sarcoma viral oncogene homolog
HSL	hormone sensitive lipase
IAyne	iodoacetamide alkyne
IDH1	isocitrate dehydrogenase 1
IGF-1/IGF-2	insulin-like growth factor 1/2
IL-6	interleukin-6
IP3	inositol triphosphate
isoTOP-ABPP	isotopic tandem orthogonal proteolysis enabled-ABPP
JAK	janus kinase
KIAA1363	aka neutral cholesterol ester hydrolase 1 (NCEH1)
KSP	kinesin spindle protein
LEPR-B	leptin receptor-B long isoform
LPA	lysophosphatidic acid
LPC	lysophosphatidyl choline
LPCAT	lysophosphatidylcholine acyltransferase
LPE	lysophosphatidyl ethanolamine
LRb	leptin receptor
MAGE	monoacylglycerol ether

MAGL	monoacylglycerol lipase
ManNAc	N-acetylmannosamine
ManNAc-6-P	N-acetylmannosamine-6-phosphate
MAPK	mitogen-activated protein kinase (ERK)
MEK	MAPK/ERK kinase (MAPKK)
mTOR	mammalian target of rapamycin
MudPIT	multidimensional protein identification technology
NADP+	nicotinamide adenine dinucleotide phosphate - oxidized
NADPH	nicotinamide adenine dinucleotide phosphate - reduced
NAE	n-acyl-ethanolamine
NAT	n-acyl-taurine
NF-κB	nuclear factor kappa-light-chain-enhancer of activated B cells
O-Glc-NAc	O-linked β-N-acetylglucosamine
PA	phosphatidic acid
PAF	platelet activating factor
PAFAH1B2/3	platelet activating factor acetylhydrolase 1B2/3
PAI-1	plasminogen activator inhibitor 1
PG	phosphatidylglycerol
PGD_2	prostaglandin D_2
PGE_2	prostaglandin E_2
PHGDH	phosphoglycerate dehydrogenase
PI	phosphatidylinositol
PI3K	phosphoinositide 3-kinase
PKC	protein kinase C
PLA2	phospholipase A2
PLK	polo-like kinase
PR	progesterone receptor
PS	phosphatidylserine
PSAT	phosphoserine aminotransferase
PSPH	phosphoserine phosphatase
Ptdins(4,5)P2	phosphatidylinositol 4,5-bisphosphate

PTEN	phosphatase and tensin homolog
PTGR1	prostaglandin reductase 1
RAC	ras-related C3 botulinum toxin substrate 1
RBBP9	retinoblastoma-binding protein 9
RHO	ras homolog gene family, member A
RNAi	ribonucleic acid interferance
S1P	sphingosine-1-phosphate
SHMT	serine methyltransferase
shRNA	short hairpin RNA (RNAi technology)
SIAE	sialic acid acetylesterase
siRNA	small interfering RNA (RNAi technology)
SK-1	sphingosine kinase 1
SM	sphingomyelin
STAT	signal transducer and activator of transcription
TAG	triacylglycerol
TAZ	transcription factor involved in cell proliferation and apoptosis
TCA	tricarboxylic acid (Krebs or citric acid cycle)
TGF-β	transforming growth factor beta
TNBC	triple negative breast cancer
TNF-α	tumor necrosis factor alpha
TZD	thiazolidinedione
UDP-GlcNAc	uridine diphosphate N-acetylglucosamine
WAT	white adipose tissue

ACKNOWLEDGEMENTS

Adapted from Biochimica et Biophysica Acta: Lipids, Volume 1831, Sharon M. Louie*, Lindsay S. Roberts*, and Daniel K. Nomura, “Mechanisms Linking Obesity and Cancer,” pp. 1499-1508. Copyright © 2013 with permission from Elsevier.
*these authors contributed equally

Adapted from Biochimica et Biophysica Acta: Lipids, Volume 1831, Sharon M. Louie*, Lindsay S. Roberts*, Melinda M. Mulvihill, Kunxin Luo, and Daniel K. Nomura, “Cancer Cells Incorporate and Remodel Exogenous Palmitate into Structural and Oncogenic Signaling Lipids,” pp. 1566-1572. Copyright © 2013 with permission from Elsevier.
*these authors contributed equally

Adapted with permission from ACS Chemical Biology, doi: 10.1021/acschembio.6b01159. Lindsay S. Roberts, Peter Yan, Leslie A. Bateman, and Daniel K. Nomura, “Mapping Novel Metabolic Nodes Targeted by Anti-Cancer Drugs that Impair Triple-Negative Breast Cancer Pathogenicity.” Copyright © 2017 American Chemical Society

CHAPTER ONE: Understanding and Identifying Metabolic Nodes Driving Cancer Cell Pathogenicity Towards Improvements in Future Therapeutic Options

Introduction

In the United States, it is estimated that over 200,000 women will be diagnosed with breast cancer and nearly 40,000 women will die of breast cancer in 2016[1]. Mortality from breast cancer is almost always attributed to metastatic spread of the disease to other organs, thus precluding resection as a treatment method.[2] Unfortunately, conventional chemotherapy fails to eradicate many aggressive breast cancers. Studies over the past decade have uncovered certain breast cancer cell-types, such as estrogen/progesterone/human epidermal growth factor receptor 2 (ER/PR/ HER2)-negative (triple-negative) breast cancers (TNBCs) that show poor prognosis and chemotherapy resistance within breast tumors.[3–5] Eliminating these breast cancer types is critical in reducing the mortality associated with breast cancer. Current therapeutic strategies for breast cancer include resection, nonspecific therapies such as radiation or chemotherapy, and targeted strategies for combating certain types of breast cancers. However, there are no targeted strategies for combating the most aggressive types of breast cancers, including TNBCs.

Genetic mutations in DNA are the unifying, initiating event that gives rise to cancers. These genetic mutations commonly lead to metabolic alterations that, in turn, fuel cancer cell malignancy and tumorigenesis.[6,7] The discovery of dysregulated metabolism was first shown in the 1920s when Otto Warburg observed that cancer cells consume much higher levels of glucose than normal cells and use that glucose-derived carbon to secrete lactate instead of fully oxidizing it for energy.[8] Since that time it has become well established that cancer cells have broadly dysregulated metabolism that drives nearly every aspect of their pathogenicity. These changes include not only those in the glycolytic pathway[9,10], but also in others including the citric acid cycle[11–13], lipogenesis[14,15] and glutaminolysis[16,17] (**Fig. 1-1**). Most research efforts have been focused on fully understanding the known alterations in central carbon metabolism. However, it is likely that other pathways, enzymes, and metabolites are also involved in or driving cancer cell pathogenicity. These changes in metabolism may lead to enhanced cancer cell phenotypes including proliferation, invasion, survival, and metastasis through modulation of cellular energy status as well as the availability of building blocks for structural and signaling metabolites.

Over the past decade, there has been a resurgence of research into dysregulated cancer metabolism and the development of therapeutics targeting metabolic enzymes and pathways. Most of the research and pharmaceuticals have focused on well-characterized, functionally annotated enzymes due to the relative ease with which these can be studied; however, we know from the mapping of the human genome that there are many more metabolic enzymes encoded in our DNA that could also have important implications in cancer development and progression. Traditional genomic, transcriptomic, and proteomic profiling strategies have undoubtedly yielded some critical insight into dysregulated metabolic pathways but fall short as they do not provide any information on enzyme activity or enzyme-metabolite relationships. For example, post-translationally modified enzymes may have no change in abundance as detected by proteomics, but have vastly different functionality. As a result, many technologies have

recently surfaced which give new promise towards uncovering the importance of these uncharacterized enzymes and pathways as well as directly assessing the function and functional states of enzymes *in situ* and *in vivo*.

Metabolomics profiling to reveal new important pathways in cancer

Metabolomics[18–20] has emerged as a very useful tool especially when coupled with other "omics"-based strategies such as genomics, transcriptomics, or proteomics[21,22]. In the context of cancer, for example, once an enzyme has been identified as dysregulated by one of the traditional profiling platforms, researchers can determine the direct effect of that enzyme in the metabolome by looking at relative abundances of the substrate(s), product(s), and other metabolites further up- or down-stream in the pathway that may be altered. This can help to reveal the direct mechanism by which a dysregulated enzyme or pathway is conferring malignant phenotypes, and these can then be confirmed through more specific biochemical experiments. Targeted metabolomic profiling (**Fig. 1-2 A**) is a powerful strategy using liquid chromatography and mass spectrometry in which researchers can easily compare the abundance of known metabolites between groups of interest.[23]

Since the discovery of the metabolic "switch" of cancer cells from oxidative to glycolytic metabolism (the Warburg effect), cancer metabolism research has primarily focused on these catalytic pathways. However, more recently it has been shown that cancer cells also undergo changes in anabolic metabolism, for example enhanced *de novo* lipogenesis. Furthermore, in 2010 Nomura *et al*. showed that the enzyme monoacylglycerol lipase (MAGL) regulates fatty acid networks high in oncogenic signaling lipids, which promote features of cancer cell malignancy including migration, invasion, survival, and *in vivo* tumor growth.[24] Monoacylglycerol lipase is the enzyme primarily responsible for releasing arachidonic acid from the endocannabinoid 2-arachidonylglycerol (2-AG), but also is active against monoacylglycerols (MAGs) with other fatty acid chain lengths. Both genetic (shRNA) and pharmacological inactivation of MAGL resulted in reductions in cancer cell malignancy as assessed by *in vitro* cell migration, invasion, and survival. So to determine the mechanism by which MAGL was exerting these effects, they performed targeted lipidomic analyses. Ovarian, breast, melanoma, and prostate cancer cells all treated with the MAGL-specific inhibitor JZL184, showed increases in several MAGs as well as decreases in the levels of free fatty acids (FFAs).

Moreover, both shMAGL cells and chronic JZL184 inhibitor-treated cells, showed reductions in lysophosphatidic acid (LPA) and prostaglandin E_2 (PGE_2), both of which are protumorigenic lipid messengers and have been shown to promote aggressiveness of cancer cells.[25,26] In normal cells, MAGL has not been shown to control the levels of FFAs and therefore also not LPA or PGE_2, so this is acts as an example of targeted metabolomic analyses revealing a unique function and importance for MAGL specifically in aggressive cancer cells.

In a separate study by Nomura *et al*. they showed that because MAGL is the enzymatic node connecting the endocannabinoid, 2-AG, with the protumorigenic signaling lipids such as LPA and PGE_2, disrupting MAGL in androgen-dependent prostate cancer led to not only decreased oncogenic lipids but also increased 2-AG, which has been shown to be antitumorigenic. This suggests that in androgen-dependent prostate cancer, MAGL exerts dual control over pro- and anti-tumorigenic signaling pathways to drive cancer.[27]

Following the discovery of the importance of MAGL in cancer cells, many other enzymes involved in lipid metabolism have been shown to be critical drivers of aggressive cancers. One such enzyme is alkylglyceronephosphate synthase (AGPS), which is a critical step in the synthesis of ether lipids, responsible for the conversion of acyl-glycerone-3-phosphate into alkyl-glycerone-3-phosphate. Ether lipids have been known to be higher in tumors and in 2013 Benjamin *et al*. showed that consistent with elevated ether lipids AGPS is up-regulated across multiple types of aggressive human cancer cells and primary tumors.[28] Furthermore, they showed that genetic ablation of AGPS reduced cell survival and *in vivo* tumor growth as well as the levels of ether lipids such as lysophosphatidic acid ether (LPAe), as predicted. Surprisingly though, using metabolomics platforms, they also showed that AGPS knockdown resulted in lower levels of free fatty acids (FFAs) including arachidonic acid, as well as arachidonic acid-derived protumorigenic signaling eicosanoids prostaglandin E_2/D_2 (PGE_2/PGD_2) in a triple negative breast cancer cell line. These data indicate that AGPS may be a metabolic node in breast cancer that modulates the ratios of structural and signaling lipids, as well as fatty acid utilization pathways. High AGPS expression, therefore promotes the generation of oncogenic signaling lipids such as lysophospholipids and eicosanoids that drive tumorigenic features of breast cancer.

A study done by Zhu *et al*. also showed that silencing of AGPS reduced the levels of both LPAe and PGE_2, leading, in turn, to reduced signaling through their respective receptors which mediate pathways involved in the expression of several multi-drug resistant genes in glioma and hepatic carcinoma cell lines.[29] Upon AGPS silencing, signaling through these pathways was reduced as well as the expression of these genes. Therefore, they concluded that high AGPS in cancer may also be important in the ability to resist chemotherapy and therefore a very attractive target for inhibitor development as it could be used to sensitize cells to other chemotherapeutics. In 2015, Piano *et al*. published a study on the discovery and validation of an AGPS inhibitor as an anti-cancer agent.[30] They show that treatment of this inhibitor yields a very similar metabolomic signature to that of AGPS knockdown by shRNA, and commensurate phenotypic impairments in cancer cell survival and migration. These data further support that AGPS is an important enzyme in cancer metabolism and therefore make it an attractive druggable target for future chemotherapies.

While the “Warburg Effect”, the hyperconsumption of glucose metabolized to lactate, is considered a hallmark of tumors, more recently the diversion of this glucose to other important metabolic pathways has begun to be appreciated. Since 2010 one such diversion, towards the serine and glycine pathways, has garnered increased attention. To enter this pathway the glycolytic intermediate 3-phosphoglycerate gets converted to

3-phosphohydroxypyruvate by the enzyme phosphoglycerate dehydrogenase (PHGDH). Following two more conversions by phosphoserine aminotransferase (PSAT) and phosphoserine phosphatase (PSPH), serine is made. Finally serine can be directly converted to glycine by the enzyme serine methyltransferase (SHMT). Several previous protein expression studies have shown increased expression of all of these enzymes in cancer cells and that several of them correlate with prognosis[31–33]; however, the mechanism by which increased flux through this pathway confers an advantage to cancer cells was not known.

In 2011, Locasale *et al*. used a metabolomics approach with stable isotope labeling to directly measure the amount of glycolytic carbon going into serine and glycine metabolism to attempt to determine this mechanism.[34] Using ^{13}C-glucose they showed that flux into the glycine pathway from glycolysis is higher in cancers and presumed that this increased flux was to allow carbons to go to many downstream pathways including maintenance of the folate pool[35,36], amino acid intermediates[37], and cellular redox status[38,39]. In another isotope tracing study in 2012, Jain *et al*. profiled the NCI-60 cancer cell lines to determine their different consumption and release rates of 219 metabolites as measured by liquid chromatography tandem mass spectrometry (LC-MS/MS)[40], so called CORE analysis. From this large-scale profiling, they found that glycine consumption and the expression of the glycine biosynthetic proteins strongly correlated with proliferation rates of cells, a proxy for aggressiveness.[41] Furthermore, metabolic tracing with ^{13}C-glycine in these cells revealed that some rapidly proliferating cells use this glycine for purine biosynthesis as well as to make glutathione, a metabolite critical for regulation of cellular redox. However, they found that sensitivity to a glutathione synthesis inhibitor was unrelated to proliferation rates in these cells, leading them to conclude that although they saw ^{13}C incorporation into glutathione, it was not involved in the rapid proliferation phenotype of the cancer cells. Another study in 2014 by Labuschagne *et al*. showed that restricting exogenous glycine consumption did not change proliferation rates, however serine restriction did. They, therefore, concluded that it is serine, not glycine, consumption that supports nucleotide synthesis and leads to enhanced proliferation rates.[42]

In addition to the aforementioned alterations in glucose metabolism seen in cancer cells, there are also fundamental changes in metabolic pathways such as the TCA cycle and amino acid biosynthesis. NMR and mass spectrometry with stable isotope labeling have been used to measure rates of flux and also fates of metabolites through these pathways. In particular, ^{13}C-glucose labeling studies have been used, as discussed above, to determine the outcomes of glucose metabolism through glycolysis, the tricarboxylic acid (TCA) cycle, hexosamine pathway, nucleotide biosynthesis, etc. Similarly, using ^{13}C-glutamine, DeBerardinis *et al*. showed that glutamine can be used in place of glucose to provide the mitochondria with carbons to then produce citric acid, a critical precursor for the synthesis of many important biomolecules including lipids, amino acids, and nucleotides, a phenomenon termed “glutaminolysis”. They showed that cancer cells primarily use this citric acid to provide acetyl-CoA for fatty acid and phospholipid biosynthesis. In 2011 Cheng *et al*. showed that suppression of glutamine anaplerosis by blockade of the enzyme glutaminase, the first step in glutamine-

dependent anaplerosis, led to reduced proliferation of glioblastoma cancer cells in culture and *in vivo* providing evidence for an attractive therapy route.[43] However, they also showed that upon this blockade, glioblastoma cells initiate a compensatory anaplerotic mechanism catalyzed through pyruvate carboxylase (PC), which enables the cells to use pyruvate derived from glucose instead of glutamine for anaplerosis. They therefore concluded that these cells are able to achieve glutamine independence and therapies targeting glutaminolysis may not be effective long term if cells can compensate through increase PC activity.

Untargeted, discovery-metabolite profiling as an unbiased metabolomics screening approach

The majority of studies using metabolomics platforms use the above-described targeted approach often because they already have a hypothesis generated based on a previous profiling effort. However, it is also possible to use an unbiased discovery based metabolomics approach, termed discovery metabolite profiling (DMP)[44], to guide the hypothesis in the first place. For DMP all metabolites are separated through liquid chromatography, measured by mass spectrometry, and then relative abundances compared between groups using bioinformatic platforms (**Fig. 1-2 B)**. This allows the researchers' hypotheses to then be guided based on the largest or most significant changes rather than their preconceptions what they choose to target for. Alternatively, researchers can utilize discovery metabolite profiling if they do not have the necessary information about the metabolites of interest from which they can set up a targeted program or if they believe a novel metabolite may be involved that they wish to identify.

One supreme example of the power of discovery metabolite profiling is with the enzyme isocitrate dehydrogenase (IDH1). This enzyme is a member of the citric acid cycle (TCA cycle) and typically catalyzes the oxidative carboxylation of isocitrate to α-ketoglutarate with coordinate reduction of $NADP^+$ to NADPH. Through genome wide analysis studies of glioma and acute myeloid leukemia patients, mutations in the active site of this enzyme have been identified.[45] Moreover, they were found to occur at a single amino acid residue, arginine 132, most commonly turning it into a histadine.[46] To understand the consequences of this mutation and why it may be involved in driving these cancers, Dang *et al*.[47] compared metabolomes between glioblastoma cells stably transfected with either wild type or mutated IDH1. They used this discovery based metabolomics approach which allowed them to simply compare relative abundances of unknown metabolites between groups, and then to try to identify those of interest based on significance and fold-change. Through doing this, these authors identified a novel "oncometabolite", 2-hydroxyglutarate (2-HG) that was significantly increased in cells with the mutated IDH1. Further metabolomic studies showed that increased 2-HG, either through mutated IDH1 or through exogenous treatment with the metabolite, led to a range of downstream metabolic changes including animo acids, choline derivaties, and TCA cycle intermediates.[10]

Initially upon discovery of 2-HG it was thought that it could only arise from the mutated form of IDH1; however, in 2011 Wise *et al*. showed that under specific conditions 2-HG

can be produced even with wild type IDH1 present, and that this increase in 2-HG leads to the same pro-malignancy phenotype. Using metabolic flux analysis[48,49], they labeled cells with either ^{13}C-glucose or ^{13}C-glutamine that were either in normoxic or hypoxic conditions. They saw that under normoxic conditions, citrate, which can be readily isomerized to isocitrate, can be formed through both glucose and glutamine-derived carbons, however under hypoxic conditions, most of the citrate comes from glutamine-derived α-ketoglutarate. They showed specifically that this reductive carboxylation by cancer cells under hypoxia is mediated by the IDH2 isoform of the enzyme, as this is the mitochondrial isoform, and that this leads to a significant increase in 2-HG levels. To further support this, they showed that 2-HG production from glutamine is significantly reduced upon knockdown of IDH2.

Activity-based protein profiling to assess enzyme functionality

One proteomic platform that has arisen to broadly study enzyme functionality is called activity-based protein profiling (ABPP)[50–52], and uses active-site directed chemical probes to directly asses the functional state of many enzymes in native biological samples (**Fig. 1-3**). Furthermore, this strategy can be used in conjunction with other profiling techniques, like metabolomics, as described above, and/or more traditional biological techniques to yield more comprehensive biochemical information on specific pathways and a more thorough understanding of the cellular consequences in cancer cells[53] or other disease states. Activity-based probes have two defining features: a reactive group which allows for covalent binding in the active site of the enzymes in the class through the enzyme's catalytic activity and a reporter tag for detection, enrichment, and identification of the labeled enzymes. One further application of ABPP is called competitive ABPP, which has been valuable in inhibitor discovery and validation.[54,55] In competitive ABPP the proteome, cell, or animal is first exposed to a small molecule, which covalently binds to and inactivates target enzymes, then the probe is introduced and those inhibited enzymes are not labeled which is detected through loss of the reporter tag output.

One of the largest and most diverse enzyme classes is the serine hydrolase superfamily, which consists of many metabolic enzymes including lipases, proteases, hydrolases and esterases. Using the serine hydrolase activity-based probe, many serine hydrolases have been implicated in tumorigenesis such as fatty acid synthase (FASN)[14], monoacylglycerol lipase (MAGL)[24,27], platelet-activating factor1B3 (PAFAH1B3)[56], retinoblastoma-binding protein 9 (RBBP9)[57], and the uncharacterized enzyme KIAA1363[58,59], to name a few. Moreover, many of these groups have used metabolomics to further understand the metabolic consequences of these enzymatic perturbations in cancer cells, and/or competitive ABPP to assess small-molecule inhibitory selectivity and potency (**Fig. 1-4)**. One of the most powerful aspects of ABPP is the ability to study cancer cell metabolism in an unbiased manner including completely uncharacterized enzymes. Furthermore, when coupled to metabolomic profiling there lies the potential to assign functionality to an enzyme through the metabolomics changes associated with a specific enzyme's functional changes.[60,61]

In 2014 Mulvihill *et al.* used ABPP to identify that platelet-activating factor acetylhydrolase 1B3 (PAFAH1B3) had heightened activity across a panel of aggressive breast cancer cell lines as compared to a non-transformed mammary epithelial cell line.[56] Upon genetic inactivation of PAFAH1B3 they saw significant impairments in various aspects of *in situ* cancer cell pathogenicity including proliferation, survival, and migration. PAFAH1B3's putative function is to remove an acetyl group from platelet-activating factor (PAF), an important oncogenic signaling lipid, thereby reducing its levels, which can lead to reductions in aspects of cancer aggressiveness. Through metabolomic profiling, as well as rigorous other biochemical assays, they were not able to confirm this putative function, nor were able to confirm a new function. While it is of future interest to understand the function of this enzyme, through ABPP they were able to confidently link PAFAH1B3 activity to breast cancer pathogenicity, despite not knowing its true function. In 2015, a paper from the same group by Kohnz *et al.* showed that a selective inhibitor against PAFAH1B3 discovered through competitive ABPP, called P11, could also confer impairments in pathogenic features of cancer.[62] While it is unfortunate that the metabolomic characterization efforts in both of these papers failed to determine the catalytic role of PAFAH1B3 in cancer cells, the phenotypic data that correlates with activity of PAFAH1B3 confirms its importance in breast cancer nonetheless and further supports the power of ABPP.

Similarly to the use of ABPP to determine the importance of the misannotated PAFAH1B3 in cancer, ABPP has also been used to identify the significance of completely uncharacterized enzymes. Coupled with metabolomics, the enzyme can then be functionally characterized, followed by competitive ABPP for the development and screening of lead small molecule inhibitors to assess potency and selectivity. One example of this is the enzyme KIAA1363, which was shown by Jessani *et al*. to be an enzyme associated with cancer cell invasiveness[63]; however, at this time the function of the enzyme was entirely unknown. In 2006 Chiang *et al.* combined ABPP with metabolomics to determine the role of this enzyme in cancer.[64] They determined that this enzyme served as a node in an ether lipid-signaling network that connects platelet-activating factor (PAF), monoalkylglycerol ethers (MAGEs), and lysophopholipids. While it was not concluded which specific metabolites controlled cancer pathogenesis in this pathway, they did show that when the enzyme KIAA1363 was genetically knocked down using shRNA, *in situ* cell survival, invasion and migratory capacity as well as *in vivo* tumor growth were significantly impaired. In 2011, Chang *et al.* developed and validated a highly selective small-molecule inhibitor, JW480, against KIAA1363.[65] Treating cells with JW480 significantly reduced cancer cell survival, migration, and invasion similarly to the shRNA against KIAA1363. Metabolomically, they show reductions specifically in several species of MAGEs, which they believe are conferring the changes in cancer cell phenotypes. Furthermore, JW480 is *in vivo*-active, safe, and showed tumor growth defects when mice were treated with it as compared to a vehicle control. Taken together, these studies have used several key chemical biology applications to 1) identify a yet-so-far unknown enzyme important in cancer, 2) characterize its functionality in this context, and 3) develop an *in vivo*-active inhibitor against it with the hopes of moving this target and inhibitor towards the clinic.

isoTOP-ABPP to map proteome-wide ligandable hotspots

While ABPP has certainly advanced our understanding of enzyme functionality, there are several limitations to this technology most notably that it cannot be used *in vivo*. Furthermore, ABPP can only assess the catalytic activity of an enzyme. Therefore, a newer platform has arisen in which bioorthogonal probes are used in place of the activity-based probes.[66,67] Bioorthogonal probes are probes that are compatible with life, meaning they can easily be used *in vivo*.[68] These probes possess a small, analytical handle, either an azide or alkyne group, that is suitable for "click chemistry" in place of the bulky reporter tag on the activity-based probe. The replacement of the reporter tag for a smaller analytical handle both enhances cell permeability and allows for experimentation *in vivo*.[69] These analytical handles can then be used for *in vitro* copper-catalyzed azide-alkyne cycloaddition to append on a detection handle like those on the activity-based probes for detection by in-gel fluorescence or enrichment, quantification, and identification by mass spectrometry-based proteomics. There are bioorthogonal probes that work similarly to activity-based probes by binding the active site of an enzyme to assess catalytic activity *in situ* or *in vivo*. As far back as 2003, many of these activity-based bioorthogonal probes were compared to the traditional activity-based probes for validation.[70] While many of the findings were expected, that the bioorthogonal probes could label the same enzymes as the original probes, in some cases, they actually found different targets *in situ* compared to *in vitro,* further supporting the need for probes suitable for *in situ* or *in vivo* studies to minimize false positives.

Another major limitation of ABPP, even with bioorthogonal probes, is that it relies on a catalytic event for covalent binding of the probe, and thus can only assess active-sites of enzymes. Therefore, there has been significant interest in developing approaches to probe non-catalytic but biologically relevant residues on proteins, such as those involved in protein-protein interactions, allosteric regulation, cofactor binding, etc. One such chemoproteomic platform that has arisen to tackle many of these challenges in target identification is isotopic tandem orthogonal proteolysis-enabled activity-based protein profiling (isoTOP-ABPP) **(Fig. 1-5).**[71,72] IsoTOP-ABPP uses reactivity-based chemical probes to covalently modify proteome-wide reactive, functional, and ligandable hotspots. There are three features specific to proteomic profiling with reactivity-based probes that enable mining of proteome-wide functional and ligandable hotspots facilitating both inhibitor and target discovery of covalently-acting small-molecules. These features are 1) an electrophilic warhead that can react with nucleophilic hotspots on proteins; 2) an alkyne handle for Copper-catalyzed azide-alkyne cycloaddition (CuAAC) or "click chemistry" conjugation of an enrichment handle for probe-labeled proteins and peptides; and 3) an azide-functionalized TEV protease recognition peptide linker bearing an isotopically light or heavy valine and a biotin group which can be appended onto probe-labeled proteins for subsequent avidin enrichment, digestion, isolation of probe-labeled tryptic peptides, and TEV release of probe-labeled peptides for subsequent quantitative proteomic analyses comparing isotopically light to heavy peptide ratios of probe-modified tryptic peptides.

These probes react not only with catalytic sites within enzymes, but also solvent-accessible binding pockets, post-translational modification sites, cysteine oxidation sites, protein-protein interaction sites, and other types of regulatory or functional domains across the entirety of the proteome. When coupled with isoTOP-ABPP to map reactivity of specific sites of probe-modification, this overall approach enables a global approach to map protein functionality and more importantly, facilitates the identification of druggable hotspots within protein targets that may have previously been undruggable. When used in a competitive manner (competitive isoTOP-ABPP), covalently-acting small-molecules can be competed against the binding of their corresponding reactivity-based probes to rapidly identify the targets of these molecules **(Fig. 1-5)**.[71]

An example of this competitive isoTOP-ABPP approach was first demonstrated by Wang *et al.* where the authors used this technology to map the proteome-wide reactivity of lipid-derived electrophiles.[73] Several groups have also used this platform to identify new druggable hotspots and find lead compounds that target them.[74–76] A recent use of this platform coupled to a chemical genetics screen of a cysteine-reactive fragment library in colorectal cancer identified cysteine 1101 on reticulon (RTN4) as an important residue in maintaining cancer cell survival, and endoplasmic reticulum (ER) and nuclear envelope morphology. Binding of this cysteine by a fragment led to significant and robust reductions in cancer cell pathogenicity indicating that this cysteine may be blocking the formation of ER tubular networks and would therefore prevent cell divisions.[75]

Conclusions

While DNA damage is considered the initiating event that gives rise to cancer, the metabolic alterations consequential to this damage may actually be responsible for driving the pathogenic features such as increased cellular survival, proliferation, migration, invasion, vascularization, etc. Due to increased understanding of dysregulated cancer metabolism, many metabolic pathways, targets, and inhibitors have been discovered for potential cancer therapy recently. These include pyruvate kinase activators that target glycolytic metabolism, isocitrate dehydrogenase mutant-specific inhibitors that impair oncometabolite synthesis, fatty acid synthase inhibitors that impair lipogenesis, and phosphoglycerate dehydrogenase inhibitors that target serine metabolism. Through the development of more advanced profiling platforms, we now know that these enzymes and pathways do not fully represent the potential druggable targets that may be exploited for cancer therapeutic development. Furthermore with these innovative technologies, we are beginning to be able to determine off-target or secondary targets of drugs and drug candidates and elucidate any mechanism through which they may be contributing to this reduction in cancer cell pathogenicity.

Figures

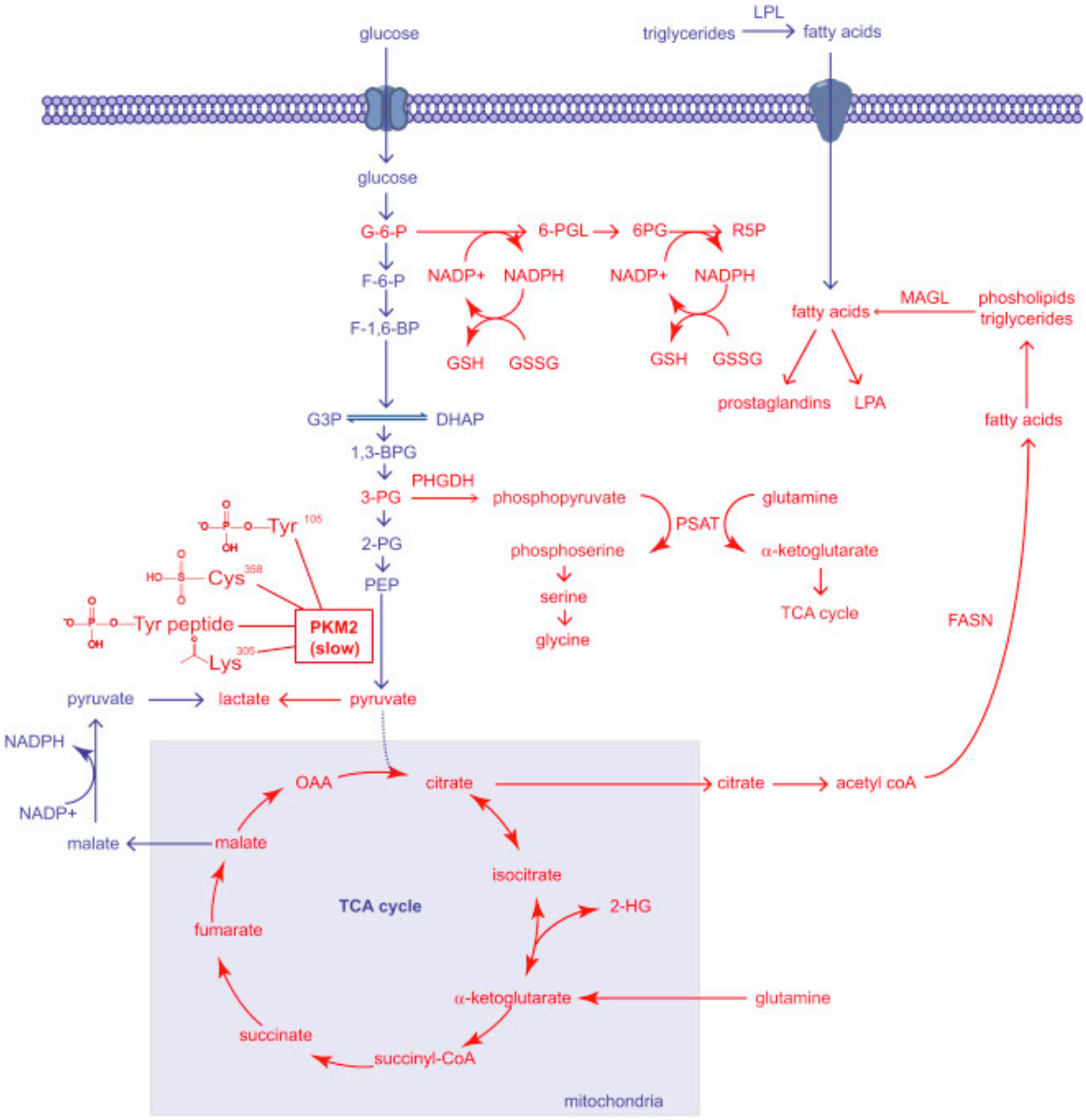

Figure 1-1. Dysregulated metabolic pathways in cancer cells identified thus far. The metabolic pathways that sustain the proliferative nature of cancer cells are very much the same pathways that constitute the metabolism of normal cells. However, cancer cells are able to aberrantly rewire many of these normal pathways to meet their excessive needs for growth and proliferation. In the figure above, we see that pathways that have been revealed to be essential in cancer cells (shown in red) are pathways that are fundamentally important for the synthesis of biological macromolecules, antioxidants, and signaling molecules that facilitate cellular growth, survival, and progression.[19] (Reproduced with permission from Elsevier).

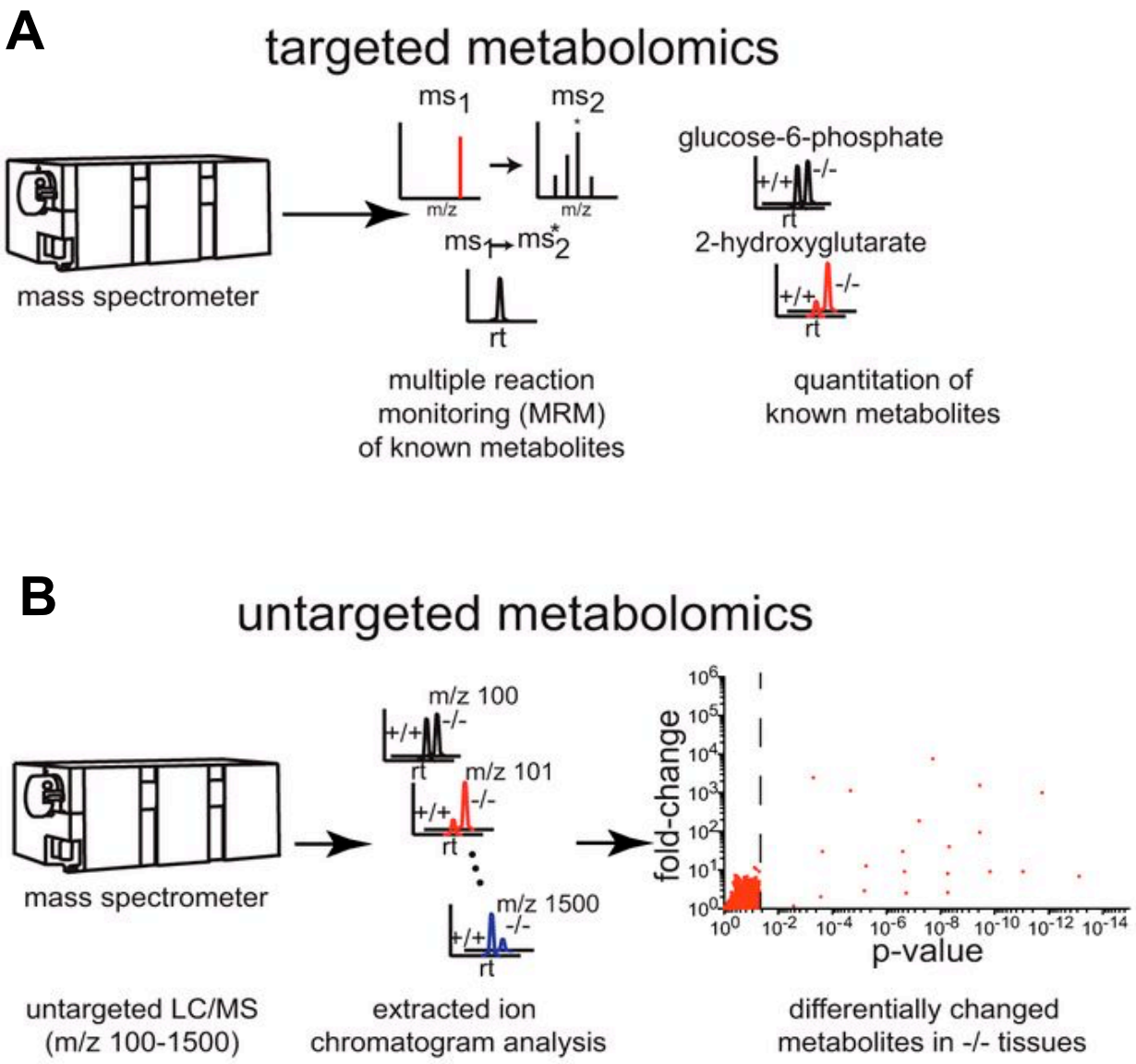

Figure 1-2. Targeted and untargeted metabolomics platforms. (A) targeted metabolomics uses multiple reaction monitoring to quantify the levels of ~100 known metabolites. **(B)** Untargeted metabolomics (or discovery-based metabolite profiling, DMP) scans for metabolites across a mass range. Coupling this with bioinformatic platforms allows for determination of relative abundances of these metabolites, however, the identity of the metabolite must be confirmed with follow-up targeted approaches.[56] (Adapted with permission from American Journal of Physiology, Endocrinology, and Metabolism)

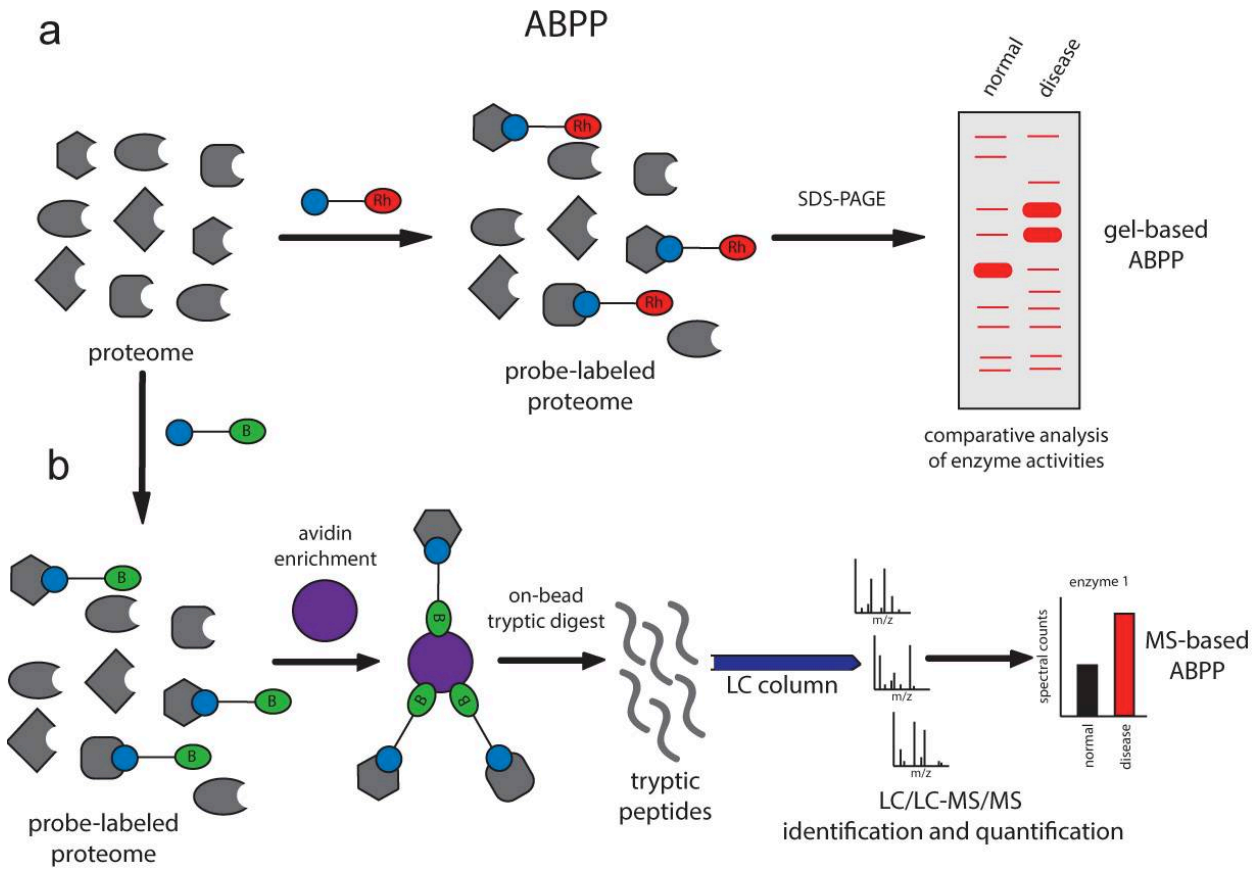

Figure 1-3. Activity-based protein profiling (ABPP). ABPP uses active site-directed chemical probes to broadly assess the functional state of enzymes across enzyme families. These probes consist of a reactive group and a detection handle, most commonly rhodamine (Rh) or biotin (B). In gel-based ABPP, native proteomes are reacted with the probe and proteins are separated by SDS-PAGE and visualized by fluorescent scanning. MS-based ABPP facilitates the identification and quantification of enzyme activities following avidin enrichment, on-bead tryptic digestion, and resolution by Multidimensional Protein Identification Technology (MudPIT)[61]. (Reproduced with permission from Elsevier)

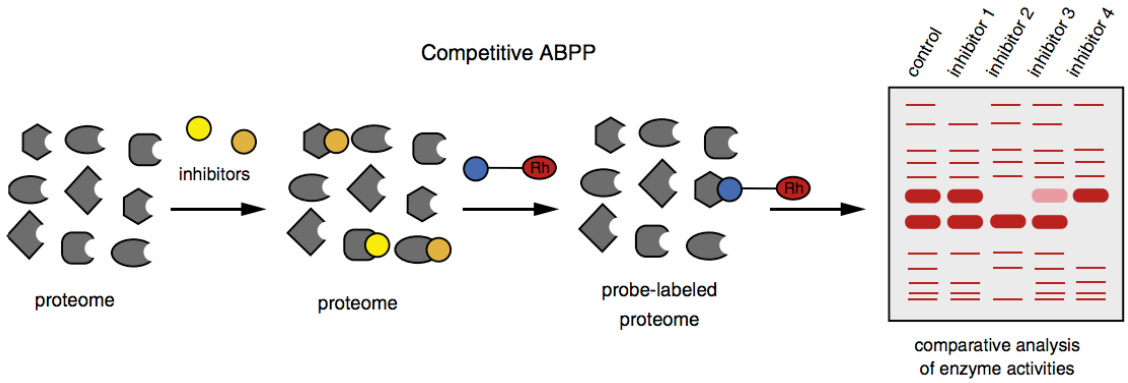

Figure 1-4. Competitive activity-based protein profiling (ABPP). Competitive ABPP assesses the potency and selectivity of small molecule inhibitors in native proteomes by competing with the ability of the probe to bind. Enzyme inhibition is indicated by a loss of fluorescent intensity by gel or a loss of spectral counts by MS.[61] (Reproduced with permission from Elsevier)

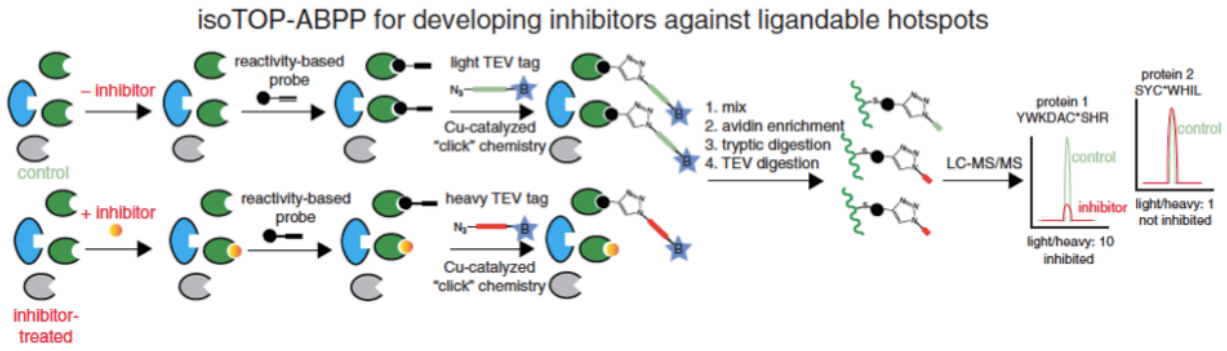

Figure 1-5. Competitive isotopic tandem orthogonal proteolysis-enabled ABPP (isoTOP-ABPP) for inhibitor development and identification of ligandable hotspots. Using isoTOP-ABPP for pharmacological interrogation of ligandable hotspots. The vehicle-treated and inhibitor-treated proteomes can be labeled with activity or reactivity-based probes, followed by appendage of isotopically light or heavy analytical biotin handles bearing a TEV protease cleavage sequences, followed by mixing of proteomes in a 1:1 ratio, avidin enrichment of probe-labeled proteins, TEV digestion to release probe-modified tryptic peptides and quantitative proteomic analysis of probe-modified peptides. This will not only map the sites of probe labeling, but also sites where the inhibitor has displaced probe labeling, facilitating both inhibitor discovery for targets of interest as well as an assessment of its proteome-wide selectivity.[71] (Reproduced with permission from Elsevier)

CHAPTER TWO: Mechanisms Linking Obesity and Cancer

Introduction

The incidence of obesity has been steadily increasing over the past few decades. In 2007–2008, the prevalence of obesity among US adults was 33.8% and of overweight 68.0%, after adjusting for age.[77] These epidemic proportions of obesity are not only mirrored in the rest of the developed world, but also now in many developing countries, making obesity one of the most serious health problems worldwide.[78] While there are many comorbidities associated with obesity, such as the well-established relationship with type 2 diabetes and cardiovascular diseases, a clear epidemiological relationship between obesity and the prevalence of a variety of cancers has also been uncovered.[79,80]

Cancer is currently the leading cause of death in developed countries and second in developing countries.[81] Several studies have shown significantly elevated risk for leukemia, lymphoma and myeloma with high body-mass index (BMI) in a dose-dependent manner[82], as well as an increased risk for pancreatic[83], prostate[84], breast[85], colon, endometrial, liver, kidney, esophagus, gastric, and gallbladder cancers[86] in obese adults. Furthermore, as childhood obesity rates continue to follow those of adults[87], their risks for cancers later in life are significantly higher.[88] Although the epidemiological associations between cancer progression and prognosis are firmly established, the link between obesity and cancer initiation and the molecular mechanisms underlying these associations are still being elucidated.

White adipose tissue has traditionally been considered an inert tissue almost exclusively for energy storage. Recently, white adipose has emerged as an important endocrine and metabolic organ as well as a key player in immunity and inflammation.[89] With this new understanding of adipose tissue function, researchers have delved into the relationship of these secondary effects of obesity, which may in fact be responsible for the increased propensities for various cancers. Considering the prevalence of obesity, the lethality of cancer, and the rise in childhood obesity, there is an imminent need for research to delineate the underlying mechanism(s) through which obesity drives cancer and to exploit those findings to develop interventions and potential therapeutics to combat this deadly combination. This review focuses on the mechanisms that have been proposed to underlie how obesity drives cancer pathogenesis, with emphasis on inflammation, insulin signaling, adipokines, elevated lipids and lipid signaling (**Fig. 2-1**).

Inflammation

In addition to simply storing excess fat, the state of obesity induces a low-grade, chronic, metabolically-linked, inflammatory state, different from traditional inflammation, called metaflammation.[90] Although it is unclear how this inflammatory state is initiated, one proposed mechanism is through hypoxia. During weight gain and adipose tissue expansion, there are times when some cells are too distant from the organ's vasculature causing them to become poorly oxygenated and resulting in localized hypoxia.[91] This then activates hypoxia-inducible factor (HIF)-1α, which mediates the infiltraton of

macrophages and monocytes into the adipose tissue and finally the secretion of tumor necrosis factor-α (TNF-α).[92]

In this metaflammatory state, TNF-α has been found to be elevated in and secreted from the white adipose tissue.[93] However, other work has shown that TNF-α is actually released from macrophages and monocytes, which have increased infiltration into the adipose tissue in obese subjects.[94] While TNF-α was originally found to mediate endotoxin-induced tumor necrosis[95], it has also been implicated in cancer angiogenesis[96] and metastasis[97] as well as cell survival[98], growth, and differentiation[99,100]. One proposed mechanism of TNF-α-induced carcinogenesis is through activation of the nuclear transcription factor NF-κB by inhibiting the inhibitor of NF-κB (IκB). This pathway has been shown to be involved in the development of lymphoma[101], pancreatic[102] and liver[103] cancers. Activated NF-κB prevents apoptosis allowing enhanced cell survival[98] and eventually inflammation-associated cancer[103]. However these effects may differ in different cell-types and experimental conditions.[104] Moreover, activation of NF-κB in cancer cells can activate cell cycling through c-Myc[98] and cyclin D1[99] leading to increased cell growth and proliferation. While both the relationship between obesity-induced inflammation and the activation of NF-κB by TNF-α are well-established, whether there are other roles of NF-κB in obesity-associated cancers remains unknown.

Interleukin-6 is another cytokine shown to be elevated in obesity and IL-6 levels are positively correlated with BMI.[105] IL-6 secretion from the white adipose tissue is induced by TNF-α[93] as well as the hypoxic conditions of the adipose[106]. Circulating IL-6 signals through the Janus kinase-signal transducer and activator of transcription-3 (JAK-STAT3) signal cascade.[107] IL-6 induced JAK-STAT3 signal transduction stimulates cell proliferation, differentiation[108] and metastasis[109]. In animal models lacking endogenous IL-6, the effect of obesity on tumorigenesis was not seen[110]. IL-6 mediated cell proliferation has been proposed to act through the mitogen-activated protein kinase (MAPK) pathway. Upon inhibition of MAPK, there was no proliferation in the presence of IL-6[111] indicating the integral role of IL-6 in cell proliferation in inflammation.

In addition to TNF-α and IL-6, there are other cytokines produced during the obesity-induced inflammatory state such as plasminogen activator inhibitor-1 (PAI-1). PAI-1 inhibits plasminogen activators such as urokinase and tissue plasminogen activator. These plasminogen activators convert plasminogen, a zymogen, to the active enzyme, plasmin. Plasmin is a serine protease, which breaks down the extracellular matrix, a critical step in cancer invasion and metastasis.[112] After the extracellular matrix is broken down and as the cancer becomes more aggressive, PAI-1 is upregulated to inhibit the aberrant activity of plasmin. Therefore, elevated PAI-1 levels are observed in subjects with poor cancer prognoses, (rates of relapse, death, etc.).[113] PAI-1 has also been shown to inhibit cell-adhesion to vitronectin and promote migration from vitronectin to fibronectin, where it has a stimulatory effect on vascularization, thus promoting angiogenesis.[114] Moreover, the absence of PAI-1 prevents invasion and tumor vascularization, both of which can be rescued upon injection of an adenoviral vector expressing PAI-1.[115] These inflammatory response data indicate the multi-faceted importance of elevated cytokine levels in cancer malignancy, their measured levels as

potential cancer malignancy biomarkers, and their inhibition as a novel cancer or obesity induced cancer drug target.

Some of these inflammatory pathways stimulated as a result of obesity intersect with other seemingly unrelated pathways altered in obesity. This interplay may lead to a synergistic effect of multiple mechanisms through which obesity drives cancer. For example, TNF-α overexpression in white adipose tissue has also been shown to play an important role in mediating insulin resistance in obesity[116] and a lack of TNF-α function results in improved insulin sensitivity in mice.[117]

Insulin signaling

Obesity is associated with an increased risk of developing insulin resistance. Insulin resistance is a major metabolic abnormality in most patients with type 2 diabetes characterized by elevated levels of circulating insulin.[118] Insulin resistance develops with the accumulation of fatty acid metabolites within insulin responsive tissues. Besides the overall increase in adiposity, distribution of body fat is a critical determinant of insulin sensitivity. Lean individuals with a more peripheral distribution of fat are more insulin sensitive than lean individuals who have their fat distributed predominantly centrally in the abdominal and chest areas.[119–121] Insulin resistance is a pathological condition characterized by a decrease in the efficiency of insulin signaling for blood sugar regulation. A recent meta-analysis of observational studies has revealed that insulin resistance is a significant risk factor for endometrial cancer.[122] Furthermore, cancer patients with preexisting type 2 diabetes have a worse cancer prognosis than matched patients without diabetes.[123,124] In addition, patients with HER2-positive breast cancer with expression of the IGF-1 receptor are more likely to be resistant to the preoperative chemotherapeutic drugs, trastuzumab and vinorelbine, compared to matched patients without expression of the IGF-1 receptor.[125] These data suggest that insulin resistance may promote a poorer response to cancer treatment or a more aggressive cancer phenotype in patients with preexisting diabetes. The dysregulation of insulin signaling is a major contributor to the increased risk of cancer associated with obesity.

In the obese state, characterized by insulin resistance, tissues are exposed to elevated levels of insulin and insulin signaling. In fed rats, acute elevation of insulin stimulates lipid synthesis and acetylCoA carboxylase activity in liver and adipose tissues.[126] Similarly, insulin also stimulates fatty acid synthesis in human breast cancer cells.[127] In addition, many groups have demonstrated the proliferative effects of elevated insulin. Insulin promotes proliferation in the human breast cancer line MCF-7 by facilitating the transit of cells through G1.[128] More recently, insulin has been shown to induce proliferation in hepatocellular carcinoma cells by upregulating AKR1B10, a tumor marker that plays a critical role in tumor development and progression by promoting lipogenesis.[129] Furthermore, Wang *et al.* recently showed that insulin has mitogenic and antiapoptotic effects on endometrial cancer.[130]

In addition to insulin, insulin-like growth factors, IGF-1 and IGF-2, also play a role in insulin signaling. IGF-1 and IGF-2 are hormones that are primarily produced in the liver

and share sequence homology with insulin.[131] Hyperinsulinemia has been shown to increase production of IGF-1 in the liver.[132] IGF-1 and IGF-2 bind to IGF receptors, which can heterodimerize with insulin receptors. Activation of the receptors results in phosphorylation of IRS proteins, which activates the oncogenic Ras-MAPK and PI3K-Akt pathways.[133,134] The PI3K/Akt signaling pathway is frequently activated in human cancers where it induces cell proliferation.[135] One downstream effector of Akt is mTOR, which promotes protein translation and cancer growth.[136] Furthermore, tumors with constitutive activation of the PI3K pathway are insensitive to dietary restrictions, which can normally delay the incidence and decrease growth of various types of tumors by reducing the levels of circulating insulin and IGF-1, suggesting a link between obesity and cancer.[137] IGF-1 has also been shown to mediate PTEN suppression and enhances cell invasion and proliferation via activation of the PI3K/Akt signaling pathway in pancreatic cancer cells.[138] Thus, the effect of obesity on the elevated levels of IGFs plays a crucial role in determining the proliferative effects of the oncogenic signaling pathways on cancer growth.

The aggressive phenotypes of various types of cancers have been linked to the IGF family. Increased expression of IGF-1, IGF-2, and/ or IGF-1R have been shown in gliobaslatomas, neuroblastomas, meningiomas[139], medulloblastomas[140], breast cancer[141], and prostate cancer[142]. Several groups have documented the role of the IGF family in cancer metastasis as well. Barozzi *et al.*[143] found that the overexpression of IGF-2 was predictive of liver metastasis. Hakam *et al.*[144] also showed an increase in the expression of IGF-1R during progression from colonic adenomas toward primary colorectal adenocarcinomas and metastases. The combined effects of insulin and the insulin-like growth factors on cell proliferation and metastasis may increase the risk for cancer in the hyperinsulinemic state that is associated with obesity. Somewhat controversially, one cross-sectional study did find a negative correlation between IGF-1 levels and both insulin resistance and BMI.[145] These results, however, only consider total IGF-1, not the relative amounts of bound and free IGF-1. Another study[146] found that in obesity total IGF-1 is unchanged compared to normal weight control. However, free IGF-1 is significantly increased and IGF binding proteins reduced. The ratio of free to bound IGF-1 may be an important factor in IGF-1-driven carcinogenesis, and this change may be induced by perturbations of the IGF-1 production and signaling pathway as a result of chronic hyperinsulinemia.

In accordance with the correlative studies, transgenic expression of IGF-1, IGF-2, or IGF-1R in mice drives development of various cancers. The transgenic overexpression of IGF-1 in mice enhances development of breast cancer[147], prostate cancer[148], and skin cancer[147]. The transgenic overexpression of IGF-2 drives development of lung cancer[149] and breast cancer[150]. Overexpression of IGF-1 receptor drives development of salivary and mammary adenocarcinomas[151] and pancreatic cancer[152]. These transgenic overexpression studies suggest that increased signaling through the IGF-1R pathway can drive cancer development, even in the presence of physiological levels of insulin.

The role of the IGF system in driving tumor development and progression in the obese state has also been explored in genetic models of obese mice with liver-specific deletion

of IGF-1. IGF-1 deficiency in the mice abolished the obesity-associated enhancement of subcutaneous tumor growth where tumors in the IGF-1 deficient mice were smaller than tumors in the control mice. Furthermore, IGF-1 deficiency in the liver showed a reduction of liver metastases of a colorectal cancer cell line that was injected into the venous circulation.[172]

Adipokines

In addition to its fat-storing capacity, adipose tissue is the largest endocrine organ, secreting adipokines. Adipokines are adipocytederived hormones that play a role in maintaining energy homeostasis. Leptin, one such adipokine, is a central mediator that regulates appetite and energy homeostasis. By secreting leptin from adipocytes, the change in leptin level communicates body energy status to the brain, which responds by activating the leptin receptor and adjusting food intake.[153] Several groups have shown an overexpression of leptin receptors in various cancers, including cancers of the breast[154], prostate, and colon[155].

Obesity can lead to alterations in leptin regulation. Chronic overexpression of leptin induces leptin resistance, resulting in increased circulating leptin, similar to the increased insulin levels seen in insulin resistance that is associated with increased adiposity.[156,157] The close association between adiposity and leptin levels may suggest a role for this neuroendocrine hormone in the increased incidence of cancer in obesity. Elevated circulating leptin has been shown to increase the risk of prostate[130], breast, colon, thyroid[158], and ovarian[159] cancer.

Elevated leptin in cancer has been suggested to have several protumorigenic effects. Leptin has been shown to have mitogenic action in cancers of the breast[160], colon[161], and endometrium[162] and have mitogenic and anti-apoptotic effects in cancers of the ovarian[159] and prostate[130]. Increases in cell migration have also been shown by elevated circulating leptin in thyroid cancer[158] and endometrial cancer[162].

Several mechanisms have been explored by which leptin contributes to tumor development and progression. Leptin signals through a transmembrane receptor (LRb) that contains intracellular tyrosine residues that become phosphorylated to mediate downstream LRb signaling, which controls STAT3 and ERK activation.[162] STAT3 signaling is required for proper leptin regulation of energy balance.[163] Leptin induces STAT3 phosphorylation in the human breast cancer line, MCF7, and blocking phosphorylation with the specific inhibitor AG490 abolished leptin-induced proliferation.[160] Furthermore, leptin increases HER2 protein levels through a STAT3 mediated upregulation of Hsp90 in breast cancer cells. Inhibition of the STAT3 signaling cascade by AG490 abrogated leptin induced HER2 expression.[164] In gastrointestinal epithelial cell specific knockout of SOCS3, leptin production was enhanced and activated STAT3 signaling to increase development of gastric tumors in mice. Administration of an anti-leptin antibody to the knockout mice reduced hyperplasia of gastric mucosa, the initiation step of gastric tumor.[165] These studies suggest that

enhancement of leptin receptor signaling by STAT3 contributes to tumor development and progression.

These signaling pathways stimulate leptin to have proliferative and mitogenic effects, contributing to the initiation and progression of cancers. Activation of leptin receptors leads to phosphorylation of MAPK and increased proliferation in MCF7 breast cancer cells[166] and in HT29 colon cancer cells[167]. Treatment with leptin and inhibitors of MAPK and PI3K inhibited the proliferative effects on prostate cancer cells[130]. Chronic elevation in leptin also caused ERK1/2[168] activation in human breast cancer cells and ERK1/2 and Akt phosphorylation in human prostate cancer cells[130]. Activation of these pathways induces cell proliferation, which plays a critical role in tumor progression.

Additional *in vivo* studies support the pro-tumorigenic effects of elevated leptin levels. Mammary tumors transplanted into obese leptin receptor deficient (db/db) mice grow to eight times the volume compared to tumors in the wild-type mice, suggesting the role of obesity in increased tumor growth.[169] Surprisingly, tumors transplanted into leptin-deficient (ob/ob) mice showed a reduction of tumor outgrowth compared to wildtype or db/db mice. Residual tumors from ob/ob mice showed reduced tumor initiating activity, suggesting fewer cancer stem cells. In contrast to the obese db/db mice, the obese ob/ob mice were leptin-deficient, suggesting that leptin deficiency is sufficient to suppress obesity induced tumor growth. The reduced outgrowth and tumor burden in leptin-deficient mice indicates that leptin can promote increased tumorigenesis in an obese state.[169]

Although db/db or ob/ob mice have been used to study the role of leptin in obesity-associated cancers, these leptin receptor or leptin deficient mice suffer from defective development of the ductal epithelium, resulting in models unsuitable to address mammary tumorigenesis. Park *et al.* focused on the role of peripheral leptin signaling in breast cancer progression through transgenic overexpression of the leptin receptor in neurons of db/db mice and crossing the brain-specific long form of leptin receptor transgenic mice into the background of the mouse mammary tumor model MMTV-PyMT, thus generating peripheral LEPR-B mutants.[170] The rate of tumor growth in the peripheral LEPR-B mutants was reduced by twofold compared to PyMT mice. Furthermore, the lack of peripheral leptin receptors reduced tumor progression and metastasis through ERK1/ 2 and Jak2/STAT3 mediated pathways. Under obese conditions, tumor cells exhibit high local levels of leptin, leading to an increase in LEPR-B mediated pathways, which increases tumor progression. Globally, the effects of elevated leptin in obesity can drive tumor growth and development.

Adiponectin is another adipokine that is associated with cancer risk. Adiponectin is a key mediator in development and progression of several types of cancers[171] and circulating adiponectin levels are decreased in patients with diabetes and obesity-associated cancers[172].

The two classical adiponectin receptors are seven transmembrane proteins[173] that activate the downstream target AMPK. Expression of the adiponectin receptors, AdipoR1 and AdipoR2, is decreased in obesity, diminishing adiponectin sensitivity.[174]

Epidemiological studies have suggested a link between circulating adiponectin levels and cancer. Adiponectin levels were inversely correlated with the risk of colorectal cancer[175], endometrial cancer[176], esophageal cancer[177], prostate cancer[178], and breast cancer[179].

Several studies have explored the mechanisms by which adiponectin inhibits carcinogenesis. Adiponectin negatively influences growth of most obesity-related cancer types, such as prostate[180] and colon[181] cancers. A study on breast cancer also proved a negative effect of adiponectin on migration[182]. MMTV-PyVT transgenic mice with reduced adiponectin expression developed mammary tumors by downregulating PTEN and upregulating PI3K/Akt signaling.[183] Thus, the proliferative effects of reduced adiponectin may be mediated through the PI3K/Akt signaling cascade. Furthermore, binding of adiponectin to its receptors provokes activation of AMPK, a critical regulator of proliferation in response to energy status.[184] AMPK plays a role in regulation of growth arrest and apoptosis by stimulating p21 and p53[185] and is also an inhibitor of mTOR, thus suppressing cell proliferation[186]. Adiponectin has also been shown to activate PPAR-alpha, thus enhancing fatty acid combustion and energy consumption, leading to a decrease of triacylglycerides in the liver and skeletal muscle, reversing the accumulation of adiposity.[173] Recently, a new mechanism has been shown whereby the balance between ceramide and S1P mediates many of the effects of adiponectin. AdipoR1 and AdipoR2 enhance ceramidase activity.[187] An accumulation of ceramide promotes an array of activities related to metabolic diseases, often in direct opposition to adiponectin.[188] The activity of ceramidase converts ceramide to S1P, a potent inducer of proliferation and inhibitor of apoptosis.[189] Contrary to the proliferative effects of S1P, it has also been shown to activate AMPK.[190] Thus, ceramidase is an essential initiator of adiponectin actions by generating S1P, which activates AMPK. Although S1P has proliferative effects, it is degraded in the liver, the primary target tissue where adiponectin plays a role in insulin sensitization. Many of the effects of adiponectin are mediated by ceramidase activity and the resulting alteration of the ratio of ceramide to S1P plays a role in cell growth.[191]

Although adiponectin levels have been shown to inversely correlate with the risk of several types of cancers, it is noteworthy to suggest that the protective effect of adiponectin may be specific to certain types of cancers and stage of tumor progression. A study comparing rates of tumor growth in the mouse mammary tumor model MMTV-PyMT and adiponectin-null mice showed defects in angiogenesis and reduced rates of tumor growth in adiponectin-null mice in early stages of tumorigenesis.[192] Despite the defects in angiogenesis, tumor growth in the adiponectin knockout mice persisted and developed into late stages of carcinoma, at which point the antiangiogenic stress at early stages led to an adaptive mechanism to bypass the dependence of adiponectindriven angiogenesis. This study suggests a proangiogenic contribution of

adiponectin toward mammary tumor growth *in vivo* in the early stages of tumorigenesis, but not in late stages.[192]

Since adiponectin levels are inversely correlated with obesity[193], studies implicating a protective effect of adiponectin in tumorigenesis and the analysis of the PyMT tumor model by Landskroner-Eiger *et al.* showing a pro-angiogenic role of adiponectin at early stage tumors indicate the complex role of adiponectin in tumorigenesis, and possibly a biphasic effect of adiponectin at early stages.[192]

Overall, the above studies suggest that leptin plays a role in tumor development and progression, whereas adiponectin plays a role in tumor inhibition. In one prostate cancer model, adiponectin reduced cell proliferation and this effect was blocked by treatment with leptin.[194] Thus, leptin and adiponectin have been suggested to have opposing roles in cancer development and progression.

Elevated lipids in cancer

Obesity is primarily characterized by excess fat storage, adipocyte mass, and coordinate increases in certain types of lipids. We will first discuss the evidence for how fat from sources including cancer cell *de novo* lipogenesis, from the breakdown of adipose tissue in cachexia, or from neighboring adipocyte lipid-transfer, can be utilized as oncogenic signaling lipids by the cancer cells and thereby influence cancer pathogenicity. This then sets the stage for potential mechanisms through which lipid stores in obesity may also influence cancer pathogenicity.

One piece of supporting evidence for the utilization of lipids by cancer cells is the upregulation of fatty acid synthase (FASN), an enzyme that makes endogenous fatty acids, which can be modified and packaged into structural lipids required for cell division. Elevated FASN enzyme, mRNA, and enzymatic activity have been seen in human breast cancer cell lines[195], ovarian tumors[196], prostate tumors[197], and cancer precursor lesions in the colon, stomach, esophagus and oral cavity[198]. The increase in FASN seems to be necessary for eliciting the malignant effects, such as proliferation and survival, though this itself is not the cause of malignancy.[14] One study found FASN inhibition as an off-target effect of the weight-loss drug Orlistat. This FASN inhibition induced an antiproliferative effect in prostate cancer cells in culture, which was rescued by addition of palmitate, the product of FASN.[199] Furthermore, when FASN was chemically inhibited in both breast and prostate cancer tumor xenografts, there was a significant antitumor effect.[198] These data together show the importance of FASN in cancer cell growth, survival and proliferation *in vitro* and *in vivo*.

This FASN overexpression in cancer is also mirrored in a variety of tissues in obesity, and one may postulate that the fatty acids formed through FASN in other tissues may also provide fatty acid sources to the cancer.[200] Additionally, in a study examining FASN polymorphisms and the risk of prostate cancer, one of the polymorphisms associated with prostate cancer was also significantly, positively correlated with BMI.[197] Between increases in FASN in obesity and a heightened propensity for an unfavorable FASN

polymorphism, there is also evidence that FASN plays an important role in the way through which obesity may drive some cancers.

The increased activity of FASN in cancer cells is also matched by an increase in lipolytic enzymes, such as monoacylglycerol lipase (MAGL), to promote the mobilization of lipid stores for remodeling of cellular lipids and generation of pro-tumorigenic signaling lipids. The MAGL pathway is upregulated in multiple types of aggressive human cancer cells and high-grade primary tumors[24] and releases FFAs, which in-turn fuel the generation of fatty acid-derived lipid signaling molecules such as lysophosphatidic acid and prostaglandins. Impairments of MAGL-dependent tumor growth are rescued by a high-fat diet *in vivo*, suggesting that exogenous sources of fatty acids can also contribute to cancer malignancy. Thus, elevated levels of fatty acids, derived either from the cancer cell or exogenous fat sources, may promote a more aggressive tumorigenic phenotype.[24]

In subjects, with late-stage, highly malignant cancer these exogenous sources of fats may be derived from the breakdown of fat mass. Cachexia commonly accompanies late-stage cancers and causes subjects to lose both muscle and fat mass through catabolic processes. In cachectic subjects, there is a marked increase in adipose triglyceride lipase (ATGL)[201] an enzyme that breaks triglycerides into diglycerides as well as hormone-sensitive lipase (HSL), an enzyme that breaks diglycerides into free fatty acids[202]. This then leads to increased levels of circulating free fatty acids, which can be repackaged into important oncogenic signaling lipids as well as membrane structural lipids necessary for cell proliferation.[203] Moreover, there is evidence that the lipids released in these processes can be directly utilized by the cancer cells for fuel.[204] While cachexia contrasts obesity in that it is a condition marked by muscle and adipose catabolism, it provides additional evidence that cancer cells can utilize free fatty acids for both fuel and oncogenic signaling lipids. In a state of obesity, however, the free fatty acid substrates for fuel or signaling molecules must be derived from adipocyte stores.

One study did show that cancer cells can access and use lipids from neighboring adipocyte stores *in vitro* by co-culture of ovarian cancer cells and adipocytes. This led to the direct transfer of lipids from the adipocytes to the cancer cells, which induced lipolysis in the adipocytes and β-oxidation in the cancer cells. This indicates that cancer cells can directly use these transferred lipids as an energy source, which, in turn, promotes tumor growth.[205] These data are of particular importance in considering the implications of obesity, mainly excess adipocyte mass, on cancer prevalence and aggressiveness and the synergistic interplay of adipocytes and cancer cells.

In another study using a mouse model, obesity was shown to facilitate tumor growth irrespective of diet, suggesting a direct role of adipose tissue in cancer progression.[206] White adipose tissue-derived mesenchymal stem cells, termed adipose stromal cells (ASC), may represent a cell population linking obesity to the increased incidence of cancer. When transplanted into mice, adipose stromal cells can promote tumor growth by serving as perivascular adipocyte progenitors. ASCs were shown to traffic from endogenous white adipose tissue (WAT) to tumors, where they can be incorporated as

pericytes into blood vessels and differentiate into adipocytes.[206] Intratumoral adipocytes were shown to be associated with an increase in tumor vascularization and an increase in proliferation of adjacent malignant cells.[206] These results suggest that ASCs recruited from adipose tissue have a direct role in inducing tumor development.

Lipid signaling

Another mechanism through which obesity may drive cancer pathogenesis is through converting high-fat diet supplied fatty acids or *de novo* synthesized fatty acids into protumorigenic signaling lipids. Signaling lipids derived from other cell types or from the cancer cell itself can then signal onto the cancer cell through paracrine or autocrine interactions. Studies have shown that aggressive cancer cells upregulate MAGL to generate fatty acids to be incorporated in oncogenic signaling lipids that in-turn drive cancer pathogenicity. However, the function of MAGL can be supplanted also by exogenous fatty acid sources that arise from high-fat diets.[24] The enzymes that synthesize or break down these signaling lipids are also often-times dysregulated in cancer to promote their signaling. There is a widerange of lipid signaling molecules that have the capacity to trigger oncogenic responses, including proliferation, motility, invasiveness, tumor growth, immunological responses, and metastasis. Imbalances in these lipid-signaling pathways can fuel various aspects of cancer.[207]

Lysophosphatidic acid (LPA) is a bioactive phospholipid that stimulates cell proliferation, migration, and survival by acting on G-protein coupled receptors.[26] LPA and LPA receptors are highly expressed in multiple cancer lines including ovarian[208], breast[209], and colon[210]. Interestingly, autotaxin (ATX), the primary enzyme producing LPA, is upregulated in highly aggressive metastatic breast cancer[209], indicating that LPA is a key contributor to the aggressive phenotypes of cancer.

LPA functions by activating G-protein coupled receptors, which in turn can feed into multiple effector systems. LPA activates Gq, which stimulates the effector molecule phospholipase C, thereby generating multiple second messengers leading to activation of protein kinase C[211]. The LPA-dependent activation of PKC mediates the activation of the β-catenin pathway, leading to its cell proliferative effects in colon cancer cells.[210] LPA also activates Gi, leading to inhibition of adenylyl cyclase and therefore inhibition of cAMP accumulation. Gi also stimulates the mitogenic Ras-MAPK cascade and also the PI3K pathway, contributing to cell proliferation and migration.[212–214] LPA has also been shown to mediate cell proliferation, invasion, and migration in human breast cancer through activation of Gi protein, which activates the ERK 1/ERK2 pathway.[215]

Debio-0719, a specific inhibitor of the LPA receptor 1, suppressed development of metastasis from the breast to the liver in the 4T1 breast cancer model.[216] Pharmacological or genetic blockade of MAGL lowers LPA levels indirectly through lowering the levels of fatty acids required for acylation of glycerol-3-phosphate through the *de novo* LPA synthesis pathway, leading to impaired cancer cell migration, invasion, and tumor growth.[24] Furthermore, knockdown of β-catenin by RNAi abolished LPA

induced proliferation in colon cancer cells[210], suggesting a critical role for LPA in the initiation and progression of cancer.

Prostaglandins play a role in regulating the migratory and invasive behavior of cells during development and progression of cancer. Many human cancers exhibit high prostaglandin levels due to upregulation of cyclooxygenase-2 (COX-2) and prostaglandin E2 synthase-1 (PGE_2-1), key enzymes in eicosanoid biosynthesis. Prostaglandins are derived from the 20-carbon chain fatty acid, arachidonic acid. COX-2 is highly expressed in metastatic breast cancer[217] and knocking out COX-2 in mice reduced mammary tumorigenesis and angiogenesis[218]. High COX-2 and PGE2 levels have been implicated in the loss of e-cadherin, and subsequently, cell migration as cells become more migratory during epithelial to mesenchymal transition.[219] The expression of COX2, along with the epidermal growth factor receptor ligand epiregulin and the matrix metalloproteinases 1 and 2, can collectively facilitate mammary tumor metastasis into the lungs by the assembly of new tumor blood vessels and the release of tumor cells into circulation.[25] In mice with orthotopically implanted mammary tumors, pharmacological intervention with antiEGFR antibody, metalloproteinase inhibitor, and a COX2 inhibitor showed reduced rates of primary tumor growth.[25] In addition, overexpression of COX-2 in transgenic mice induced increases in microvessel density and tumor growth, suggesting the role of prostaglandins in the upregulation of angiogenic factors.[220] Furthermore, prostaglandin E2 promotes colon cancer growth through the G-protein coupled receptor, EP2, by signaling the activation of PI3K and Akt, which subsequently inactivates glycogen synthase kinase and activates the β-catenin signaling pathway.[221]

The hydrolytic pathways that release the arachidonic acid from complex phospho- or neutral-lipid stores to generate prostaglandins have also been implicated in cancer progression. Phospholipase A2 (PLA2) is an enzyme that releases fatty acids from phospholipids, generating arachidonic acid and lysophospholipids.[222] Mice deficient for cytosolic phospholipase A2 are protected against the development of lung tumors, suggesting that PLA2 plays a key role in tumorigenesis by altering cytokine production.[223] MAGL blockade also leads to reduced prostaglandins by reducing the arachidonic acid precursor pool required for generating prostaglandins, leading to impaired cancer cell pathogenicity.[24] These mechanisms suggest a profound role for prostaglandins in promoting cancer development and growth.

Sphingolipids play an important role in modulating growth and survival. Sphingosine-1-phosphate (S1P) is a biologically active lipid that plays a role in regulating growth, survival, and migration. S1P is generated by the conversion of ceramide to sphingosine by the enzyme ceramidase, which is subsequently catalyzed by sphingosine kinase-1 (SK-1) to S1P.[224] High expressions of SK-1 and S1P have been implicated in various types of cancers, including ovarian[225], gastric[226], and colon[227] cancers. SK-1 plays a critical role in determining the balance between pro-apoptotic ceramide and pro-survival S1P. Increased SK-1 expression and subsequently S1P levels reduce sensitivity to ceramide-mediated apoptosis and overexpression of pro-survival protein Bcl-2 in human melanoma cells.[228] Overexpression of SK-1 also activates the proliferative and anti-

apoptotic PI3K/Akt pathways.[229] In addition, SK-1 promotes tumor progression in colon cancer by regulation of the focal adhesion kinase pathway, which stimulates cell motility, and thus cell invasion and migration. Accordingly, S1P stimulates migration and invasion in OVCAR3 ovarian cancer cells.[225] Furthermore, S1P lyase, which degrades S1P, has been shown to be downregulated in colon cancer and S1P expression promotes apoptosis.[230] Taken together, the upregulation of SK-1, which generates S1P, stimulates proliferative pathways, contributing to the growth and survival of cancers.

Platelet-activating factor (PAF) is a proinflammatory lipid-signaling molecule that can be generated by the remodeling of phosphatidylcholine, a membrane lipid, to PAF by the action of lysophosphatidylcholine acyltransferase (LPCAT).[231] PAF activity has been implicated in several cancers, including thyroid[232] and breast[233] cancers. PAF promotes proliferation, migration, and angiogenesis in human breast cancer cells[233]. One mechanism for the tumorigenic properties of PAF is through the overexpression of cAMP-response element binding protein (CREB). PAF has been shown to activate CREB, which modulates gene expression in response to cAMP and cell stimulation with growth factors. Addition of PAF to melanoma cells stimulates CRE-dependent transcription and metastasis.[234] Taken together, PAF contributes to the onset and development of tumors through inducing angiogenesis and metastasis.

Phosphatidylinositols can be reversibly phosphorylated at three distinct positions on the inositol headgroup, generating unique phosphoinositides that have diverse roles in signaling.[207] Phosphoinositides signal through cytosolic effector proteins to activate downstream signaling molecules. The plasma membrane localized phosphatidylinositol-4,5-bisphopshate (PtdIns(4,5)P2) serves as the substrate for two phosphoinositide-dependent signaling events. Cleavage of PtdIns(4,5)P2 by phospholipase C generates two second messengers, membrane-bound diacylglycerol (DAG) and the soluble inositol-1,4,5- trisphosphate (IP3).[207] In addition, PtdIns(4,5)P2 can alternatively be converted to phosphatidylinositol-3,4,5-trisphosphate (PtdIns(3,4,5) P3) by phosphoinositide 3-kinase (PI3K).[207] PtdIns(3,4,5)P3 is another second messenger involved in cell growth signaling and elevated levels have been implicated in cancer.[235] PI3K, the enzyme that generates PtdIns(3,4,5)P3, plays a key regulatory function in cell survival, proliferation, migration, and apoptosis.[236] PI3K has been shown to play a mitogenic and anti-apoptotic effect in endometrial cancer.[130] Furthermore, inhibition of the enzyme blocks growth and promotes apoptosis in small-cell lung cancers.[237] Altogether, phosphoinositides have been implicated to play a profound role in the promotion of tumorigenesis.

Conclusions

Several mechanisms have been suggested to explain the association between cancer and obesity, involving elevated lipid levels and lipid signaling, inflammatory responses, insulin resistance, and adipokines. However, it remains unclear how the convergence of these pathways drives obesity-linked cancer. Thus, whether therapeutic interventions can prevent the effect of obesity on cancer is still controversial.

One potential therapeutic intervention for patients with obesity and type 2 diabetes is to take insulin, drugs that increase insulin secretion like sulphonylureas, or insulin-sensitizing drugs, such as metformin or thiazolidinediones (TZDs). Data suggest that patients who take insulin or drugs that increase insulin secretion have a higher risk of cancer than patients taking insulin-sensitizing drugs.[238,239] In addition, patients taking insulin or insulin secreting drugs have a worse cancer outcome than those taking insulin-sensitizing drugs.[240,241] Epidemiological data also show that taking metformin or TZDs may be associated with lower cancer incidence, possibly due to a reduction in circulating insulin levels.[242] Although not all data sets have shown this association, the association between high circulating insulin levels and cancer risk is evident.

Another potential therapeutic implication is through lowering inflammation as a strategy for chemoprevention. Epidemiological data showed that in patients with higher BMI, aspirin is more effective in preventing colorectal cancers[243], possibly by reducing circulating cytokines. Although this effect was not seen at lower doses[243], there seems to be a therapeutic potential in modulating inflammation. Although the effectiveness of therapeutic interventions is controversial, the growing incidence of obesity suggests that lifestyle changes and therapeutics may reduce or prevent adiposity that could additionally reduce the incidence and mortality from cancer.

Figures

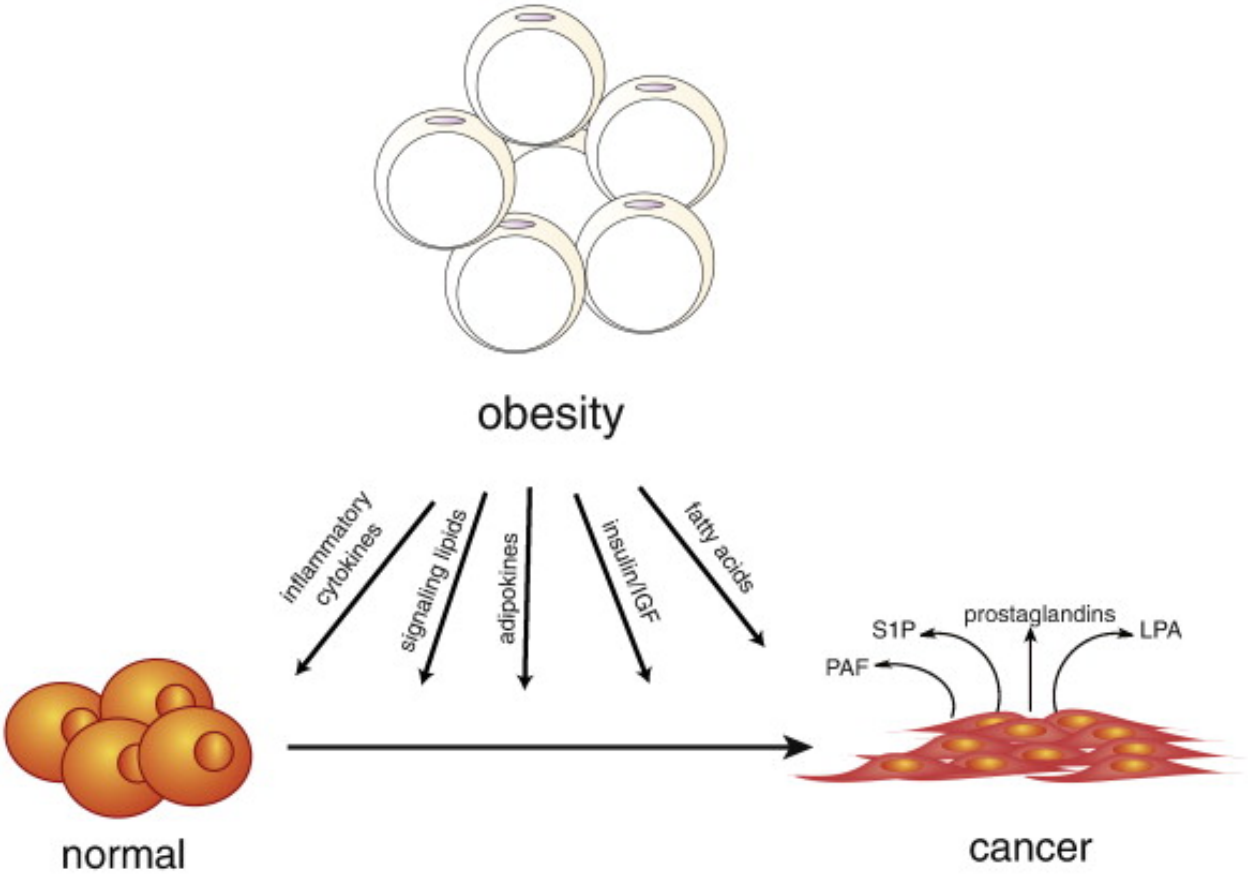

Figure 2-1. Obesity-related mechanisms underlying cancer. Cancer cells have heightened *de novo* lipogenesis through elevated fatty acid synthase (FASN) and both obesity or cancer cell-derived lipolytic enzymes generate free fatty acids to the tumor to provide structural and oncogenic lipid signaling molecules such as platelet activating factor (PAF), sphingosine-1-phosphate (S1P), lysophosphatidic acid (LPA), and prostaglandins. Obesity also causes a low-grade inflammation and the release of inflammatory cytokines. Obesity can also lead to type II diabetes and hyperinsulinemia and insulin signaling which can fuel cancer. Furthermore, obesity leads to dysregulation in adipokines including elevated leptin and reduced adiponectin levels, which can collectively stimulate tumor growth.

CHAPTER THREE: Cancer Cells Incorporate and Remodel Exogenous Palmitate into Structural and Oncogenic Signaling Lipids

Introduction

One metabolic hallmark of cancer cells is heightened *de novo* lipogenesis, which is required for cellular transformation and cancer progression. Fatty acid synthase, the enzyme responsible for *de novo* synthesis of fatty acids, is upregulated across multiple types of human tumors and blocking FASN has been shown to attenuate cell proliferation, tumorigenicity, and cancer malignancy.[14] Early studies, using radioactivity-based methods measuring bulk lipids, have shown that *de novo* synthesis of fatty acids from glucose and other carbon sources account for 93% of the total cellular lipid content in certain cancer types.[244] Cancer cells are thus thought to rely almost solely on *de novo* lipogenesis, rather than exogenous fatty acids for generation of cellular lipids.[6] In addition to lipogenic pathways that subserve cancer proliferation, we have previously shown that aggressive human cancer cells also upregulate lipolytic pathways to mobilize free fatty acids to generate oncogenic signaling lipids that in-turn fuel aggressive features of cancer.[24] We found that the tumorigenic impairments conferred by inactivating a lipolytic enzyme monoacylglycerol lipase (MAGL) in cancer cells, could be rescued by exogenous fatty acids *in situ* or by high-fat diet feeding *in vivo*.[24] These results put forth the possibility that exogenous fatty acids, despite the dominant role of *de novo* fatty acid synthesis, may also play an important role in cancer pathogenesis.

In this study, we investigated whether cancer cells are capable of incorporating exogenous free fatty acids (FFA) and used advanced metabolomic platforms to comprehensively understand how FFAs are remodeled within cancer cells, and whether this exogenous FFA-derived lipid metabolism is altered during cancer progression.

Isotopic fatty acid tracing-based metabolomics reveals that cancer cells incorporate exogenous fatty acids into structural and signaling lipids

To understand how cancer cells incorporate exogenous lipids and whether this lipid metabolism is altered during cancer progression, we treated a panel of aggressive versus non-aggressive human cancer cells from breast, ovarian, prostate, and melanoma cancers *in situ* with nonisotopic or isotopic palmitic acid (C16:0 free fatty acid (C16:0 FFA)), 10 μM in 0.5% fatty-acid free BSA for 4 h). These aggressive human cancer cells (231MFP, SKOV3, PC3, and C8161) have been previously shown to possess heightened motility, invasiveness, and *in vivo* tumor growth rates, compared with their non-aggressive counterparts (MCF7, OVCAR3, LNCaP, and MUM2C) [24,27,245]. We also profiled a human breast cancer progression model consisting of: 1) MCF10A nontransformed mammary epithelial cells; 2) MCF10A cells transformed with the activated HRAS (MCF10A-T1k cells or M2 cells); 3) M2 cells transduced with the constitutively activated transcription factor TAZ S89A (M2T cells) that have been previously shown to induce epithelial-to-mesenchymal transition (EMT), poor breast cancer prognosis, and stem-cell-like features in breast cancer; and 4) M4 (or MCF10A-CA1a) cells that are malignant derivatives of M2 cells through spontaneous malignant evolution *in vivo*. These cells are highly tumorigenic, metastatic, and display increased stem-like features and an upregulation of TAZ.[245] We then extracted the lipidome of these cells and quantitatively measured isotopic incorporation into cellular lipids using a

combination of targeted SRM-based and untargeted discovery-based metabolomic profiling[60,246] to globally track the isotopic incorporation and remodeling of exogenous fatty acids into cancer cells (**Fig. 3-1**). Our SRM methods included ~ 60 representative lipid species that could potentially incorporate isotopic palmitate, including phospholipids, neutral lipids, sphingolipids, and ether lipids. Our untargeted methods collected mass spectrometry data over a large mass range (m/z 50–1200) and subsequent datasets were analyzed by the XCMS Online software[247] to integrate all detectable ions (~5000–10,000 ions), and identify significant alterations in the metabolomes. We combined both targeted and untargeted data to gain a global understanding of exogenous FFAderived lipid metabolism in cancer cells and mapped these data onto metabolic pathway maps.

Our metabolomic profiling of isotopic palmitic acid incorporation revealed that cancer cells robustly incorporate exogenous fatty acids into cancer cells, which are in-turn remodeled into acyl carnitines (AC), phospholipids such as phosphatidyl cholines (PC), lysophosphatidyl cholines (LPC), phosphatidic acids (PA), lysophosphatidic acids (LPA), phosphatidyl ethanolamines (PE), lysophosphatidyl ethanolamines (LPE), phosphatidyl inositols (PI), phosphatidyl glycerols (PG) and phosphatidyl serines (PS), neutral lipids such as triacylglycerols (TAG) and diacylglycerols (DAGs), sphingolipids such as ceramide, sphingomyelin (SM), and ceramide-1-phosphate (C1P), and ether lipids such as alkyl PCs, alkyl PEs, alkyl PIs, alkyl PGs, alkyl PSs, alkyl PIs, platelet activating factor (PAF), and lysoPAF (**Fig. 3-2 A–E**). These incorporated lipids not only include structural lipids (e.g. PC, LPC, SM, PE, LPE, PS, PG, PI, alkyl PCs, alkyl PEs, alkyl PIs, alkyl PGs, alkyl PSs, and alkyl PIs) and lipid stores (e.g. TAGs and DAGs), but also signaling lipids such as LPA, ceramide, DAG, and C1P. Several of these signaling lipids, such as LPA, DAG, and C1P or their associated signaling pathways have been shown to promote cancer pathogenicity.[26,207,248,249] We also find that C16:0 FFA also contributes to the generation of C18:0 FFA (stearic acid) and is incorporated into several C18:0 FFA-containing lipids. As such, with our targeted methods monitoring the m/z 184 phosphocholine ms2 fragment, we acknowledge the possibility that C16:0 PAF (1-O-hexadecyl-2-acetyl-sn-glycero-3-phosphocholine) may be a combination of C16:0 PAF and C18:0 LPC (1-stearoyl-2-hydroxysn-glycero-3-phosphocholine).

Isotopic fatty acids are incorporated into oncogenic signaling lipids in tumors *in vivo*

We also wanted to investigate whether fatty acids can be incorporated *in vivo* into tumor xenografts in mice. Mice bearing M4 tumors were treated with d_4-C16:0 FFA (100 mg/kg oral gavage, 4 h), and isotopic incorporation into tumor lipids was measured by mass spectrometry. Consistent with our *in situ* studies, we found that exogenous d_4-C16:0 FFA was incorporated into certain lipid species including LPC, PAF, and C1P (**Fig. 3-2 F**). Our studies suggest that exogenous fatty acid-derived lipids, which include oncogenic signaling lipids PAF and C1P, are found in tumors or tumor-associated cells *in vivo*.

Fatty acid incorporation into structural and oncogenic signaling lipids are heightened in aggressive cancer cells

We next wanted to understand alterations in lipid metabolism that may underlie cancer progression. We therefore compared isotopic fatty acid incorporation across aggressive versus non-aggressive cancer cells from multiple cancer types, and filtered for isotopic lipid levels that were commonly altered across three out of the five aggressive cancer cells (231MFP, M4, PC3, SKOV3, and C8161) compared to their non-aggressive counterparts (MCF7, MCF10A, LNCaP, OVCAR3, and MUM2C). We intriguingly found a common signature of altered lipid metabolism shared among aggressive cancer cells in which there are lower levels of isotopically labeled ACs, and increased levels of isotopically labeled phospholipids such as PA, PS, PC, and PI, sphingolipids such as ceramide and SM, ether lipids such as alkyl PE and alkyl PC, as well as oncogenic signaling lipids PAF, LPA, and C1P (**Figs. 3-2 A-E, 3-3**). While we believe that these changes are reflective of reduced or heightened fatty acid incorporation into these lipids, we note that in this comparative analysis, we cannot formally distinguish between alterations in synthetic and degradation rates of each lipid. Using the KEGG pathway database[250] as a guide, fatty acid incorporation into cellular lipids was mapped onto a pathway diagram. We find that FFA incorporation and remodeling into phospholipid, sphingolipid, and ether lipids is heightened across aggressive cancer cells indicating that aggressive cancer cells rely more heavily on exogenous FFAs for cancer cell lipids (**Fig. 3-4**).

Taken together, our results reveal that cancer cells incorporate and utilize exogenous fatty acids not only for generation of cellular membranes for cell division, but also for synthesis of signaling lipids, such as C1P, PAF, DAG, and LPA, that have been previously shown to fuel cancer cell pathogenicity.[26,207,248,249] While recent studies have shown that carnitine palmitoyltransferase (CPT)1A or CPT1C activity promotes cell survival, tumor growth, or cellular motility in certain types of cancer cells and that blocking CPT may be a novel cancer therapeutic strategy[250–252], our data would suggest that CPT and fatty acid oxidation pathways are attenuated during cancer progression to shunt fatty acids from betaoxidation pathways (i.e. carnitine palmitoyltransferase (CPT)-mediated AC production) to generate more structural and oncogenic lipids. These results are reinforced by our previous genomic profiling efforts showing that the aggressive cancer cells used in this study possess lower levels of CPT expression compared to their non-aggressive counterparts (**Fig. 3-5**).[27] Nonetheless, blocking CPT may be an attractive therapeutic strategy for combatting less aggressive or low-grade tumors.

Of particular interest are the exogenous fatty acids that are incorporated significantly more into the signaling lipids C1P, PAF, and LPA across several types of aggressive human cancer cells compared with their less aggressive counterparts. C1P is formed by ceramide kinase and has been shown to oppose the apoptotic effects of ceramide and promote cell proliferation and survival through activating intracellular signaling pathways such as MEK, ERK, PI3K/AKT, and JNK, activate in- flammatory responses by activating cytosolic phospholipase A2 for generating pro-inflammatory prostaglandins, and stimulate cell migration through stimulating a yet unknown extracellular Gi-coupled receptor11c. PAF, an inflammatory lipid that acts through PAF receptors and causes

inflammation and platelet aggregation, has also been shown to be produced by melanoma cancer cells and promote invasiveness and metastasis through stimulating cancer cell PAF receptors in an autocrine mechanism.[234,253] LPA is a potent oncogenic signaling lipid that acts through stimulating LPA receptors leading to activation of multiple downstream effector pathways including phospholipase C, PI3K-AKT, RAS-ERK, and RHO and RAC GTPases leading to proliferation, survival, migration, invasion, and increased endothelial permeability11a. Increased incorporation of exogenous fatty acids into C1P, PAF, and LPA in aggressive cancer cells can thus potentially fuel cancer initiation, progression, and metastasis.

Beyond the generation of these oncogenic signaling lipids, we also show that palmitic acid incorporation into complex lipids is globally increased in aggressive cancer cells into glycerophospholipid, sphingolipid, and ether lipid pathways. While there have been many studies into the bioactive roles of glycerophospholipids and sphingolipids11b, the role of ether lipids in cancer remains relatively poorly understood, despite its established correlation with aggressive cancers.[254] It will be of future interest to understand the role of heightened ether lipid synthesis in cancer progression.

Previous studies have indirectly suggested that cancer cells utilize exogenous fatty acids for energy or membrane formation. Nieman *et al.* showed that ovarian cancer cells use lipids derived from neighboring adipocyte stores *in vitro* by co-culture of ovarian cancer cells and adipocytes.[205] Studies have also shown that adipose stromal cells transplanted into mice promote tumor growth by serving as perivascular adipocyte progenitors. Intratumoral adipocytes can also fuel tumor vascularization and cancer cell proliferation.[206]

Conclusions

While we show here that cancer cells take up exogenous free nonesterified palmitic acid, we do not yet understand the mechanism for palmitic acid uptake. Previous studies have shown that breast cancer and sarcoma cells expressing lipoprotein lipase and CD36, involved in lipoprotein-associated triglyceride lipolysis and fatty acid transport, respectively, treated with triglyceride-rich lipoproteins led to accelerated cell proliferation.[255] These authors also found that providing lipoprotein lipase to prostate cancer cells with triglyceride-rich lipoproteins prevented the cytotoxic effects of fatty acid synthesis inhibition. The expression of fatty acid binding proteins that are involved in fatty acid uptake and transport have also been associated with poor survival in triple-negative breast cancers.[256] Intriguingly, Kamphorst *et al.* recently demonstrated that under hypoxic conditions or Ras activation, cells switch from *de novo* lipogenic pathways to scavenging of serum fatty acids esterified to lysophospholipids to fuel membrane production.[257] Interestingly, this study also shows that this phenomenon is also linked to reduced glycolytic flux to acetyl-CoA and an increased flux of glutamine to fatty acid synthesis. While these authors were also unable to ascertain the mechanism of lysophopholipid import, they show yet another mechanism through which cancer cells take up fatty acid sources. It will also be of future interest to determine the interplay

between glycolytic and glutamine metabolism and fatty acid uptake and metabolism during cancer progression.

Our results provide a potential alternate and more direct mechanism linking obesity to increased incidence of cancer deaths by directly taking in exogenous fatty acids into structural and signaling lipids that can drive cancer pathogenicity. This mechanism adds to previous studies linking obesity-induced inflammation, hyperinsulinemia and increased insulin growth factor signaling, and heightened adipokine signaling to cancer cell proliferation and malignancy.[258]

In summary, we have used advanced metabolomic platforms to globally map exogenous fatty acid incorporation and metabolism into cancer cells *in situ* and *in vivo*. We find a commonly dysregulated metabolic signature of lipid metabolism that underlies aggressive human cancer cells where there is an overall increase in exogenous fatty acid incorporation that is redirected from oxidative pathways to the generation of structural and signaling glycerophospholipids, sphingolipids, and ether lipids. Targeting fatty acid uptake into cancer cells, in combination with inhibitors of key nodal lipid metabolism pathways, may provide a potential alternate strategy for treating cancer.

Materials and methods

Cell Culture

C8161, MUM2C, 231MFP, MCF7, SKOV3, OVCAR3, PC3, and LNCaP cells were obtained from Benjamin Cravatt at The Scripps Research Institute or from ATCC. MCF10A, M2, M2T, and M4 cells were obtained from Stefano Piccolo at the University of Padua[245]. Cells were cultured as previously described[24,27,245].

Isotopic Fatty Acid Labeling of Cancer Cells and Mice

Cancer cells were seeded (1.5×10^6 cells) and upon adherence, cells were serum starved and treated with d_0-palmitic acid or (7,7,8,8-d_4)- palmitic acid (10 μM in 0.5% FFA-free BSA) for 4 h. Cells were then washed twice in phosphate-buffered saline (PBS) and harvested by scraping. Cells were collected on ice and centrifuged at 1000 ×g and cell pellets were frozen at −80°C until lipid extraction.

For isotopic fatty acid labeling of mouse tumor xenografts *in vivo*, M4 cancer cells (2×10^6 cells) were subcutaneously injected into the flank of immune-deficient SCID mice and tumors were grown out to 800 mm^3. Mice were treated with vehicle or d_4-palmitic acid (100 mg/kg oral gavage in polyethylene glycol 300 (PEG300)) for 4 h. Mice were then sacrificed and tumors were removed and flash frozen.

Metabolomic Analyses

Cell and tumor lipids were extracted as previously described[24]. Briefly, cells and tumors were extracted in 2:1:1 chloroform:methanol:phosphate-buffered saline with inclusion of internal standards (10 nmoles of dodecylglycerol and 10 nmoles of pentadecanoic acid). The organic layer was collected and the remaining aqueous layer was acidified with 0.1% formic acid and re-extracted in chloroform. Organic layers were combined and dried down under a stream of nitrogen. Dried extracts were resolubilized in 120 μl of chloroform and an aliquot (10 μl) was injected onto an Agilent 6430 triple quadrupole (QQQ)-liquid chromatography-mass spectrometry (LC-MS) instrument.

Targeted mass spectrometry analysis was performed as previously described[259,260]. Briefly, single-reaction monitoring (SRM) programs were derived from non-isotopic standards and databases. SRM programs for isotopic lipids were based on the ms2 fragments and optimized collision energies of non-isotopic standards. Metabolites were quantified by integrating the area under the curve and normalized against internal standards and external standard curves.

Untargeted mass spectrometry analysis was performed by LC-MS in scanning mode collecting mass spectral data from m/z 50 to 1200. Data files were extracted as m/z data files and analyzed by XCMS Online (xcmsserver.nutr.berkeley.edu) to identify isotopic fatty acid incorporation into cellular lipids[24,247]. Structures of metabolites from untargeted analysis were identified based on database searches (METLIN[261]) and

incorporation of d_4-palmitate, as well as co-elution of metabolites with standards within the same class of metabolites.

Lipids were separated by reverse phase chromatography with a Luna C5 column (Phenomenex) starting with 100% 95:5 water:methanol with a gradient to 100% 60:35:5 isopropanol:methanol:water as previously described. Formic acid (0.1%) with 50 mM ammonium formate or ammonium hydroxide (0.1%) was added for positive and negative ionization mode, respectively. Metabolites were quantified by integrating the area under the curve, normalizing to internal standards, and then calculating levels based on external standard curves with representative lipid standards from each lipid species. For those metabolites for which there was a background peak for the isotopic d_4-lipid in the d_0-C16:0 FFA-treated group, we subtracted the average of the background from both d_0- and d_4-C16:0 FFA-treated groups. For all metabolites, the isotopic d_4-lipid peak for the d_0-C16:0 FFA-treated group was less than 20% of the d_4-C16:0 FFA-treated group.

Figures

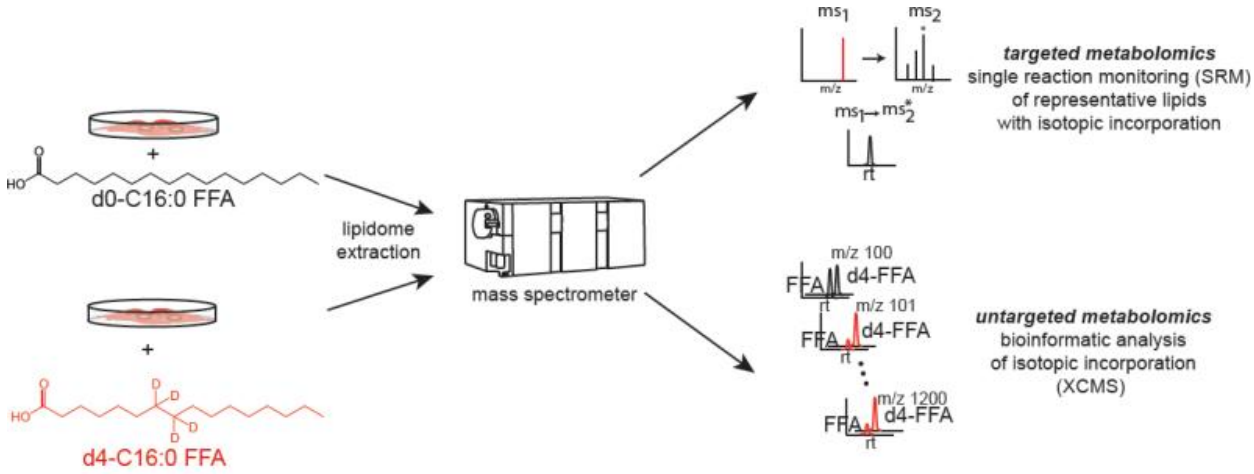

Figure 3-1. Metabolomic mapping of exogenously-derived isotopic FFA metabolism in cancer cells. Cells were treated with either d_0-C16:0 FFA or d_4-C16:0 FFA for 4 h. Lipids were extracted and analyzed by LC-MS using targeted SRM-based approaches and untargeted approaches. The large datasets resulting from untargeted metabolomics were analyzed by XCMS Online to determine masses that were altered between d_0- and d_4-C16:0 FFA to identify isotopic-FFA-incorporated lipids.

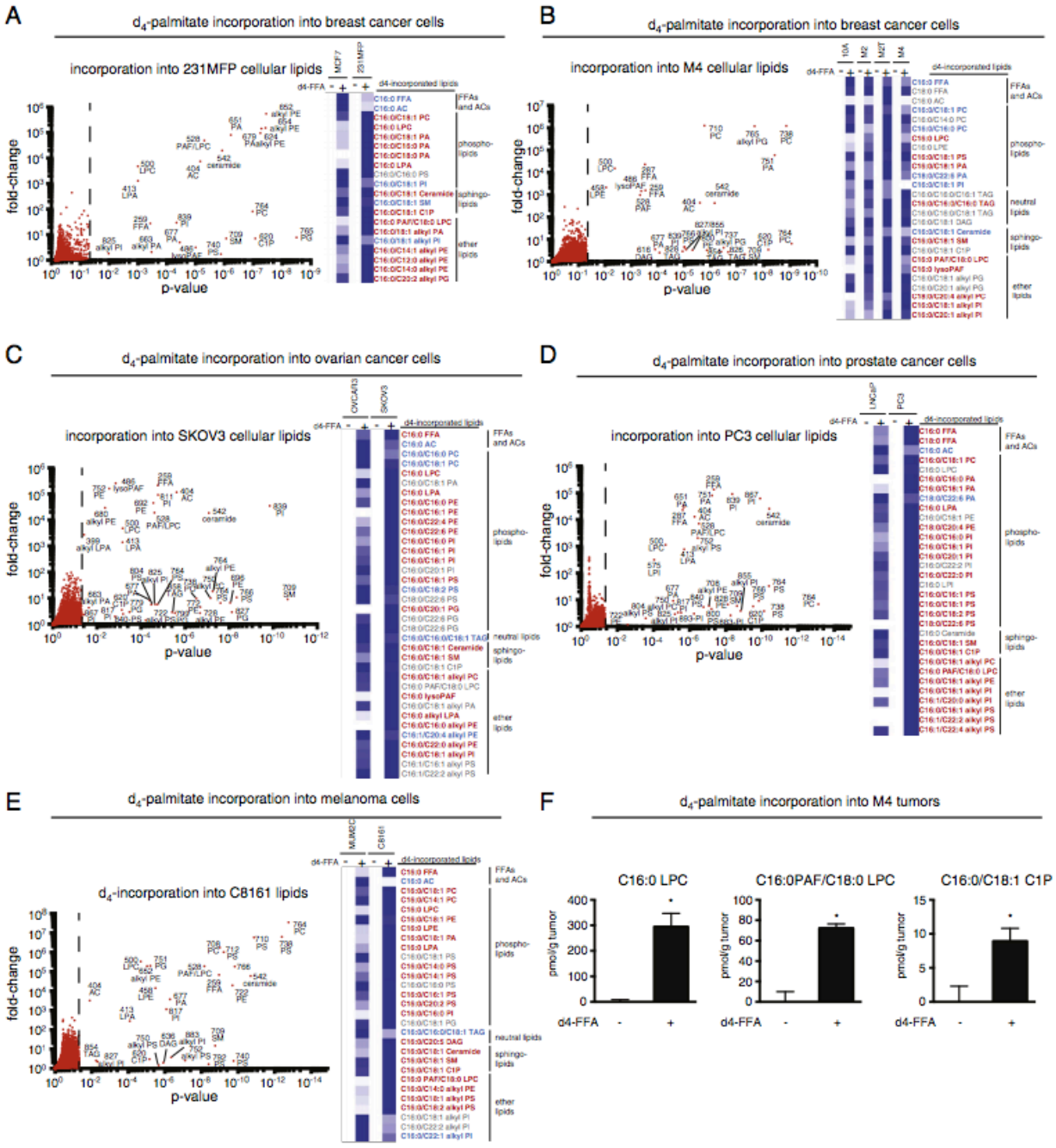

Figure 3-2. Mapping exogenous isotopic FFA-derived lipid metabolism in human cancer cells. (A–E). Shown on the left are all ions detected in 231MFP, M4, SKOV3, PC3, or C8161 aggressive human cancer cells. For the volcano plot, points that are to the left of the dotted line ($P > 0.05$) represent ions that were not statistically altered in levels between d_0-C16:0 FFA versus d_4-C16:0 FFA-labeled cells. All points to the right of the dotted line ($P < 0.05$) represent ions that had significantly higher ion intensity in the d_4-C16:0 FFA labeled group compared to d_0-C16:0 FFA labeled group, i.e. d_4-incorporated lipids. In total, at least ~5000–10,000 ions were detected and analyzed

between targeted and untargeted analysis comparing d_0-C16:0 FFA labeled to d_4-C16:0 FFA labeled M4, 231MFP, C8161, SKOV3, or PC3 cells. The y-axis denotes fold-change between raw integrated values of isotopically-incorporated ions by either targeted or untargeted analysis between d_0 versus d_4-C16:0 FFA-labeled samples. For the ions that exhibited no background peak corresponding to the m/z of the d_4-lipid in the d_0-C16:0 FFA-treated cells, we considered this value to be 1 to obtain a fold-change value compared to the raw integration values of d_4-C16:0 FFA-treated cells. For the ions for which there was a background peak, we obtained a fold-change value by dividing the ion intensity for the d_4-C16:0 FFA compared to d_0-C16:0 FFA groups.

The heat-map on the right shows relative levels of d_4-C16:0 FFA-incorporated lipids in nonaggressive (MCF7, OVCAR3, LNCaP, MUM2C) or non-transformed (MCF10A) cells compared to aggressive (231MFP, M2T, M4, SKOV3, PC3, C8161) or transformed (M2) cells. In the heatmap, relative levels of each d_4-incorporated lipid metabolite are shown (darker blue shading corresponds to higher level of metabolite). The lipid designations next to the heat map are color-coded red for significantly higher, blue for significantly lower, and gray for unchanged d_4-metabolites in aggressive cancer cells (231MFP, M4, SKOV3, PC3, and C8161) compared to non-aggressive (MCF7, MCF10A, OVCAR3, LNCaP, and MUM2C, respectively) cells (*$p < 0.05$).

(F) Shown are lipids species that exhibited significant d_4-C16:0 FFA incorporation *in vivo* in mice bearing a tumor xenograft from M4 cells. Mice were subcutaneously injected with 2 × 106 M4 cells and tumors were grown out to ~800–1000 mm^3 . Mice were treated with vehicle (polyethylene glycol 300 (PEG300)) or d_4-C16:0 FFA (100 mg/kg in PEG) by oral gavage (4 h). Tumors were harvested and lipids were extracted and analyzed by SRM-based metabolomics. For A–F, those metabolites where there was a background peak for the d_4-lipid m/z in the d_0-C16:0 FFA-treated cells, the average of the background ion intensity was subtracted from both d_0 and d_4-C16:0 FFA-treated groups. For all lipid shown here, any background peak for a d_4-lipid detected in d_0-C16:0 FFA-treated cells was assumed to either be a co-eluting isobaric metabolite or natural isotopic abundance of the lipid. We have only presented here the d_4-incorporated lipids that showed >5-fold significantly ($p < 0.05$) higher ion intensity in the d_4-C16:0 FFA-treated group compared to the d_0-C16:0 FFA-treated group. All data from A–E is shown in Supplemental Table 1 and certain lipids are quantified in Fig. 3. Data in **(A–E)** are average values of n = 4–6 biological replicates. Data in F are mean ± standard error of n = 4–6 biological replicates. Significance in F is represented as *$p < 0.05$ in d_4-C16:0 FFA-treated mice compared with vehicle treatment.

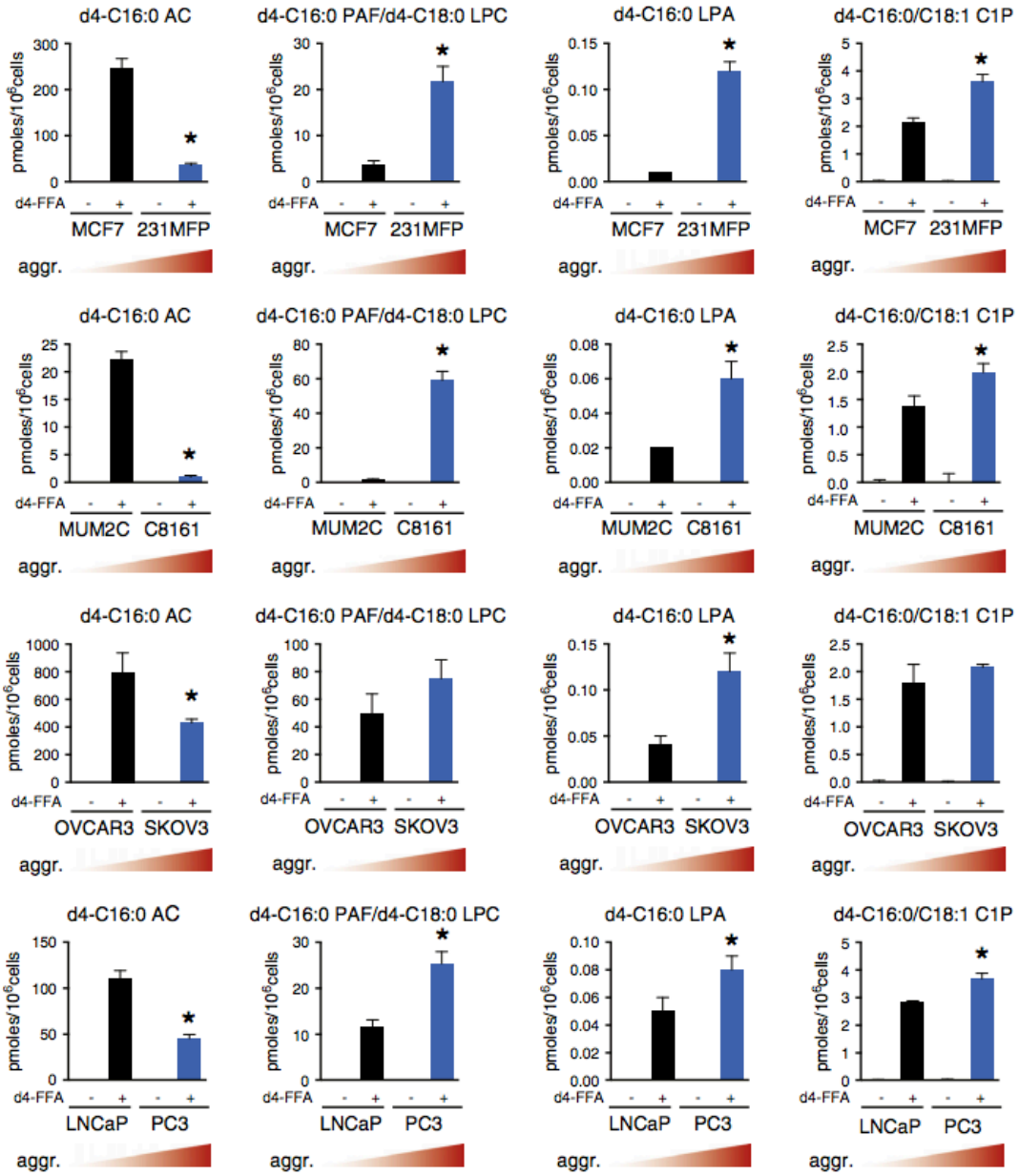

Figure 3-3. Aggressive cancer cells increase incorporation of fatty acids into oncogenic signaling lipids and reduce incorporation into oxidative pathways. Representative lipids with significant fatty acid incorporation from Fig. 3-2 are quantitated and shown as bar graphs. In comparing d_4-C16:0 FFA incorporation into aggressive (C8161, PC3, SKOV3, and 231MFP cells) compared with non-aggressive cancer cells (MUM2C, LNCaP, OVCAR3, and MCF7 cells), we find that there is reduced incorporation into C16:0 AC and increased incorporation into phospholipids, sphingolipids, and ether lipids, including the signaling lipids C1P, PAF/LPC, and LPA. Data are average values of n = 4–6 biological replicates and are presented as mean ± standard error. Significance is represented as *$p < 0.05$ comparing aggressive versus non-aggressive d_4-FFA groups.

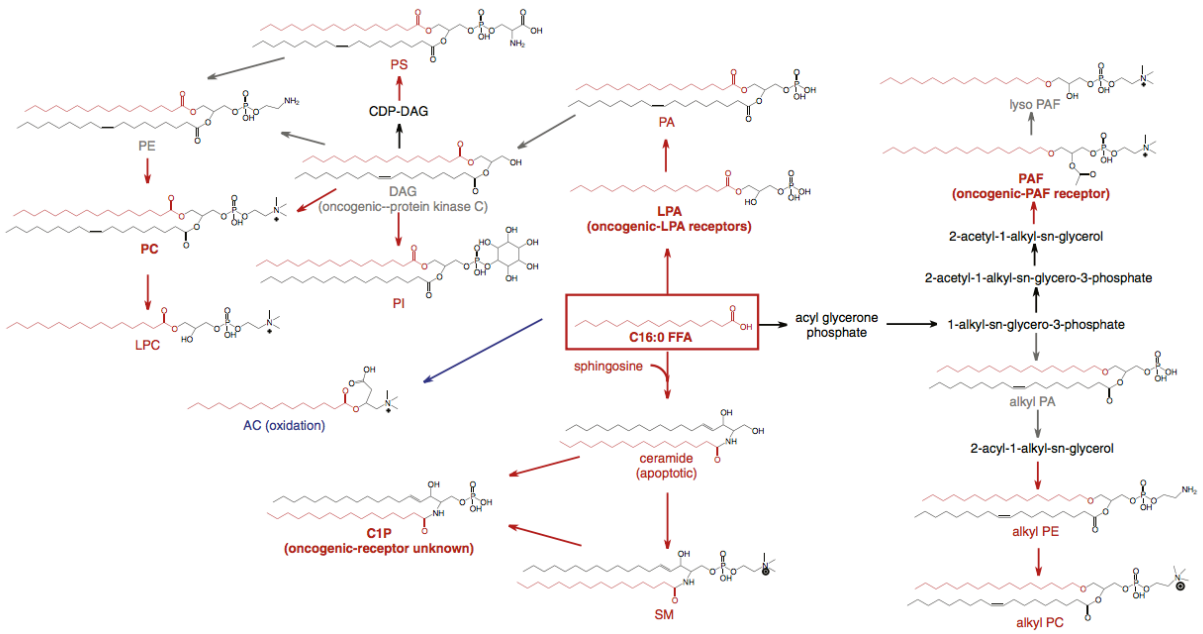

Figure 3-4. Map of lipid metabolism in aggressive cancer cells. The data gathered from isotopic tracing of d_4-C16:0 FFA labeled cancer cells was compiled into a metabolic pathway map using the KEGG pathway database as a guide. d_4-C16:0 FFA incorporation into the lipid structures is noted in red. The color of arrows and metabolites notes increased (in red), decreased (in blue), or unchanged (in gray) levels of d_4-lipid in three out of five comparisons of aggressive (231MFP, M4, SKOV3, PC3, and C8161) versus non-aggressive (MCF7, MCF10A, OVCAR3, LNCaP, and MUM2C, respectively) cancer cells. Metabolites and arrows in black were not detected in either targeted or untargeted analysis. LPA, C1P, DAG, and PAF are oncogenic signaling lipids that act through LPA receptors, unknown receptor, protein kinase C, and PAF receptors, respectively.

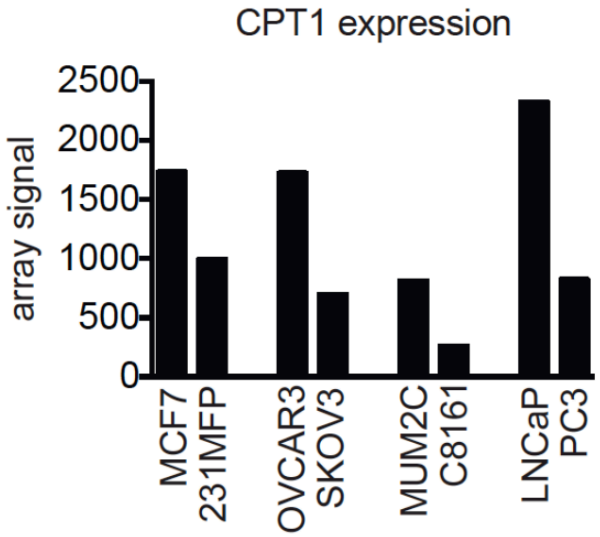

Figure 3-5. CPT1 expression is downregulated in aggressive human cancer cells compared to non-aggressive cancers of the same tissue. This figure shows the relative signals of carnitine palmitoyltransferase 1 (CPT1) expression in pairs of aggressive and non-aggressive cancer cells within the same tissue type. MCF7 and 231MFP are breast cancer. OVCAR3 and SKOV3 are ovarian. MUM2C and C8161 are melanoma. LNCaP and PC3 are prostate. These data are derived from a microarray transcriptomic experiment from Nomura *et al*. 2011.[27]

CHAPTER FOUR: Coupling Chemoproteomics and Metabolomics to Identify Novel Drivers of Triple Negative Breast Cancer

Introduction

Alterations in cancer cell metabolism are now considered one of the hallmarks of cancer, however, most of the research surrounding cancer cell metabolism has focused on a relatively narrow window of cellular metabolism. While we know cellular metabolism extends far beyond these well-studied networks, studying the alterations of these pathways in cancer has proven difficult. Moreover, to understand the importance of different alterations requires an agnostic approach to identify these dysregulations. Innovative mass spectrometry-based proteomic and metabolomic approaches, especially when coupled together, have helped to address this technological roadblock in the cancer metabolism field.

Classic shotgun proteomics is a powerful mass spectrometry-tool researchers have used for a long time to identify differences in protein expression across many proteins in a discovery-based manner. This approach, however, is limiting in that a) it only can detect the most abundant proteins in the proteome and b) it only informs about the expression of the proteins, which doesn't necessarily correlate to their activity due to post-translational modifications or allosteric regulation. Therefore, the development of activity-based protein profiling (ABPP), a mass spectrometry-based proteomics platform discussed above, (**Fig. 4-1 A**) has arisen.[60] Activity-based probes have been developed to study the activities of many classes of enzymes. These probes are designed to have a reactive group which has cross-reactivity with all or most members of the enzyme family, a linker region, and a moiety for detection either through the use of a fluorophore for in-gel fluorescence readout, or an enrichment handle such as biotin, for enrichment, identification and quantification by mass spec. One such probe, which bears a fluorophosphonate reactive group (**Fig. 4-1 B**), has reactivity with the serine hydrolase enzyme superfamily. The serine hydrolase superfamily is one of the largest metabolic enzyme classes in the human genome with a broad range of functions including lipases, proteases, and hydrolases, many of which have already been shown to be important in cancer[262], therefore by using this probe we can directly and quantitatively assess the activity of many metabolic enzymes. Using this approach we can directly compare the relative activities of enzymes between different cell types, treatment groups, disease states, etc. even for fully uncharacterized enzymes. After identification of dysregulated enzymes, we can perform follow-up studies with classic biochemistry and molecular and cellular biology as well as mass spectrometry-based metabolomics, to fully understand the role and importance of the enzyme(s) of interest.

Identification of sialic acid acetylesterase as a metabolic enzyme driving triple negative breast cancer malignant phenotypes

To identify metabolic enzymes that may be driving cellular transformation and malignant features of breast cancer, we performed activity-based protein profiling across a breast cancer progression model. This breast cancer progression model consisted of: 1) MCF10A non-transformed mammary epithelial cells; 2) MCF10A cells transformed with the activated HRAS (MCF10A-T1k cells or M2 cells); 3) M2 cells transduced with the constitutively activated transcription factor TAZ S89A (M2T cells) that have been

previously shown to induce epithelial-to-mesenchymal transition (EMT), poor breast cancer prognosis, and stem-cell-like features in breast cancer; and 4) M4 (or MCF10A-CA1a) cells that are malignant derivatives of M2 cells through spontaneous malignant evolution *in vivo*. These cells are highly tumorigenic, metastatic, and display increased stem-like features and an upregulation of TAZ.[245]

For this study we first performed shotgun proteomics to see differences in protein expression in the most abundant proteins in these cell lines (**Fig. 4-1 C**). Additionally, we performed ABPP of this breast cancer progression model using the serine hydrolase activity-based fluorophosphonate biotin probe and identified many metabolic enzymes with increased activity in some or all of the aggressive lines as compared to the non-transformed MCF10A line (**Fig. 4-1 D)**. The enzymes identified through shotgun proteomics include enzymes involved in glycolysis, *de novo* lipogenesis, and glycogen metabolism (**Fig. 4-1 C bar graphs**). Enzymes found to have increased activity across the four aggressive cell lines through ABPP included fatty acid synthase (FASN), dipeptidyl peptidase 9 (DPP9), acylpeptide hydrolase, prolyl endopeptidase, platelet activating factor acetylhydrolase 1B2 and 1B3 (PAFAH1B2 and PAFAH1B3) and sialic acid acetylesterase (SIAE) (**Fig. 4-1 D bar graphs**). Many of these pathways have previously been shown to be altered in cancer cell transformation or malignancy corroborating our findings of their importance.[56]

To determine the individual roles and significance of these enzymes, we used RNA interference to knock each gene down in MII TAZ S89A cells and performed phenotypic cell based assays for proliferation, serum-free survival, and transwell migration (**Fig. 4-2 A-D**). From this screen we found that sialic acid acetylesterase (SIAE) conferred the largest migratory defect, indicating that perhaps this enzyme plays a role specifically in processes that support metastases.[56] Finding a target that seemed to have somewhat specific regulation over migratory capacity was of interest to us as most deaths from breast cancer are due to the metastatic spread of the disease rather than the primary tumor. Furthermore, the most lethal subtype of breast cancer is triple negative breast cancer (TNBC), breast cancer that lacks three cell surface receptors which are common targets for therapeutics, so we wondered if SIAE might be a TNBC and migration specific target.

In comparing a panel of three triple negative breast cancer cell lines (231MFP, HCC38, and MDA-MB-468) to three receptor positive breast cancer cell lines (MCF7, MDA-MB-361, and T47D), we found that there was significantly higher SIAE mRNA expression in the TNBC cells (**Fig. 4-3 A**). We also looked at the correlation between SIAE expression and recurrence free survival using the cancer genome database and found that among breast cancers negative for two of the three receptors (estrogen receptor and progesterone receptor) high SIAE expression was correlated with significantly worse recurrence-free survival (**Fig. 4-3 B**). Together all of these data show that high SIAE expression and activity correlate with malignant phenotypes and worse prognosis suggesting that it might be a viable therapeutic target especially for metastatic triple negative breast cancers which currently lack any targeted therapies.

Determining the cellular and metabolic consequences of altered SIAE activity

After determining increased SIAE expression in TNBC cells compared to non-TNBC cells, we decided to further explore the role of this enzyme in a TNBC cell line. Using the 231MFP cell line, a line derived from a breast cancer patient adenocarcinoma MDA-MB-231 that has been *in* vivo passaged in mice to derive a malignant and more aggressive variant[63], we knocked down SIAE expression with two independent oligonucleotide shRNAs (**Fig. 4-4 A**). We then confirmed the phenotypic alterations we saw with the MII TAZ S89A siSIAE – reduced serum-free survival (**Fig. 4-4 B**), reduced migration (**Fig. 4-4 C**), as well as reduced *in vivo* tumor growth in a xenograft study in which either shControl or shSIAE cells were implanted into the flank of immune-deficient mice and tumor growth was monitored (**Fig. 4-4 D**). These cell-based assays solidified a role for SIAE in triple negative breast cancer cell survival, growth, and migration. However, the way through which this enzyme was conferring these pathogenic features remained elusive.

Sialic acid acetylesterase (SIAE) is a secreted enzyme annotated as the only enzyme responsible for removing an O-linked acetyl group from the 9 position on sialic acid. Sialic acids are a family of about 50 monosaccharides with a nine-carbon backbone. They are primarily synthesized *de novo* through the hexosamine biosynthetic pathway and are incorporated at the terminal position of glycan chains on membrane proteins or lipids (**Fig. 4-5 A**). Once conjugated to proteins, different secreted enzymes can transfer or remove a variety of moieties onto or off of this sialic acid backbone.[263,264]

These sialic acid residues are commonly involved in interaction between different cells or between a cell and the extracellular matrix (ECM) through specific receptor-ligand pairs. Therefore, it tracks that by changing the cell surface sialic acid landscape cancer cells with heightened SIAE activity would potentially be more able to break free from the ECM and help in seeding metastases. Additionally these interactions could be between different cell types, for example, immune cells, and could initiate cell-signaling cascades either in the cancer cell or the other type and could aid in the cell evading the immune system, which also supports metastases.[264]

Sialic acids from the cell surface can be recycled back into the cell for conjugation onto different proteins or lipids in response to signals or if the protein onto which it is added is degraded. Sialic acid removal is performed by sialidase enzymes, which, in mammalian systems, only recognize the parent molecule, sialic acid, not any of the derivatives.[265] Therefore, all modifications on sialic acid must be removed before it can reenter the cycle. Increased SIAE activity would therefore promote this recycling pathway through heightened removal of the 9-O-acetyl moiety and, in doing so, potentially shift the cell's balance of sialylated proteins. Conversely, knocking down SIAE in cell culture, would reduce the flux through this recycling pathway and could cause an accumulation of 9-O-acetylsialylated proteins on the cell surface. While the specific role for 9-O-acetylsialylated proteins or lipids has not been uncovered, general hypersialylation of cancer cells is a well-established feature that confers or is involved in malignancy.[264] Furthermore, it has been shown that a global reduction of cell surface sialylation

through knockdown of the enzyme that activates it for conjugation to glycans, leads to cell survival defects as well as tumor growth defects *in vivo*.[266]

Using mass spectrometry based targeted metabolomics to profile the polar metabolites in the shControl compared to shSIAE cells, we saw a reduction in many of the hexosamine pathway intermediates including uridine diphosphate N-acetylglucosamine (UDP-GlcNAc), N-acetyl-D-mannosamine-6-phosphate (ManNAc-6-P), sialic acid itself, and its downstream metabolite CMP-sialic acid (**Fig. 4-5 A, B**). This could indicate that by interrupting the recycling pathway of sialic acid from the cell surface, the cell is forced to deplete those stores to make other sialylated proteins, and then also depletes upstream metabolites to continue compensating for this lack of recycled sialic acid. While we believe that the direct effect of SIAE knockdown reducing the cancer cell pathogenicity to be through alterations in cell surface sialylation and those interactions, we wondered if we could rescue our migratory defect by replenishing intracellular hexosamine pathway intermediates.

Adapted from a method published by Laughlin and Bertozzi[267], we treated cells with tetra-acetyled D-mannosamine (Ac_4-ManNAc). This derivative of N-acetylmannosamine (ManNAc) is more membrane permeable than the metabolite lacking the acetyl groups so it is readily taken up by the cell. Within the cell, nonspecific esterases hydrolyze the acetyl groups, freeing ManNAc to be utilized normally in the hexosamine biosynthetic pathway (**Fig. 4-6 A**). We treated our shControl and our shSIAE cells with either this ManNAc or vehicle control, and saw that there was an almost complete rescue of the migratory defect conferred by knockdown of shSIAE (**Fig. 4-6 B**). This suggests that one of two things might be happening. The first being that by knocking down SIAE we block the recycling of sialic acid and accumulate 9-O-acetylsialylated proteins on the cell surface, and restoring the intracellular sialic acid levels allows for the cell to modify proteins and lipids with other sialic acid derivatives to return the sialyl-landscape to the preferred relative levels. An alternative explanation may be that by depleting hexosamine pathway intermediates the cell increases flux through that pathway shunting glucose away from other life-sustaining pathways. The former of these options could be uncovered though isolation of glycan chains from the cell surface and identification and quantification by mass spectrometry, while the latter could be further explored through isotopic tracing analyses using C^{13}-glucose to determine its fate and the rate through which it fluxes through different pathways.

Conclusions

While we see the importance of SIAE and 9-O-acetylated sialic acids and have gained some insight on how these may function to confer advantages to cancer cells, we are still interested in learning the identity of the sialylated proteins as well as any receptors on other cells or the ECM that they might interact with, or any intracellular signaling programs they might be involved in. Studying 9-O-acetylsialic acids and the proteins they are on has proven challenging due to the lability of the 9-O-acetyl group. Recently, one group has developed a chemical biology approach to address this obstacle. They report that by changing the oxygen atom to a nitrogen atom, biologically stable 9-N-

acetylated sialic acids can be formed.[268] We are hopeful that chemical biology advances like this will enable further comprehension of the role of these biologically important glycan sugars as this area of metabolism seems to be a relatively unstudied one with some great potential for future cancer therapeutic developments.

Materials and Methods

Materials

Ac_4-ManNAc (2-Acetamido-1,3,4,6-tetra-O-acetyl-2-deoxy-b-D-mannopyranose) was purchased through Carbosynth Limited.

Cell Culture

HCC38, MD-MB-468, MCF7, T47D, MDA-MB-361, and 231MFP Benjamin Cravatt at The Scripps Research Institute or from ATCC. MCF10A, M2, M2T, and M4 cells were obtained from Stefano Piccolo at the University of Padua. Cells were cultured as previously described[24,27,245].

Shotgun Proteomics

Pellets were precipitated in 20% trichloroacetic acid at −80°C overnight and centrifuged at 10,000 × g at 4°C for 10 min to pellet protein. Pelleted proteins were washed three times with 8 M urea in PBS. After solubilization, 30 µl of 0.2% ProteaseMAX Surfactant (Promega) was added and the resulting mixture was vortexed followed by the addition of 40 µl of 100 mM ammonium bicarbonate and 10 mM tris(2-carboxyethyl)phosphine (TCEP). After 30 min, 12.5 mM iodoacetamide was added and allowed to react for 30 min in the dark before adding 120 µl of PBS and 1.2 µl of 1% ProteaseMAX Surfactant. The protein solution was vortexed, and 0.5 µg/µl sequencing-grade trypsin (Promega) was added and allowed to react overnight at 37°C. The peptide solution was then centrifuged at 10,000 × g before the supernatant was subsequently analyzed by LC-MS/MS.

Activity-Based Protein Profiling

ABPP-MudPIT analysis was performed as previously described[24]. Briefly, 1mg of protein was labeled with 5µM fluorophosphonate-biotin (FP-biotin) probe in PBS for 1 h at room temperature. Then solubilized in 1% Triton X-100 for 1 h, denatured, and labeled enzymes were enriched using avidin beads. They were then reduced, alkylated, and trypsinized. The tryptic peptides were analyzed on a Thermo LTQ-XL MS/MS.

RNA Interference of Enzymes

For siRNA knockdown, cells were treated with ON-TARGETplus SMARTpool siRNA (Dharmacon) using the manufacturer's protocol. 200,000 cells were treated with 50 nM siRNA using DharmaFECT 1 Transfection Reagent. All assays were performed after 48 h of treatment and knockdown was confirmed by qPCR.

Cell Survival

Cells were trypsinized, centrifuged, and then resuspended in serum-free L15 medium. Cells were counted and 40,000 cells were seeded in 200 μL serum-free medium in a 96-well plate. Cells were allowed to adhere overnight at which point cells were stained with Hoechst and a time-0 measurement was taken to confirm even seeding between lines. After 48 h cells were stained with Hoechst and measured. Data shown are the fluorescent readings with background subtracted, normalized first to their own day 0 average and then to the average of control at 48 h.

Cell Migration

Cells were serum starved for 2 hours before being trypsinized, centrifuged, and then resuspended in serum-free L15 medium. Transwell membranes were coated in collagen V for 1 h prior to cells being added. To each well 700 μL of serum-free L15 medium was added and the transwell membrane was placed inside. Cells were counted and 50,000 cells in 200 μL were added on top of each transwell membrane. Cells were allowed to migrate for 6 h at which point those on the bottom of the membrane were fixed and stained. Triplicate images of each well were taken, counted and averaged to give the number of migrated cells/well.

ManNAc Treatment and Migration

Cells were pretreated for 18 h with 10 μM Ac_4-ManNAc dissolved in water or water-vehicle control. During the final 2 hours of this pretreatment, cells were serum starved. They were then trypsinized, centrifuged and resuspended in serum-free L15 medium. Migration procedure was the same as described above, except that Ac_4-ManNAc was added to the wells for a final concentration of 10μM and a total treatment time of 24 h.

SIAE Knockdown

Targets were knocked down stably with shRNA as previously described[28,269]. shControl (targeting GFP) or shSIAE constructs (Sigma) were transfected into HEK293T (ATCC) cells alongside lentiviral vectors using lipofectamine 2000 (Thermo Fisher Scientific). Lentivirus was collected from filtered cultured medium 48 h post-transfection and used to infect the target cancer cell line with Polybrene (0.01 mg/mL). Target cells were selected over 3 days with 1 mg/mL puromycin. The short hairpin sequences for the generation of SIAE knockdown lines were
shSIAE−1:
CCGGGCTTTGCTTCATACATCAATACTCGAGTATTGATGTATGAAGCAAAGCTTTTTG
shSIAE−2:
CCGGCATCGAAGACTGGCGTGAAACCTCGAGGTTTCACGCCAGTCTTCGATGTTTTTG

control shRNA against GFP: GCAAGCTGACCCTGAAGTTCAT. Knockdown was confirmed by qPCR.

qPCR

qPCR was performed using the manufacturer's protocol for Fisher Maxima SYBR Green. Primer sequences are as follows:
SIAE forward: AGGACCTTGTTGCGGTTGAC
SIAE reverse: GATCAGCCCGATGGGATACTG
Cyclophilin forward: CCCACCGTGTTCTTCGACATT
Cyclophilin reverse: GGACCCGTATGCTTTAGGATGA

Tumor Xenograft Studies

Tumor xenografts of 231MFP human derived breast cancer cells were established by transplantation ectopically into the flank of C.B17 severe combined immunodeficiency (SCID) mice (Taconic Farms) as previously described[24]. Briefly, cells were washed with PBS, trypsinized, and harvested in complete L15 medium. Once harvested, cells were wasted twice with serum-free L15 medium, resuspended at a concentration of 2.0×10^4 cells/μL, and 100μL were injected. Tumors were measured with calipers every 2 days. Animal experiments were conducted in accordance with the guidelines of the Institutional Animal Care and Use Committees of the University of California, Berkeley.

Polar Metabolomic Profiling of Cancer Cells

Metabolomic studies and analyses were performed as previously described. In brief, 2 million cells were plated overnight, serum starved for 2 hours prior to harvesting, at which time cells were washed twice with PBS, scraped, and flash frozen. Frozen cell pellets were extracted using 180μL of 40:40:20 acetonitrile:methanol:water with inclusion of 1 nmole d_3N^{15} - serine as an internal standard. The samples were then vortexed and bath sonicated to lyse the cells, and then centrifuged to isolate the polar metabolite fraction (supernatant). A 20 μL aliquot was injected and analyzed by single-reaction monitoring (SRM)-based LC-MS/MS. Relative levels of each metabolite were determined by integrating the area under the curve, normalizing to internal standard values, and then normalizing again to average values from the control.

Figures

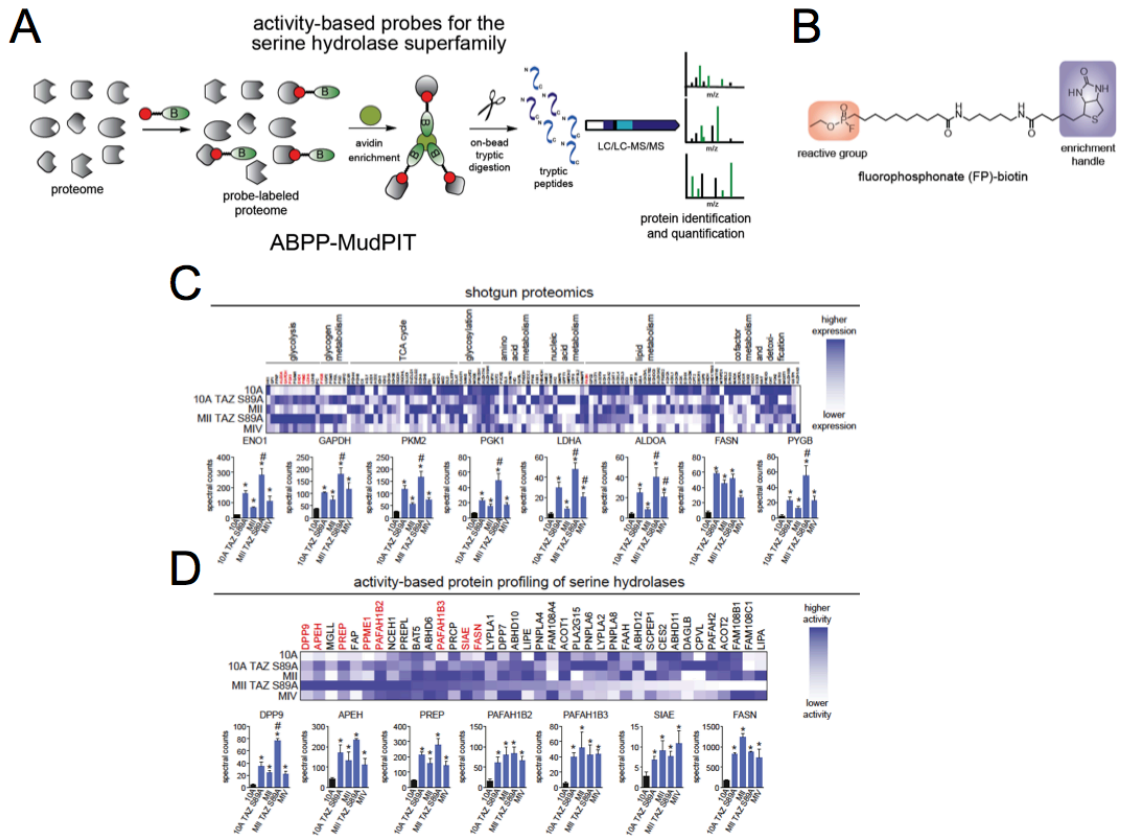

Figure 4-1. Activity-based protein profiling of breast cancer cells. (a) schematic of activity-based protein profiling (ABPP) for quantitative activity-based proteomics. **(b)** Structure of an activity-based probe for the serine hydrolase enzyme superfamily. This possesses a fluorophosphonate reactive group for covalent binding in the active site of the enzyme, a linker region, and an enrichment handle (biotin) for use in mass spectrometry based quantitative activity-based protein profiling. **(c)** Shotgun proteomic profiling of metabolic enzyme expression in the breast cancer progression model by MudPIT. Heatmap shows relative protein expression of each protein, normalized to highest expression of each protein across the five cell lines. Dark blue corresponds to high expression, and white or light blue corresponds to lower expression. Bar graphs show the metabolic enzymes that were significantly upregulated across 10A TAZ S89A, MII, MII TAZ S89A, and MIV cells. **(d)** ABPP of serine hydrolase activities in the breast cancer progression model by MudPIT. Heat map shows relative protein activity of each protein, normalized to the highest expression of each protein across the 5 cell lines. Dark blue corresponds to high expression and white or light blue corresponds to lower expression. Bar graphs show the serine hydrolase activities that were significantly upregulated across 10A TAZ S89A, MII, MII TAZ S89A, and MIV cells. Data in bar graphs are presented as mean ± sem; n = 4-6/group. Significance is presented as *p < 0.05 compared to MCF10A controls, #p < 0.05 compared to MII cells.[56] Adapted from Mulvihill *et al.* Chem. Biol. 2014.

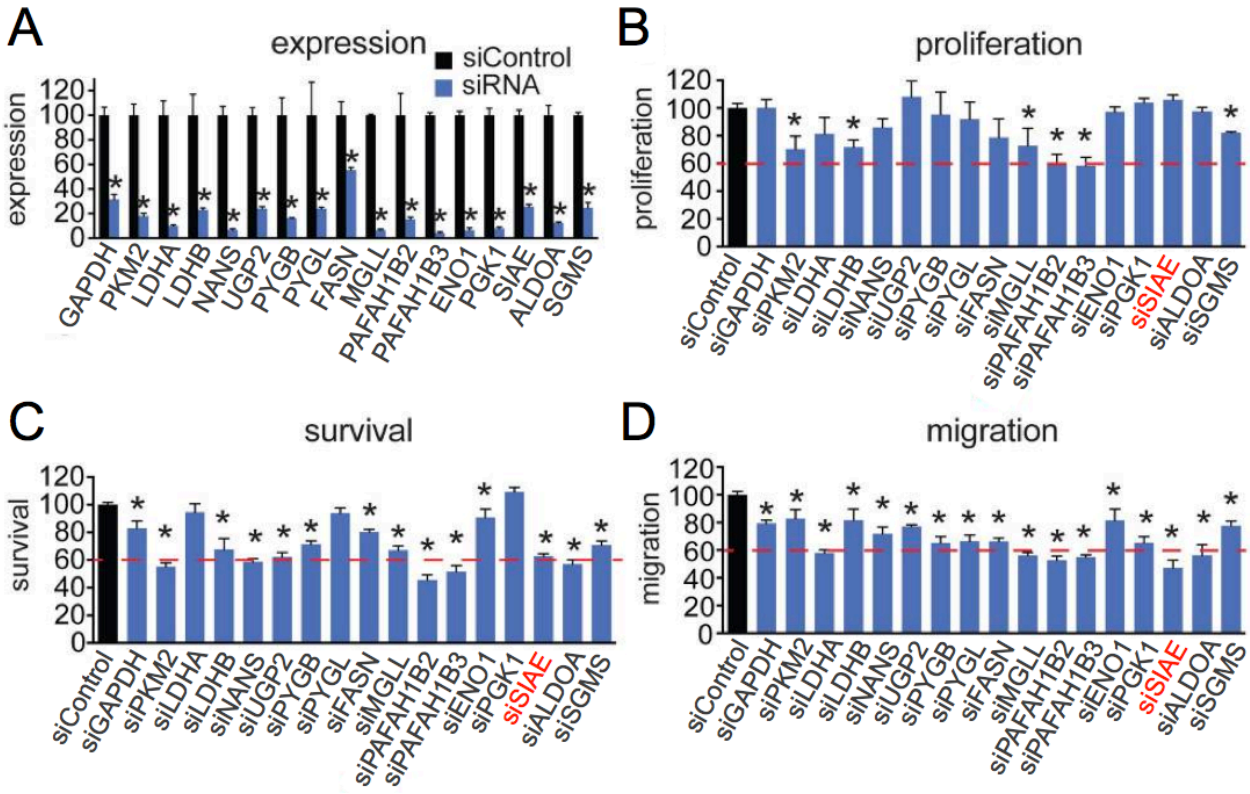

Figure 4-2. Screening for nodal metabolic enzymes in breast cancer. (a) We transiently knocked down the expression of representative metabolic enzymes in the pathways that we identified as consistently dysregulated in the breast cancer prgression model with siRNA in MII TAZ S89A cells. Knockdowns were confirmed by qPCR 48 h after siRNA transfection **(b-d)**. We screened for enzymes that, when inactivated, impaired various aspects of cancer pathogenicity including cellular proliferation **(b)**, serum-free cell survival **(c)**, and cell migration **(d)** in MII TAZ S89A cells. Cells were transfected with siRNA for 48 h before seeding into phenotypic experiments. Proliferation and cell survival were assessed at 48 h after seeding cells by the WST1 cell viability assay. Migration was assessed by counting the number of cells migrated through transwell chambers over 24 h. Data in bar graphs are presented as mean ± sem; n=3-5/group normalized to siControl. Significance is presented as *p < 0.05 compared to siControl MII TAZ S89A control cells.[56] Adapted from Mulvihill *et al.* Chem. Biol. 2014.

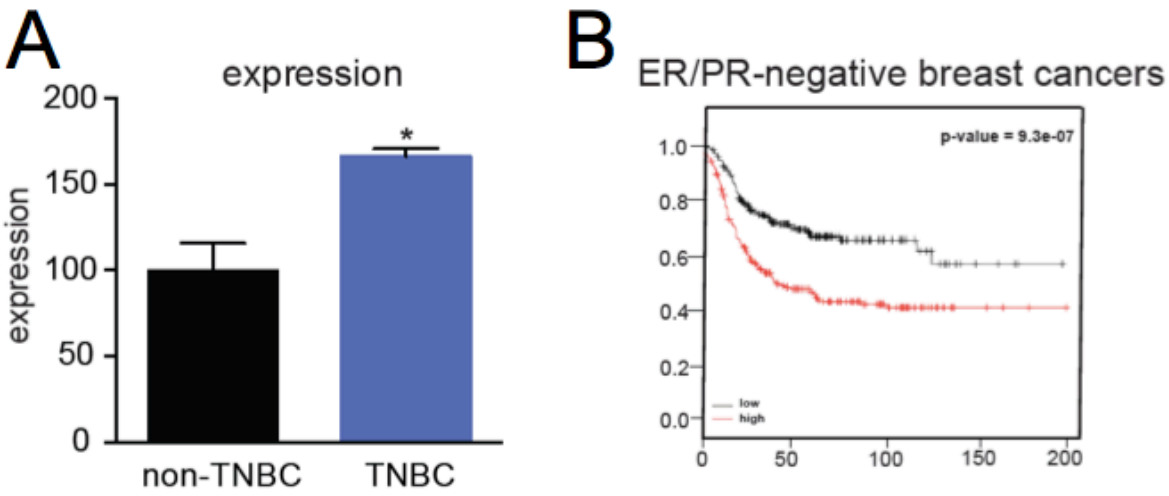

Figure 4-3. SIAE in TNBC vs. receptor positive cells. (A) mRNA expression of SIAE in non-triple negative breast cancer cells (non-TNBC) compared to TNBC. A panel of three non-TNBC cell lines and three TNBC cell lines (obtained from ATCC) were used. Data shown are for n=3/cell line, *p < 0.05. **(B)** Kaplan-Meier plot generated from kmplot.com using The Cancer Genome Atlas (TCGA) data for breast cancer patients with estrogen receptor and progesterone receptor positive breast cancer, and any HER2 status. Data generated from ~80 patients/group, x-axis is in months.

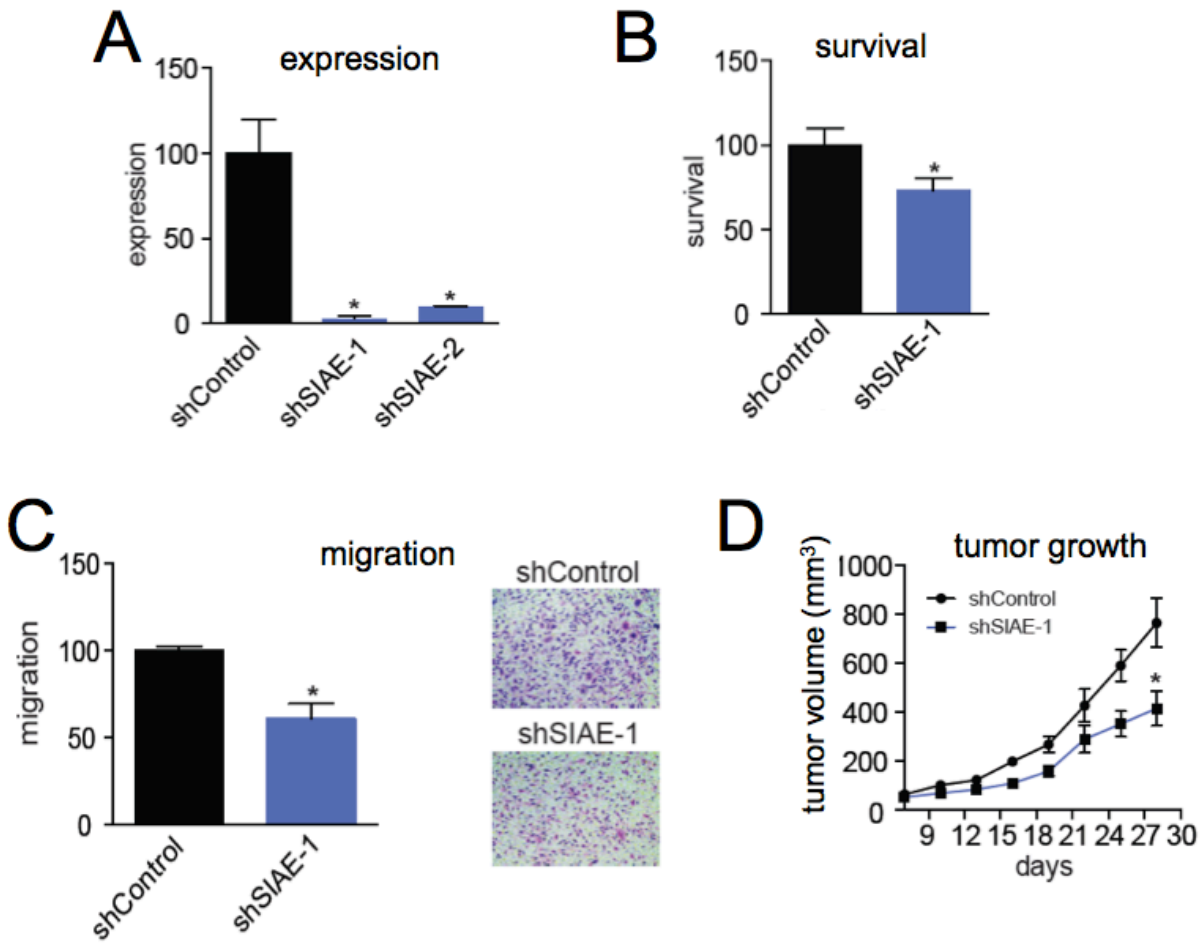

Figure 4-4. Knockdown of SIAE in 231MFP TNBC cells recapitulates phenotypes seen in siRNA screen. (A) mRNA expression of SIAE in 231MFP shControl compared to two short hairpin RNAs for SIAE (shSIAE-1 and shSIAE-2) as determined by qPCR. Data shown are n=3/group, *p < 0.05. **(B)** Cell survival of 231MFP shControl or shSIAE-1 cells. Cells were seeded at 40,000/well, allowed to adhere, and after 48 h survival was assessed by Hoechst staining. Data are n=5/group, *p < 0.05. **(C)** Cell migration in 231MFP shControl or shSIAE-1 cells through a transwell membrane for 6 h. Pictures on right are representative pictures showing the difference in migration. Bar graphs on left are quantification of n=3/group, *p < 0.05. **(D)** *In vivo* tumor growth of shControl of shSIAE-1 cells implanted subcutaneously into SCID mice. Data shown are n=5-6/group, *p < 0.05.

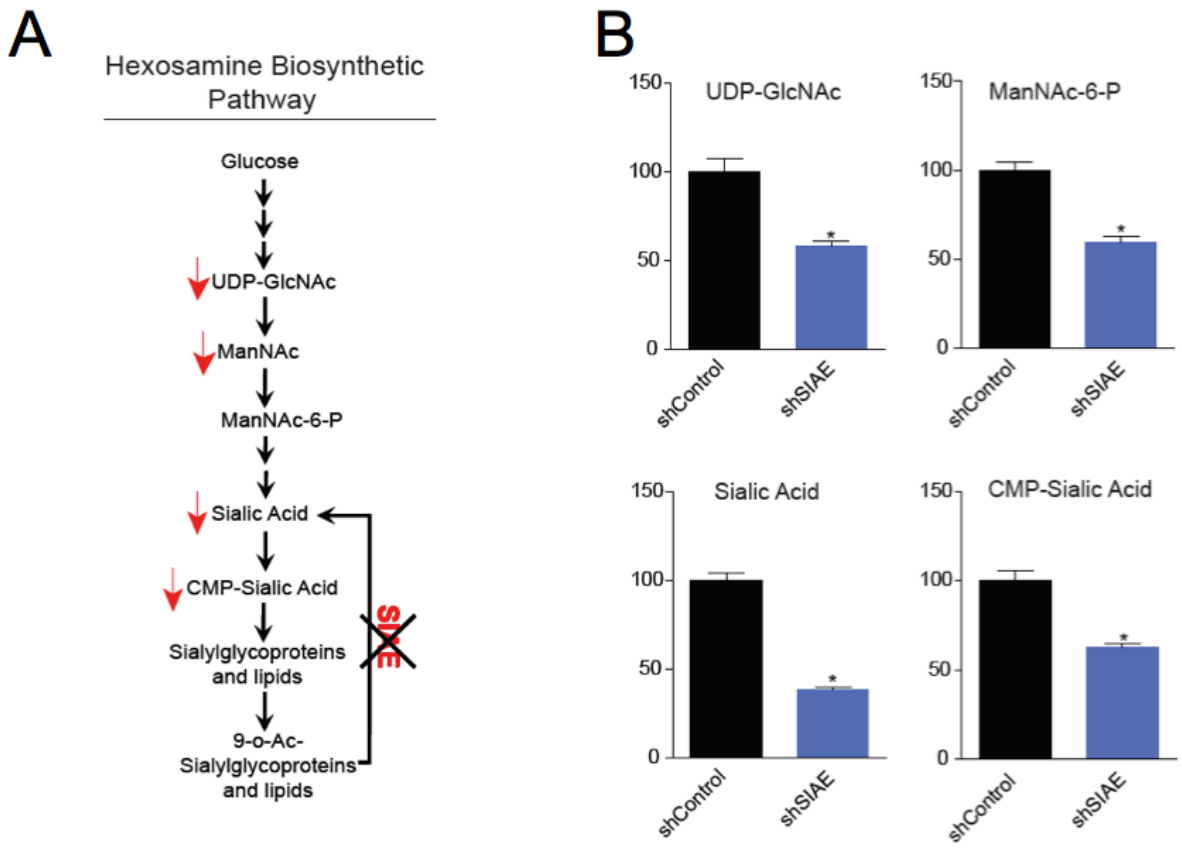

Figure 4-5. Metabolomic alterations in hexosamine biosynthetic pathway upon SIAE knockdown. (A) Hexosamine biosynthetic pathway from glucose to sialylated glycoproteins. Red arrows indicate the changes seen in these intermediates upon SIAE knockdown. **(B)** Quantification of the hexosamine metabolite changes from SIAE knockdown in 231MFP cells. Data are n=5/group, *p < 0.05.

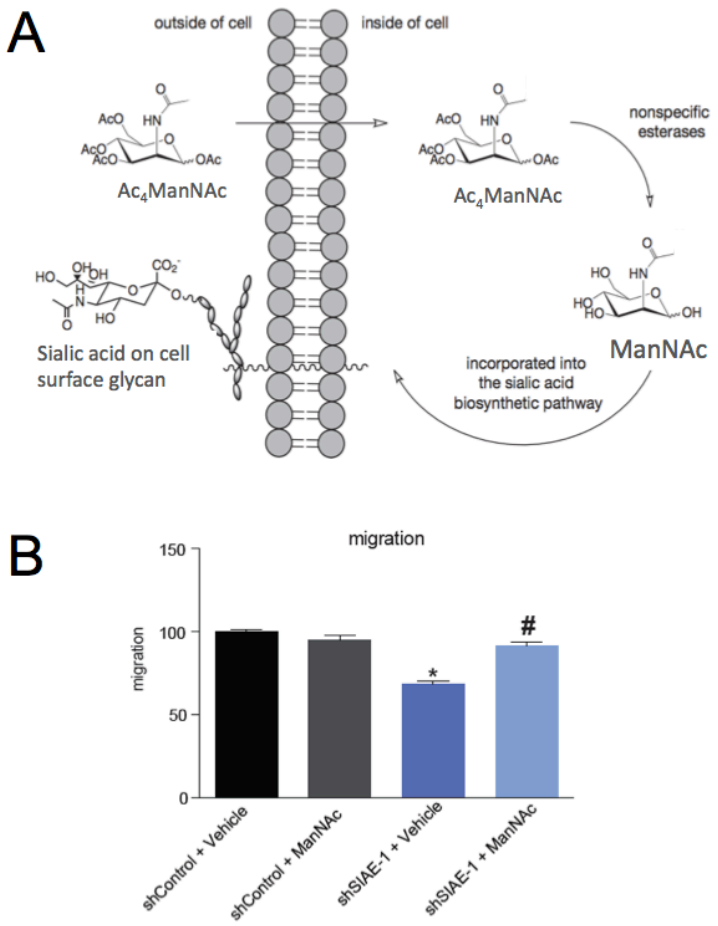

Figure 4-6. Treatment of shSIAE cells with Ac4-ManNAc rescues migratory defect. **(A)** Schematic of treatment of Ac_4-ManNAc showing that it can readily be taken up by cells, hydrolyzed to ManNAc, and incorporated completely normally into the hexosamine biosynthetic pathway. **(B)** Migration of 231MFP shControl or shSIAE-1 cells pretreated with 10 μM Ac_4-ManNAc or vehicle (water) for 18 h, followed by 6 h treatment during transwell migration. Migration data shown here are n=3/group, *p < 0.05 compared to shControl + vehicle, #p < 0.05 compared to shSIAE-1 + vehicle.

CHAPTER FIVE: Mapping Metabolic Targets of Anti-Cancer Agents to Identify Druggable Proteins and Drivers of Triple Negative Breast Cancer

Introduction

Current therapeutic strategies for breast cancer include resection, nonspecific therapies such as radiation or chemotherapy, and targeted strategies for combating certain types of breast cancers.[270] However, there are not targeted strategies for combating the most aggressive types of breast cancers, including TNBCs. Due to the reignited interest in targeting metabolic drivers of cancer for therapy, in this study, we combined chemoproteomic and metabolomic profiling to elucidate protein targets and metabolic effects of known anti-cancer drugs and drug candidates. Through this profiling effort, we have uncovered novel metabolic mechanisms and anti-TNBC activities of the phytoestrogenic natural product licochalcone A and deubiquitinase inhibitors. Considering these compounds are approved or in clinical trials, further understanding their mechanisms could help clinicians prescribe the most effective compounds for each specific cancer.

Chemical genetics screen of anti-cancer agents yields 20 compounds that cause significant cell death

To discover drugs and drug candidates that impair TNBC pathogenicity, we screened an anticancer library consisting of 424 compounds spanning a diverse range of molecular targets to identify small-molecules that impaired serum-free cell survival in 231MFP and HCC38 TNBC cells (**Fig.5-1, Fig. 5-2, Appendix 1-1**). We then filtered this list for those compounds that showed >75% survival impairments in both 231MFP and HCC38 cells. We subsequently retested the filtered list of compounds to identify agents that significantly ($p < 0.05$) impaired cell survival across 231MFP, HCC38, and HCC70 TNBC cells by over 50%. This resulted in a list of 20 compounds spanning 15 different molecular targets that reproducibly and significantly impaired cell survival by >50% across three TNBC lines (**Fig. 5-2**).

Several of these 20 compounds inhibit proteins that are currently being targeted in TNBC patients or are in clinical development including proteasome inhibitors MLN2238 and MLN9708; topoisomerase inhibitors daunorubicin, doxorubicin, idarubicin, and mitoxantrone; JAK2 inhibitor TG101348; mTOR inhibitor Torin 2; EGFR inhibitor dacomitinib; pololike kinase 1 (PLK) inhibitor BI6727; kinesin spindle protein (KSP) inhibitor ispenisib; and aurora kinase (AURK) inhibitor AT9283.[4,172–177] Other compounds modulate protein targets that have been previously shown to be important in TNBCs including HDAC inhibitors SB939 and romidepsin.[277] The remaining compounds and their targets, while previously shown to be important in cancer, are less understood in regard to their efficacy or roles in advanced-stage breast cancers or TNBCs. These include deubiquitinase inhibitor WP1130, exchange proteins directly activated by cAMP isoform 1 (EPAC) inhibitor ESI-09, kinesin inhibitor ARQ 621, FXR activator GW4064, and the phytoestrogen natural product licochalcone A[278–282] and may represent promising therapeutic strategies for combating TNBCs. Among these compounds with poorly understood roles in TNBCs, licochalcone A showed the greatest impairment (>95%) in cell survival across the three TNBC cells tested here with a 50% effective concentration (EC50) of 8.4 μM (**Fig. 5-3**).

The target of licochalcone A is the estrogen or progesterone receptor based on previous characterization of this compound as an estrogenic flavonoid.[280] Licochalcone A is a flavonoid extracted from licorice root that has been shown to possess anticancer, anti-inflammatory, and antiparasitic activity and has been tested on humans as an anti-inflammatory moisturizer.[109,280,283–287] However, the cell survival impairments of licochalcone A in TNBC cells resistant to ER and PR signaling indicated that this compound may be acting through alternate targets. In addition to acting through the esterogen or progesterone receptors, some previous studies have also shown that it can inhibit janus kinase (JNK) activity. JNK is a kinase that transduces cytokine-mediated signals through the JAK-STAT pathway. Activation of this pathway initiates transcription of genes involved in cell proliferation, and can also activate apoptosis. JNK activiation is critical for cell survival, and, therefore, inhibition of this pathway results in a dramatic reduction in cell viability.[288] While the survival defect seen with licochlacone A treatment (**Fig. 5-4 A**) may be acting through inhibition of JNK, we saw that selective inhibition of JNK by two different JNK inhibitors in the library showed low or no survival defect (**Fig. 5-4 B**). This indicated to us that there may be other, yet unknown, targets of licochalcone A causing the survival defects.

Chemoproteomic analysis of lead compound

Licochalcone A belongs to a larger group of natural products known as chalcones characterized by their aromatic enone structures (**Fig. 5-5 A**). These enones can undergo Michael addition to cysteine thiols on proteins to modulate protein function.[289] To identify the potential anticancer targets of licochalcone A, we mapped the cysteine reactivity of this compound in TNBC cells using a chemoproteomic platform termed isotopic tandem orthogonal proteolysis-enabled activity-based protein profiling (isoTOP-ABPP). IsoTOP-ABPP uses reactivity-based probes to map proteome-wide reactive, functional, and ligandable hotspots directly in complex proteomes. When used in a competitive manner, small molecules like licochalcone A can be competed against reactivity-based probes to map the proteome-wide reactivity and targets of covalently acting compounds (**Fig. 5-5 B**).[73,74,290] We profiled the proteome-wide cysteine-reactivity of licochalcone A through competition of this agent against the broad cysteine-reactive iodoacetamide-alkyne probe in 231MFP proteomes using the isoTOP-ABPP platform.[71,74] We subsequently appended probe-labeled proteins with a biotin-azide handle bearing an isotopically light (for control) or heavy (for licochalcone-treated) mass tag bearing a TEV protease recognition sequence by copper-catalyzed azide−alkyne cycloaddition (CuAAC), followed by mixing vehicle-treated and licochalcone-treated proteomes in a 1:1 ratio, avidin enrichment of probe-labeled proteins, digestion of enriched proteins by trypsin, and subsequent isolation and elution of probemodified tryptic peptides by TEV protease for subsequent quantitative proteomic analysis of light to heavy peptide ratios (**Fig. 5-5 B**). Through this profiling effort, we identified 1410 probe-modified tryptic peptides that were present in at least two out of four biological replicates (**Fig. 5-5 C, Appendix 1-2**). Most peptides showed light to heavy isotopic ratios of ~1, indicating that most sites were not inhibited. We interpreted those sites that

showed light to heavy isotopic ratios >10 as true targets of licochalcone A (**Fig. 5-5 C; Appendix 1-2**).

From this study, we found the primary target of licochalcone A to be cysteine 239 of the metabolic enzyme target prostaglandin reductase 1 (PTGR1) with the highest isotopic light to heavy ratio of 27 (**Fig. 5-5 C; Appendix 1-3**). We validated this target using gel-based ABPP methods where we observed competition of licochalcone A against iodoacetamide-alkyne labeling of pure human PTGR1 protein (**Fig. 5-5 C**). PTGR1 is involved in inactivating prostaglandins, including 15-ketoprostaglandins and leukotriene B4.[291291294293292311310] While recently shown to be important in lung and prostate cancers, PTGR1 represents a novel target for breast cancer.[292,293] Leukotriene B4, through stimulating leukotriene B4 receptor BLT1, has also been shown to fuel TGF-β−mediated proliferation in breast cancer cells.[294] Interestingly, C239 of PTGR1 represents the binding region for NADP+, required for the reductase catalytic activity of this enzyme[295] (**Fig. 5-5 D**), suggesting that licochalcone A binding to this site would displace NADP+ binding and inhibit PTGR1 activity. To further confirm the importance of PTGR1 in TNBC pathogenicity, we knocked down the expression of PTGR1 in 231MFP TNBC cells using three independent shorthairpin RNA oligonucleotides and show that PTGR1 knockdown dramatically impairs 231MFP cell survival and proliferation, thus recapitulating the effects observed with licochalcone A (**Fig. 5-5 E−G**). Thus, we put forth a novel metabolic mechanism of licochalcone A, in which it inhibits PTGR1 to impair TNBC pathogenicity.

We next sought to take a broader approach toward identifying unique metabolic mechanism underlying agents that impair TNBC pathogenicity. We performed lipidomic profiling to map metabolic changes conferred by treatment of 231MFP TNBC cells with the 20 lead compounds that impaired TNBC cell survival (**Fig. 5-6 A**). We focused this study on measuring ∼100 lipid metabolites spanning phospholipids, fatty acids, neutral lipids, sphingolipids, sterols, and fatty acid derivatives such as acyl carnitines, Nacyl ethanolamines (NAEs), and N-acyl taurines (NATs). We performed lipidomic profiling on cells that were treated for 6 h before any cell death to avoid confounding effects that may arise from differing cell numbers. Interestingly, we find that each compound gives a unique lipidomic signature, suggesting that metabolomic profiling may be used as a potential biomarker of drug response (**Fig. 5-6 A**; **Fig. 5-7**). We also see common changes in specific metabolites that correlate with certain mechanisms of action. For example, we observe that topoisomerase inhibitor-treated cells show reduced levels of C18:0/C18:1 diacylglycerol (DAG) and C18:0 ceramide, not seen with most of the other drug treatments, potentially indicating that these lipid species may be more specifically controlled by topoisomerase-mediated pathways **(Fig. 5-7)**. We also see certain lipid classes that are similarly regulated by multiple drugs that do not necessarily share a common mechanism of action. For example, C16:0 and C18:0 lysphosphatidylethanolamines (LPE), C16:0 lysophosphatidylcholine (LPC), and C18:0e lysophosphatidylcholineether (LPCe) levels are significantly elevated upon treatment of 231MFP cells with proteasome inhibitors MLN2238 and MLN9708, HDAC inhibitor romidepsin, JAK2 inhibitor TG101348, KSP inhibitor ispinenib, PLK inhibitor BI6727, EGFR inhibitor dacomitinib, and licochalcone A **(Fig. 5-7)**. Perhaps this common

regulation of different types of lysophospholipids by compounds that act through different targets may suggest a common downstream pathway targeted across all of these mechanisms potentially through an activation of phospholipase enzymes that would generate lysophospholipids. We do not believe these lipidomic signatures to be a general signature of cell death, as all 20 of these drugs impair TNBC cell survival. Rather, we believe that these lipidomic signatures likely represent unique metabolic mechanisms underlying the action of each drug.

Among the lipidomic profiles, the most significant changes were in acyl carnitine (AC) levels with a >60-fold elevation in C16:0 AC with the deubiquitinase inhibitor WP1130 and a >10-fold elevation with the EPAC inhibitor ESI09 and FXR activator GW4604 (**Fig. 5-6 B**). ACs are metabolites generated by carnitine palmitoyltranferase 1 (CPT1) at the mitochondrial membrane to import fatty acids into the mitochondria for fatty acid oxidation.[296] We show that other deubiquitinase inhibitors PR619 and P5091 also impair 231MFP cell survival and elevate AC levels (**Fig. 5-6 C, D**).
While PR619 and WP1130 inhibit several deubituitinases, P5091 selectively inhibits USP7 and USP47, which may explain the less dramatic AC elevations with P5091. We show that AC treatment impairs cell survival (**Fig. 5-8 A**). We also find that treatment of 231MFP cells with a concentration of AC that does not impair cell survival dramatically sensitizes cells to WP1130, likely because AC treatment synergizes with WP1130-mediated elevations in AC to impair 231MFP viability (**Fig. 5-8 B**). Previous studies have shown that ischemic injury elevates the levels of AC and that AC uncouples the mitochondria and impairs cellular respiration.[297–299] We show that treatment of 231MFP cells with both AC and WP1130 impairs maximal cellular respiration to a comparable degree (**Fig. 5-8 C**). Our data thus suggest that inhibition of deubiquitinase enzymes leads to elevation in AC levels, which, in turn, impair cellular respiration and may contribute to the cell survival impairments.

We also tested the role of LPE, since lysophospholipid species were among the lipid species dramatically changed with several drugs. We show that LPE treatment also impairs 231MFP cell survival and potentiates the cell survival impairments conferred by the proteasome inhibitor MLN9708 that elevates LPE levels (**Fig. 5-7, 5-9**). We further demonstrate that, unlike AC treatment, LPE or palmitate treatment in 231MFP cells does not affect cellular respiration, indicating that the lysophospholipid effects are driven through an alternate mechanism (**Fig. 5-9**).

Conclusions

In summary, we reveal several unique and novel metabolic effects underlying small-molecule drugs and drug candidates that impair TNBC pathogenicity by coupling drug screening with chemoproteomic and metabolomic profiling. In our first example, using isoTOP-ABPP platforms, we show here that licochalcone A impairs TNBC cell survival by >95% through inhibiting PTGR1. In our second example, using metabolomic platforms, we identify that deubiquitinase inhibitors also impair TNBC cell survival and that inhibiting these enzymes elevates AC levels by >60-fold to potentially impair cellular respiration and contribute to the viability impairments. Both PTGR1 inhibition and acyl

carnitine-mediated respiratory impairments in TNBC cells represent novel metabolic modalities that affect TNBC pathogenicity. Future studies should focus on better understanding the inhibitory mechanisms of licochalcone A on PTGR1, developing potent and selective PTGR1 inhibitors, and ascertaining the role of PTGR1, leukotriene B4, and BLT1 signaling pathways on TNBC pathogenicity. Future studies also include understanding the mechanisms and molecular targets through which AC impairs mitochondrial respiration. Collectively, our data point to the utility of using chemoproteomic and metabolomic platforms to uncover novel metabolic regulators of cancer, toward developing novel cancer therapies.

Materials and Methods

Materials

The anticancer compound library consisting of 424 compounds at 10mM in DMSO was purchased from Selleck Chemicals. IAyne was obtained from CHESS Gmbh. Heavy and light TEV-biotin tags were synthesized per previously described methods.[72,290] Palmitoyl carnitine was obtained from Sigma-Aldrich and resuspended in deionized water to 100mM stock. Lysophosphatidyl ethanolamine was obtained from Avanti Polar Lipids and resuspended in 2:1 chloroform/methanol to a 10mM stock.

Cell Culture

The 231MFP cells were obtained from Professor Benjamin Cravatt and were generated from explanted tumor xenografts of MDA-MB-231 cells. HCC38, HCC70, and HEK293T cells were obtained from the American Type Culture Collection (ATCC). 231MFP cells were cultured in L15 (HyClone) medium containing 10% FBS, supplemented with 2% glutamine (200 mM stock), and maintained at 37°C with 0% CO2. HCC38 and HCC70 cells were cultured in RPMI (Gibco) medium containing 10% FBS, supplemented with 2% glutamine (200 mM stock), and maintained at 37°C with 5% CO2. HEK293T cells were cultured in DMEM (Corning) containing 10% FBS, supplemented with 2% glutamine (200 mM stock) and maintained at 37°C with 5% CO2.

Cellular Survival and Proliferation Studies

Cell survival assays were performed as previously described using Hoechst 33342 dye (Invitrogen) according to the manufacturer's protocol.[269] Cells were seeded into 96-well plates (40,000 cells) in a volume of 150 µL of serum-free media and allowed to adhere overnight. Once adhered, an additional 50 µL of serum-free media containing 1:250 dilution of 1000× compound stock in DMSO was added to each well and allowed to incubate for 48 h before fixation. The medium was removed from each well, and 100 µL of staining solution containing 10% formalin and Hoechst 33342 dye was added to each well and incubated for 15 min in the dark at RT. Staining solution was then removed, and 100 µL of PBS was added for imaging on a SpectraMax i3 fluorescent plate reader. Studies with HCC38 cells and HCC70 were also performed as above but were seeded with 20,000 and 30,000 cells, respectively. Cell proliferation assays were performed as above, but cells were seeded (20,000 for 231MFP cells) and treated in medium containing FBS.

isoTOP-ABPP

IsoTOP-ABPP studies were done as previously reported.[74,290] Cell proteomes were prepared by sonicating harvested cell pellets in PBS, followed by centrifugation of proteomes at 1000g to remove any cell debris. Proteome samples diluted in PBS were treated with licochalcone A or vehicle for 30min at 37°C. Then, IAyne labeling was performed for 1h at RT. CuAAC was used by sequential addition of tris(2-

carboxyethyl)phosphine (1mM, Sigma), tris[(1- benzyl-1H-1,2,3-triazol-4-yl)methyl]amine (34μM, Sigma), copper- (II) sulfate (1mM, Sigma), and biotin-linker-azide, the linker functionalized with a TEV protease recognition sequence along with an isotopically light or heavy valine for treatment of control or treated proteome, respectively. After click reactions, proteomes were precipitated by centrifugation at 6500g, washed in ice-cold methanol, combined in a 1:1 control/treated ratio, washed again, then denatured and resolubilized by heating in 1.2% SDS/PBS to 80°C for 5 min. Insoluble components were precipitated by centrifugation at 6500g, and soluble proteome was diluted in 5mL of 0.2% SDS/PBS. Labeled proteins were enriched using avidin-agarose beads (170μL beads/ sample, Thermo Pierce) while rotating overnight at 4°C. Probelabeled proteins were enriched by washing three washes each with PBS and water, followed by resuspension of beads in 6 M urea/PBS and reduction of cysteines in TCEP (1mM), alkylation with iodoacetamide (18mM), washing and resuspension of beads in 2M urea, and trypsinization overnight with 0.5 μg/μL sequencing grade trypsin (Promega). Tryptic peptides were eluted off. Beads were then further washed in PBS and water, washed in TEV buffer solution (water, TEV buffer, 100mM dithiothreitol), and resuspended in buffer with Ac-TEV protease and incubated overnight. Peptides were diluted in water and acidified with formic acid (1.2M), and tryptic peptides were stored at −80 °C until MS analysis.

MS Analysis

Total peptides eluted from TEV protease release of probe-modified peptides were pressure-loaded onto 250μm inner diameter fused silica capillary tubing packed with 4 cm of Aqua C18 reverse-phase resin (Phenomenex # 04A-4299), which was previously equilibrated. This capillary tubing containing the loaded peptides was then attached using a MicroTee PEEK 360 mm fitting (Thermo Fisher Scientific #p-888) to a nanospray column consisting of 10 cm of C18 reverse-phase and 3 cm of strong-cation exchange resin. Samples were analyzed using an Q Exactive Plus mass spectrometer (Thermo Fisher Scientific) using a Multidimensional Protein Identification Technology (MudPIT) program, using 0%, 25%, 50%, 80%, and 100% salt bumps of 500 mM ammonium acetate and using a gradient of 5−55% buffer B in buffer A (buffer A. 95:5 water/acetonitrile, 0.1% formic acid; buffer B. 80:20 acetonitrile/water, 0.1% formic acid). Data were collected in data-dependent acquisition mode with dynamic exclusion enabled (60 s). One full MS (MS1) scan (400−1800 m/z) was followed by 15 MS2 scans of the most abundant ions. Heated capillary temperature and nanospray voltage were 200 °C and 2.75 kV, respectively.

Data were extracted in the form of MS1 and MS2 files using Raw Extractor 1.9.9.2 (Scripps Research Institute) and searched against the Uniprot human database using ProLuCID search methodology in IP2 v.3 (Integrated Proteomics Applications, Inc.).[300] Cysteine residues were searched with a static carboxyaminomethylation (+57.02146) modification for up to two differential modifications for methionine oxidation and either the light or heavy TEV tags (+464.28596 or +470.29977, respectively). Peptides were required to have at least one tryptic end and to contain the TEV modification. Data were filtered through DTASelect to ensure a peptide false-positive less than 1%.

Gel-Based ABPP

Gel-based ABPP methods were performed as previously described.[301] Recombinant PTGR1 (0.1μg) protein (Origene) was pretreated with DMSO or licochalcone A, respectively, for 1h at 37°C in an incubation volume of 50μL of PBS and was subsequently treated with IAyne (1μM final concentration) for 30min at 37°C. CuAAC was performed to append rhodamine-azide onto IAyne probe-labeled proteins. The samples were separated by SDS/ PAGE and scanned using a ChemiDoc MP (Bio-Rad Laboratories, Inc.). Inhibition of target labeling was assessed by densitometry using ImageStudio Light software.

Metabolomic Profiling

Metabolomic profiling was performed as previously reported.[28,269] For metabolomic profiling, 2 million cells were seeded in complete media and allowed to adhere overnight. They were then washed with PBS and refed with serum-free media containing 10μM of compound in DMSO or DMSO vehicle control at 0.1% DMSO final concentration for 6h. The cells were harvested and flash-frozen, and metabolomes were extracted in 3mL of 2:1 chloroform/methanol and 1mL of PBS with inclusion of internal standards dodecylglycerol (10nmol, Santa Cruz Biotechnology) and pentadecanoic acid (10nmol, Sigma-Aldrich). Organic and aqueous layers were separated by centrifugation at 1000g for 5min, and the organic layer was collected, dried under a stream of nitrogen, and dissolved in 120μL of chloroform. A 10μL aliquot of the 120μL sample in chloforom was then injected into an Agilent 6430 QQQLC/MS/MS. Metabolomes were separated using reverse-phase chromatography with a Luna C5 column (50 mm × 4.6 mm with 5μm diameter particles, Phenomenex) using previously reported methods.[28,269]

Metabolites were identified by single-reaction monitoring of the transition from precursor to product ions at associated optimized collision energies and retention times as previously described.[28,269] Metabolites were quantified by integrating the area under the curve and then normalized to internal standard values. Metabolite levels are expressed as relative abundances as compared to controls.

PTGR1 Knockdown

Targets were knocked down stably with shRNA as previously described.[28,269] shControl (targeting GFP) or shPTGR1 constructs (Sigma) were transfected into HEK293T (ATCC) cells alongside lentiviral vectors using lipofectamine 2000 (Thermo Fisher Scientific). Lentivirus was collected from filtered cultured medium 48 h post-transfection and used to infect the target cancer cell line with Polybrene (0.01mg/mL). Target cells were selected over 3 days with 1mg/mL puromycin. The short hairpin sequences for the generation of PTGR1 knockdown lines were
shPTGR1−1:
CCGGCTTGGATTTGATGTCGTCTTTCTCGAGAAAGACGACATCAAATCCAAGTTTTT
shPTGR1−2:

CCGGCTATCCTACTAATAGTGACTTCTCGAGAAGTCACTATTAGTAGGATAGTTTTT
shPTGR1−3:
CCGGGCCTACTTTGGCCTACTTGAACTCGAGTTCAAGTAGGCCAAAGTAGGCTTTT
T
control shRNA against GFP: GCAAGCTGACCCTGAAGTTCAT. Knockdown was confirmed by qPCR.

qPCR

qPCR was performed using the manufacturer's protocol for Fisher Maxima SYBR Green. Primer sequences are as follows:
PTGR1 forward: AGCACTTTGTTGGCTATCCTAC
PTGR1 reverse: CCCCATCATTGTATCACCTTCC
Cyclophilin forward: CCCACCGTGTTCTTCGACATT
Cyclophilin reverse: GGACCCGTATGCTTTAGGATGA

Cellular Respiration Measurements

231MFP cells were seeded at 50 000 cells/well in an XF24 cell culture microplate (Seahorse Bioscience) and analyzed the following day. On the day of analysis, cells were washed once with Seahorse respiration buffer made up of XF base medium minimal DMEM containing 25mM glucose and 5mM sodium pyruvate with the pH adjusted to 7.4. The cells were then placed in 0.5mL of Seahorse respiration buffer and incubated in a CO2-free incubator for 1 h. The 10× port injection solutions, in Seahorse respiration buffer all pH adjusted to 7.4, were prepared as follows (final concentrations in parentheses): port A, 10μM oligomycin (1μM final); port B, 1mM palmitoyl carnitine (100μM final) or 100μM WP1130 (10μM final); port C, 3μM FCCP (0.3μM final); port D, 5μM rotenone and 5μM antimycin A (0.5μM final). The Seahorse program ran as follows: basal measurement, three cycles; inject port A (oligomycin), three cycles; inject port B (compounds), three cycles; inject port C (FCCP), three cycles; inject port D (rotenone and antimycin A), three cycles. Each cycle consisted of mix for 3min, wait for 2min, measure for 3min.

Figures

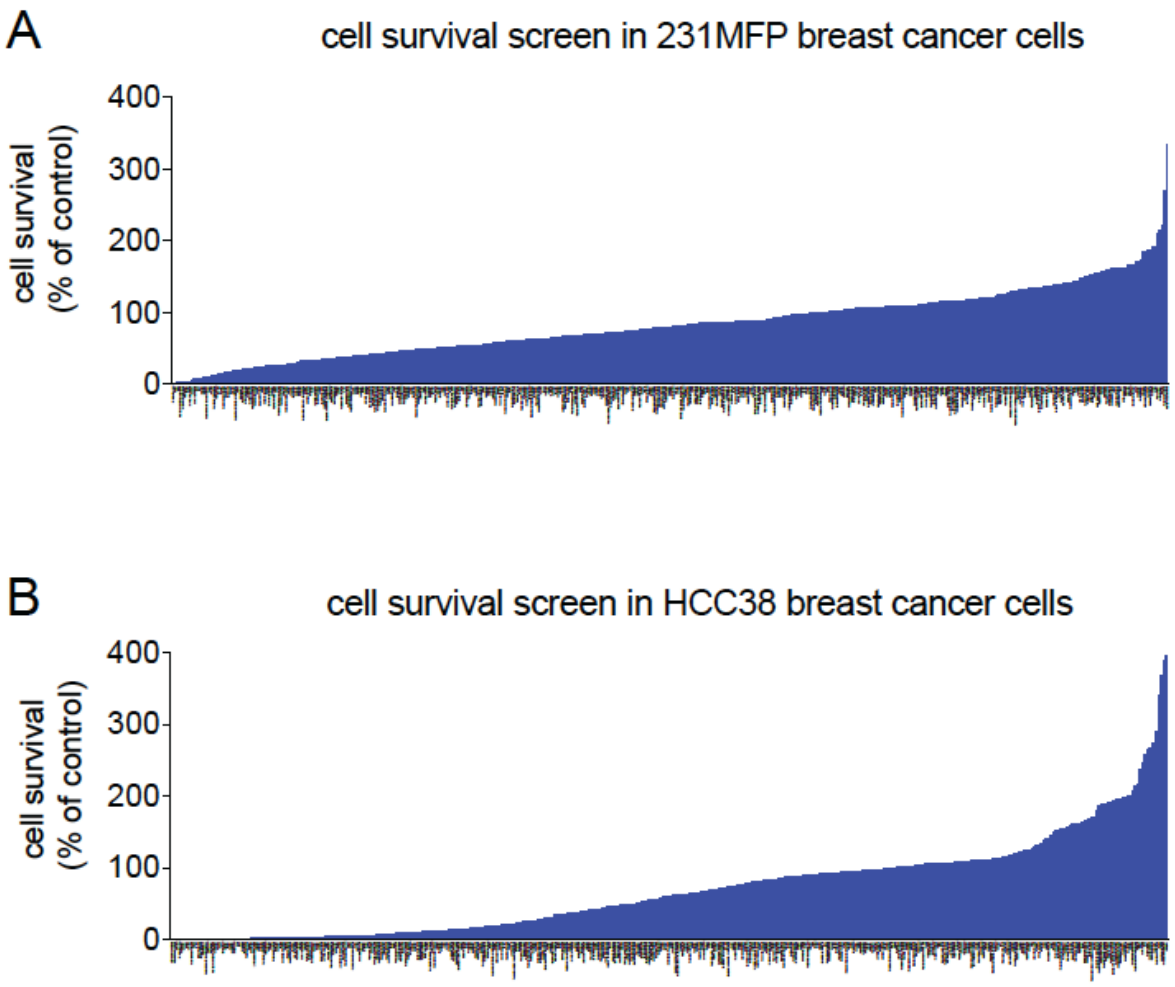

Figure 5-1. Screening a library of anti-cancer drugs and drug candidates in TNBC cells. (A,B) A library of anti-cancer drugs and drug candidates were screened in 231MFP **(A)** and HCC38 **(B)** TNBC cell lines for impairments in serum-free cell survival. Cells were treated with DMSO vehicle or compound (10μM) in serum-free media and cell survival was assessed 48h after treatment by Hoechst staining. Data in **(A, B)** are from an n=1 screen.

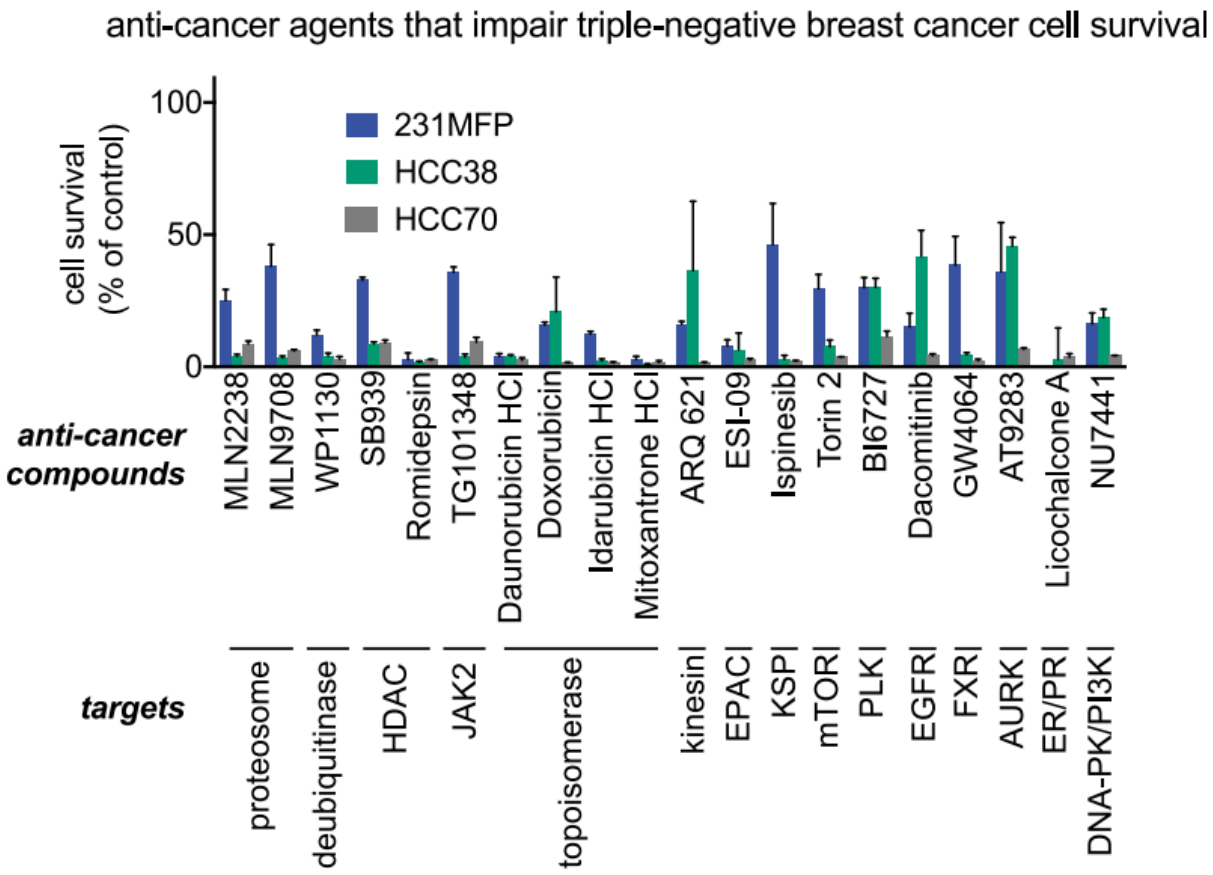

Figure 5-2. Screening a library of anti-cancer drugs and drug candidates in TNBC cells. A library of anti-cancer drugs and drug candidates were screened in 231MFP and HCC38 TNBC cell lines for impairments in serum-free cell survival. These data are shown in **Fig. 5-1** and **Appendix 1-2**. Shown here are drugs and drug candidates that reproducibly and significantly impaired 231MFP, HCC38, and HCC70 serum-free cell survival by >50%. Cells were treated with DMSO vehicle or compound (10μM) in serum-free media, and cell survival was assessed 48 h after treatment by Hoechst staining. Data are presented as mean ± SEM, n = 3/group, and all compounds shown in this figure showed significant ($p < 0.05$) cell survival impairments compared to DMSO treated controls.

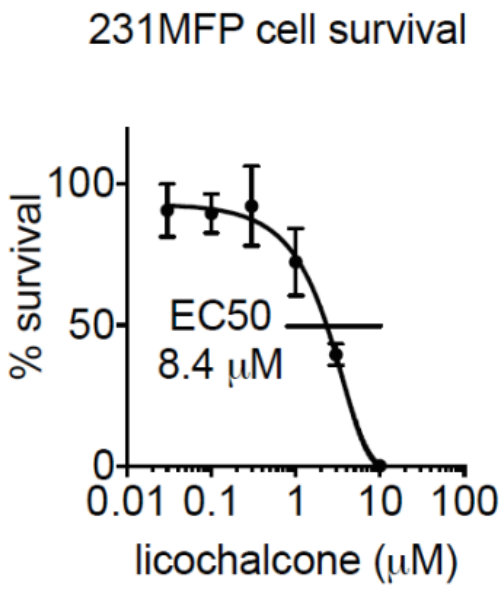

Figure 5-3. Licochalcone A dose-response in 231MFP Cells. 231MFP cells were treated with DMSO vehicle or licochalcone A and serum-free cell survival was assessed 48h post treatment by Hoechst staining. Survival values are expressed in relation to vehicle-treated controls. Data are presented as mean ± sem, n=3/group.

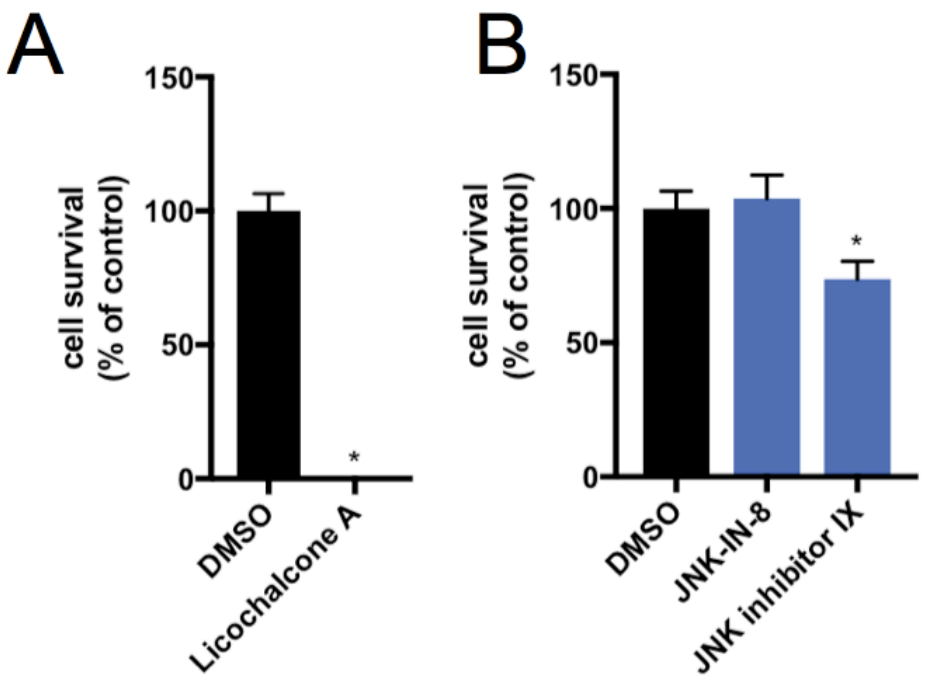

Figure 5-4. Licochalcone A yields a greater survival defect than selective JNK inhibitors. Cells were treated with DMSO vehicle, **(A)** licochalcone A or **(B)** JNK-IN-8 or JNK inhibitor X (10μM) in serum-free media, and cell survival was assessed 48 h after treatment by Hoechst staining. Data are presented as mean ± SEM, n = 5/group, *p < 0.05 compared to DMSO treated controls.

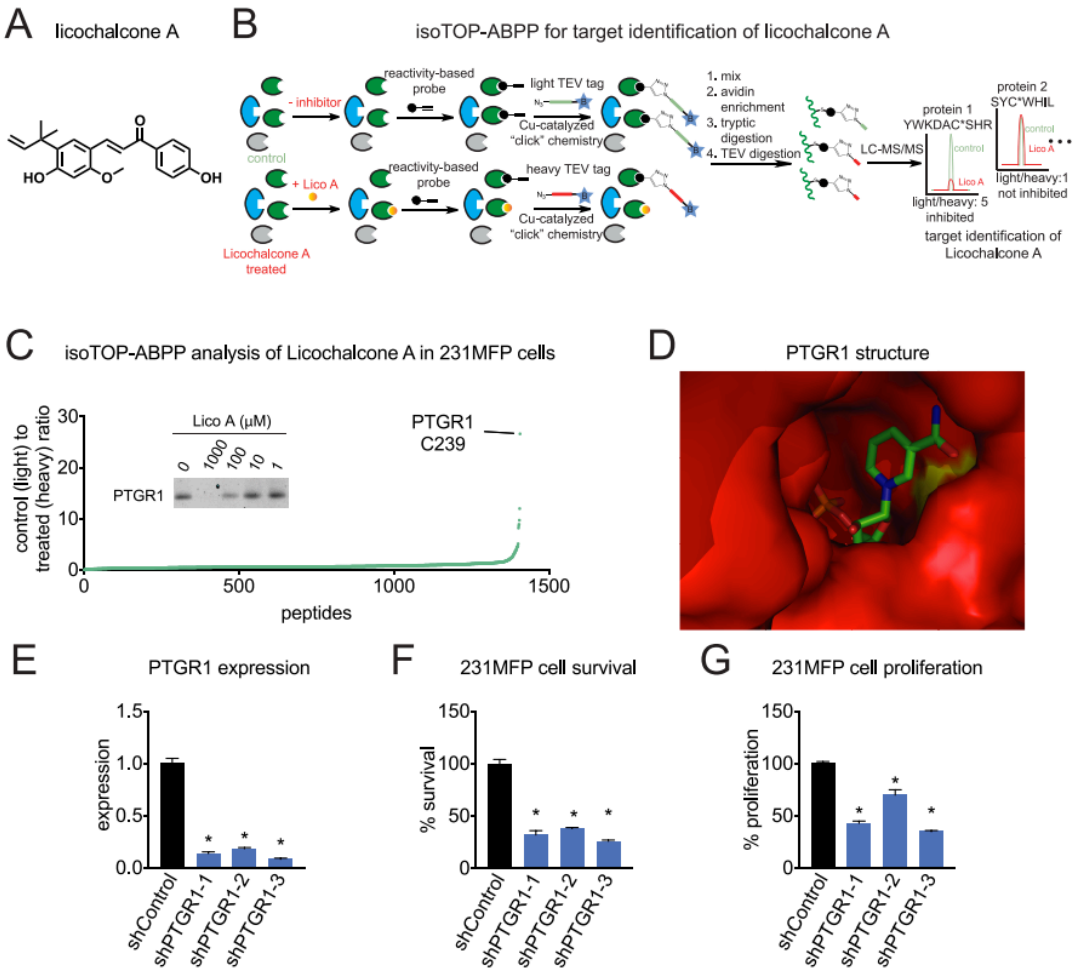

Figure 5-5. IsoTOP-ABPP analysis of Licochalcone A in TNBC cells. (A) Structure of licochalcone A. **(B)** Competitive isoTOP-ABPP to map licochalcone targets. Licochalcone A bears a Michael acceptor that is potentially cysteine-reactive. We mapped the cysteine-reactivity of licochalcone A by preincubating licochalcone A (10μM) for 30 min in 231MFP breast cancer cell proteomes, prior to labeling with the cysteine-reactive iodoacetamide-alkyne (IAyne) probe (100μM, 30 min). Probe labeled proteins were then tagged with an isotopically light (for control) or heavy (for licochalcone A-treated) biotin-azide tag bearing a TEV protease recognition site by CuAAC. Control and treated proteomes were then mixed in a 1:1 ratio. Probe labeled proteins were avidin-enriched and tryptically digested. Probe-labeled tryptic peptides were avidin-enriched again and released by TEV protease and analyzed by quantitative proteomic methods, and light to heavy peptide ratios were quantified. **(C)** Competitive isoTOP-ABPP analysis of licochalcone A cysteine reactivity in 231MFP breast cancer cell proteomes. Light to heavy ratios of ~1 indicate peptides that were labeled by IAyne, but not bound by licochalcone A. We designate light to heavy ratios of >10 as targets that were bound by licochalcone A. The top target was C239 of PTGR1. Shown in this figure is also validation of PTGR1 as a target of licochalcone A. Licochalcone A was preincubated with pure human PTGR1 protein followed by IAyne. Probe-labeled

proteins conjugated to rhodamine-azide by CuAAC and analyzed by SDS/PAGE and in-gel fluorescence. Shown are average isotopic ratios of probe-modified tryptic peptides that were present in at least two out of four biological replicates. **(D)** Crystal structure of PTGR1 showing C239 (shown in yellow) and NADP+ shown in ball and stick form. PDB structure used is 2Y05. **(E)** PTGR1 expression in shPTGR1 231MFP cells. PTGR1 was stably knocked down with three independent shRNA oligonucleotides, and expression was determined by qPCR. **(F, G)** Serum-free cell survival and proliferation in shPTGR1 231MFP cells. Cell survival and proliferation were assessed 48h after seeding by Hoescht staining. Data in **(E−G)** are presented as mean ± SEM, n = 3−5/group. Significance is presented as *$p < 0.05$ compared to shControl cells.

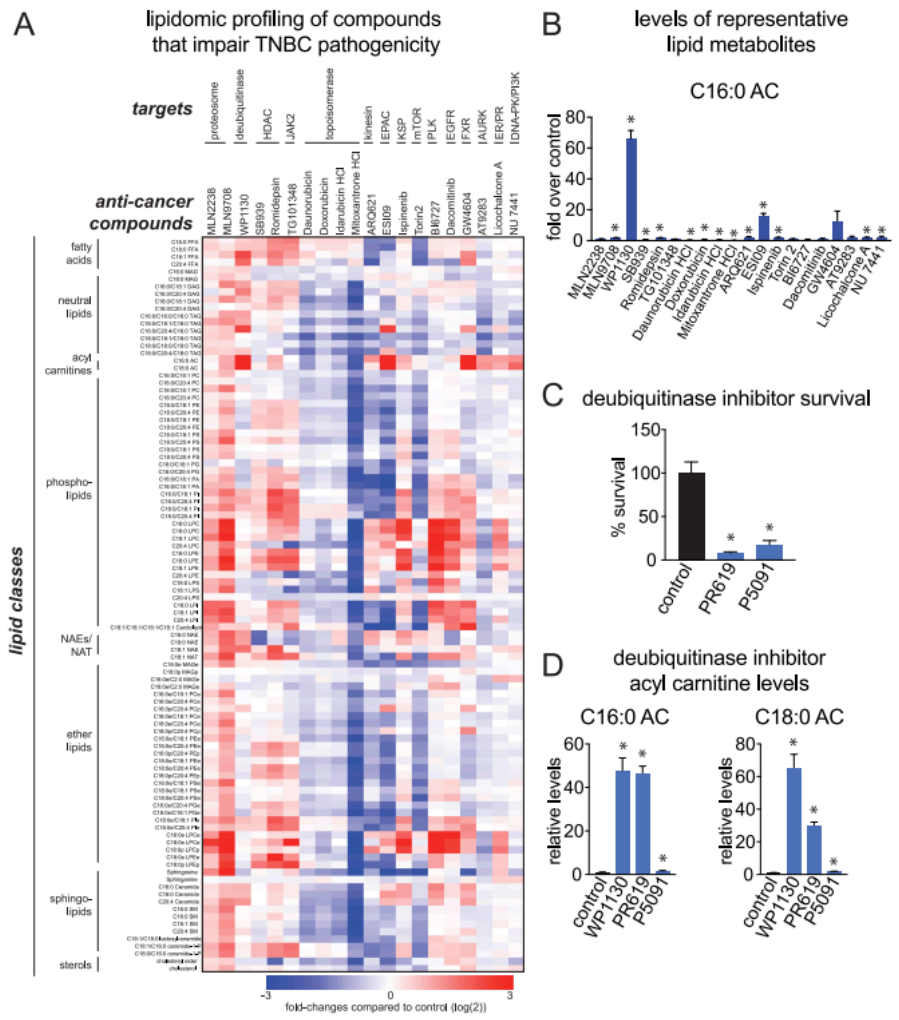

Figure 5-6. Metabolomic profiling of drug responses in TNBC cells. (A) Metabolomic profiling of 231MFP TNBC cells treated with the 20 compounds that impaired TNBC cell survival. 231MFP cells were treated with DMSO-vehicle or each compound (10μM) for 6 h. Lipid levels were analyzed by single reaction monitoring (SRM)-based liquid chromatography−mass spectrometry (LC-MS/MS). Heatmap shows fold changes in log (2) compared to vehicle-treated controls where red and blue designates increased and decreased levels, respectively. **(B)** C16:0 AC levels in 231MFP cells treated with each of the 20 compounds that impaired TNBC cell survival. Data are from the experiment described in A. **(C)** Cell survival in 231MFP cells. 231MFP cells were treated with DMSO control or deubiquitinase inhibitors PR619 and P5091 (10μM), and serum-free cell survival was assessed 48h after treatment by Hoechst staining. **(D)** AC levels in 231MFP cells treated with deubiquitinase inhibitors. Cells were treated with DMSO vehicle or inhibitors (10μM) for 6h, and AC levels were determined by SRM-based LC-MS/MS. Data in **(A)** are from an n = 5/group. Data in **(B−D)** are presented as mean ± SEM, n = 5/group. Significance is presented as *p < 0.05 compared to vehicle-treated control cells.

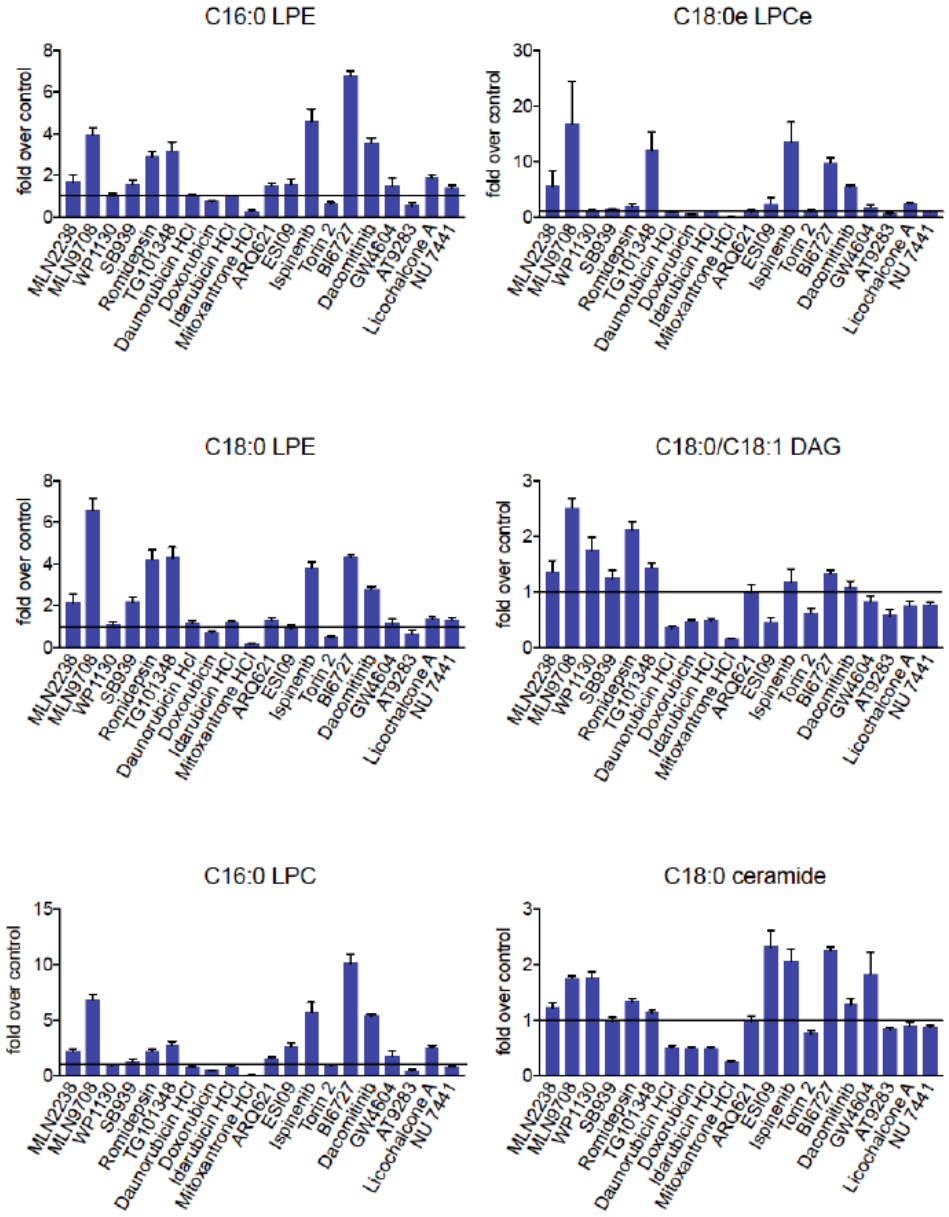

Figure 5-7. Levels of representative lipids. Levels of representative lipids from 231MFP TNBC cells treated with the 20 compounds that impaired TNBC cell survival. These data are taken from **Fig. 5-5 A**. 231MFP cells were treated with DMSO vehicle or each compound (10μM) for 6h. Lipid levels were analyzed by single reaction monitoring (SRM)-based liquid chromatography-mass spectrometry (LC-MS/MS). Data are presented as mean ± sem, n=5/group.

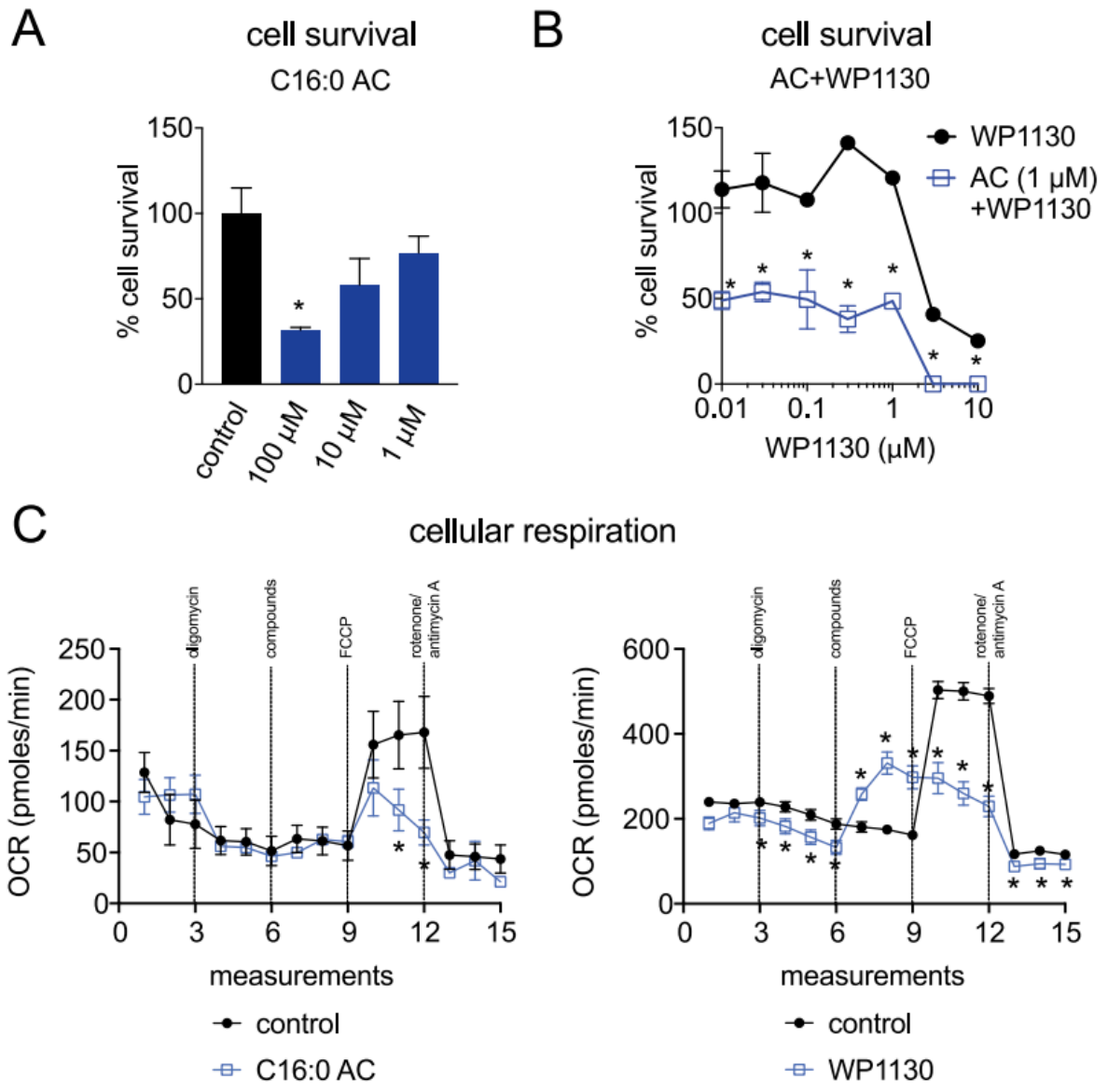

Figure 5-8. The role of AC in deubiquitinase inhibitor-mediated cell survival impairments in TNBC cells. (A) 231MFP cell survival upon treatment of cells with AC. Cells were treated with AC, and serum-free cell survival was assessed 48h after treatment by Hoechst staining. **(B)** 231MFP cell survival upon treatment of cells with AC and deubiquitinase inhibitor WP1130. Cells were co-treated with water or C16:0 AC (1μM), a concentration that does not impair viability when treated alone, and DMSO or WP1130, and cell survival was assessed 48h after treatment by Hoechst staining. **(C)** Oxygen consumption rates in cells treated with DMSO vehicle or AC or WP1130. Compounds were treated at cycle 6 (injection from port B). Oxygen consumption was measured using a Seahorse XF24 Analyzer. Data in A−C are presented as mean ± SEM, n = 3−5/group. Significance is presented as *p < 0.05 compared to vehicle treated control cells.

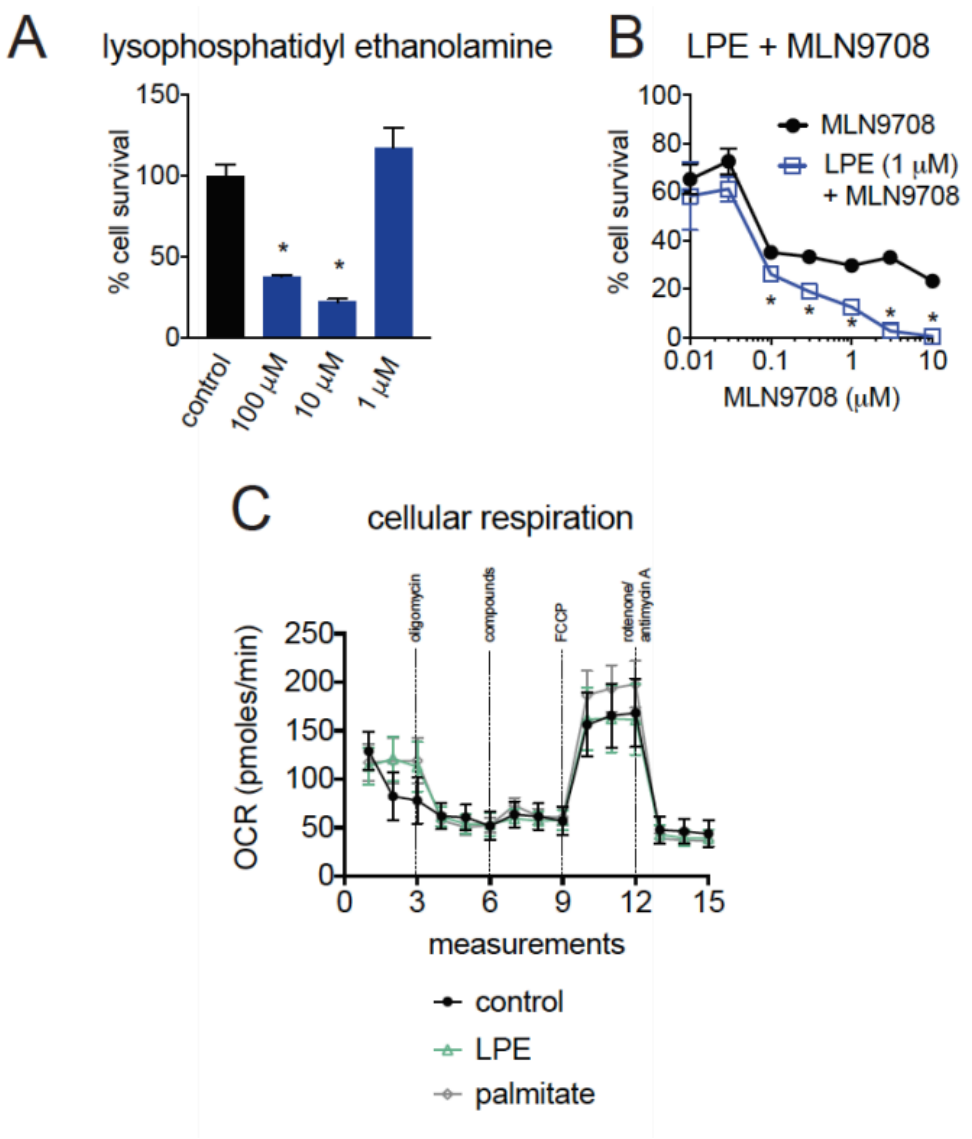

Figure 5-9. Chacterizing the role of LPE in TNBC cell survival. (A) 231MFP cell survival upon treatment of cells with LPE. Cells were treated with LPE and serum-free cell survival was assessed 48h after treatment by Hoechst staining. **(B)** 231MFP cell survival upon treatment of cells with LPE and proteasome inhibitor MLN9708. Cells were co-treated with 2:1 chloroform:methanol or C16:0 LPE (1μM), a concentration that does not impair viability when treated alone, and DMSO or MLN9708 and cell survival was assessed 48h after treatment by Hoechst staining. **(C)** Oxygen consumption rates in cells treated with 2:1 chloroform:methanol vehicle or LPE or palmitate. Lipids were treated at cycle 6 (injection from port B). Oxygen consumption was measured using a Seahorse XF24 Analyzer. Data in **(A-C)** are presented as mean ± sem, n=3-5/group. Significance is presented as *p < 0.05 compared to vehicle treated control cells.

Conclusions

Final remarks

Nearly a century has passed since the initial discoveries of Otto Warburg ignited the interest and awareness of dysregulated metabolism as a hallmark of cancer cells. Since that time much of metabolism research has focused on central carbon metabolism pathways due to the relative ease with which it is to study. The mapping of the human genome, however, uncovered a large number of genes encoding proteins with unknown function including many uncharacterized metabolic enzymes. These findings revealed the lack of completeness in our understanding of cellular metabolism and motivated many researchers to develop tools to further uncover this unmapped landscape of metabolism. As cancer cell metabolism research has advanced, many drugs have been developed and used that target metabolic enzymes. Therefore, more thorough understanding of cancer cell metabolism and how these alterations may be candidate targets for therapeutic development is of great interest. In this dissertation I show how mass-spectrometry based metabolomic and proteomic platforms can facilitate this discovery process.

As cancer is becoming classified as a metabolic disease, it is also of interest to understand the relationship between it and other metabolic diseases, such as obesity, to see how these metabolic changes, signaling metabolites, and symptoms may synergize to fuel each other. In this dissertation, I first review the mechanisms that link the metabolic diseases obesity and cancer, followed by a study using metabolomics to show that exogenous fatty acids can be utilized by cancer cells for structural and signaling molecules. These together provide new information about the way cancer cell lipid metabolism works and how high levels of circulating fatty acids may fuel this disease.

In addition to alterations in lipid metabolism, I show that proteomic profiling of breast cancer cells reveals many other dysregulated metabolic enzymes. Continuing to gather a more complete picture of cellular metabolism and the alterations seen in cancer cells has huge implications for the development of more effective and targeted therapies. The identification of sialic acid acetylesterase (SIAE) as a dysregulated enzyme in triple negative breast cancer and understanding the importance it has in cell migration and potentially the relationships between cancer cells and immune cells is one example of this. Perhaps there will be future drugs developed to target SIAE or other enzymes in this area of metabolism that will prove effective in reducing the metastatic potential of these cells or their ability to evade immune cell detection.

Taking a slightly different approach, by profiling the targets of drugs and drug candidates currently in the clinic or clinical trials, I find that in triple negative breast cancer there may be yet unknown targets of well-characterized drugs, such as licochalcone A which is reported to target the estrogen and progesterone receptors. Taking this approach we can find important targets in triple negative breast cancer cells that are hit by the drugs. Furthermore, finding multiple targets of a drug can inform the potentially combinatorial mechanism through which it is working, as well as what cancers might be sensitive to the therapy. Finally, using an approach with drugs already

approved or in an approval pipeline hastens the rate at which the therapy could actually be used in the clinic.

Cancer cell metabolism remains an evolving field for both uncovering the basic biological mechanisms underlying why cancer cells behave the way they do as well as identifying viable druggable targets for therapeutic applications. Recent innovations in chemical biology techniques have enabled accelerated discoveries in these areas. By coupling advanced metabolomic and proteomic platforms with chemical genetics and RNAi screens in this dissertation I have been able to elucidate some new areas of interest in cancer metabolism and some potential candidate drug targets. Advancements in our tools have revealed new areas of cancer cell metabolic dysregulation and lend hope that someday we will have a complete picture and, with that, finally be able to develop targeted therapies to combat and eradicate these lethal cancers.

Appendices

Appendix 1-1. Drugs and Drug Candidates Screened. List of compounds screened in this study and characterization of these compounds and their targets (adapted from Selleck Chemicals' Website).

ABT-263 (Navitoclax)	Bcl-2	Apoptosis
ABT-737	Bcl-2	Apoptosis
Linifanib (ABT-869)	PDGFR, VEGFR	Protein Tyrosine Kinase
Veliparib (ABT-888)	PARP	DNA Damage
Axitinib	VEGFR, PDGFR, c-Kit	Protein Tyrosine Kinase
Saracatinib (AZD0530)	Src, Bcr-Abl	Angiogenesis
Selumetinib (AZD6244)	MEK	MAPK
Nintedanib (BIBF 1120)	VEGFR, PDGFR, FGFR	Protein Tyrosine Kinase
Afatinib (BIBW2992)	EGFR	Protein Tyrosine Kinase
BMS-536924	IGF-1R	Protein Tyrosine Kinase
Bortezomib (PS-341)	Proteasome	Proteases
Bosutinib (SKI-606)	Src	Angiogenesis
Cediranib (AZD2171)	VEGFR, Flt	Protein Tyrosine Kinase
Dovitinib (TKI-258, CHIR-258)	c-Kit, FGFR, Flt, VEGFR, PDGFR	Angiogenesis
PD184352 (CI-1040)	MEK	MAPK
Dasatinib	Src, Bcr-Abl, c-Kit	Angiogenesis
Gefitinib (ZD1839)	EGFR	Protein Tyrosine Kinase
Imatinib Mesylate (STI571)	PDGFR, c-Kit, Bcr-Abl	Protein Tyrosine Kinase
Lapatinib (GW-572016) Ditosylate	EGFR, HER2	Protein Tyrosine Kinase
Lenalidomide (CC-5013)	TNF-alpha	Apoptosis
Motesanib Diphosphate (AMG-706)	VEGFR, PDGFR, c-Kit	Protein Tyrosine Kinase
Nilotinib (AMN-107)	Bcr-Abl	Angiogenesis
PD0325901	MEK	DNA Damage
PI-103	DNA-PK, PI3K, mTOR	Neuronal Signaling
Rapamycin (Sirolimus)	mTOR	DNA Damage
Sorafenib Tosylate	VEGFR, PDGFR, Raf	Neuronal Signaling
Sunitinib Malate	VEGFR, PDGFR, c-Kit, Flt	Microbiology
Temsirolimus (CCI-779, NSC	mTOR	Neuronal Signaling
Trichostatin A (TSA)	HDAC	Others
Vorinostat (SAHA, MK0683)	HDAC	Endocrinology & Hormones
VX-680 (Tozasertib, MK-0457)	Aurora Kinase	Endocrinology & Hormones
Y-27632 2HCl	ROCK	Others
Elesclomol (STA-4783)	HSP	Angiogenesis
Entinostat (MS-275)	HDAC	Transmembrane Transporters
Enzastaurin (LY317615)	PKC	Neuronal Signaling
AC480 (BMS-599626)	HER2	Neuronal Signaling
Obatoclax Mesylate (GX15-070)	Bcl-2	Neuronal Signaling
Olaparib (AZD2281, Ku-0059436)	PARP	Protein Tyrosine Kinase
Nutlin-3	Mdm2	Neuronal Signaling
Masitinib (AB1010)	c-Kit, PDGFR, FGFR, FAK	Others
GDC-0941	PI3K	Metabolism
SB431542	TGF-beta/Smad	Others
Crizotinib (PF-02341066)	c-Met, ALK	Others
AUY922 (NVP-AUY922)	HSP	Others
PHA-665752	c-Met	Others
ZSTK474	PI3K	Neuronal Signaling
SB216763	GSK-3	Others
SB203580	p38 MAPK	Transmembrane Transporters
MK-2206 2HCl	Akt	Others
SU11274	c-Met	Neuronal Signaling
Vismodegib (GDC-0449)	Hedgehog, P-gp	Neuronal Signaling
Brivanib (BMS-540215)	VEGFR, FGFR	GPCR & G Protein

Belinostat (PXD101)	HDAC	Others
Iniparib (BSI-201)	PARP	Others
Refametinib (RDEA119, Bay 86-	MEK	Others
PCI-24781 (Abexinostat)	HDAC	Others
OSI-906 (Linsitinib)	IGF-1R	Others
KU-55933 (ATM Kinase Inhibitor)	ATM	Others
GSK1904529A	IGF-1R	Others
PF-04217903	c-Met	Others
Quisinostat (JNJ-26481585)	HDAC	Others
BTZ043 Racemate	Others	Others
Rucaparib (AG-014699,PF-	PARP	Others
Vatalanib (PTK787) 2HCl	VEGFR, c-Kit, Flt	Others
GDC-0879	Raf	Others
LY294002	PI3K	Others
Danusertib (PHA-739358)	Aurora Kinase, FGFR, Bcr-Abl, c-	Others
BI 2536	PLK	Others
GSK690693	Akt	Others
JNJ-38877605	c-Met	Others
Triciribine	Akt	Others
Everolimus (RAD001)	mTOR	Others
TW-37	Bcl-2	Others
Mocetinostat (MGCD0103)	HDAC	Others
SRT1720	Sirtuin	Others
YM155 (Sepantronium Bromide)	Survivin	Others
Alisertib (MLN8237)	Aurora Kinase	Others
AT9283	Bcr-Abl, JAK, Aurora Kinase	Others
Andarine	Androgen Receptor	Others
17-AAG (Tanespimycin)	HSP	Others
17-DMAG (Alvespimycin) HCl	HSP	Others
SNS-032 (BMS-387032)	CDK	Others
Barasertib (AZD1152-HQPA)	Aurora Kinase	Others
Docetaxel	Microtubule Associated	Others
Paclitaxel	Microtubule Associated	Others
Roscovitine (Seliciclib,CYC202)	CDK	Others
SNS-314 Mesylate	Aurora Kinase	Others
Capecitabine	DNA/RNA Synthesis	Others
Ganetespib (STA-9090)	HSP	Others
Lenvatinib (E7080)	VEGFR	Protein Tyrosine Kinase
ABT-751 (E7010)	Microtubule Associated	Cytoskeletal Signaling
Valproic acid sodium salt (Sodium	GABA Receptor, HDAC	Neuronal Signaling
CYC116	Aurora Kinase, VEGFR	Cell Cycle
JNJ-26854165 (Serdemetan)	p53	Apoptosis
WZ4002	EGFR	Protein Tyrosine Kinase
MK-2866 (GTx-024)	Androgen Receptor	Endocrinology & Hormones
BIIB021	HSP	Cytoskeletal Signaling
Plinabulin (NPI-2358)	VDA	Angiogenesis
Regorafenib (BAY 73-4506)	c-Kit, Raf, VEGFR	Protein Tyrosine Kinase
XAV-939	Wnt/beta-catenin	Stem Cells & Wnt
ENMD-2076	Flt, Aurora Kinase, VEGFR	Angiogenesis
BIBR 1532	Telomerase	DNA Damage
Anastrozole	Aromatase	Endocrinology & Hormones
Aprepitant	Substance P	Others
Bicalutamide	Androgen Receptor, P450	Endocrinology & Hormones
Fulvestrant	Estrogen/progestogen Receptor	Endocrinology & Hormones
Raltitrexed	DNA/RNA Synthesis	DNA Damage
Thalidomide	Others	Apoptosis
CUDC-101	HDAC, EGFR, HER2	Epigenetics
Exemestane	Aromatase	Endocrinology & Hormones
Irinotecan	Topoisomerase	DNA Damage

Cladribine	DNA/RNA Synthesis	DNA Damage
Decitabine	DNA/RNA Synthesis	Epigenetics
Dimesna	Others	Others
Tivozanib (AV-951)	VEGFR, c-Kit, PDGFR	Protein Tyrosine Kinase
Doxorubicin (Adriamycin)	Topoisomerase	DNA Damage
Fluorouracil (5-Fluoracil, 5-FU)	DNA/RNA Synthesis	DNA Damage
Methotrexate	DHFR	Metabolism
Bendamustine HCl	Others	Others
Nelarabine	DNA/RNA Synthesis	DNA Damage
Bleomycin Sulfate	DNA/RNA Synthesis	DNA Damage
Clofarabine	DNA/RNA Synthesis	DNA Damage
YM201636	PI3K	PI3K/Akt/mTOR
OSI-930	c-Kit, VEGFR	Protein Tyrosine Kinase
Dacarbazine	DNA/RNA Synthesis	DNA Damage
Oxaliplatin	DNA/RNA Synthesis	DNA Damage
Etoposide	Topoisomerase	DNA Damage
KU-0063794	mTOR	PI3K/Akt/mTOR
Raloxifene HCl	Estrogen/progestogen Receptor	Endocrinology & Hormones
Fludarabine Phosphate	DNA/RNA Synthesis	DNA Damage
Flavopiridol (Alvocidib)	CDK	Cell Cycle
Topotecan HCl	Topoisomerase	DNA Damage
2-Methoxyestradiol (2-MeOE2)	HIF	Angiogenesis
Letrozole	Aromatase	Endocrinology & Hormones
Temozolomide	Others	Ubiquitin
Vincristine	Autophagy,Microtubule Associated	Cytoskeletal Signaling
Amuvatinib (MP-470)	c-Met, c-Kit, PDGFR, Flt, c-RET	Protein Tyrosine Kinase
JNJ-7706621	CDK, Aurora Kinase	Cell Cycle
Enzalutamide (MDV3100)	Androgen Receptor, P450	Endocrinology & Hormones
Celecoxib	COX	Neuronal Signaling
PD173074	FGFR, VEGFR	Angiogenesis
WYE-354	mTOR	PI3K/Akt/mTOR
Vemurafenib (PLX4032, RG7204)	Raf	MAPK
BX-795	PDK-1, IKK	PI3K/Akt/mTOR
Altretamine	Others	Others
Carmofur	Antimetabolites	DNA Damage
Epothilone A	Microtubule Associated	Cytoskeletal Signaling
Floxuridine	DNA/RNA Synthesis	DNA Damage
FT-207 (NSC 148958)	DNA/RNA Synthesis	DNA Damage
Ifosfamide	DNA/RNA Synthesis	DNA Damage
Megestrol Acetate	Androgen Receptor	Endocrinology & Hormones
Mercaptopurine (6-MP)	DNA/RNA Synthesis	DNA Damage
Streptozotocin (STZ)	Others	Others
Dexamethasone (DHAP)	IL Receptor	Others
Rigosertib (ON-01910)	PLK	Cell Cycle
Epothilone B (EPO906, Patupilone)	Microtubule Associated	Cytoskeletal Signaling
Bafetinib (INNO-406)	Bcr-Abl	Angiogenesis
Ruxolitinib (INCB018424)	JAK	JAK/STAT
Isotretinoin	Hydroxylase	Metabolism
Pelitinib (EKB-569)	EGFR	Protein Tyrosine Kinase
Zileuton	Others	Others
Ispinesib (SB-715992)	Kinesin	Cytoskeletal Signaling
Tipifarnib	Farnesyltransferase, Ras	Metabolism
Zibotentan (ZD4054)	ETA Receptor	GPCR & G Protein
Doxercalciferol	Others	Others
SB525334	TGF-beta/Smad	TGF-beta/Smad
AEE788 (NVP-AEE788)	EGFR, Flt, VEGFR, HER2	Protein Tyrosine Kinase
PHA-793887	CDK	Cell Cycle
PIK-93	PI3K, VEGFR	PI3K/Akt/mTOR
Ponatinib (AP24534)	Bcr-Abl, VEGFR, FGFR, PDGFR, Flt	Angiogenesis

Fludarabine	STAT, DNA/RNA Synthesis	JAK/STAT
Mycophenolate Mofetil	Others	Metabolism
Pracinostat (SB939)	HDAC	Cytoskeletal Signaling
SAR245409 (XL765)	PI3K, mTOR	PI3K/Akt/mTOR
AT7519	CDK	Cell Cycle
MK-1775	Wee1	Cell Cycle
Quizartinib (AC220)	Flt	Angiogenesis
AZD7762	Chk	Cell Cycle
R406 (free base)	Syk	Angiogenesis
DMXAA (Vadimezan)	VDA	Angiogenesis
EX 527 (Selisistat)	Sirtuin	Epigenetics
Febuxostat	Others	Others
Dapagliflozin	SGLT	GPCR & G Protein
AZD8055	mTOR	PI3K/Akt/mTOR
BMS-777607	c-Met	Protein Tyrosine Kinase
Pomalidomide	TNF-alpha, COX	Apoptosis
KU-60019	ATM	DNA Damage
BIRB 796 (Doramapimod)	p38 MAPK	MAPK
RO4929097	Y-Secretase	Proteases
Tie2 kinase inhibitor	Tie-2	Protein Tyrosine Kinase
Prednisone	Others	Others
Triamcinolone Acetonide	Others	Others
Allopurinol Sodium	Others	Others
Tretinoin	Others	Others
Ezetimibe	Others	Others
Estrone	Others	Endocrinology & Hormones
Aminoglutethimide	Aromatase	Endocrinology & Hormones
Disulfiram	Others	Others
Meprednisone	Others	Others
Busulfan	NULL	Others
Hydrocortisone	Others	Others
Estradiol	Others	Others
Gemcitabine	Others	DNA Damage
Azathioprine	Others	Others
Mesna	Others	Others
Toremifene Citrate	Others	Endocrinology & Hormones
Azacitidine	DNA/RNA Synthesis	DNA Damage
Teniposide	Others	Others
Simvastatin	Others	Others
Ranolazine	Others	Others
Lomustine	Others	Others
Mitoxantrone	Topoisomerase	Cell Cycle
Hydroxyurea	Others	Others
Flutamide	P450	Endocrinology & Hormones
Fluvastatin Sodium	HMG-CoA Reductase	Metabolism
Tamoxifen Citrate	Estrogen/progestogen Receptor	Endocrinology & Hormones
Maraviroc	CCR5	Microbiology
PF-573228	FAK	Angiogenesis
Cyclophosphamide Monohydrate	Others	Others
Bexarotene	Others	Others
Lapatinib	EGFR, HER2	Protein Tyrosine Kinase
LDE225 (NVP-	Smoothened	Stem Cells & Wnt
AZD1480	JAK	JAK/STAT
AG-14361	PARP	DNA Damage
MLN2238	Proteasome	Proteases
MLN9708	Proteasome	Proteases
GSK461364	PLK	Cell Cycle
CYT997 (Lexibulin)	Microtubule Associated	Cytoskeletal Signaling
SGI-1776 free base	Pim	JAK/STAT

BMS-794833	c-Met, VEGFR	Protein Tyrosine Kinase
OSI-420	EGFR	Protein Tyrosine Kinase
Formestane	Aromatase	Endocrinology & Hormones
DAPT (GSI-IX)	Gamma-secretase, Beta Amyloid	Proteases
Irinotecan HCl Trihydrate	Topoisomerase	DNA Damage
CYT387	JAK	JAK/STAT
SB590885	Raf	MAPK
TAME	APC	Cell Cycle
CAL-101 (Idelalisib, GS-1101)	PI3K	PI3K/Akt/mTOR
LY2157299	TGF-beta/Smad	TGF-beta/Smad
Telatinib	VEGFR, PDGFR, c-Kit	Protein Tyrosine Kinase
Volasertib (BI 6727)	PLK	Cell Cycle
Degrasyn (WP1130)	DUB, Bcr-Abl	Angiogenesis
BKM120 (NVP-BKM120, Buparlisib)	PI3K	PI3K/Akt/mTOR
CX-4945 (Silmitasertib)	PKC	Others
(-)-Epigallocatechin Gallate	Others	Others
Cyclosporin A	Others	Others
Gossypol	Dehydrogenase	Others
Limonin	HIV Protease	Microbiology
Oridonin	Others	Others
Phloretin	Others	Others
Tanshinone I	Phospholipase (e.g. PLA)	Metabolism
Quercetin	PI3K, PKC, Src, Sirtuin	Epigenetics
Chrysophanic Acid	EGFR, mTOR	Protein Tyrosine Kinase
Mitoxantrone HCl	Others	Others
Mycophenolic acid	Others	Others
Rosiglitazone	PPAR	DNA Damage
Medroxyprogesterone acetate	Estrogen/progestogen Receptor	Endocrinology & Hormones
Pioglitazone	Others	Others
Mifepristone	Estrogen/progestogen Receptor	Endocrinology & Hormones
Lonidamine	Others	Others
TAK-733	MEK	MAPK
LY2603618	Chk	Cell Cycle
GW3965 HCl	Liver X Receptor	Others
DCC-2036 (Rebastinib)	Bcr-Abl	Angiogenesis
GSK2126458 (GSK458)	PI3K, mTOR	PI3K/Akt/mTOR
MK-0752	Gamma-secretase	Proteases
PF-3845	FAAH	Metabolism
Trametinib (GSK1120212)	MEK	MAPK
Flavopiridol HCl	CDK	Cell Cycle
Ibrutinib (PCI-32765)	Src	Angiogenesis
NVP-BSK805 2HCl	JAK	JAK/STAT
XL335	FXR	Others
A-769662	AMPK	PI3K/Akt/mTOR
CH5132799	PI3K, mTOR	PI3K/Akt/mTOR
KX2-391	Src	Angiogenesis
YO-01027	Gamma-secretase	Proteases
Geldanamycin	HSP	Cytoskeletal Signaling
AMG-900	Aurora Kinase	Cell Cycle
PH-797804	p38 MAPK	MAPK
Dacomitinib (PF299804, PF299)	EGFR	Protein Tyrosine Kinase
Crenolanib (CP-868596)	PDGFR	Protein Tyrosine Kinase
AZ 3146	Kinesin	Cytoskeletal Signaling
TG101348 (SAR302503)	JAK	JAK/STAT
PAC-1	Caspase	Apoptosis
AZ 628	Raf	MAPK
Canagliflozin	SGLT	GPCR & G Protein
3-Methyladenine	PI3K	PI3K/Akt/mTOR
Dalcetrapib (JTT-705, RO4607381)	CETP	Metabolism

Nocodazole	Microtubule Associated	Cytoskeletal Signaling
GW4064	FXR	Others
Tofacitinib (CP-690550,Tasocitinib)	JAK	JAK/STAT
Sotrastaurin	PKC	TGF-beta/Smad
Sirtinol	Sirtuin	Epigenetics
CEP-33779	JAK	JAK/STAT
INK 128 (MLN0128)	mTOR	PI3K/Akt/mTOR
Torin 2	mTOR	PI3K/Akt/mTOR
RG108	Transferases	Epigenetics
TPCA-1	IKK	NF-κB
PF-562271	FAK	Angiogenesis
S-Ruxolitinib (INCB018424)	JAK	JAK/STAT
BAY 11-7082	IκB/IKK	NF-κB
CHIR-99021 (CT99021) HCl	PI3K/Akt/mTOR	PI3K/Akt/mTOR
Pazopanib	VEGFR	Protein Tyrosine Kinase
Daunorubicin HCl	Telomerase	DNA Damage
Dexamethasone Acetate	Others	Others
Anagrelide HCl	PDE	Metabolism
Triptolide (PG490)	Others	Others
Cabozantinib malate (XL184)	VEGFR	Protein Tyrosine Kinase
Vinorelbine Tartrate	Microtubule Associated	Cytoskeletal Signaling
Chloroambucil	DNA/RNA Synthesis	DNA Damage
Danthron	others	Others
Sulfabenzamide	others	Others
5-Chloro-8-hydroxy-7-iodoquinoline	others	Others
Vitamin E	others	Others
JNK-IN-8	JNK	MAPK
Fingolimod (FTY720) HCl	S1P Receptor, Bcr-Abl, PKC	GPCR & G Protein
VS-5584 (SB2343)	PI3K	PI3K/Akt/mTOR
Z-VAD-FMK	Caspase	Apoptosis
RG-7112	Mdm2	Apoptosis
CX-6258 HCl	Pim	JAK/STAT
LY2874455	FGFR	Protein Tyrosine Kinase
GSK2334470	PDK-1	PI3K/Akt/mTOR
GSK923295	Kinesin	Cytoskeletal Signaling
PF-3758309	PAK	Cytoskeletal Signaling
HSP990 (NVP-HSP990)	HSP (e.g. HSP90)	Cytoskeletal Signaling
AZD1208	Pim	JAK/STAT
RO5126766 (CH5126766)	Raf	MAPK
ABC294640	S1P Receptor	GPCR & G Protein
PF-543	S1P Receptor	GPCR & G Protein
CNX-2006	EGFR	Protein Tyrosine Kinase
GF109203X	PKC	TGF-beta/Smad
GSK650394	Others	Others
Deltarasin	PDE	Metabolism
IOX1	Histone demethylases	Epigenetics
Ro3280	PLK	Cell Cycle
PD173955	Bcr-Abl	Angiogenesis
PFK15	Others	Others
AZD9291	EGFR	Protein Tyrosine Kinase
AZ5104	EGFR	Protein Tyrosine Kinase
CPI-203	Epigenetic Reader Domain	Epigenetics
GSK2606414	PERK	Apoptosis
SF1670	Others	Others
TMP269	HDAC	Epigenetics
6H05	Rho	Cell Cycle
K-Ras(G12C) inhibitor 9	Rho	Cell Cycle
CW069	Microtubule Associated	Cytoskeletal Signaling
SH-4-54	STAT	JAK/STAT

CH5138303	HSP (e.g. HSP90)	Cytoskeletal Signaling
ARQ 621	Kinesin	Cytoskeletal Signaling
HS-173	PI3K	PI3K/Akt/mTOR
Phosphoramidon Disodium Salt	Others	Others
MI-2 (MALT1 inhibitor)	Others	Others
SB-3CT	MMP	Proteases
TAPI-1	Others	Others
VER-50589	HSP (e.g. HSP90)	Cytoskeletal Signaling
LDC000067	CDK	Cell Cycle
PI-1840	Proteasome	Proteases
FH535	Wnt/beta-catenin	Stem Cells & Wnt
YH239-EE	Mdm2	Apoptosis
WIKI4	Wnt/beta-catenin	Stem Cells & Wnt
INH1	Microtubule Associated	Cytoskeletal Signaling
INH6	Microtubule Associated	Cytoskeletal Signaling
ESI-09	Others	Others
HJC0350	Others	Others
HO-3867	STAT	JAK/STAT
JNK Inhibitor IX	JNK	MAPK
Voreloxin (SNS-595)	Topoisomerase	DNA Damage
Afuresertib (GSK2110183)	Akt	PI3K/Akt/mTOR
XMD8-92	ERK	MAPK
ML323	DUB	Ubiquitin
EW-7197	TGF-beta/Smad	TGF-beta/Smad
PF-06463922	ALK	Protein Tyrosine Kinase
PTC-209 HBr	Others	Others
G-749	FLT3	Angiogenesis
GDC-0623	MEK	MAPK
4SC-202	HDAC	Epigenetics
ODM-201	Androgen Receptor	Endocrinology & Hormones
AT13148	Akt	PI3K/Akt/mTOR
INCB024360	IDO	Metabolism
Santacruzamate A (CAY10683)	HDAC	DNA Damage
BV-6	IAP	Apoptosis
PX-478 2HCl	HIF	Angiogenesis
Tasquinimod	HDAC	Angiogenesis
Pilaralisib (XL147)	PI3K	PI3K/Akt/mTOR
MI-773 (SAR405838)	Mdm2	Apoptosis
PND-1186 (VS-4718)	FAK	Angiogenesis
CB-839	Others	Others
CH5183284 (Debio-1347)	FGFR	Angiogenesis
Picropodophyllin (PPP)	IGF-1R	Protein Tyrosine Kinase
AZD6738	ATM/ATR	PI3K/Akt/mTOR
AZD8186	PI3Kβ, PI3Kδ	PI3K/Akt/mTOR
LY2584702 Tosylate	S6 Kinase	PI3K/Akt/mTOR
Dovitinib (TKI258) Lactate	FLT3	Angiogenesis
Pexmetinib (ARRY-614)	p38 MAPK	MAPK
AT7519 HCl	CDK	Cell Cycle
4-Hydroxytamoxifen	Estrogen/progestogen Receptor	Endocrinology & Hormones
Licochalcone A	Estrogen/progestogen Receptor	Endocrinology & Hormones
CB1954	others	Others
Endoxifen HCl	Estrogen/progestogen Receptor	Endocrinology & Hormones
BI-847325	MEK	MAPK
SGI-7079	VEGFR	Protein Tyrosine Kinase
Oltipraz	Others	Others
Xanthohumol	COX	Metabolism
Epacadostat (INCB024360)	IDO	Metabolism
WZB117	Others	Others
TIC10	Akt	PI3K/Akt/mTOR

PU-H71	HSP	Cytoskeletal Signaling
Nutlin-3a	Mdm2	Apoptosis
Nutlin-3b	Mdm2	Apoptosis
C-DIM12	others	Others
Mitomycin C	DNA/RNA Synthesis	DNA Damage
NSC348884	p53	Apoptosis
RSL3	Ferroptosis	Metabolism
Cucurbitacin B	Microtubule Associated	Cytoskeletal Signaling
ML264	Others	Others
LTX-315	Others	Others
PRI-724	Wnt/beta-catenin	Stem Cells & Wnt
Palbociclib (PD-0332991) HCl	CDK	Others
LY2228820	p38 MAPK	MAPK
Nedaplatin	DNA/RNA Synthesis	DNA Damage
Calcium Levofolinate	Others	Others
Miltefosine	Akt	PI3K/Akt/mTOR
Fosbretabulin (Combretastatin A4	Microtubule Associated	Cytoskeletal Signaling
APTSTAT3-9R	STAT	JAK/STAT

Appendix 1-2. Anti-Cancer Library Cell Viability Screen in 231MFP and HCC38 TNBC Cells. Cells were treated with DMSO vehicle or compound (10μM) in serum-free media and cell survival was assessed 48h after treatment with Hoechst staining. Data shown from n=1.

231MFP cell survival data	% cell survival		HCC38 cell survival data	% cell survival
Mitoxantrone HCl	-1.908376526		AEE788 (NVP-AEE788)	-40.12247571
ESI-09	-1.541708049		Vemurafenib (PLX4032)	-30.58806103
TIC10	2.812653634		Gossypol	-13.35135511
Romidepsin (FK228,	3.512183612		Mitoxantrone HCl	-10.64719695
Crizotinib (PF-02341066)	4.107905344		PHA-793887	-4.719065747
Mitoxantrone	4.107905344		SH-4-54	-4.179075234
AT9283	4.130286532		ESI-09	-3.574578309
MI-773 (SAR405838)	4.281458811		WP1130	-3.363815593
SH-4-54	6.934049502		Doxorubicin (Adriamycin)	-2.856011894
NU7441 (KU-57788)	7.621014326		PIK-93	-2.443460449
INH6	8.639425001		G-749	-2.37515363
INH1	8.923843239		BI6727 (Volasertib)	-1.749088795
MLN2238	9.150508737		Pelitinib (EKB-569)	-1.084071325
MLN9708	9.938593952		Licochalcone A	-1.006910367
Daunorubicin HCl (Daunomycin	10.63641794		Daunorubicin HCl (Daunomycin	-0.627581154
YM155	10.76697426		CX-6258 HCl	-0.417933091
WP1130	11.52071047		Mitoxantrone	-0.275278653
TG101348 (SAR302503)	12.29910214		Romidepsin (FK228,	-0.153216502
Idarubicin HCl	12.31238834		PF-3758309	-0.00394579
JNK-IN-8	14.42327641		RG-7112	0.195600055
GW4064	14.46262059		Torin 2	0.240897022
Doxorubicin (Adriamycin)	14.72363329		Xanthohumol	0.337998892
GSK461364	16.16659552		AZD9291	0.57637588
PTC-209 HBr	16.3971773		AZ5104	0.742428596
RG-7112	16.4575742		KX2-391	0.742721024
SRT1720	18.70862372		GSK650394	1.011342629
Dacomitinib (PF299804,PF-	19.3149325		GW3965 HCl	1.033118965
Torin 2	19.909106		BV-6	1.228478527
Licochalcone A	20.15291092		INH6	1.375602608
Imatinib (Gleevec)	21.43210959		Deltarasin	1.483752494
BI6727 (Volasertib)	21.43284631		GSK2126458	1.487950823
PF-3758309	22.00695433		Tretinoin (Aberela)	1.557501045
MLN8237 (Alisertib)	22.52418219		Triptolide	1.603584829
Danusertib (PHA-739358)	22.60910118		BMS 794833	1.705751226
Bafetinib (INNO-406)	23.07540336		(-)-Epigallocatechin gallate	1.761037477
ARQ 621	23.38506038		Lapatinib	1.857163044
Ispinesib (SB-715992)	24.54926773		PF-562271	1.924322407
Axitinib	24.89495838		BI-847325	2.0149795
SB939 (Pracinostat)	24.89495838		TG101348 (SAR302503)	2.031154942
TMP269	25.52629165		Idarubicin HCl	2.033908371
Quercetin (Sophoretin)	25.63618227		YM201636	2.148114488
PD173074	25.97817673		ABT-737	2.170527851
Dovitinib (TKI258) Lactate	26.04752461		Plinabulin (NPI-2358)	2.24619149
HS-173	26.67148492		LY2874455	2.395310387
Triciribine (Triciribine phosphate)	26.74959449		CUDC-101	2.401968061
Fingolimod (FTY720)	27.01883792		Tubacin	2.53596296
YM201636	27.56284609		DCC-2036 (Rebastinib)	2.554596267
Cabozantinib malate (XL184)	27.6097823		MLN9708	2.555575756
AZD9291	28.38719188		Tivozanib (AV-951)	2.640235921
CUDC-101	28.56324898		Crenolanib (CP-868596)	2.719564749
GSK2126458	28.92111935		Bexarotene	2.746633856
PCI-24781	29.30462007		SNS-314 Mesylate	2.774146106

LY3009120	30.84395073		Vinorelbine Tartrate	2.794689327
BI-847325	32.23818435		AZD7762	3.116441335
Refametinib (RDEA119, Bay 86-	32.65334689		NU7441 (KU-57788)	3.131586627
KX2-391	33.03928241		MLN2238	3.191179412
Linifanib (ABT-869)	33.857604		Bortezomib (Velcade)	3.235929879
LY2228820	33.857604		Ponatinib (AP24534)	3.342370436
XL147	33.89938793		Evista (Raloxifene HCl)	3.419971591
ABT-263 (Navitoclax)	33.91430132		Vincristine	3.427270972
Ponatinib (AP24534)	33.91430132		GW4064	3.49127938
TAK-733	34.31868854		ABT-751	3.804422603
PCI-32765 (Ibrutinib)	34.37331979		Ispinesib (SB-715992)	3.813344143
CH5183284 (Debio-1347)	34.64607464		ABT-263 (Navitoclax)	3.883369103
Rucaparib (AG-014699 , PF-	35.19565733		Cyt387	4.231346868
MK-2206 2HCl	35.79438404		Sorafenib (Nexavar)	4.325752841
Masitinib (AB1010)	36.45714661		Tamoxifen Citrate (Nolvadex)	4.344193502
Simvastatin (Zocor)	36.45714661		Geldanamycin	4.580948665
SB590885	36.68937827		GSK461364	4.654202066
ABT-751	37.07916328		HS-173	4.663584949
Vatalanib 2HCl (PTK787)	37.24644893		JNJ 26854165 (Serdemetan)	4.667205791
G-749	37.76715202		INK 128 (MLN0128)	4.902912728
Belinostat (PXD101)	37.97595291		Flavopiridol (Alvocidib) HCl	4.972050181
Picropodophyllin (PPP)	38.36525636		PIK-75	5.002126727
PD 0332991 (Palbociclib) HCl	38.94289704		BX-795	5.089232428
SU11274	39.07131633		Cyclosporin A (Cyclosporine A)	5.511745723
AZ 3146	39.07387428		TW-37	5.613091554
HJC0350	39.26447092		BIBR 1532	5.65735372
LDC000067	39.55518725		Amuvatinib (MP-470)	5.771821953
BI 2536	39.64142357		Clofarabine	5.809953523
BIBF1120 (Vargatef)	39.90727717		Cladribine	5.907124343
MK-1775	39.90727717		YM155	5.92357235
SNS-032 (BMS-387032)	41.51582886		Teniposide (Vumon)	5.970945402
Rigosertib (ON-01910)	42.20299615		ENMD-2076	6.164470257
Phloretin (Dihydronaringenin)	42.48398192		BKM120 (NVP-BKM120)	6.324858016
Mocetinostat (MGCD0103)	42.93320482		Trichostatin A (TSA)	6.532751524
Bortezomib (Velcade)	43.20140284		Ganetespib (STA-9090)	6.541333663
R406 (free base)	43.20140284		Belinostat (PXD101)	6.902822019
Barasertib (AZD1152-HQPA)	43.53923408		JNJ-26481585	7.093617364
PF-3845	43.89754318		Voreloxin (SNS-595)	7.960840337
Lapatinib	43.99683987		CX-4945 (Silmitasertib)	8.147054149
Amuvatinib (MP-470)	44.20904051		AT7519	8.360746367
FH535	44.90487355		BIIB021	8.417186668
INCB024360	45.55599742		Picropodophyllin (PPP)	8.824116229
CYT997 (Lexibulin)	46.09085079		CYT997 (Lexibulin)	9.112472497
NVP-BSK805 2HCl	46.47008901		Gemcitabine (Gemzar)	9.326444963
Vinorelbine Tartrate	46.7461337		PTC-209 HBr	9.335779204
GSK1904529A	47.32419084		Regorafenib (BAY 73-4506)	9.340201705
GSK923295	47.404962		SB939 (Pracinostat)	9.408225445
HO-3867	47.43743765		Topotecan HCl	9.433932613
GSK2334470	47.97487488		PD173074	9.823029821
Motesanib Diphosphate (AMG-	48.50431293		PCI-24781	9.899313139
Tie2 kinase inhibitor	48.50431293		XL765 (SAR245409)	10.32148891
JNJ-26481585	48.68164736		Tipifarnib (Zarnestra)	10.68738428
Cyt387	48.94477048		Tie2 kinase inhibitor	11.04439529
Linsitinib (OSI-906)	48.95130687		E7080 (Lenvatinib)	11.6136469
Nocodazole	49.39099332		MK-1775	11.82177166
BMS-536924	49.88833537		Roscovitine (Seliciclib, CYC202)	11.89800227
AZD7762	49.88833537		AT7519 HCl	11.93148803
Tivozanib (AV-951)	50.04947774		Cabozantinib malate (XL184)	12.43397355
WZ4002	50.71516752		4SC-202	12.80815138

GSK2606414	50.88368506		JNJ-7706621	12.92971595
CB-839	50.88496422		PF 573228	13.0293685
GDC-0879	51.25725494		FH535	13.22131001
AZD6244 (Selumetinib)	52.51650667		CYC116	13.25866725
AT7519	52.51650667		KU-60019	13.43839863
GSK1120212 (Trametinib)	52.60243342		Azacitidine (Vidaza)	13.61250222
Evista (Raloxifene HCl)	52.62399703		Fludarabine (Fludara)	13.81663556
Sorafenib (Nexavar)	53.48429952		Dovitinib (TKI258) Lactate	14.24631235
Ezetimibe (Zetia)	53.48429952		Obatoclax mesylate (GX15-070)	14.30218542
6H05	53.59330952		AZD8055	14.38443652
EW-7197	53.59430463		Etoposide (VP-16)	14.88708282
AEE788 (NVP-AEE788)	53.70706391		AT9283	15.18416912
Y-27632 2HCl	53.73795896		Nocodazole	15.27581174
Estradiol	53.73795896		AZD1480	15.41433817
CW069	53.95007644		BMS-536924	15.43260326
SB 216763	54.17662809		Vorinostat (SAHA)	16.60464694
Pexmetinib (ARRY-614)	54.18137853		Docetaxel (Taxotere)	16.66745524
Sotrastaurin (AEB071)	54.45274815		Ku-0063794	17.2391062
BX-795	56.06058745		Mocetinostat (MGCD0103)	17.28511071
WAY-362450	56.61915652		Cediranib (AZD2171)	18.06198795
PF-562271	57.18322924		2-Methoxyestradiol	18.33456384
LY294002	57.22575603		BI 2536	18.98864479
JNJ-38877605	57.39125005		Dacomitinib (PF299804,PF-	19.05538606
Dalcetrapib (JTT-705)	57.6653694		WYE-354	19.26942737
Triptolide	57.71627179		HSP990 (NVP-HSP990)	19.53873584
PND-1186 (VS-4718)	58.53674642		OSI-930	19.63049615
XMD8-92	58.65820631		SGI-1776 free base	20.55352276
Cyclosporin A (Cyclosporine A)	59.24061694		PU-H71	20.71870028
CH5132799	59.97810961		Floxuridine (Fludara)	20.86523537
AZ5104	60.04077146		ARQ 621	21.21554014
Brivanib (BMS-540215)	60.17911237		JNK Inhibitor IX	21.66467105
SGI-1776 free base	60.42322259		Toremifene Citrate (Fareston,	22.09742875
Pilaralisib (XL147)	60.50393664		VER-50589	23.52145647
ZSTK474	60.92461996		Isotretinoin	24.07813686
Fluvastatin sodium (Lescol)	60.92461996		Fingolimod (FTY720)	24.31320755
PF-06463922	61.93981605		Paclitaxel (Taxol)	24.75284079
MI-2 (MALT1 inhibitor)	62.0524951		Nilotinib (AMN-107)	24.95603029
Topotecan HCl	62.11346675		Phloretin (Dihydronaringenin)	25.71199329
Tofacitinib (CP-690550,	62.14927875		Raltitrexed (Tomudex)	26.02576622
JNJ-7706621	62.4691454		GF109203X	26.29599688
Temsirolimus (Torisel)	62.47360199		CNX-2006	26.70783697
Aminoglutethimide (Cytadren)	62.47360199		Rosiglitazone (Avandia)	28.17190732
CYC116	62.50105174		Epothilone B (EPO906)	28.83193426
TPCA-1	62.50149801		Quizartinib (AC220)	28.96416689
YH239-EE	63.14297697		Entinostat (MS-275, SNDX-275)	29.38988154
4SC-202	64.01298582		HO-3867	30.09500629
Maraviroc	64.82826217		LDC000067	30.45752773
KU-55933	65.21065245		Sunitinib Malate (Sutent)	31.38851827
AG14361	66.31599246		Rigosertib (ON-01910)	34.21621053
CH5138303	66.61879225		SF1670	34.72596831
AZD1208	66.64600359		Ro3280	35.10636362
Lapatinib Ditosylate (Tykerb)	67.21189966		Bafetinib (INNO-406)	35.35408628
BIRB 796 (Doramapimod)	67.21189966		CH5138303	35.76193347
E7080 (Lenvatinib)	67.83367065		Fludarabine Phosphate (Fludara)	36.00035179
Tubacin	68.50609508		SB 525334	36.0097242
Phosphoramidon Disodium Salt	68.60850287		MI-773 (SAR405838)	36.50464103
ABT-888 (Veliparib)	68.73578815		PAC-1	37.10775119
Mycophenolate mofetil (CellCept)	68.73578815		LY3009120	37.65127144
RG108	68.73587182		LY2603618 (IC-83)	38.30724442

Pioglitazone (Actos)	68.89580682		GSK2606414	39.11486521
Lenalidomide (Revlimid)	69.49509838		AUY922 (NVP-AUY922)	39.81578144
RO4929097	69.49509838		AZD6738	40.29420456
Gossypol	69.95198105		LY2228820	41.0253037
VER-50589	70.29389882		Simvastatin (Zocor)	41.07178452
AMG 900	70.30111629		Adrucil (Fluorouracil)	41.36311421
PF 573228	70.38250576		SU11274	41.59005503
Lonidamine	70.50731502		Bosutinib (SKI-606)	41.73144374
PF-04217903	71.05902505		Flavopiridol (Alvocidib)	42.08034108
Z-VAD-FMK	71.270382		Dovitinib (TKI-258)	44.17245433
BMS-599626 (AC480)	71.35263943		17-AAG (Tanespimycin)	44.28286393
Toremifene Citrate (Fareston,	71.35263943		17-DMAG HCl (Alvespimycin)	45.97563373
Mifepristone (Mifeprex)	71.65437012		TPCA-1	46.12191194
Gefitinib (Iressa)	72.04705365		Quercetin (Sophoretin)	46.1375507
Pomalidomide	72.04705365		SNS-032 (BMS-387032)	46.38284689
Afuresertib (GSK2110183)	72.07577382		Pilaralisib (XL147)	46.97561873
WIKI4	72.09996808		K-Ras(G12C) inhibitor 9	47.76027227
Tipifarnib (Zarnestra)	72.20017566		Carmofur	47.90657199
SGX-523	74.09816009		BIRB 796 (Doramapimod)	48.22950671
TW-37	74.2362518		CI-1040 (PD184352)	48.40501889
BV-6	74.46617475		Abitrexate (Methotrexate)	48.81151133
CHIR-99021 (CT99021) HCl	74.7258394		Vandetanib (Zactima)	48.86152373
SB 203580	74.72766281		Afuresertib (GSK2110183)	49.96303927
CEP33779	74.76552504		Temozolomide	50.58818593
Vismodegib (GDC-0449)	76.15572655		Mercaptopurine	52.02287964
MK-0752	76.70230018		Imatinib (Gleevec)	52.35915084
Oltipraz	76.84746169		VS-5584 (SB2343)	53.0446924
2-Methoxyestradiol	77.07279276		Dasatinib (BMS-354825)	54.24386824
Ifosfamide	77.22188878		CH5183284 (Debio-1347)	54.8764843
Bexarotene	77.68888638		PCI-32765 (Ibrutinib)	55.25948727
Medroxyprogesterone acetate	78.0577761		Aprepitant (MK-0869)	55.97065684
Santacruzamate A (CAY10683)	78.26657007		Bleomycin sulfate	56.06045043
AUY922 (NVP-AUY922)	78.53211632		Endoxifen HCl	56.47273736
Hydroxyurea (Cytodrox)	78.53211632		SB590885	57.89264948
BKM120 (NVP-BKM120)	78.83965609		TAK-733	59.07877626
Imatinib Mesylate	79.12871769		ZSTK474	59.51090087
KU-60019	79.12871769		GSK1120212 (Trametinib)	59.54902721
GDC-0623	80.16498406		PI-103	60.85211007
Endoxifen HCl	80.92629544		CH5132799	62.15006279
ODM-201	81.01088109		Irinotecan HCl Trihydrate	62.29177194
CPI-203	81.46619038		Refametinib (RDEA119, Bay 86-	62.41895876
LDE225 (NVP-LDE225,	81.52068206		PD173955	62.63431578
Flavopiridol (Alvocidib) HCl	82.15180818		R406 (free base)	63.02966486
Tasquinimod	82.41512949		CEP33779	63.30373667
Flavopiridol (Alvocidib)	83.29965367		PHA-665752	63.38181395
LY2584702 Tosylate	83.38406769		Pexmetinib (ARRY-614)	63.81548011
IWP-2	84.0732548		Axitinib	63.84605775
Afatinib (BIBW2992)	84.19664961		PD0325901	64.97728468
Quizartinib (AC220)	84.19664961		GDC-0623	65.04722127
Adrucil (Fluorouracil)	85.05181534		Flutamide (Eulexin)	65.38007033
Epothilone A	85.2227361		CPI-203	66.24214705
A-769662	85.34297281		NVP-BSK805 2HCl	66.57782402
PI-1840	85.36277895		XMD8-92	67.5614955
Doxercalciferol (Hectorol)	85.49407426		AZ628	68.4740327
CI-1040 (PD184352)	85.54270726		Fluvastatin sodium (Lescol)	69.62633415
Dapagliflozin	85.54270726		Afatinib (BIBW2992)	69.63599514
Fulvestrant (Faslodex)	85.92187819		GDC-0941	70.63503946
YO-01027	86.13083709		Doxercalciferol (Hectorol)	70.98220356
Enzastaurin (LY317615)	86.42223745		Danusertib (PHA-739358)	71.29582168

Mesna (Uromitexan, Mesnex)	86.42223745		VX-680 (MK-0457, Tozasertib)	71.76252314
JNK Inhibitor IX	86.85716099		JNK-IN-8	72.53503903
Obatoclax mesylate (GX15-070)	87.11159241		Rucaparib (AG-014699 , PF-	74.11942893
Azacitidine (Vidaza)	87.11159241		XL147	74.57059843
PU-H71	87.23374962		Irinotecan	74.87762882
Bosutinib (SKI-606)	87.54619498		MLN8237 (Alisertib)	75.19164564
DMXAA (ASA404)	87.54619498		AMG 900	76.26230989
ABC294640	87.90865336		PF-3845	76.4800716
GF109203X	88.0867043		BIBF1120 (Vargatef)	77.11800588
PHA-665752	88.16102235		Pazopanib	77.3771596
Flutamide (Eulexin)	88.16102235		CHIR-99021 (CT99021) HCl	77.74435627
WYE-354	88.27277352		Brivanib (BMS-540215)	79.41590537
AT7519 HCl	88.2805787		YH239-EE	80.22600183
Entinostat (MS-275, SNDX-275)	88.4271641		Azathioprine (Azasan, Imuran)	80.92275745
Azathioprine (Azasan, Imuran)	88.4271641		Lapatinib Ditosylate (Tykerb)	81.82963989
Docetaxel (Taxotere)	89.513609		EW-7197	81.89719864
	89.64463878		PND-1186 (VS-4718)	81.96813519
Tamoxifen Citrate (Nolvadex)	89.64463878		KU-55933	82.89480661
ML323	90.2023186		GSK923295	83.15858068
PF-543	90.33458846		Crizotinib (PF-02341066)	83.63703207
LY2603618 (IC-83)	91.37750136		LY294002	83.85708204
Cyclophosphamide monohydrate	92.8217561		Temsirolimus (Torisel)	84.03503703
Erlotinib HCl	93.37214517		AZD6244 (Selumetinib)	84.15828302
BMS 777607	93.37214517		GSK2334470	84.44224221
ENMD-2076	93.71011234		Rapamycin (Sirolimus)	86.01199434
Ganetespib (STA-9090)	94.9652184		Barasertib (AZD1152-HQPA)	86.08527707
OSI-930	95.25064807		SRT1720	87.61130602
(-)-Epigallocatechin gallate	96.04825919		PI-1840	87.7228868
Bendamustine HCL	96.71815304		Gefitinib (Iressa)	88.69480383
LY2157299	97.05991414		MI-2 (MALT1 inhibitor)	88.72261347
Chloroambucil	97.12781066		Mifepristone (Mifeprex)	88.79492501
Vincristine	97.3257498		Nutlin-3b	88.87424258
GSK690693	97.8534939		Nutlin-3a	88.92289085
SB-3CT	97.90720478		BMS-599626 (AC480)	89.28874314
AZD1480	98.21845866		ML323	89.31948309
XAV-939	98.50583179		PD 0332991 (Palbociclib) HCl	89.39364892
Streptozotocin (Zanosar)	99.33124579		AZD8186	89.89258904
Epacadostat (INCB024360)	99.56603726		WIKI4	90.48264708
Nilotinib (AMN-107)	99.63499767		Sirtinol	91.04673622
Prednisone (Adasone)	99.63499767		PFK15	91.31827426
Fludarabine Phosphate (Fludara)	99.92476781		HJC0350	91.33413672
AZ628	100.0137501		Lenalidomide (Revlimid)	91.55717488
Pazopanib	100.3592941		INH1	91.83181141
PIK-93	100.8942144		Saracatinib (AZD0530)	91.87176126
Etoposide (VP-16)	101.3809439		Dalcetrapib (JTT-705)	91.92009871
MDV3100 (Enzalutamide)	102.5526562		AZ 3146	91.98618472
DAPT (GSI-IX)	102.7049244		SB-3CT	92.16269382
Dasatinib (BMS-354825)	102.7685559		INCB024360	92.51327892
AZD8055	102.7685559		Olaparib (AZD2281)	93.07571759
LY2874455	103.2647176		Everolimus (RAD001)	93.80260355
PX-478 2HCl	103.4202461		TAPI-1	93.99283909
Exemestane	104.6639003		Motesanib Diphosphate (AMG-	94.14586693
Crenolanib (CP-868596)	105.0422437		AZD1208	94.24137034
Dovitinib (TKI-258)	105.159239		RG108	94.7489834
Febuxostat (Uloric)	105.159239		Erlotinib HCl	94.79329124
SB 431542	105.8589469		GDC-0994	94.90591078
Lomustine (CeeNU)	105.8589469		CW069	95.34274392
PH-797804	106.1110378		Canagliflozin	95.4535463
Altretamine (Hexalen)	106.2898141		PF-06463922	96.31195587

Paclitaxel (Taxol)	106.5147212		S-Ruxolitinib	96.67249908
Epothilone B (EPO906)	106.9255818		AG14361	96.68477025
Zibotentan (ZD4054)	107.0059014		PH-797804	96.79701351
Cediranib (AZD2171)	107.1380094		Tasquinimod	96.81122457
EX 527	107.1380094		YO-01027	96.95746435
Vemurafenib (PLX4032)	107.165192		ABT-888 (Veliparib)	97.23132451
Floxuridine (Fludara)	107.7566408		Lonidamine	97.29833303
Andarine (GTX-007)	107.8951812		Linifanib (ABT-869)	97.30644848
Cladribine	108.1642116		ODM-201	98.55993318
Thalidomide	108.3584064		MK-0752	98.73909747
BMS 794833	108.4707884		Triciribine (Triciribine phosphate)	99.36367601
Itraconazole (Sporanox)	108.5773153		Oltipraz	99.533884
AZD8186	108.7172082		Nutlin-3	99.55032009
Rapamycin (Sirolimus)	109.0119252		Epothilone A	100.9350337
Tretinoin (Aberela)	109.0119252		LY2584702 Tosylate	100.9988301
Chrysophanic acid	109.4044026		Santacruzamate A (CAY10683)	101.3153694
GW3965 HCl	109.5285492		Linsitinib (OSI-906)	101.336166
BIIB021	109.6658595		SGX-523	101.337636
Celecoxib	109.8967164		Mycophenolate mofetil (CellCept)	101.8645319
GDC-0941	110.2036468		A-769662	102.4659034
Ranolazine (Ranexa)	110.2036468		Epacadostat (INCB024360)	102.543853
Regorafenib (BAY 73-4506)	110.2685364		3-Methyladenine	103.7662107
Ku-0063794	110.4949241		PX-478 2HCl	103.7940306
Sunitinib Malate (Sutent)	111.1082207		SB 431542	104.0053278
Estrone	111.1082207		Phosphoramidon Disodium Salt	104.3019871
CX-4945 (Silmitasertib)	111.6540694		IWP-2	105.0085369
Formestane	113.0804839		Imatinib Mesylate	105.0233505
Saracatinib (AZD0530)	113.4980709		GSK1904529A	105.0964555
XL765 (SAR245409)	113.4980709		Anagrelide HCl	105.1485957
Abitrexate (Methotrexate)	114.4934767		Ostarine (MK-2866)	105.1951896
Letrozole	114.8953775		CB-839	105.4119383
GDC-0994	115.0313741		TIC10	105.546209
AZD6738	115.1569811		Enzastaurin (LY317615)	105.6223968
Clofarabine	115.5816553		Vatalanib 2HCl (PTK787)	105.7737841
Rosiglitazone (Avandia)	115.8311093		Hydroxyurea (Cytodrox)	105.9399024
Roscovitine (Seliciclib, CYC202)	115.8605481		PF-04217903	106.1204599
BAY 11-7082 (BAY 11-7821)	116.1845797		BTZ043 racemate	106.2642354
Mycophenolic (Mycophenolate)	117.0151058		Iniparib (BSI-201)	107.4337243
JNJ 26854165 (Serdemetan)	117.0527511		Estradiol	107.7912026
Ro3280	117.1828766		Pioglitazone (Actos)	107.7981907
K-Ras(G12C) inhibitor 9	117.237382		Z-VAD-FMK	108.7984223
3-Methyladenine	117.2763689		Y-27632 2HCl	109.1845489
INK 128 (MLN0128)	117.7837405		GSK690693	109.4857447
Nutlin-3a	117.7991029		WAY-362450	109.6574131
Dacarbazine (DTIC-Dome)	117.9346082		Medroxyprogesterone acetate	109.8806389
Geldanamycin	118.1073334		BAY 11-7082 (BAY 11-7821)	110.1368523
PD173955	118.3128733		WZ4002	110.2937651
VS-5584 (SB2343)	119.6671485		Dexamethasone acetate	110.4425091
Decitabine	119.871525		Chloroambucil	111.1260191
DCC-2036 (Rebastinib)	120.5264891		Masitinib (AB1010)	111.4797971
SF1670	120.6556887		AT13148	111.5592005
Vorinostat (SAHA)	120.9333592		SB 216763	111.7017359
Busulfan (Myleran, Busulfex)	120.9333592		Sotrastaurin (AEB071)	111.7093531
TAME	121.1943909		Tofacitinib (CP-690550,	112.4571867
Telatinib (BAY 57-9352)	123.8923559		Elesclomol	112.5586248
Olaparib (AZD2281)	124.3738688		OSI-420	112.5845149
Teniposide (Vumon)	124.3738688		IOX1	113.1421651
ABT-737	125.4566648		Vismodegib (GDC-0449)	114.4254826
Fludarabine (Fludara)	125.4566648		ABC294640	115.1168546

OSI-420	127.4591032		MK-2206 2HCl	116.2816082
Irinotecan HCl Trihydrate	128.7394096		RO5126766 (CH5126766)	116.9694693
AT13148	129.1647655		SB 203580	117.9081319
Valproic acid sodium salt	129.2583845		Dacarbazine (DTIC-Dome)	118.9224242
Anagrelide HCl	130.8050012		Andarine (GTX-007)	119.0861493
CAL-101 (GS-1101)	131.0469702		XAV-939	122.508988
17-AAG (Tanespimycin)	131.2266488		BMS 777607	123.0919449
Xanthohumol	131.6855923		JNJ-38877605	124.4474405
TAPI-1	131.7010989		Oxaliplatin (Eloxatin)	124.9117422
PD0325901	134.0517784		GDC-0879	124.9547729
Triamcinolone Acetonide	134.0517784		6H05	126.3565814
S-Ruxolitinib	134.389637		Lomustine (CeeNU)	130.2311699
Voreloxin (SNS-595)	134.4829674		Decitabine	131.6609769
VX-680 (MK-0457, Tozasertib)	134.5447984		DMXAA (ASA404)	131.8975205
Hydrocortisone (Cortisol)	134.5447984		LY2157299	133.5468666
Nutlin-3b	135.6710785		PF-543	138.3020677
Bicalutamide (Casodex)	135.6859198		Letrozole	140.2842843
Sirtinol	136.1287988		Ranolazine (Ranexa)	140.3742589
Zileuton	136.8871366		EX 527	144.6046813
Capecitabine (Xeloda)	138.7621863		Celecoxib	149.7156144
17-DMAG HCl (Alvespimycin)	139.0593276		Megestrol Acetate	152.3425796
GSK650394	139.2333409		Febuxostat (Uloric)	152.3477795
Megestrol Acetate	139.9786217		Mycophenolic (Mycophenolate)	154.0199048
Everolimus (RAD001)	140.1821893		Bendamustine HCL	154.5632931
PI-103	140.406734		Thalidomide	155.1051417
Allopurinol Sodium	140.406734		Fulvestrant (Faslodex)	157.8328077
Ruxolitinib (INCB018424)	141.478535		Exemestane	158.5130014
SB 525334	142.9187981		Nelarabine (Arranon)	160.2777132
Ftorafur	143.4540163		Capecitabine (Xeloda)	161.2276684
CNX-2006	144.5581916		Anastrozole	161.8861615
SNS-314 Mesylate	148.1513603		Dapagliflozin	162.0609436
Bleomycin sulfate	148.4715224		Estrone	162.5702627
Nelarabine (Arranon)	151.3708809		Itraconazole (Sporanox)	165.2444851
Ostarine (MK-2866)	151.4513753		Bicalutamide (Casodex)	165.5874025
Iniparib (BSI-201)	152.8426043		Ezetimibe (Zetia)	168.0184203
Pelitinib (EKB-569)	153.1810319		Valproic acid sodium salt (Sodium	169.4623
CX-6258 HCl	154.1400409		Dimesna	169.9111782
Dexamethasone acetate	155.3702715		Mesna (Uromitexan, Mesnex)	179.980469
Oxaliplatin (Eloxatin)	155.7297833		Chrysophanic acid (Chrysophanol)	186.3453518
Carmofur	157.4817614		Betapar (Meprednisone)	187.7299582
Canagliflozin	157.9003752		Busulfan (Myleran, Busulfex)	187.8931226
Trichostatin A (TSA)	159.8765262		Prednisone (Adasone)	188.2197775
Disulfiram (Antabuse)	159.8765262		Allopurinol Sodium	191.5667058
Aprepitant (MK-0869)	160.9443236		Telatinib (BAY 57-9352)	191.7901884
PIK-75	161.2730466		LDE225 (NVP-LDE225,	193.7440649
Vandetanib (Zactima)	161.4737973		Hydrocortisone (Cortisol)	195.4609968
Betapar (Meprednisone)	161.4737973		Aminoglutethimide (Cytadren)	195.7427478
IOX1	162.0456602		Triamcinolone Acetonide	195.7642154
BTZ043 racemate	162.155318		Pomalidomide	197.7372836
Isotretinoin	162.8502138		Disulfiram (Antabuse)	198.5571952
BIBR 1532	165.5628392		RO4929097	199.5604139
Elesclomol	166.7656768		TMP269	201.3144769
Gemcitabine (Gemzar)	166.7656768		MDV3100 (Enzalutamide)	207.3042652
PAC-1	170.7247235		Cyclophosphamide monohydrate	213.3913561
PHA-793887	171.2063806		Maraviroc	216.0180155
Mercaptopurine	173.525835		Zileuton	236.6315384
Irinotecan	185.7418056		DAPT (GSI-IX)	246.0788329
HSP990 (NVP-HSP990)	185.9571238		TAME	257.1355255
Anastrozole	186.3942161		Dexamethasone	264.0818655

Raltitrexed (Tomudex)	187.1635175		CAL-101 (GS-1101)	266.277771
Deltarasin	190.8723018		Zibotentan (ZD4054)	272.8664507
PFK15	191.5894548		Formestane	274.0358862
Temozolomide	210.7396069		Ruxolitinib (INCB018424)	289.2887178
Dexamethasone	214.6822913		Ftorafur	339.6059876
Dimesna	222.7723316		Altretamine (Hexalen)	367.5165282
Plinabulin (NPI-2358)	269.8391253		Streptozotocin (Zanosar)	388.2813237
RO5126766 (CH5126766)	333.7477799		Ifosfamide	395.9289247

Appendix 1-3. isoTOP-ABPP Analysis of Licochalcone A in 231MFP TNBC Cells. Competitive isoTOP-ABPP to map licochalcone A targets. We mapped the cysteine-reactivity of licochalcone A by pre-incubating licochalcone A (10μM) for 30min in 231MFP breast cancer cell proteomes, prior to labeling with the cysteine-reactive iodoacetamide-alkyne (IAyne) probe (100μM, 30min). Probe labeled proteins were the tagged with an isotopically light (for control) or heavy (for licochalcone A-treated) biotin-azide tag tag bearing a TEV protease recognition site by CuAAC. Control and treated proteomes were then mixed in a 1:1 ratio, probe labeled proteins were avidin-enriched and tryptically digested. Probe-labeled tryptic peptides were avidin-enriched again and released by TEV protease and analyzed by quantitative proteomic methods and light to heavy peptide ratios were quantified. Light to heavy ratios of ~1 indicate peptides that were labeled by IAyne, but not bound by licochalcone A. We designate light to heavy ratios of >10 as targets (in red) that were bound by licochalcone A. Table shows processed isoTOP-ABPP proteomic data showing those probe-modified peptides that were identified in at least 2 out of 4 biological replicates.

Peptide	Modified Residue	Avg. area ratio	Uniprot ID	seen in
IAIC*GAISTYNR	C239	26.64651434	Q14914 F2Z3J9	4
VMALQEAC*EAYLVGLFEDTNLCAIHAK	C97	12.01466035	P68431	3
ANSSVVSVNC*K	C596	9.73063	O60502 O60502	2
LVFLAC*CVAPTNPR	C301	8.945675	Q14566	2
VVDNGSGMC*K		8.604373333	Q562R1	2
GNLNFTC*DGNSVISPVGNR	C24	8.215105	Q15269	2
RVDDFEAGAAAGAAPGEEDLC*AAFNVI	C105 C98	5.125065523	Q13158	2
C*QLEINFNTLQTK	C351	4.710625621	P12814 O43707	2
AATMSAVEAATC*R	C266	4.59163599	A0A0A0MQS1	3
GLVLIAFSQYLQQC*PFDEHVK		4.469170189		3
C*FIVGADNVGSK		4.444024639	P05388	2
C*GALLACLLLVLPVSEANFCLYFR		4.148601046	H7BXT0	2
C*DSSPDSAEDVR		3.918607674	P02765	4
GHVLGNGSQVTQAANSGC*SK	C560	3.915851031	Q86V48 Q86V48	2
C*PSIAAAIAAVNALHGR	C456	3.727171496	Q14498 Q14498	2
TGQYSGIYDC*AK	C311	3.717025	Q6NUK1 Q6NUK1	2
PVMSGNTAYPVISC*PPLTPDWGVQDV	C350	3.578791026	P22234	2
ELQEGTYVMVAGPSFETVAEC*R	C206	3.29322	P00491	2
ISSINSISALC*EATGADVEEVATAIGMD	C174	3.264903657	O60701 O60701	3
LGEWVGLC*K		3.203577976	P25398	3
VELTVTSSDHPEDTANVTVTVLSTKQTE		3.069587158	H3BSM2	2
ITNSLTVLC*SEK	C153 C66	2.99806	H0YGJ7 O75822	2
SGETEDTFIADLVVGLC*TGQIK		2.765956403	P06733	3
DLIMDNC*EELIPEYLNFIR		2.684615185	Q58FG1	2
SIPLEC*PLSSPK	C147	2.683542166	Q92667 I3L2N7	2
NLAVAMC*SR	C55	2.490719469	Q5JS54 E2QRC7	3
IIDLEEAEDEIEDIQQEITVLSQC*DSPYV	C77	2.474442851	Q9Y6E0 B4DR80	2
AKENDENC*GPTTTVFVGNISEK	C83	2.44639	P49756	2
C*LLIHPNPESALNEEAGR	C147	2.356570836	Q16763 K7EPJ1	3
AIANEC*QANFISIK	C535	2.331095	P55072	2
LAEQC*GGLQGFLIFRSFGGGTGSGFT	C96	2.313799006	A6NHL2 A6NHL2	4
RPLNPLASGQGTSEENTFYSWLEGLC*	C241	2.238316667	Q96HE7	2
VAHALAEGLGVIAC*IGEK	C127	2.236486046	P60174 P60174	4
LSLQNC*CLTGAGCGVLSSTLR		2.15108	P13489	2
SNTGGQAFPQC*VFDHWQILPGDPFDN	C812	2.10366	P13639	2
TFVDFFSQC*LHEEYR		1.998479289	Q53GQ0	3
VFNVFC*LYGNVEK		1.997432177	M0QXS5 P14866	2

LGMAVSSDTC*R	C35	1.966753333	Q7Z4G1 Q7Z4G1	2
LYQVEYAMEAIGHAGTC*LGILANDGVL	C34	1.959703333	H0YL69 P25789	2
MPC*QLHQVIVAR	C640	1.942539996	P17655	2
AQDIEAGDGTTSVVIIAGSLLDSC*TK	C90	1.882056504	P50991 P50991	3
GALVTVGQLSC*YDQAK		1.862405	B4DLN1	2
NIELIC*QENEGENDPVLQR		1.859772378	Q15691	2
QLPSLAC*K		1.765435083	P42166	2
VPADTEVVC*APPTAYIDFAR	C42	1.733110759	P60174 P60174	2
LFTEVEGTC*TGK	C38 C34	1.73142	P62487 H0YEE4	2
C*SWLVPSPK	C210	1.718206663	Q3SXM5 Q3SXM5	3
C*VYTYIQEFYR	C948 C892	1.715629268	B5MCI0	2
FGANAILGVSLAVC*K		1.712474043	P06733	2
EVFGSGTAC*QVCPVHR	C250 C342 C334	1.678385418	B3KSI3 M0QZP4	2
VVVAENFDEIVNNENKDVLIEFYAPWC*		1.632490473	P30101	4
TTANAIYC*PPK	C29	1.63058855	O00231 O00231	2
IIAIANYVC*R	C525 C637	1.605206486	A0A0A0MRB1	2
ATC*IGNNSAAAVSMLK	C163	1.601672534	H0YL69 P25789	3
PGENC*SPAWGAAPAAYDAADTHLR	C16	1.600415783	Q14353 Q14353	2
ETAAAC*VEK		1.59218877	E9PGT1 Q15631	4
APVAGTC*YQAEWDDYVPK	C168	1.58679365	P30086	3
AASLLLEILGLLC*K	C1385 C1188 C1297	1.578038522	Q04637 Q04637	2
TIDGQQTIIAC*IESHQFQPK	C157	1.574920928	P52907	2
SSILLDVKPWDDETDMAQLEAC*VR	C193 C174 C217 C583	1.561461622	P29692 E9PRY8	2
LLC*GLLAER	C81	1.54361107	P14174	3
LISPNLGVVFFNAC*EAASR	C316	1.543356956	Q66K74 Q66K74	2
VIVVGNPANTNC*LTASK	C155	1.528476206	C9JRL4 P40925	4
ALPAAAWSLYQAGC*SLR		1.520821536	Q9H6W3	3
GLPFGC*SKEEIVQFFSGLEIVPNGITLP	C122	1.519627923	P31943 G8JLB6	3
C*GLVASNLNLKPGECLR	C3	1.518540497	P09382	2
GCC*LEKMPWSQLCGELPPLYGAEPEA	C264	1.508846265	Q9P209	2
LQEVPHEGPMC*DLLWSDPDDR		1.47993	E5RHC1 P67775	2
LLNLVYDVTPPELVDLVITELGMIPC*SS	C530 C508 C506	1.47812652	E7ERK9 Q9UI10	3
IALESEGRPEEQMESDNC*SGGDDDWT		1.473997354	Q13501	2
TQLGAIYIDASC*LTWEGQQFQGK	C38	1.467751744	H3BRV9 P61970	3
TQLAVC*QQR	C396	1.466527045	Q02790 H0YFG2	2
VNPC*IGGVILFHETLYQK	C127	1.466357477	P04075 P04075	3
IYEGQVEVTGDEYNVESIDGQPGAFTC*	C144	1.465278527	P46777 Q5T7N0	2
MAC*PLDQAIGLLVAIFHK	C3	1.446075354	P06703 R4GN98	2
ASVSVMEEEFLLEAMEGPPELYIPDMA	C534 C550 C376	1.443807552	Q6ZRS4 Q6ZRS4	2
YLLQYQEPIPC*EQLVTALCDIK	C107 C83	1.431774324	H0YL69 H0YN18	2
LMHLFTSGDC*K	C91	1.42968	Q8WXD5	2
IDLLDDSC*IKNEEAEALAK	C130	1.428318242	Q9ULC3	2
DIAQQLQATC*TSLGSSIQGLPTNVKDQ	C340	1.428142982	O60664 O60664	2
IINDNATYC*R		1.425314412	O00567	3
LDYFLLSHSLLPALC*DSK		1.416047357	P27695	2
ILQMEEEYIQQLC*EDIIQLKPDVVITEK	C234	1.410842485	P49368 B4DUR8	2
WHLC*PTLYESR	C264	1.410245389	Q9H3H3 Q9H3H3	3
YSYVC*PDLVK	C235	1.401510825	P61158	2
FVLSGANIMC*PGLTSPGAK	C113	1.395733968	Q9ULC4	3
IIYGGSVTGATC*K	C218	1.39304724	P60174 P60174	3
NNAFPC*QVNIK	C675	1.392166058	Q9NQW6	3
ILLLC*VGEAGDTVQFAEYIQK		1.391115	P49721	2
VLFPGCTPPAC*LLDGLVR	C414	1.387656906	Q66K74 Q66K74	2
VSNSPSQAIEVVELASAFSLPIC*EGLTQ	C233	1.38543	Q96EY7 Q96EY7	2
LHAVNAEEC*NVLQGR	C333	1.380975273	O75521	2
MLPDKDC*R	C80 C118	1.378335981	E9PK25 G3V1A4	3
APPWVPAMGFTLAPSLGC*FVGSR	C19	1.372239545	B1AH87 P30536	4
TFC*QLILDPIFK	C290	1.371150443	P13639	3
LTVVDTPGYGDAINC*R	C83 C71 C122 C121	1.368160958	C9J2Q4 C9J938	3

			C9IZU3 Q15019	
VVNSETPVVVDFHAQWC*GPCK	C90	1.366216659	Q99757 F8WDN2	2
PPVLFSSALSQPDFLQMLSETC*RWLP	C142	1.365307389	P52952	2
KITIADC*GQLE	C161	1.363956844	P62937	3
AETSDVANAVLDGADC*IMLSGETAK	C401	1.361728232	P30613 P30613	3
EGILSDEIYC*PPETAVLLGSYAVQAK	C117	1.356818418	P15311 E7EQR4	2
ENVPPGPEVC*ITHQEGEK	C316 C156 C14	1.35051616	Q9UHB6 F8VS07	2
GLYGIKDDVFLSVPC*ILGQNGISDLVK	C322	1.347871433	P00338 P00338	4
QYDADLEQILIQWITTQC*R	C38	1.347709467	P37802 P37802	3
GFC*FLEYEDHK	C153 C137 C194 C191	1.343605	B4DT28 O43390	2
LALFNPDVC*WDR	C44	1.335553767	O00483	4
ITVVGVGQVGMAC*AISILGK		1.335248398	P07195	4
LFVSDGVPGC*LPVLAAAGR	C12	1.333419374	P56192 F8VPL7	2
VGLTNYAAAYC*TGLLLAR	C100	1.330457931	P46777 Q5T7N0	4
TLIQNC*GASTIR	C410	1.330040886	P49368 B4DUR8	3
SC*VEEPEPEPEAAEGDGDK	C101	1.327689974	P51858 P51858	2
GC*ELVDLADEVASVYQSYQPR		1.326855245	Q7Z434	2
TIIPLISQC*TPK	C212 C105	1.323479281	P40926 P40926	3
YYSSEPQAVDFLEC*AEEAR		1.319086295	P05120	4
KQVVIDGETC*LLDILDTAGQEEYSAMR	C51	1.311975	P01116 P01112	2
VIGSGC*NLDSAR	C192	1.311839551	P00338 P07195	2
LNQSAENGSSLPSAASSC*AEAR	C27	1.309064529	Q8NB90 Q8NB90	2
LC*AAAASILGKPADR		1.303835199	J3KQ18	4
IIPGFMC*QGGDFTR	C62	1.301088781	P62937	2
EGILNDDIYC*PPETAVLLASYAVQSK		1.30069681	P26038	4
EKIEAELQDIC*NDVLELLDK	C94	1.297269431	P31946 P31946	4
YHALLIPSC*PGALTDLASSGSLAR	C18 C94 C32	1.291373045	Q8NB37 H0YF25	2
GLPWSC*SVEDVQNFLSDCTIHDGAAG		1.29056	P52597	2
IETELRDIC*NDVLSLLEK		1.287924392	E7EX29	4
EEFASTC*PDDEEIELAYEQVAK		1.286052638	O00299	4
APPSSGAPPASTAQAPC*GQAAYGQFG	C78	1.283604667	G5EA31 P53992	2
LADDVDLEQVANETHGHVGADLAALC*	C415	1.27884015	P55072	2
C*ATSKPAFFAEK		1.275133092	P04083	2
C*YEMASHLR		1.269260017	P07737	4
ALANSLAC*QGK	C393	1.26872056	P04075 P04075	3
HTGPGILSMANAGPNTNGSQFFIC*TAK	C115	1.265182349	P62937	4
YASIC*QQNGIVPIVEPEILPDGDHDLKR	C232	1.259998688	P04075 P04075	3
SIC*TTVLELLDKYLIANATNPESK	C94	1.259732351	P27348	4
GLAAALLLC*QNK	C645	1.259335457	O43290	3
C*AMTALSSK		1.253965705	Q99832	2
YADLTEDQLPSC*ESLKDTIAR		1.252050796	P18669	4
LMEPIYLVEIQC*PEQVVGGIYGVLNR	C751	1.24832524	P13639	3
TCNC*ETEDYGEKFDENDVITCFANFES	C372	1.248325	Q00839 Q00839	2
AVASQLDC*NFLK		1.239416529	A0A087X2I1	3
VAVSADPNVPNVVVTGLTLVC*SSAPG	C79	1.236977289	J3KTF8 P52565	4
AVLFC*LSEDKK	C39 C77	1.235654476	E9PK25 G3V1A4	4
SQEATEAAPSC*VGDMADTPR	C241 C84	1.233456336	Q9UHD8 Q9UHD8	3
GISEFIVMAADAEPLEIILHLPLLC*EDK	C73	1.232554821	B1AHD1 P55769	2
IYLCDIGIPQQVFQEVGINYHSPFGC*K	C499	1.229935	Q96F86	2
ALLYLC*GGDD		1.229854284	P07355 P07355	2
SCFLCMVC*K		1.226065246	P21291	2
LC*SAHGVLVPGGFGVR	C362	1.225093712	P17812 P17812	2
ELLTEFGYKGEETPVIVGSALC*ALEGR		1.223815	P49411	2
AAAIGIDLGTTYSC*VGVFQHGK		1.21674	A0A0G2JIW1	2
DGTVLC*ELINALYPEGQAPVKK	C63	1.216121058	P37802 P37802	4
SLHDALC*VVK		1.215029545	P17987	2
GMYGIENEVFLSLPC*ILNAR		1.214216343	P07195	4
TVPFC*STFAAFFTR	C394	1.210104201	A0A0B4J1R6	2
GDFYVIEYAAC*DATYNEIVTLER		1.20866233	P51116	3

C*PQIVIAFYEER	C160	1.20562	Q13185	2
YAYLNVVGMVGSIDNDFC*GTDMTIGTD		1.205076607	Q01813	3
LTESPC*ALVASQYGWSGNMER	C645	1.200929731	P14625	3
MMYSPIC*LTQDEFHPFIEALLPHVR	C7	1.199608329	O00712 Q5VW26	3
YLEC*SALQQDGVKEVFAEAVR	C157	1.178853325	P84095	4
YLC*DEQKELQALYALQALVVTLEQPPN	C1517 C1320 C1429	1.177801941	Q04637 Q04637	4
C*LTQSGIAGGYKPFNLETCR	C57	1.176730838	P30626 B4DHQ6	2
AITIAGIPQSIIEC*VK	C158	1.173084584	Q15366 Q15366	2
YC*PNSVLVIIDVKPK		1.172077985	P51665	4
SLLINAVEASC*IR	C262	1.169475585	E2QRB3 P32322	2
ILQDDIESLMPIVYTPTVGLAC*SQYGHI	C120	1.167237565	P23368	2
GEAYNLFEHNC*NTFSNEVAQFLTGR	C108	1.165417275	Q6ICB0	4
VWAVLPSSPEAC*GAASLQER	C170	1.165106745	Q5T440	2
ATPPQIVNGDQYC*GDYELFVEAVEQN	C204	1.162018245	A0A087WV23	4
YGQC*WVFAAVACTVLR	C277	1.160425	P21980	2
LNEDMAC*SVAGITSDANVLTNELR	C74	1.159678388	H0YL69 P25789	3
VLC*ELADLQDKEVGDGTTSVVIIAAELL	C76	1.159174809	E7ERF2 P17987	3
AAAGELQEDSGLC*VLAR	C172	1.15802	Q96C19	2
NESC*SENYTTDFIYQLYSEEGK		1.15676541	Q01813 Q01813	4
C*YSAEVVTLWYRPPDVLFGAK	C157	1.147793507	Q00535 Q00535	3
C*EFQDAYVLLSEKK		1.146143609	P10809	4
NTNDANSC*QIIIPQNQVNR	C317	1.144016667	P50395 P50395	2
WTLGFC*DER	C78	1.140619863	O95336	2
NC*LALADDKK	C296	1.139473806	O75367 O75367	2
LSLEPLPC*YQLELDAAVAEVK		1.13917915	Q96RS6	3
GELSGHFEDLLLAIVNC*VR	C246	1.132408158	P12429 D6RA82	3
FQSSAVMALQEACEAYLVGLFEDTNLC	C111	1.131258279	P68431	4
LNCQVIGASVDSHFC*HLAWVNTPK	C83	1.13071602	Q06830	3
GLGTDEDSLIEIIC*SR		1.130100977	P07355 P07355	4
GFGFVC*FSSPEEATK		1.129403866	Q13310 H0Y5F5	3
NALANPLYC*PDYR		1.129316986	P22695	3
VLC*LAVAVGHVK		1.126875	P62906	2
SHPLDPIDTVDFEREC*GVGVIVTPEQIE	C100	1.125442665	P47897 P47897	4
EGVVEC*SFVK	C275	1.125295	P40926	2
NVDAILEEYANC*KK	C165	1.12428	Q15014	2
LQHINPLLPAC*LNK	C325	1.122731183	Q9BTE3 Q9BTE3	4
SHLLAADAPSSAAWVQTLC*R	C115	1.121764363	Q99704	2
ALDVGSGSGILTAC*FAR	C153 C64 C95	1.121570382	A0A0A0MRJ6	3
GSSLC*DIAILVVDIMHGLEPQTIESINLL	C720	1.119283476	A0A087WUT6	2
VDASVAVFC*EIQNTLINTLIR	C37	1.113802012	P45954 P45954	3
VPQC*PSGR	C88	1.110738284	Q16186	2
AITIAGVPQSVTEC*VK	C158	1.108988538	Q15365	4
C*FLAQPVTLLDIYTHWQQTSELGR	C38	1.106640647	E7ETY2 Q13428	4
QLFALSC*TAEEQGVLPDDLSGVIR	C75 C96	1.10109804	P04899 P04899	3
EKVETELQGVC*DTVLGLLDSHLIK		1.101017561	P31947	4
IC*ELLPEAAINDVYLAPLLQCLIEGLSAE	C250 C291	1.098764116	J3KTM9 Q14974	3
VGMGSGSIC*ITQEVLACGRPQATAVYK		1.094134712	P12268	3
FLGPEIFFHPEFANPDFTQPISEVVDEVI	C307	1.09353632	P61158	3
IYGETPEAC*R		1.092876208	P51116	2
GFEVVYMTEPIDEYC*VQQLK	C521	1.091229876	P08238	3
ALLLLC*GEDD		1.091226172	D6RBL5 P08758	3
ILC*FYGPPGVGK	C456 C177 C406	1.087914429	P36776 K7EKE6	2
NIIQPPSCVLHYYNVPLC*VTEETFTK	C430	1.080807037	Q8WVV9 Q8WVV9	2
ECISIHVGQAGVQIGNAC*WELYCLEHG	C20 C90	1.080752007	Q9BQE3 F5H5D3	4
YFTQGNC*VNLTEALSLYEEQLGR	C318	1.079416443	P52788 P52788	3
ILALC*MGNHELYMR		1.07888	P26038	2
IC*SLHSLPPQS	C59	1.075998172	P03928	2
GLC*GAIHSSIAK	C103	1.07590354	P36542 P36542	4
C*LYASVLTAQPR	C728	1.075355	P13639	2

SVAFPCISTGVFGYPC*EAAAEIVLATLR	C276	1.07445701	Q9BQ69	3
LLGSTIPLC*SAQWER	C304	1.067963423	P50416 P50416	2
ELEAVC*QDVLSLLDNYLIK	C97	1.067221113	P61981	4
ELETVC*NDVLSLLDKFLIK	C97	1.066169119	Q04917	4
NFNYHILSPC*DLSNYTDLAMSTVK	C461	1.064581716	G5E9W3 Q9UKF6	4
AGAVVAVPTDTLYGLACAASC*SAALR	C99	1.064447457	Q86U90	3
IAVAAQNC*YK	C67	1.063689666	P60174 P60174	3
GDLENAFLNLVQC*IQNKPLYFADR		1.063129235	P07355 P07355	4
LESLSAESHRPPGNC*GEVNGVIAGVA	C32	1.061502675	P40123 F8WDB9	2
LYGIQAFC*KDLLEVADVLEK	C108	1.060432515	Q9HAV7	2
NQC*LFTNTQCK	C68	1.056579294	B7Z6B6 Q9UL40	3
GFGHIGIAVPDVYSAC*K		1.052615	Q04760 Q04760	2
VLILDEATSALDVQC*EQALQDWNSRG		1.049931892	X5CMH5 Q03519	4
NC*SETQYESK	C112	1.045234204	P61981	2
DSC*LPSQGLSFSYGDILHVINASDDEW	C182	1.044424777	Q92796 Q5JUW8	4
LC*FLDKVEPHATIAEIK		1.04064	Q9NZ01	2
GVLAC*LDGYMNIALEQTEEYVNGQLK	C36	1.040453866	P62312	2
SIKDTIC*NQDER	C147 C351 C509	1.038891531	B4E3S0 Q9ULV4	3
DYVLNC*SILNPLLTLLTK		1.035929331	O60684	2
C*LAFHDISPQAPTHFLVIPK	C38	1.0355896	P49773	4
DC*GGAAQLAGPAAEADPLGR	C8	1.034686056	Q9Y508	4
NSPVFELLPC*GIIQGEPGAQPQLITFHP	C444	1.030235	Q9NRG9	2
LCLNIC*VGESGDR	C25	1.029456421	P62913 Q5VVC8	3
VPTANVSVVDLTC*R	C247	1.028635223	P04406	4
AVEEYSC*EFGSAK	C56	1.028606293	F8VVM2 Q00325	2
ICELLPEAAINDVYLAPLLQC*LIEGLSAE	C310	1.027785	Q14974	2
IISNASC*TTNC*LAPLAK	C152 C156	1.02355018	P04406	4
STFLSLMTSTASEAASYEFTTLTC*IPGV	C99	1.023534543	A8MZF9 P55039	3
ALSVGNIDDALQC*YSEAIK	C73	1.022383214	P31948 P31948	2
TGTELVLLTAAPPPPPRPGPC*AYAAHG	C44 C64	1.021572615	Q96B36 H9KV91	3
NAFAC*FDEEATGTIQEDYLR		1.020021826	P19105 J3QRS3	4
AVSTGVQAGIPMPC*FTTALSFYDGYR	C409	1.014701512	P52209 P52209	3
AKFENLC*K	C564	1.012213195	P08238	2
GIFPVLC*KDPVQEAWAEDVDLR	C474	1.011815623	P14618	4
AAVEEGIVLGGGC*ALLR		1.011189469	P10809	4
MPC*ESSPPESADTPTSTR	C1372	1.011145	A0A087WV66	2
TALKEDGVLCCQGEC*QWLHLDLIK		1.004972175	P19623	4
DAFEHIVTQFSSVPVSVVSDSYDIYNAC	C287	1.00415664	P43490	4
AGC*AVTSLLASELTK	C1218 C1183	0.997136759	O60610 O60610	4
LGPVDMLVNC*AGMAVSGK	C26	0.996312972	K7ERC8	2
INALTAASEAAC*LIVSVDETIKNPR		0.995866992	Q99832	2
MC*LFAGFQR	C575	0.99550464	Q00839 Q00839	2
VLQSEFC*NAVR	C47	0.993855271	Q9NUP9 G3V1D4	2
LITIEINPDC*AAITQR	C95	0.993071309	P21964 P21964	2
NSNVDSSYLESLYQSC*PR	C645 C106	0.989055	Q7Z2W4 C9J6P4	2
VC*TLAIIDPGDSDIIR	C92	0.988914445	P62888 E5RI99	2
VVMALGDYMGASC*HACIGGTNVR		0.988008089	P60842	4
SGTIC*SSELPGAFEAAGFHLNEHLYNM	C200	0.98680055	A0A0C4DGQ5	4
ITGC*ASPGK	C349	0.982393137	P50991 P50991	2
LVTSPCC*IVTSTYGWTANMER	C598	0.981774879	P07900 P07900	2
DSGAALGLGIALHSPC*YAQVR	C269	0.981227128	K7ESE6 Q9BUM1	3
CPLC*DMTCPLPSSLR	C260	0.981034659	Q9BQA5 Q9BQA5	2
FVPFAAVAAANC*INIPLMR	C189 C190	0.979864785	A0A0A0MS41	3
VIEINPYLLGTMAGGAADC*SFWER	C111	0.978414239	P28074 P28074	3
TILQC*ALNRPAFFAER	C413	0.978213025	P20073 P20073	4
ETGANLAIC*QWGFDDEANHLLLQNNL	C302	0.977793241	E9PCA1 B7ZAR1	3
ITQSNAILC*YIAR	C44 C78 C37	0.971771224	P09488 A6NNT0	2

			B9ZVX7 E7EWW9	
NADMSEEMQQDSVEC*ATQALEK		0.970811401	P63167	3
VSC*SPVSAQLLSVLQGLLHLEPTLR	C284	0.970743689	Q27J81 Q27J81	4
EDPTVSALLTSEKDWQGFLELYLQNSP	C209	0.969345466	P78417 P78417	4
AQLNIGNVLPVGTMPEGTIVC*CLEEKP	C114	0.968204203	E9PKU4 E9PKZ0	2
ILYSQC*GDVMR	C32	0.967494125	G3V1V0 P60660	3
GYEVIYLTEPVDEYC*IQALPEFDGKR	C576	0.967432134	P14625	2
VICAEEPYIC*KDFPETNNILK	C456	0.96702	P49915	2
VADSSPFALELLISDDCFVLDNGLC*GK	C275	0.966212435	P40121 P40121	4
ITSC*IFQLLQEAGIK	C63	0.961451841	E9PBS1 P22234	4
HGGEDYVFSLLTGYC*EPPTGVSLR	C219	0.9601477	P08574	4
C*CSGAIIVLTK	C349	0.959217562	P14618 B4DNK4	3
AVLLASDAQEC*TLEEVVER	C332	0.957259024	Q27J81 Q27J81	2
ETC*SLWPGQALSLQVEQLLHHR		0.956223595	P19623	4
ATFHTPFSHLGQSPEGC*SSYTFPK	C247	0.9562	O75521	2
GLQGVGPGC*TDETLLSAIASALHTSTM	C172 C116	0.955324514	O95983 K7EIE8	2
IVEDEPNKIC*EADR	C85	0.955293179	P55060	2
AVAAGNSC*R	C2196	0.953374839	Q9Y490	3
IIPTLEEGLQLPSPTATSQLPLESDAVEC		0.95332553	P61978 P61978	4
LC*YVALDFENEMATAASSSSLEKSYEL	C219	0.952111703	P68133 P68032	4
VTLADITVVC*TLLWLYK	C166	0.95177724	P26641 P26641	2
TSSVSNPQDSVGSPC*SR	C108	0.951033433	P49023 F5GZ78	2
YVEPIEDVPC*GNIVGLVGVDQFLVK	C466	0.950751327	P13639	3
AEPYC*SVLPGFTFIQHLPLSER	C391 C302 C291	0.950121322	M0QYZ0 Q9BUJ2	4
TPDTSTYC*YETAEK		0.947585002	P46821	3
GPAVGIDLGTTYSC*VGVFQHGK	C17	0.946806765	P11142 P11142	3
LPQPPEGQC*YSN	C218 C100 C102	0.946698423	A0A0A0MSL3	2
NLSDLIDLVPSLC*EDLLSSVDQPLK	C65 C24	0.943510354	P47756 P47756	4
LNQTTFTATRPGVYYGQC*SEICGANHSFMPIVLELIPLK		0.94242	P00403	2
YQIDPDAC*FSAK	C232	0.939966895	P21796	2
AVILDLLQEALTESGLTSQDIDC*IAYTK	C73	0.934854298	Q9NPF4	2
LLDLVQQSC*NYK	C30	0.934500952	B1AHD1 P55769	3
YFAGNLASGGAAGATSLC*FVYPLDFA	C129	0.932449765	P05141	4
C*VLPEEDSGELAKPK	C318	0.931897401	Q9Y3F4 Q9Y3F4	2
LC*WFLDEAAAR	C237	0.931292842	O95336	2
FAC*HSASLTVR	C56	0.927057551	Q15233 Q15233	3
HDDSSDNFC*EADDIQSPEAEYVDLLLN	C166	0.927044682	Q96HE7	4
SGANVLICGPNGC*GK	C367	0.926372722	P28288 P28288	2
SSEC*MKDDPITLFVALSPQGTAQGELF	C844	0.925987672	Q14697 Q14697	3
ENDPIQGPDGKVHGNTC*SMCEVFFQA	C400 C381	0.925403609	E7EWP9 Q9NQ38	2
IRPLNSEGTLNLLNC*EPPR		0.924771962	Q9Y5S2	2
TYADYESVNECMEGVC*K	C33	0.924770351	G3V279 P84090	2
VTHLVANC*TQGEK	C221 C189	0.924682277	Q9H8V3 Q9H8V3	4
SVYLGTGC*GK	C516	0.923613697	Q9NXV6	3
LICC*DILDVLDKHLIPAANTGESK	C98	0.923167663	P62258 P62258	4
VADSSPFALELLISDDC*FVLDNGLCGK	C267	0.917625175	P40121 P40121	3
CHEFVTFSC*PGADKGPDTDLFSPVLLV	C84	0.917327769	J3KN97	2
VAAALENTHLLEVVNQC*LSAR	C158	0.916110464	Q9Y3D0	4
EIGLWFHPEELVDYTSC*AQNWIYE	C170	0.915720055	P15531 P15531	4
C*RELDTWTQDLTLPAVVWLSGFFNPQ	C4358	0.913127814	Q96DT5	2
LPITVLNGAPGFINLC*DALNAWQLVK	C240	0.912245369	P31939 P31939	3
VITVDGNIC*TGK	C67	0.911063006	Q8N1B9 E7ESZ7	2
AYCHILLGNYC*VAVADAK	C62	0.910279908	Q9Y2Z0 Q9Y2Z0	2
ALQSNIIPFC*DEVMQLLLENLGNENVH	C544 C503	0.909768384	J3KTM9 Q14974	3
KDC*EVVMMIGLPGAGK	C478	0.908255	Q00839 Q00839	2
IIGVHQEDELLEC*LSPATSR	C961	0.907229478	Q93009 H3BND8	2
VQTDPPSVPIC*DLYPNGVFPK	C120 C98 C97 C85	0.906831907	P50579 F8VY03	2
GEVPC*TVTSASPLEEATLSELK	C141	0.905026322	H7C068 P48047	2
C*PTQFPLILWHPYAR		0.902970954	Q96TA1 Q96TA1	2

MSSYAFFVQTC*R	C23	0.901311831	P26583 Q5T7C4	2
TSC*GSPNYAAPEVISGR	C174 C200	0.900696526	A0A087WXX9	4
GVTIIGPATVGGIKPGC*FK	C362	0.898035542	P53396 P53396	3
YLPDTLLLEEC*GLLR	C157	0.897811575	P21964 P21964	2
ALDLDSSC*K	C508	0.897439142	P31948 P31948	4
QVLIRPC*SK	C30	0.894444491	H3BV27 I3L303	3
KPPC*GSTPYSER	C374 C616 C394 C586	0.893315	O15231 O15231	2
YTIVVSATASDAAPLQYLAPYSGC*SMG	C244	0.892283333	P25705 P25705	2
FIITALPTIYHC*K	C106	0.890016794	Q9H3N1	4
SCCSCCPVGC*AK	C41 C42	0.889332473	P13640 P80297	2
WPISYC*R		0.888998009	Q8NBX0	4
LATTAC*TLGDGEAVGADSGTSSAVSLK	C13 C63	0.887915407	O94901 O94901	3
LC*GSGFQSIVNGCQEICVK	C37 C92	0.887057143	K7ER88	3
EGTDSSQGIPQLVSNISAC*QVIAEAVR		0.884913312	Q99832	4
ITLDNAYMEKC*DENILWLDYK	C152	0.88458	P14618 P14618	3
DTQTSITDSC*AVYR	C100	0.88303193	Q9Y5M8	3
LNPPAQLPNSEGLC*EFLEYVAESLEPP	C182	0.878896552	Q66K74 Q66K74	2
AFQYVETHGEVC*PANWTPDSPTIKPS		0.878489581	P30048	3
DFTPVC*TTELGR	C47	0.878385	P30041	2
ELELMFGC*QVEGDAAETPPRPR	C277	0.877022813	H3BRW9 Q02750	3
C*TGGEVGATSALAPK	C17	0.876147226	P30050 P30050	4
LAQIC*SSIR		0.875864647	Q53HL2	3
ASLNGADIYSGC*CTLK		0.87455	M0QXS5 P14866	2
LQDSFC*SGQTLWELLSHFPQIR		0.87454	Q9BZE9 Q9BZE9	2
SLC*NLEESITSAGRDDLESFQLEISGFL		0.871434045	Q52LJ0 Q52LJ0	4
GNLNFTC*NGNSVISPVGNR		0.869937807	A0A0B4J2E5	2
VC*EDLDTSVNLAWTSGTNCTR	C199	0.863081416	A0A0A0MR02	4
GLPWSC*SADEVQR	C22	0.862941523	P31943 G8JLB6	3
FVVDVDKNIDINDVTPNC*R	C104	0.862250692	J3QLH6 J3QRW1	3
YIYDQC*PAVAGYGPIEQLPDYNR	C453	0.861342222	P31930	3
GFTDADNTWEPEENLDC*PELIEAFLNS	C69	0.857751279	Q13185	3
TDVNKIEEFLEEVLC*PPK	C100	0.85756	Q9Y696	2
ANSWFNC*R	C466	0.85361969	P03956	2
LSLQNCC*LTGAGCGVLSSTLR		0.851990524	P13489	4
VMALQEAC*EAYLVGLFEDTNLC*AIHA	C97 C111	0.8479985	P68431	2
EQSDFC*PWYIGLPFIPYLDNLPNFNR	C282 C413	0.845568428	H3BR35 P15170	3
EVIQSDSLWLVEFYAPWC*GHCQR	C107 C60	0.844397304	Q15084 Q15084	4
TAIC*NLILGNPPSK		0.844345	Q9NRX1	2
DIDFLKEEEHDC*FLEEIMTK		0.844318078	P12268	3
NTGIIC*TIGPASR	C49	0.844231434	P14618 P14618	3
IDPENAEFLTALC*ELR	C476	0.842299607	Q13325 Q13325	2
MVSDINNAWGC*LEQVEK		0.841963171	P12814	3
VSVHC*PVFDYVPPELITLFISNIGGNAP	C310	0.83918273	P49770	3
LLAIC*QPLTYSTR	C136	0.83908	P47893 P47888	2
C*GAETQHEGLELR	C128	0.834182415	B5MC98 Q9HCU5	2
LEFSIYPAPQVSTAVVEPYNSILTTHTTL	C213	0.833663107	P68366 P68363	2
FALNNPEMVEGLVLINVNPC*AEGWMD	C102	0.830705	Q92597 Q92597	2
STLTDSLVC*K	C41	0.829880657	P13639	4
YTVIMNPQLC*TQMAITIWVIGFFHALLH		0.829831258	P58182	2
ELDLSNNC*LGDAGILQLVESVR		0.829657936	P13489	2
ATELFVQC*LATYSYR		0.827403886	Q9NRG0	4
VTFSC*AAGFGQR	C1113 C165 C1210	0.825026346	Q14203 E7EWF7	4
TNTAVRPYC*FIEFDNFIQR	C111	0.822870167	C9JRY4 Q96IW7	3
FMC*AQLPNPVLDSISIIDTPGILSGEK	C152	0.8186	A0A024R571	2
GQGVYLGMPGC*LPVYDALAGEFIR		0.817602601	F8VY02 P30040	3
SVSAFAPICNPVLC*PWGK	C152	0.816090758	X6RA14 P10768	2
QGFGNLPIC*MAK	C841 C906 C907	0.815875881	P11586	2
KLDTNSDGQLDFSEFLNLIGGLAMAC*H		0.813439062		4
FMGGGGESC*SLIAEGLSTALQLFDDFK	C111	0.81332719	B9TX33	2

			Q71SY5 Q71SY5	
LALDCSGQQVAVDLFLLSGQYSDLASL		0.812222704	O95486	2
SC*SGVEFSTSGHAYTDTGK		0.811942593	Q9Y277	4
LIC*CDILDVLDKHLIPAANTGESK	C97	0.81081805	P62258 P62258	3
YVDIAIPC*NNK	C163	0.810416255	A0A0C4DG17	3
C*GVPDVAQFVLTEGNPR	C92	0.809655116	P03956	2
EATQILSVPKVDDEILGFISEATPLGGIQAASTESC*NQQLDLALCR		0.808354868	P42166	4
LVILANNC*PALR	C52	0.806664295	P62888 E5RI99	3
ECISIHVGQAGVQIGNACWELYC*LEHG	C95 C25	0.805692622	Q9BQE3 F5H5D3	4
AAAPAPVSEAVC*R	C151 C336 C166 C290	0.805166595	P20810 P20810	2
LAAC*VNLIPQITSIYEWK	C73 C96	0.804912248	O60888 C9IZG4	3
AGAIAPC*EVTVPAQNTGLGPEK	C119	0.804381449	F8VWS0 P05388	4
AASVFVLYATSC*ANNFAMK		0.803969634	Q9NRF9	3
KIWC*FGPDGTGPNILTDITK	C651	0.803791766	P13639	2
ISC*MSKPPAPNPTPPR		0.803562239	P46734 P46734	4
AGSNMLLIGVHGPTTPC*EEVSMK	C2376 C2532 C2587	0.801015	O75369 O75369	2
GLC*ESVVEADLVEALEK	C84	0.800496164	Q8WVV9 Q8WVV9	4
SPGVVISDDEPGYDLDLFC*IPNHYAED	C23	0.800422996	P00492	4
DIPDGATVLVGGFGLC*GIPENLIDALLK		0.800374683	P55809	3
AALANLC*IGDVITAIDGENTSNMTHLEA	C45	0.800345	O00151	2
TTASEPVEQSEATSKDC*SR		0.800019626	Q15007	2
GKLVDC*K	C234	0.797186323	P35270	3
C*SENKLPAELQELPGLSHQYWSAPSD		0.796998702	P27695	2
AQC*ETLSPDGLPEEQPQTTK	C3649 C3658	0.796008028	Q7Z6Z7 Q7Z6Z7	2
VQTDAFVSNELDDPDDLQC*K	C464 C462	0.795706291	Q9UI10 Q9UI10	2
TAFQEALDAAGDKLVVVDFSATWC*GP		0.795090496	P10599	4
DIIEHLNTSGAPADTSDPLQQIC*K		0.794531341	M0QXN5 P37198	2
DC*FLELAPDFVGDILWEHLEILQK	C112	0.793380748	P14921 P14921	2
C*HTPPLYR		0.793020682	M0R117 Q02543	4
LDVGNFSWGSEC*CTR		0.792795764	P62241	3
VGIGPGSVC*TTR	C171 C204	0.792607821	H0YLV5 H0YNJ6	4
GC*STVLSPEGSAQFAAQIFGLSNHLV	C374	0.792054842	E9PBS1 P22234	4
VTAVIPC*FPYAR	C91 C24	0.788319068	B1ALA9 P60891	3
ADELLC*WEDSAGHWLYE	C158	0.786570106	H3BPR2 Q13232	3
VIGIEC*SSISDYAVK	C101	0.785661726	Q99873	4
AAQLEPITYMQGLSAC*EQIR		0.785469693	Q9HBH0	3
IQFNDLQSLLC*ATLQNVLR	C399 C440	0.784237034	J3KTM9 Q14974	4
C*GYAGSNFPEHIFPALVGRPIIR	C20	0.78399674	P61160 P61160	3
LQVIQC*IDVAEQALTALEMLSR	C583	0.782234041	Q14669 Q14669	3
LC*SGVLGTVVHGK		0.78146893	Q9Y6C9	4
RPYGVGLLIAGYDDMGPHIFQTC*PSAN	C154	0.781391628	P25786 P25786	3
LSTAC*PGRVPSMVSTSLNAEALQYLQ	C883	0.780138923	P55060 P55060	3
LVAFC*PFASSQVALENANAVSEGVVH		0.779939896	O00567	4
GC*GVVKFESPEVAER		0.77885444	P52272 P52272	2
SKDGVC*VR	C185	0.77807291	P55786 E9PLK3	3
TFVGTPC*WMAPEVMEQVR	C218	0.778016667	Q9UEW8 O95747	2
DTAQQGVVNFPYDDFIQC*VMSV	C194	0.77767	P30626 C9J0K6	2
VCEDLDTSVNLAWTSGTNC*TR	C216	0.777641887	A0A0A0MR02	3
SSYLNIVGLVGSIDNDFC*GTDMTIGTDS	C241 C170	0.7775	P08237 P08237	2
C*PGESLINPGFK		0.7764188	Q9BUH6	2
ATLQAALC*LENFSSQVVER	C21 C40	0.776372232	P59998 F8WE39	3
LC*VQNSPQEAR	C150	0.775864961	P33240 P33240	2
STVLSLDWHPNNVLLAAGSC*DFK	C115 C162	0.77568	Q92747 Q92747	2
LVTSPC*CIVTSTYGWTANMER	C597	0.774302273	P07900 P07900	3
AAAYNLVQHGITNLC*VIGGDGSLTGANI	C114	0.771336667	P17858 P17858	2
TVPFLPLLGGC*IDDTILSR	C180	0.771278927	Q7Z7H8 Q7Z7H8	3
ILGNTFGMC*VLQDFEALTPNLLAR	C121	0.771093583	E9PJN6 E9PMU0	3
TAFQEALDAAGDKLVVVDFSATWC*GP		0.770038568	P10599	4
GLSNLFLSC*PIPK	C36	0.769615	Q9Y570 Q9Y570	2

EVC*PVLDQFLCHVAK	C22	0.769237095	F8WCA1 Q9NY27	2
VPFLVLEC*PNLK	C14	0.768565565	A0A087WUD3	3
FTLDC*THPVEDGIMDAANFEQFLQER		0.766604526	P35268	4
AVILGPPGSGKGTVC*QR	C22	0.765748075	P27144	3
FNAHGDANTIVC*NSK	C61	0.76514813	P09382	2
YWLC*AATGPSIK	C205	0.765086971	D6RAC2 J3KPE3	3
AAVLVQQWVSYADTELIPAAC*GATLPA	C112	0.764127735	P26640 A2ABF4	4
ILLNACC*PGWVR		0.76256303	P16152	3
SC*CSCCPVGCAK	C34 C33	0.760085855	P13640 P80297	3
SELAALPPSVQEEHGQLLALLAELLRGP	C1144 C1183	0.760051322	H7BXY3 Q7L2E3	3
GEETPVIVGSALC*ALEGRDPELGLK		0.759730956	P49411	4
ADEASELAC*PTPK	C2202	0.757776086	P49327	2
KSAYC*PYSHFPVGAALLTQEGR		0.757725	P32320	2
AFVNPFPDYEAAAGALLASGAAEETGC*VRPPATTDEPGLPFHQD		0.75757084	Q9NS86	2
LNQVC*FDDDGTSSPQDR	C299	0.754700754	H3BVG0 Q8N1F7	3
HLYTLDGGDIINALC*FSPNR	C196	0.753791616	D6RAC2 J3KPE3	2
SAGAC*TAAAFLKEFVTHPK	C462	0.753451856	P28838 P28838	3
TDVLVLSC*DLITDVALHEVVDLFR	C106	0.752383556	Q9NR50 Q9NR50	2
SVLLCGIEAQAC*ILNTTLDLLDR	C114	0.752342746	K7ENV7 K7EKW4	3
C*MPTFQFFKK		0.749945445		4
YMLDC*R	C230	0.749420732	Q9Y277 Q9Y277	2
NLSFFLTPPC*AR	C492	0.747088779	P42224 P42224	3
MALDALLQEIALSEPQLC*EVLQVAGPD	C38	0.746721054	Q7Z2W4 C9J6P4	3
ENFDEVVNDADIILVEFYAPWC*GHCK	C206	0.746613792	P13667	4
SGIQPLC*PER		0.745589446	P42166	3
LC*PQFLQLASANTAR	C264	0.743169146	O95630 O95630	4
TLC*GTPNYIAPEVLSK	C212	0.74316	P53350	2
GLYDGPVC*EVSVTPK	C468	0.74299782	Q16555 Q16555	2
VTEEDIVELFC*VCGALKR	C272	0.742652741	Q9BY77 F6VRR5	3
RPPGGTSPPNGGLPGPLATSAAPPGPP	C58	0.742390542	H3BUF6 Q8WWM7	2
AINC*ATSGVVGLVNCLR	C1448	0.74083056	P49327	4
LRPLSYPDTDVILMC*FSVDSPDSLENIP		0.74081	P62745	2
ICDGCIIVVDAVEGVC*PQTQAVLR	C73	0.739936712	Q7Z2Z2 Q7Z2Z2	2
TC*ETGEPMEAESGDTSSEGPAQVYLP	C11	0.73955	Q9BQ67	2
KC*DLISIPK	C315 C111 C473	0.739415802	B4E3S0 Q9ULV4	3
FVIHCNSPVWGADKC*EELLEK	C285	0.738478606	O75367 O75367	2
METYC*SSGSTDTSPVIDAVTHALTATT	C288	0.738285765	Q02338 E9PCG9	3
ILVALC*GGN		0.737669418	P04083	2
ADIIVSELLGSFADNELSPEC*LDGAQHF	C278 C388	0.737263247	O14744 O14744	4
AALAAC*PSSPFPPAMPR	C463	0.736756157	Q8N2G8 Q8N2G8	3
LLHVFACAC*PGCSTGGAR		0.736191331	Q9BRP1 U3KQA4	2
ANC*IDSTASAEAVFASEVKK	C268 C183	0.735902988	M0QXL5 M0R299	2
TPC*SSLLPLLNAHAATSGK	C307 C367 C397	0.734888691	B8ZZZ7 Q9NUQ6	3
VVVFIKPTC*PYCR	C23	0.734720936	P35754	4
C*PIQLNEGVSFQDLDTAK		0.734584992	A6NDU8	3
EADQKEQFSQGSPSNC*LETSLAEIFPL	C102 C161	0.734430524	Q9NQ88	3
VQEAPIDEHWIIEC*NDGVFQR	C91	0.732669373	Q14353	4
GFSDEDNTWEPEENLDC*PDLIAEFLQS	C60	0.730901641	B5MD17 P83916	2
YLAEVAC*GDDRK	C134	0.730735675	P27348	3
SWC*PDCVQAEPVVR	C43	0.729487136	I3L0K2 I3L3M7	3
VLC*LVEMSEKPYILEAALIALGNNAAYA	C128	0.72764241	Q9UH62	2
VTEDENDEPIEIPSEDDGTVLLSTVTAQ	C39	0.726460322	A0A087X260	3
LC*SGPGIVGNVLVDPSAR		0.726022232	Q9Y5P6 Q9Y5P6	2
IAQLIC*ER	C134 C91 C137 C199	0.725213871	H0YMP1	2
LWNTLGVC*K	C94	0.725107187	J3KPE3 P63244	2
VC*QGIGMVNR	C133	0.724474687	Q9Y3C6	2
NAGNC*LSPAVIVGLLK		0.724438557	O43175 Q5SZU1	2
DLC*FSPGLMEASHVVNDVNEAVQLVF	C192 C362	0.724072369	Q9BXW7 Q9BXW7	4
VQYPQSQAC*K		0.723837999	Q14204	2

LAAQSC*ALSLVR		0.72344	Q08211	2
TIYAGNALC*TVK	C155	0.72327974	P13804 H0YLU7	4
AEPPQC*TSLAWSADGQTLFAGYTDNL	C242	0.723267764	D6RAC2 J3KPE3	4
C*TPSVISFGSK	C34	0.722847442	Q92598 Q92598	3
IC*PVEFNPNFVAR		0.722336723	Q9UI30 Q9UI30	2
EC*SNPSNLLELYTQAILDMTYFEENKLVDEDFPEDSSSQK		0.719703229	A6NDU8	3
LEVDAIVNAANSSLLGGGGVDGC*IHR	C186	0.717034589	Q9BQ69	2
YYALCGFGGVLSC*GLTHTAVVPLDLVK	C75	0.71667259	F8VVM2 Q00325	4
NMITGTSQADC*AVLIVAAGVGEFEAGI	C111	0.716356641	P68104	4
GIDQC*IPLFVEAALER		0.716266941	O95373	3
GTEAGQVGEPGIPTGEAGPSC*SSASD	C241	0.716150086	O15355	4
HTLDGAAC*LLNSNKYFPSR	C170 C102	0.716095862	Q9Y3A3 S4R3N1	2
DKEPEVVFIGDSLVQLMHQC*EIWR	C55	0.71596152	Q15102 M0R389	2
C*YVQPQWVFDSVNAR	C386 C252 C374	0.715647183	B3KXD6 O00541	2
DAANC*WTSLLESEYAADPWVQDQMQ		0.715515099	Q8WVJ2	3
HVLALTGC*GPGR	C51	0.714864498	E9PIX0 Q9BTY7	2
AGKPVIC*ATQMLESMIK	C326	0.714373194	P14618	3
IAQLFSISPC*QISQIYK	C355 C402 C453	0.71424263	Q12800 Q12800	2
VFAEC*NDESFWFR	C38	0.71398	D6R918 Q9NX40	2
VMQPQILEVNFNPDC*ER	C612 C33	0.713724498	Q14166 V9GY16	2
SEGGSGGGAAGGGAGGAGAGAGC*G	C32	0.71371507	Q9NSY1 Q9NSY1	3
LVSSPC*CIVTSTYGWTANMER	C589	0.712273375	P08238	4
TVVNISSLC*ALQPFK	C159	0.711044659	P35270	4
SVTYTLAQLPC*ASMALQILWEAAR	C137	0.711021253	O14684	3
AVLLVGLC*DSGK	C73	0.71082684	Q9Y5M8	4
LLHVFAC*ACPGCSTGGAR		0.710668894	Q9BRP1	3
EITSLDTENIDEILNNADVALVNFYADWC	C58	0.709214971	Q9BS26	4
VWAEPC*LIDAAKEEYNGVIEEFLATGE		0.709124981	C9JMZ3 Q9H4A4	2
LALNC*VGGK	C136 C187	0.707455757	H3BM30 Q9BV79	2
SYIEGYVPSQADVAVFEAVSSPPPADL	C50	0.706909544	P24534 F2Z2G2	3
GIGMNEPLVDC*EGYPR	C59	0.706219194	O00233 O00233	3
AVLC*PQPTR		0.705531899	P15153	3
LAPEEVPLSAEAQAQQLAQELAWC*VE		0.7035749	Q9H7E9	2
EIITLQLGQC*GNQIGFEFWK	C13	0.703085	P23258 Q9NRH3	2
VC*EDLDTSVNLAWTSGTNC*TR	C216 C199	0.70293497	A0A0A0MR02	3
QPAIMPGQSYGLEDGSC*SYKDFSESR		0.702726102	M0QXS5 P14866	4
VFDPSC*GLPYYWNADTDLVSWLSPHD	C49 C60	0.701582314	O60828 O60828	3
VSDTVVEPYNATLSVHQLVENTDETYC*	C201 C183	0.701510063	P68371 Q9BVA1	4
SESELIDELSEDFDRSEC*K	C263 C96 C309 C139	0.701249485	P20810 P20810	4
ALGWAAVYLSTC*K	C353	0.700718633	A0A0G2JH37	2
FSFC*CSPEPEAEAEAAAGPGPCER		0.700649964	Q13501	3
GLC*AIAQAESLR		0.698975345	P23396	4
KAQC*PIVER	C66	0.698892573	P46782 M0R0R2	2
ADVSFVLFFDC*NNEIC*IER	C122 C127	0.698529959	P30085	3
LYC*PVEFSK	C337	0.698304643	P52788 P52788	2
QQSACIGGPPNAC*LDQLQNWFTIVAE	C255	0.697168564	P42224 P42224	2
CPEALFQPSFLGMESC*GIHETTFNSIM		0.696838425	P60709	4
AYHEQLSVAEITNAC*FEPANQMVK	C295	0.696770543	P68366 P68363	4
LVVPASQC*GSLIGK	C141 C109	0.696258305	P57721 P57721	4
VILITPTPLC*ETAWEEQCIIQGCK	C117 C137 C112 C24	0.695455748	Q2TAA2 C9JE02	4
LNPAVTC*AGK		0.695014686	Q8TD19	3
LC*SSSSSDTSSR	C385	0.693925257	Q86WB0 Q86WB0	2
AEGSDVANAVLDGADC*IMLSGETAKG	C358	0.693014114	P14618 P14618	4
LFNTAVC*ESK		0.691987086	Q9BXJ9	3
FIC*TTSAIQNR	C20	0.691629017	P53396 P53396	3
SYC*NDQSTGDIK	C106	0.691271003	P00492	4
EIVHIQAGQC*GNQIGTK	C12	0.690505822	K7ESM5 Q9BUF5	2
SILSPGGSC*GPIK	C215	0.690394443	P78347 P78347	3
VLPSGIGHTTNC*FLR		0.690281019	O95140	2

AC*DLPAWVHFPDTER	C181	0.689658785	A0A087WXU3	2
SGLTPNDIDVIELHDC*FSTNELLTYEALGLCPEGQGATLVDRGDN		0.689622524	P22307	3
WAELLPLLQQC*QVVR		0.689125019	P13489	2
LTTLPSDFC*GLTHLVK		0.688887838	Q96AG4	2
VLSSSGSEAAVPSVC*FLVPPPNQEAQ	C855 C859 C882 C833	0.68775003	Q15149 Q15149	2
LLACIASRPGQC*GR		0.687667619	P62241	4
FSGDLDDQTC*R	C245	0.686646976	P05455	2
ENSTLNC*ASFTAGIVEAVLTHSGFPAK		0.686257972	Q8IUR0	4
VVLLGEGC*VGK	C29	0.685305176	Q9UL25	3
FQSSAVMALQEASEAYLVGLFEDTNLC*		0.684741871	Q71DI3	4
LGTVEELANLAAFLC*SDYASWINGAVIK		0.6836434	Q16698 Q16698	4
ALLVTASQC*QQPAENK	C93 C92	0.68182906	Q01518 Q5T0R1	4
LC*DFGVSGQLIDSMANSFVGTR	C207	0.681444026	H3BRW9 Q02750	4
LNIISNLDC*VNEVIGIR	C390	0.680587981	B3KQV6 P30153	4
VGSFC*LSEAGAGSDSFALK	C73	0.680582882	P45954 P45954	2
NGYDYGQC*R	C80	0.680438188	S4R3G0 Q13242	2
QNSDFLC*QMDLLQEFYETTLEALKDAK	C130	0.680408292	P61201	4
AIYHSLGMTGIPIINVNNNC*ATGSTALF		0.68039	P22307	2
ASC*LYGQLPK		0.680225991	P09211	3
GEPGLEQPFWISSVAALLNTDLVATGS		0.680161022	O43818	3
QGAESDQAEPIIC*SSGAEAPANSLPSKVPTTLMPVNTVALK		0.679365	Q7Z434	2
IIQFQATPC*PK	C238 C298 C299	0.678999289	Q06330 Q06330	3
SLHDALC*VLAQTVK	C348	0.678944277	P78371 F8VQ14	3
QVEVDAQQC*MLEILDTAGTEQFTAMR	C51	0.678435224	E7ESV4 P61224	3
IISNASC*TTNCLAPLAK	C152	0.677565134	P04406	4
EIEQKYDC*GEEILITVLSAMTEEAAVAIK	C129	0.677222283	P63241 P63241	4
ELDVEEAHAASTEEKEAGVGNGTC*AP	C37	0.676866359	Q96C86	2
FEETGQELAELLEEEKLSC*VPVLIFANK		0.676172665	P36405	4
NLSGQPNFPC*R		0.676099575	Q9HD45	3
GLIAAIC*AGPTALLAHEIGFGSK	C86	0.675817774	Q99497 K7ELW0	4
TLQNTMINLGLQNAC*DEAIYQLGLDIEE	C109	0.675361814	E9PK47 P06737	2
AIVDALPPPCESAC*TVPTDVDKWFHH		0.675080511	Q15181	2
LVSSPCC*IVTSTYGWTANMER	C590	0.675072582	P08238	4
GVAQTPGSVEEDALLC*GPVSK	C79	0.674882244	Q5QPE7 Q5QPE8	2
WNTDNTLGTEIAIEDQIC*QGLK	C92	0.674106079	A0A0A0MR02	4
C*GFSELYSWQR	C91	0.673735	Q9NSE4	2
VFIMDSC*DELIPEYLNFIR	C366	0.673144917	P08238	4
VC*NFLASQVPFPSR	C205	0.67305027	Q99714	4
C*TAKPSSSGK	C17	0.671354743	Q14738 E9PFR3	3
IIMC*AWNPR	C97	0.669963333	P04818	2
AGSDGESIGNC*PFSQR	C35	0.669534801	Q9Y696	4
FQTIDIEPDIEALLSQGPSC*A		0.669215307	A0A087WUQ6	2
NIC*FTVWDVGGQDR		0.66906998	P18085	4
HFVLDEC*DK	C197 C173	0.668939687	K7EPJ3 O00148	3
GVLFGVPGAFTPGC*SK	C48	0.668798801	P30044 P30044	4
SVAWAPSGNLLATC*SR	C123	0.668079724	O76071	2
C*APAPPPPPPPPTSGPIGGLR	C20	0.667141301	Q12830 F5GXF5	4
VGVGPGSVC*TTR		0.667131624	P36959	3
YC*VRPNSGIIDPGSTVTVSVMLQPFDY	C60	0.666323873	Q9P0L0 Q9P0L0	3
VC*ALLSCTSHK	C299	0.665585769	P15121	3
HLSC*DLMPNENIPELAAELVQLGFISEA		0.664286667	F8W6G1 Q9UHY1	2
C*PEALFQPSFLGMESCGIHETTFNSIM		0.66412731	P63261 P60709	4
ATILDLSC*NK		0.663603476	Q96AG4	2
LPLC*SLPGEPGNGPDQQLQR	C75	0.662872616	Q96GX2	3
VAC*ITEQVLTLVNKR		0.662829558	P04843	4
SGQGAFGNMC*R	C96	0.662630725	P36578	4
VPAFEGDDGFC*VFESNAIAYYVSNEEL	C68	0.661815512	P26641 P26641	4
STSSSC*HAPAVTQHAPYFK		0.661053223	P30048	2
NIC*FTVWDVGGQDK		0.661023931	P84085	4

QVQSLTC*EVDALKGTNESLER	C328 C146	0.660999253	B0YJC5 B0YJC4	4
QILLGIQELLNEPNIQDPAQAEAYTIYC*	C138	0.660546433	P63279	3
IYHPNINSNGSIC*LDILR	C79 C56 C47 C85 C87	0.660349034	P61077 P61077	3
TLETANC*MSSQTK	C96	0.660316163	P50416 P50416	3
SNELGDVGVHC*VLQGLQTPSCK		0.660284121	P13489	3
VGLGIC*YDMR		0.658166667	Q9NQR4	2
LPLGFTFSFPC*HQTK		0.657323819	E9PB90 P52789	3
FASGGC*DNLIK	C233 C173 C190	0.657238882	P55735 A8MXL6	3
LC*PGGQLPFLLYGTEVHTDTNK		0.656552757	O00299	3
NTPSFLIAC*NK	C179	0.656384873	Q9Y5M8	2
MVSGC*QTR	C249	0.656345	Q8N1G4	2
SYILTQGPLPNTC*GHFWEMVWEQK		0.656270505	P18031	2
TC*ATDLQTK	C42	0.655924929	F8VVW8 O95861	3
ALRLDVGNFSWGSECC*TR		0.6552249	P62241	3
IIC*SAGLSLLAEER		0.655128323	Q9BV86 S4R338	4
GLVVLGFPC*NQFGHQENAKNEEILNSL		0.653970807	A0A087WUQ6	3
QQIACIGGPPNIC*LDRLENWITSLAESQ	C259 C161	0.653542701	P40763 G8JLH9	3
GAPSPGVLGPHASEPQLAPPAC*TPAA	C186	0.652437501	O96013 O96013	4
FTPTVPHC*SLATLIGLCLR	C90	0.652321	H0YKV4 Q9H5X1	2
FPDFLDC*LPGTNVDLGTLESEDLIPLFN	C363	0.65217	Q9GZV5	2
C*PFTGNVSIR	C60	0.652001283	P62280	4
TFC*GTPEYLAPEVLEDNDYGR	C310 C167	0.651842007	P31749	3
QMEKDETVSDC*SPHIANIGR	C194 C235	0.65146024	P47756 P47756	3
ILEDLDSLGVLIC*YMHNK	C137 C95	0.651120409	Q9Y305 Q9Y305	3
GTELDCGIETDSGVDDDMAC*HKIPVEA	C184	0.65095	P42574	2
AAC*NGPYDGKWSK	C249	0.65083	Q9HC38 F6TLX2	3
FSFCC*SPEPEAEAEAAAGPGPCER		0.650805687	Q13501	4
IQCTLQDVGSALATPC*SSAR	C80 C132	0.650753058	Q96EY8 S4R3P5	3
YINENLIVNTDELGRDC*LINAAK	C147	0.650521455	E7ERF2 P17987	4
CPALYWLSGLTC*TEQNFISK	C27	0.650479199	X6RA14 P10768	4
QHC*AYTIAK		0.649599596	Q6YN16	2
ELEVLLMC*NK	C91 C109	0.648290474	P62910 F8W727	4
YSNVIFLEVDVDDCQDVASEC*EVK		0.64818	P10599	2
YGAVDPLLALLAVPDMSSLAC*GYLR	C223	0.647421366	P52292	3
HGFC*GIPITDTGR		0.646031885	P12268	4
LFVSGAC*DASAK	C204	0.645815	P62873 P62873	2
SAFLC*GVMK	C99 C96	0.644653982	O43390 O60506	2
SC*SLVLEHQPDNIK	C91 C136	0.644439847	Q14318 Q14318	2
QVLMGPYNPDTC*PEVGFFDVLGNDR		0.644332167	Q9H3P7	3
VC*EEIAIIPSK	C35	0.64421071	P08708	4
FFFQMC*QPIPSYLIALAIGDLVSAEVGP	C223	0.642057522	A6NKB8 C9JMZ3	2
ALLDLC*AAPGGWLQVAAK	C52	0.64179076	Q8IY81	2
SSTETC*YSAIPK	C2321 C2477 C2532	0.641365753	O75369 O75369	3
VLDALFPCVQGGTTAIPGAFGC*GK	C221	0.640895407	P38606 P38606	2
ALANVNIGSLIC*NVGAGGPAPAAGAAPAGGPAPSTAAAPAEEK		0.640513494	P05386 P05386	4
YLEC*SALTQR	C157	0.639411847	P15153 P60763	3
LQEVEC*EEQR	C318 C100	0.638887813	Q13596 Q13596	3
TIC*SHVQNMIK	C74	0.638879209	H0Y9V9 E7ESE0	4
GNC*LPPLPLPR	C106 C129	0.638861846	E9PKV2 Q9NRX2	3
KLLAPDC*EIIQEVGK	C215	0.638604862	Q9NQT5	2
ATGHSGGGC*ISQGR		0.638090769	I3L407 I3L139	4
LSLLGGALPMFELVELQPSHLAC*PDVL	C361	0.637909525	Q9Y4P1	2
VQAQYPGVC*INNEVVEPSAEQIAK		0.637693128	P50135	2
LSDQC*TGLQGFLVFHSFGGGTGSGFT		0.636886667	P68366	2
LWQADC*SSRPLLLAGYEDGSVVLWDV	C175	0.636815	Q9BYB4 Q9BYB4	2
ANPDPNCC*LGVFGLSLYTTER	C19 C119	0.636658008	P62995 P62995	2
AWVWNTHADFADEC*PKPELLAIR	C209 C132	0.636627898	C9JXG8 P43487	4
SELEC*VTNITLANVIR	C27	0.636609985	Q9Y6W5 Q9Y6W5	4
LLPAITILGC*R		0.636530376	Q96IJ6 Q96IJ6	3

TGC*TFPEKPDFH	C318 C336	0.636424602	P55263 P55263	4
MVYSTC*SLNPIEDEAVIASLLEK	C85	0.635750267	Q08J23 Q08J23	3
GCITIIGGGDTATC*CAK	C351	0.63564	P00558 P00558	2
VFIMDNC*EELIPEYLNFIR	C374	0.634853729	P07900 P07900	4
DVLKEEGVSFLINTFEGGGC*GQPSGIL		0.634050515	P78527 P78527	2
ESFIIEEQSFLLC*EDLLYGR	C49	0.633398612	H3BNT4 Q99547	2
EAFEETHLTSLDPVKQFAAWFEEAVQC	C72	0.633069337	Q9NVS9 Q9NVS9	3
VVMALGDYMGASCHAC*IGGTNVR		0.633002013	P60842	4
LAIIVDEGGDALLVSLVC*R		0.632906064	A0A0B4J2E5	2
VPC*CTHSLPIEDPQWSTDPAQIR	C252	0.632820954	A2RU30 A2RU30	2
TVEEIEACMAGC*DK	C482 C418	0.632820687	P12955 P12955	2
YSNSALGHVNC*TIK	C108 C254 C75 C301	0.632233799	Q9NQC3 Q9NQC3	3
SPWLAGNELTVADVVLWSVLQQIGGC*SVTVPANVQR		0.632149503	F8W950 Q13155	4
SGVVPC*GTPWGQWYQTLEEVFIEVQV		0.63206174	Q8WVJ2	4
GPDAASKLPLVTPHTQC*R	C58	0.63168813	P62191	2
ADHQPLTEASYVNLPTIALC*NTDSPLR	C148	0.631093601	A0A0C4DG17	2
FLENTPSSLNIEDIEDLFSLAQYYC*SK	C283 C146	0.630815549	Q9NUY8 E9PGE5	3
STFFNVLTNSQASAENFPFC*TIDPNES		0.630439046	J3KQ32 Q9NTK5	4
AEIPC*EDEQEQEHNGPLDNK	C471 C439	0.630413011	Q5R363 Q96SB4	3
AIVDC*GFEHPSEVQHECIPQAILGMDV	C62 C63	0.630166667	Q13838 Q5STU3	3
VVSLIPAVVSGNC*QDLK	C24	0.629153129	H3BLY8 Q8N9A8	2
VLTC*TDLEQGPNFFLDFENAQPTESEKEIYNQVNVVLK		0.628240347	Q9NUQ9	4
C*ALLASEVPQLALQLLQDPESYVR		0.628188836	Q6PJG6	2
EMSC*IAEDVIIVTSSLTK	C97	0.628027513	Q9Y678	2
C*QNALQQVVAR	C620	0.627326667	Q06210 Q06210	2
ALNVEPDGTGLTC*SLAPNIISQL	C152	0.627039157	P30044 P30044	3
AIVFSGC*GR	C70	0.62619713	Q9BUL9	2
GC*LLYGPPGTGK		0.626133174	A0A087X2I1	4
IGTSGGIGLEPGTVVITEQAVDTC*FK		0.625140637	Q16831	2
GNSPPSSGEAC*R	C179	0.624958757	P41227 P41227	2
LITWSPVC*R		0.624950144	A0A087WUQ6	3
LECVEPNC*R	C77	0.62370231	P83881 Q969Q0	3
LFTESC*SISPK	C68	0.623597915	C9JUC3 C9J7N0	2
YMAC*CLLYR	C315 C282	0.622870596	P68366 P68363	3
INISEGNC*PER	C54 C86	0.622862932	P57721 P57721	3
PSWADQVEEEGEDDKC*VTSELLK	C25	0.62251	O75821 K7ENH0	2
VQVSDPESTVAVAFTPTIPHC*SMATLIG	C93	0.622463106	Q9Y3D0	4
GISCMNTTLSESPFKC*DPDAAR		0.622422426	Q15181	2
MVAAVAC*AQVPK	C393	0.622398414	D6RD67 Q9HCC0	4
ADPDGPEAQAEAC*SGER	C18	0.621975449	D6RCB9 D6RC52	4
LQSGIC*HLFR		0.621778456	P14868 P14868	3
TC*TTVAFTQVNSEDKGALAK		0.621730828	P62424 Q5T8U2	3
VC*ENIPIVLCGNK		0.621466714	F5H018	4
HEEFEEGC*K	C245	0.621008218	F6TLX2	3
HELQANC*YEEVKDR	C139 C177	0.620738948	E9PK25 G3V1A4	3
C*EVNGAGAHPLFAFLR		0.620378336	A0A087WUQ6	3
QGEYGLASIC*NGGGGASAMLIQKL		0.6198	P24752	3
C*SGVMEFSTSGHAYTDTGK	C36	0.619670126	Q9Y277	2
SGGSGGC*SGAGGASNCGTGSGR		0.619597547	E9PI68 E9PL01	3
KPTDGASSSNC*VTDISHLVR	C342 C710	0.619570302	P49321 P49321	4
YMACC*LLYR	C283 C316	0.619403995	P68366 P68363	3
IC*LQPPPTSR	C41	0.617886469	P26640 A2ABF4	2
FGVIC*LEDLIHEIAFPGK		0.617735305	Q6DKI1	4
VAASC*GAIQYIPTELDQVR	C134	0.6148105	Q7L2H7 J3KNJ2	2
AQNTWGC*GNSLR	C148 C522 C410	0.613904112	P02545 P02545	3
APAMC*SSPRVPR	C337	0.613875383	Q96GM1	2
YEAAFPFLSPC*GR	C90	0.6137525	Q6P1X6 H0YF29	2
TC*LPGFPGAPCAIK	C1817 C1930	0.613668904	P51610 P51610	4
TEYGDLELC*IEVVDNVQDAIDHIHK	C674	0.613122447	P54886 P54886	2

SVNSLDGLASVLYPGC*DTLDKVFTYAK	C85	0.612883388	O95573	2
LTNTYCLVAIGGSENFYSVFEGELSDTIPVVHASIAGC*R		0.612731638	P56537	3
NVQLLSQFVSPFTGC*IYGR		0.612329681	Q9Y3D5	3
AC*QSIYPLHDVFVRK	C201	0.612106637	D6R9B6 P61247	3
DSAQC*AAIAER		0.612084921	Q96RS6	3
LDINLLDNVVNC*LYHGEGAQQR		0.612014546	O14980	4
NC*LTNFHGMDLTR	C96	0.611360802	D6RB09 D6RAT0	4
AQVPGSSPGLLSLSLNQQPAAPEC*K	C290	0.611253743	Q86W42	3
GNVAGDSKNDPPMEAAGFTAQVIILNH	C342	0.610421795	P68104 P68104	4
AVLPVTC*HR	C2085 C2094	0.610293266	Q96N67 Q96N67	3
KIPC*DVTEAEIISLGLPFGK	C71 C40	0.610240387	X6R242 O95758	3
ETARPCYSLALAQLLQSFEDLPLC*SILQ	C29 C109	0.609973822	Q9BQG0 I3L1L3	2
DPTTKPFSVLLYIGTC*DNPDYLGPAPLEDIAEQIFNAAGPSGR		0.609745	Q8WUX2	2
AHTVLAASC*AR		0.609527014	Q8WUY1	3
LVC*GMVSYLNDLPSQR	C411	0.609307497	Q15067 Q15067	2
GSQMGTVQPIPC*LLSMPTR	C559	0.608812051	Q9NZB2 Q9NZB2	3
YQQELEEEIKELYENFC*K	C429	0.608709726	Q6DD88 F5H6I7	2
TYSHLNIAGLVGSIDNDFC*GTDMTIGTD	C170	0.607294817	P17858	3
NMITGTAPLDGC*ILVVAANDGPMPQTR		0.607286054	P49411	2
LEGDLTGPSVGVEVPDVELEC*PDAK		0.607240672	Q09666	4
PC*GEDWLSHPLGIVQGFFAQNGVNPD	C3	0.607111187	Q9BTE3 Q9BTE3	3
IC*EPGYSPTYK	C211	0.60651	P07858	2
EKTAC*AINK	C293	0.606348413	Q8NCA5 E9PH82	2
ASHIQLDSLPEVPLLVDVPC*LSAQLDD		0.606259824	Q8IUI8 Q8IUI8	2
ALAPLLLAFVTKPNSALESC*SFAR		0.606207673	P46060	3
EVFSSC*SSEVVLSGDDEEYQR		0.605449582	Q09666	4
TWYVQATC*ATQGTGLYEGLDWLSNEL		0.605076395	P18085	4
DCIGGC*SDLVSLQQSGELLTR	C83	0.60506849	P35754	4
VCENIPIVLC*GNK		0.604863905	P62826 J3KQE5	2
YLC*DFTYYTSLYQSHGR		0.604750562	Q9NXJ5 Q9NXJ5	2
C*EGINISGNFYR		0.60454	M0QYS1	2
AVC*MLSNTTAIAEAWAR	C376	0.604408421	P68366 P68363	4
HSMNPFC*EIAVEEAVR	C133	0.604153898	P38117 P38117	2
C*ESAFLSK	C36	0.60318079	C9JNW5 C9JXB8	4
NMSVHLSPC*FR	C116	0.60290972	P62280	4
DQVAQLDDIVDISDEISPSVDDLALSIYP	C172 C300	0.602736667	O95273 O95273	2
LLAC*IASR		0.601458245	P62241	3
ITSAVWGPLGEC*IIAGHESGELNQYSA	C160	0.600714932	Q13347	2
GTLTLC*PYHSDR		0.600638407	Q13200	4
ILDILGETC*K	C225 C156	0.600625977	Q15424 Q14151	2
VFPLSC*AVQQYAWGK	C11	0.60060654	H3BUZ9 P34949	2
QSLLFC*PK	C27	0.600509541	Q56VL3	4
GAVEKGEELSC*EER	C38	0.600492603	P31947	4
MYGISLC*QAILDETKGDYEK		0.600485783	P04083	4
LPACVVDC*GTGYTK	C12	0.599719701	P61158	3
LLQPPKGVLLYGPPGC*GK	C137	0.599457709	Q8NBU5 Q8NBU5	3
AGEVVPPAMYQFSQYVC*QQTGLQIPQ	C82 C60	0.599307287	K7EIR2	2
NFEATLGWLQEHAC*SR	C519	0.598715434	Q9P2J5 Q9P2J5	3
LSAPGC*WAACTNFSR		0.598196137	Q04941 Q04941	3
LLGPTVMLGGC*EFSR	C667	0.597944166	Q8N9T8	2
GC*WDSIHVVEVQEK	C135 C176	0.59757213	P47756 P47756	3
INPYMSSPC*HIEMILTEK	C106 C144	0.597535654	J3KRX5 P18621	3
YVFNLAELAELVPMEYVGIPEC*IK	C416 C173 C295	0.597048478	Q12982 Q12982	3
DQQEAALVDMVNDGVEDLRC*K		0.596998	P09211	2
DINAYNC*EEPTEKLPFPIIDDR	C91	0.596660175	P30041	4
EVIAVSCGPAQC*QETIR	C162	0.596053435	P38117 P38117	2
ATC*APQHGAPGPGPADASK	C2503 C2516 C2535	0.594836558	P21333 Q60FE5	4
FQLTDC*QIYEVLSVIR	C143	0.593585775	Q16555 Q16555	2
VQPQWSPPAGTQPC*R	C40 C110	0.593326741	P49589 B4DKY1	4

TGLC*YLPEELAALQK	C46	0.592891369	Q13045 Q13045	2
NC*IVLIDSTPYRQWYESHYALPLGR		0.591821864	P62241	4
LQDAFSSIGQSC*HLDLPQIAVVGGQSA	C27	0.591578023	P50570 P50570	4
PMC*IPPSYADLGK		0.591451667	A0A0A0MR02	4
SLC*LGPALIHTAK	C73 C54	0.591239851	Q99643 Q99643	4
LADQC*TGLQGFLVFHSFGGGTGSGFT	C129	0.590586258	P68363 Q71U36	4
KIVEAC*K	C182	0.590208622	Q9NT62 Q9NT62	2
IIFVVGGPGSGKGTQC*EK	C41	0.590202007	Q5T9B7 P00568	3
CDVTQSQPLGAVPLPPADCVLSTLC*LDAACPDLPTYCR		0.589712851	P40261	2
DHQPC*IIFMDEIDAIGGR		0.58957	A0A087X2I1	2
SSSSVTTSETQPC*TPSSSDYSDLQR		0.589406926	P50552 K7EM16	4
SLITSDKGFVTMTLESLEEIQDVSC*AW	C603	0.5892575	Q9BQ39	2
ETTEAAC*R	C164	0.58895	Q9Y2Q3 E9PFN5	2
SC*EGQNPELLPK	C309	0.58891818	Q9NQW6	2
TC*PVQLWVDSTPPPGTR	C102 C141	0.588598921	P04637 J3KP33	3
ISGPNPLSC*LK		0.588547303	Q9BRU9	4
LFIFETFC*R	C345	0.588388764	P60228	2
QASC*SGDEYR	C119 C200	0.588369343	A0A087WT27	2
VIIVQAC*R	C328 C173 C258 C202	0.58832218	P51878 P49662	4
DGSDYEGWC*WPGSAGYPDFTNPTMR	C524	0.587695	Q14697 Q14697	2
FC*DNSSAIQGK		0.58716	O15067	2
VTDGALVVVDCVSGVC*VQTETVLR	C136	0.586542547	P13639	4
VLAELPQC*LRK		0.586193333	Q9BZG1 A8MYQ9	2
GAEPETGSAVSAAQC*QGPTR	C67 C69	0.586140406	Q9UI10 Q9UI10	3
C*SEGSFLLTTFPRPVTVEPMDQLDDEE		0.586116406	Q15233	3
QFNC*SPHPYWLPNFMDVFTWSLPFVG	C332 C336 C104 C238	0.585843861	P16298 P48454	2
GC*TATLGNFAK	C131	0.585725004	P15880 H0YEN5	4
VLVTTNVC*AR	C393 C392 C310	0.585485985	I3L0H8 Q9NUU7	2
ERESLNASIVDAINQAADC*WGIR	C167	0.585293702	Q9UJZ1	4
FC*IWTESAFR	C250	0.585169695	P36578	3
VDLNSNGFIC*DYELHELFK		0.585010555	P13797	4
GNHEC*ASINR	C136 C83 C126 C127	0.584875294	F8VYE8 P62136	4
GSC*STEVEKETQEK	C69	0.584599143	O75348	4
SCSSSC*AVHDLIFWR	C46	0.58456419	O95197 O95197	4
TILTLTGVSTLGDVKNNQESDC*VSK		0.584366097	A6NDG6 H3BV17	3
GVPGAIVNVSSQC*SQR		0.584241196	Q7Z4W1	4
LNGGLGTSMGC*K	C112 C123	0.584101807	C9JUW1 Q16851	4
IAVYSC*PFDGMITETK	C225	0.584048583	P50990	3
LDVGNFSWGSEC*C*TR		0.583473563	P62241	3
VEEEDDAEHVLALTMLCLTEGAKDEC*		0.583362047	O75607	2
NEC*DPALALLSDYVLHNSNTMR	C300	0.582912351	Q13200 Q13200	2
AISTIC*SLEK	C259	0.582601262	Q9UJX3 Q9UJX3	2
SVPLC*ILYEK	C545	0.582546834	P21980	3
VVQHLC*QR		0.581643419	Q8WUY1	2
LANVQLLDTDGGFVHSDGAISC*HDMFDFLHLTGGGYAK		0.581623167	P68402	4
ADAEDLLDSFLSNILQDC*R	C313	0.58127744	Q96T76 Q96T76	2
C*MQLTDFILK	C54	0.581191542	E7EPB3 P50914	2
C*LAQEVNIPDWIVDLR	C98	0.580737448	Q9Y4W2 Q9Y4W2	2
KGTVLLADNVIC*PGAPDFLAHVR	C173	0.580501885	P21964 P21964	4
C*ELSSSVQTDINLPYLTMDSSGPK	C22	0.580422592	P38646 H0YBG6	4
TGQATVASGIPAGWMGLDC*GPESSKK	C288	0.580335	P00558 P00558	2
LLVLEAFQVSHPC*R	C150 C191	0.580226324	G3V267 O43708	4
YGVGTC*GPR		0.57920068	O15269 O15269	2
LTPGC*EAEAETEAICFFVQQFTDMEHN	C2359	0.578727893	P49327	4
AQIIELLC*IVEALKK	C595	0.578125374	Q9Y5K6	4
LPLALPPASQGC*SSGGGGGGGGGSSAGGSGNSRPPR		0.577975189	Q9NZL4 Q9NZL4	4
LSSC*DSFTSTINELNHCLSLR		0.577574338	P07814	4
FAAAYC*R	C311 C280	0.577090352	P08559 P08559	3
QTISNAC*GTIGLIHAIANNK	C95	0.577012646	P15374	2

DVIELTDDSFDKNVLDSEDVWMVEFYA	C242 C195	0.576505	Q15084 Q15084	2
ALVDGPC*TQVR	C42	0.576129016	E7EPB3 P50914	4
GC*LWALNPAKIDK		0.576040496	O15353	2
IVNLAC*K		0.575910473	O00116	2
LGGTC*VNVGCVPK	C102	0.57570752	H0YC68 P00390	3
NVGIAFQLIDDVLDFTSC*SDQMGKPTS	C276	0.575407221	Q5T2R2 Q5T2R2	2
GPFVEAEVPDVDLEC*PDAK		0.575200683	Q09666	4
TDVC*VFAAQEDLETMQAFAQVFNK	C100 C96	0.575156683	C9JWF5 Q7L1Q6	3
EGIC*ALGGTSELSSEGTQHSYSEEEKY		0.574836296	P13797	4
FQSAAIGALQEASEAYLVGLFEDTNLC*		0.574477997	K7EK07 P84243	4
NTLANSC*GTGIR	C393	0.574282021	Q96BF6 Q96RE7	3
KAVVVC*PK	C588	0.574126392	Q00839 Q00839	4
LLAPDC*EIIQEVGKLYPLEIVFGMNGR	C215	0.573944556	Q9NQT5	4
DVTEVLILQLFSQIGPC*K	C35	0.573821523	Q01085 Q01085	2
FNNWGGSLSLGHPFGATGC*R	C413	0.573193349	P55084 B5MD38	4
NC*PHVVVGTPGR	C164	0.573083283	O00148	4
NC*PHIVVGTPGR	C165	0.572955149	Q13838 Q5STU3	3
PPMEAAGFTAQVIILNHPGQISAGYAPV	C349	0.572816096	P68104 P68104	4
QIETGPFLEAVSHLPPFFDC*LGSPVFT	C36	0.571609894	Q9NZD2 F5GZ49	2
NMVHPNVICDGC*NGPVVGTR		0.56998	E7EMC7 Q13501	2
SC*SPLAFSAFGDLTIK	C231	0.569189958	Q96EY5 Q96EY5	3
C*EFEEVQGFLDQVAHKLPFAAK		0.569080106	E9PI14 Q9NX20	3
AFAFVTFADDQIAQSLC*GEDLIIK	C244	0.568481715	A0A087X260	4
AIELNPANAVYFC*NR	C129	0.568183289	K7EMD6 O43765	2
FC*DNVWTFVLNDVEFR	C33	0.567498373	P52657	4
GFLFGPSLAQELGLGC*VLIR		0.567053042	P07741	3
VAC*AEEWQESR	C87	0.566282521	O75663 O75663	4
NYLPAINGIVFLVDC*ADHER		0.565912085	Q9Y6B6	4
VTEPSAPC*QALVSIGDLQATFHGIR		0.565902966	Q9UPN7	3
C*KPVPLLELAEGQK		0.56587325	Q8NHV4 Q8NHV4	4
TVFAEHISDEC*K	C141 C114	0.56467778	H7C422 P39023	3
LTTPTYGDLNHLVSATMSGVTTC*LR	C239 C221	0.563472607	Q13885 P68371	4
GPSIALDTAC*SSSLMALQNAYQAIHSG	C161	0.56328	P49327	2
IHMGSC*AENTAK		0.563272689	P24752	4
AWSTGDC*DNGGDEWEQEIR		0.563123751	Q9BRF8 Q9BRF8	4
GVLMYGPPGC*GK	C179	0.562886515	P43686 P43686	2
IEGC*IIGFDEYMNLVLDDAEEIHSK		0.562519563	P62304	4
GFSAISC*TVEGAPASFGK	C33	0.562195	Q96EY5 Q96EY5	2
TVNCLLVGAIAIPHC*VLK		0.561877881	Q5SY16	2
C*LSIMLAEWEANPLICPVCTK	C122	0.559517504	A0A0B4J1T3	2
VNAAGTDPSSPVGFVLGVDLLHIFPLEGATFLC*PADVTDPR		0.559150747	Q9UI43	3
VAC*IGAWHPAR	C253	0.559091324	P39023	2
NNMNC*EAR	C182	0.558546238	J9JIC5 Q9HAS0	2
ITAFVPNDGC*LNFIEENDEVLVAGFGR		0.557480398	P62266	4
FFACAPNYSYAALCEC*LR		0.557345127	Q96RS6	3
LLQC*DPSSASQF		0.556922837	P84074 P37235	2
AGVC*AALEAWPALQIAVENGFGGVHS		0.55637023	Q969E8	3
LPSLPLVQGELVGGLTC*LTAQTHSLLQ	C213	0.556191981	Q7Z7H8 Q7Z7H8	2
VC*NVAPIAGETK	C188 C336	0.556109823	H0YG10 Q13823	2
NLVFSSSATVYGNPQYLPLDEAHPTGG	C79	0.555229157	Q14376	3
YIELFLNSC*PK		0.555078143	Q12849	3
YGIIC*MEDLIHEIYTVGKR	C186	0.554033727	P18124 A8MUD9	4
TPC*NAGTFSQPEK	C129	0.553499686	O43684 J3QT28	4
THPSAAVPVC*PR	C361	0.552849883	Q3KQU3 Q3KQU3	2
TIC*AILENYQTEK		0.552166667	Q5T5C7 P49591	2
VSLDPELEEALTSASDTELC*DLAAILGM	C132	0.552028017	Q9NYL9	3
STC*SLTPALAAHFSENLIK		0.551970518	Q9BTA9 Q9BTA9	3
FMADC*PHTIGVEFGTR	C40	0.551880121	X6RFL8 P61106	2
SAC*SLESNLEGLAGVLEADLPNYK	C44	0.55168024	Q09161 F2Z2T1	3

IGIASQALGIAQTALDC*AVNYAENR	C285	0.551678207	P16219 E9PE82	2
C*IADVVSLFITVMDK	C128 C111	0.551305414	E9PM90 Q9UK41	4
NC*LLLLTYLISELEAAR	C108	0.551288057	Q8NCA5 E9PH82	3
AAAAVAAAASSC*RPLGSGAGPGPTGAAPVSAPAPGPGPAGK		0.549783165	Q9NRL3 Q9NRL3	4
IGEGLDQALPC*LTELILTNNSLVELGDL	C89	0.549683297	P09661 H0YKK0	4
NYLPAINGIVFLVDC*ADHSR	C102	0.548858187	Q5SQT8 Q9NR31	4
C*LHNFLTDGVPAEGAFTEDFQGLR	C268 C316	0.548843809	G3V1A6 P57764	4
ATVAPEDVSEVIFGHVLAAGC*GQNPV	C94	0.548479007	Q9BWD1 Q9BWD1	4
YKVC*NYGLTFTQK	C66	0.547675194	Q9Y277 Q9Y277	4
IEC*SDNGDGTCSVSYLPTKPGEYFVNI	C1087 C918	0.547551356	O75369 E7EN95	2
FSC*EPAGGLTSLTEPPKGPGFGVQAG	C228	0.547212142	P19404 E7EPT4	2
HTGCC*GDNDPIDVCEIGSK		0.547088376	Q15181	3
HC*SQVDSVR	C112	0.545955601	Q14247	4
C*SDAAGYPHATHDLEGPPLDAYSIQG	C201	0.545698859	Q15365	3
VELC*SFSGYK	C6	0.545664302	C9JNW5 C9JXB8	3
YAGLSTC*FR		0.545395	Q5T5C7 P49591	2
NQSFC*PTVNLDKLWTLVSEQTR	C70	0.544563971	P46776 E9PLL6	4
IAILTC*PFEPPKPK	C253	0.544493949	E9PCA1 B7ZAR1	3
C*NYLALVGGGK	C63	0.544129737	I3L4S6 Q5MNZ6	2
HSDGNLC*VK		0.54368	P49458	2
AVC*MLSNTTAVAEAWAR		0.542700959		4
MAYQEYPNSQNWPEDTNFC*FQPEQVVDPIQTDPFK		0.542505	E7EVA0 P27816	2
AVAILC*NHQR		0.542453953	P11387	4
FQSSAVMALQEAREAYLVGLFEDTNLC	C111	0.54141	Q5TEC6	2
AWC*VNCFACSTCNTK	C309 C334	0.541322483	P48059 P48059	3
STPYEC*GFDPMSPAR	C39	0.540655209	P03897	2
IHEGC*EEPATHNALAK	C870	0.540015	A0A087WVQ6	2
SNLQEIFLPAFPC*HER	C337	0.539485	Q9NPG8	2
YLLPLSALGTVAGAAVLLKDYVTGGAC*	C30	0.538795	G8JLA1 Q8NBN7	2
YTC*GEAPDYDR		0.538468733	P21266	3
EAVFPFQPGSVAEVC*ITFDQANLTVK	C89	0.538043567	P09382	4
RGHQDPSQATGTTGSSVSC*TEEK	C77	0.537880352	Q96KR6	3
FQMQVLPQC*GHAVHEDAPDKVAEAVA		0.53741	Q9Y570 Q9Y570	2
TLSFYFPPC*GK	C388	0.537020098	Q9UG63 Q9UG63	3
KAEEATEAQEVVEATPEGAC*TEPR	C189	0.536960887	O75683	2
AGMAAVASPTGNC*DLER		0.536816728	Q6P1M0 Q6P1M0	2
IYHPNVDENGQICLPIISSENWKPC*TK	C105 C32	0.536610185	E9PKW8 O14933	3
LAPILC*DGTATFVDLVPGFR		0.536562666	O43264 O43264	3
KC*EAEEAEPPAATQPQTSETQTSHLP		0.536263282	Q9UKV3 S4R3H4	2
DADADAGGGADGGDGRGGHSC*R		0.535956104	Q14657	3
VQENSAYIC*SR	C585	0.535281919	Q9Y3T9	2
ALIVGHC*MPGPR		0.535148871	Q6P1L8	4
AILFSQPLQITDTQQGC*IAPVELR		0.534974232	Q8NBF2 Q8NBF2	2
LVVPATQC*GSLIGK	C109	0.534865788	Q15365	3
EPFDLGEPEQSNGGFPC*TTAPK	C277 C213	0.534235693	Q99961 Q99961	2
GAVEC*CPNCR		0.534209107	P31689 P31689	3
IAVHC*TVR	C72	0.534018066	P62913 Q5VVC8	3
LTWHSC*PEDEAQ	C177	0.533499393	Q13185	4
C*LTQQAVALQR	C1138	0.533252011	O75153 K7EIG1	3
NMMAAC*DPR	C285 C650 C303 C266	0.533144184	Q13885 P68371	4
AATGEEVSAEDLGGADLHC*R		0.532956643	Q9HCC0	2
DQLQELC*IPQDLVGDLASVVFGSQRPL	C117	0.53292513	E9PJE4 H0YEQ6	2
C*IPYAVLLEALALR	C110	0.532246994	F5H248 Q9UBW8	3
EC*LPLIIFLR		0.532086915	P62701	4
TIQFVDWC*PTGFKVGINYQPPTVVPGG	C417 C347	0.531898229	Q9BQE3 F5H5D3	4
ASVGFGGSC*FQKDVLNLVYLCEALNLP	C209	0.530996247	O60701 O60701	4
NSSC*GGGISSSSSSR		0.530967389	Q9BXB4	3
SIQFVDWC*PTGFK		0.530806084	P68366 P68366	4
QAVLGAGLPISTPC*TTINK	C119	0.530402191	P24752	4

LQEALDAEMLEDEAGGGGAGPGGAC*	C57	0.529947655	H3BQZ7 Q1KMD3	4
C*RDVFEPAR		0.529479133	Q9NX46	2
LLDRDAC*DTVR	C247	0.52849	Q9NZL4	2
WTQTLSELDLAVPFC*VNFR	C188	0.528488342	Q9Y266	4
AAAGEDYKADC*PPGNPAPTSNHGPDA	C21 C62	0.528385078	G3V3P2 G3V2Y7	3
SC*LLHQFTEK	C26	0.528142672	X6RFL8 P61106	3
LILDVFC*GSQMHFVR	C476 C446	0.527906276	P11413 P11413	2
FPEELTQTFMSC*NLITGMFQR	C339	0.527348917	P26641 P26641	3
ERFDPTQFQDC*IIQGLTETGTDLEAVA	C35 C39	0.527119054	Q7L1Q6 Q7L1Q6	4
WC*EYGLTFTEK	C65	0.527066264	A0A0A0MR02	4
DSGAASEQATAAPNPC*SSSSR	C671	0.527000173	Q9BU23 Q9BU23	3
NLPFPTYFPDGDEEELPEDLYDENVC*	C365 C338	0.52676013	E7ETU7 H0Y9G6	2
ADIDVSGPKVDVEC*PDVNIEGPEGK		0.526154557	Q09666	3
PAGALVALVVAPLC*WK	C284	0.526054694	Q2T9J0 Q2T9J0	3
AFLDNPGILSELC*GTLSR	C272	0.525684711	B4E1N1 Q6NXE6	3
YFNPTGAHASGC*IGEDPQGIPNNLMPY	C122	0.525115061	Q14376	4
NDPPMEAAGFTAQVIILNHPGQISAGYAPVLDC*HTAHIACK		0.525053849	P68104	2
AIVDALPPPC*ESACTVPTDVDK		0.525033854	Q15181	3
LSSQEESIGTLLDAIIC*R	C206	0.524416979	Q9Y3C4 Q9Y3C4	3
GLLDVTC*K	C120	0.523929514	P63208	2
TGSQGQC*TQVR	C27	0.523379744	P62857	4
C*AGPTPEAELQALAR	C52	0.52315755	Q15050	3
TWYVQATC*ATQGTGLYDGLDWLSHEL		0.522744321	P84085	4
EILKWEALHAAECPC*GPSLIR		0.521533333	P53701	2
LQTEAQEDDWYDC*HR	C366	0.51997679	Q9UHI6 E9PJ60	2
SYC*AEIAHNVSSK	C114 C96	0.519937873	P62910 F8W727	4
DLTTAGAVTQC*YR		0.518861473	M0R117 Q02543	3
TGC*VDLTITNLLEGAVAFMPEDITK	C325	0.518675292	Q9Y679 Q9Y679	3
SISSSSFGAEPSAPGGGGSPGAC*PAL	C34	0.518593026	O95197 O95197	3
NVGC*LQEALQLATSFAQLR	C947	0.517376322	P49588 P49588	4
VC*FGIQLLNAVSR	C114 C218 C182 C208	0.517274502	E7EWX8 Q99685	4
KENQWC*EEK		0.517228169	P63208	3
HEASDFPC*R		0.51693281	P18031	2
FLSQIESDC*LALLQVR		0.51667438	E9PB90 P52789	3
GSSC*FECTHYQSFLEYR	C188	0.516473734	P21964 P21964	3
LFFIQAC*R	C219 C271	0.515844837	P55210 P55210	3
NEANQPLC*LPALLIYTEASDYIPDDHQD	C834	0.515828207	Q01970 Q01970	3
LTGAGGGGC*GITLLKPGLEQPEVEATK	C287	0.515810797	F5H8H2 Q03426	3
GSDC*GIVNVNIPTSGAEIGGAFGGEK	C450 C441 C414	0.515356989	P49419 P49419	3
GQVC*LPVISAENWKPATK	C144	0.515267899	P68036 P68036	4
NSQWVPTLPNSSHHLDAVPC*STTINR	C138 C147	0.514978247	C9JTA6	4
DVQIGDIVTVGEC*RPLSK	C131	0.514698451	P62280	4
HGGPQYC*R	C59	0.514503157	O14684	2
WLSDEC*TNAVVNFLSR	C345	0.513701476	O75521	4
VLQFNEVGANAVTPMTPENFTSC*GFM		0.511744317	P05120	3
IVPVDIYIPGC*PPTAEALLYGILQLQR		0.511009936	O75251	2
AAAPAPEEEMDEC*EQALAAEPK	C266	0.510021542	P26641 P26641	4
VIEINPYLLGTMSGC*AADCQYWER		0.509866237	P28062 X5D2R7	2
IGLIQFC*LSAPK	C222	0.508798287	P50991 P50991	4
EEHLC*TQR	C217 C208 C212 C233	0.507528786	J3KN67 P06753	3
SPAAEC*LSEKETEELMAWMR	C573	0.5067	Q12931 Q12931	2
LVEALC*AEHQINLIK		0.506674591	P25398	2
VLLSIC*SLLCDPNPDDPLVPEIAR	C78 C109 C101	0.506217471	P61077 P61077	3
LDNWLNELETYC*TR	C139	0.506200854	Q9NP72 Q9NP72	4
GC*EVVVSGK		0.505952077	P23396	2
QPPWC*DPLGPFVVGGEDLDPFGPR	C185	0.505818145	F5H4Z3 Q5QPM7	2
ILTFDQLALDSPKGC*GTVLLSGPR	C105	0.505469659	J3QQ67 G3V203	4
SEETNTEIVEC*ILK	C902	0.50507	A0A087WV66	2
VVVVDDLLATGGTMNAAC*ELLGR		0.503670902	P07741	4

ISAFGYLEC*SAK	C159	0.503434029	Q5JR08 P08134	4
AC*PRPEGLNFQDLK	C227	0.503432481	P15927 P15927	3
ANNNAAVAPTTC*PLQPVTDPFAFSR	C46	0.502308277	F1T0I1 J3KNL6	3
GC*IVDANLSVLNLVIVK		0.501928278	P62753	4
LLLC*GGAPLSATTQR	C450	0.501736682	O95573	4
LVIYGGMSGC*R	C227	0.501615	P51610 P51610	2
LEGDLTGPSVDVEVPDVELEC*PDAK		0.501221497	Q09666	4
C*AGNEDIITLR		0.500824769	P12004	3
IGEMPLTDSILCDGLTDAFHNC*HMGITA	C187	0.500626381	Q9BWD1 Q9BWD1	2
VLGLGLGC*LR		0.500353136	Q9BRJ7 W4VSQ8	3
AC*LIFFDEIDAIGGAR	C133	0.499587024	P35998 P35998	4
ASATGMIIMDGVEVPEENVLPGASSLG	C289	0.499547218	Q92947 Q92947	2
KC*GETAFIAPQCEMIPIEWVCR	C81	0.499321487	E9PBS1 P22234	3
TC*QVLEALNVLVNRPNIR	C36 C109	0.498741449	E9PKW8 O14933	3
SVLC*STPTINIPASPFMQK	C22	0.498072304	Q96KB5 Q96KB5	3
DNTIEHLLPLFLAQLKDEC*PEVR	C377	0.498023661	B3KQV6 P30153	3
APVPSTC*SSTFPEELSPPSHQAK	C160	0.498017584	F5H763	3
SVPC*ESNEANEANEANK		0.497462064	Q9NS25	4
SAGDLGIAVCNVPAASVEETADSTLC*H	C123	0.497234884	Q13363 Q13363	3
LGGSLIVAFEGC*PV	C146	0.497216991	P60981 P60981	3
ADDTFEALC*IEPFSSPPELPDVMKPQD	C84	0.496671936	I3L0M9 Q15370	2
NC*GCLGASPNLEQLQEENLK	C32	0.496596075	E5RH09 P54136	2
TTC*MSSQGSDDEQIKR	C13 C22	0.496051462	Q9P0V9 Q9P0V9	2
IGFPETTEEELEEIASENSDC*IFPSAPD	C353	0.495454684	Q9Y3F4 Q9Y3F4	4
QC*MMFSATLSK	C223	0.49478	O00148	2
AIVDCGFEHPSEVQHEC*IPQAILGMDV	C75 C74	0.494714568	Q13838 Q5STU3	3
SHLNFSMLESPALHC*QPSTSSAFPIGS	C148	0.494381872	P49790 P49790	2
SIGYDDTDESHC*AEHIESR	C302	0.493562485	Q99541	3
QVLVAPGNAGTAC*SEK		0.493530271	P22102	2
APEILLGC*K	C177	0.493420404	P24941 G3V5T9	4
VWNLANC*K	C138	0.493257034	D6RAC2 J3KPE3	4
TIAEC*LADELINAAK	C172	0.492074607	P46782 M0R0R2	4
HLSSC*AAPAPLTSAER		0.492053155	Q6IBS0 D6RG15	2
LLEQFVC*AHTGIIFYAPYTGVCVK		0.491462336	Q9Y676	3
LVIVGDGAC*GK	C16	0.491083308	Q5JR08 P61586	4
LNISFPATGC*QK		0.490161509	P62753	4
LTLPNGEPVPC*LLLANK	C96	0.489915	O14966 O14966	2
LMWLFGC*PLLLDDVAR		0.489794005	O15067	3
LGPGRPLPTFPTSEC*TSDVEPDTR	C73	0.488620627	Q8TDD1 Q8TDD1	4
YAIC*SALAASALPALVMSK	C125	0.487392909	P36578	4
LTEGC*SFR	C93 C77	0.487034995	H0YMV8 Q71UM5	3
LNLPINIIGLAPLC*ENMPSGK	C335	0.486804752	P28838 P28838	3
SSSSSSASAAAAAAAASSSASC*SR	C100	0.486697484	Q07065	4
IMKDLDQC*R		0.484861563	P60903	3
VLLSICSLLC*DPNPDDPLVPEIAR	C113	0.484330489	P61077 P61077	3
TDICQGALGDC*WLLAAIASLTLNEEILA	C105	0.484033786	P17655	4
GTPEQPQC*GFSNAVVQILR	C67	0.483878829	Q86SX6	4
C*FLSWFCDDILSPNTK		0.483314259	Q9NRW3	2
GYGC*AGVSSVAYGLLAR	C115	0.483262718	Q92947 Q92947	2
TYDPSGDSTLPTC*SK		0.482832838	Q9Y2X3	2
C*DGETDKHWR	C24	0.482814905	Q9NXV6	3
LHDAIVEVVTC*LLR	C470 C267	0.482415656	O00429 O00429	4
VSDTVVEPYNATLSVHQLVENTDETYC*	C193 C211 C201 C183	0.481740876	P68371 Q9BVA1	4
YSSSFC*THDR	C66	0.481075304	P04183 K7ERV3	2
VVSGMVNC*NDDQGVLLGR	C230	0.48086	P21980	3
NQC*PAKPDGGGAPNGVR		0.47983984	Q9BX95	2
TVQTIEAC*IANFFNQVLVLGR	C242	0.478880411	Q29RF7	3
QMFEPVSC*TFTYLLGDR	C34	0.478234867	O95571 M0QXB5	3
C*TPACISFGPK	C34	0.477952908	A0A087WTS8	4

			P34932	
NC*LNPQFSK		0.477890874	O75131	3
VFSANSTAAC*TELAK	C48	0.477731663	Q14558 Q14558	3
AYGGSMC*AK		0.477626546	P49207	2
FMTPVIQDNPSGWGPC*AVPEQFR	C19	0.477431805	B0QYA8 O15371	3
LQAEVLEC*VSLVELTSLK		0.477072327	P07741	4
TGTQEVGGQDPGEAVQPC*R	C391 C443	0.476891434	A0A0A0MRN5	2
LVFLAC*C*VAPTNPR	C301	0.476478128	Q14566	3
IEEDVVVTDSGIELLTC*VPR	C467 C403	0.475695081	P12955 P12955	2
DKPELQFPFLQDEDTVATLLEC*K	C29	0.475040633	P09543 P09543	3
FSFC*C*SPEPEAEAEAAAGPGPCER		0.474274985	Q13501	3
SGEEDFESLASQFSDC*SSAK	C113	0.47328122	K7EN45 K7EMU7	4
VLQNMEQC*QK		0.473106104	J3KND1 E9PRZ1	2
VNQAIWLLC*TGAR	C155	0.472824768	P46782 M0R0R2	4
ALNALC*DGLIDELNQALK		0.471449464	P30084	4
VC*ISILHAPGDDPMGYESSAER		0.471122103	P60604 P60604	2
ALC*HLNVPVTVVLDAAVGYIMEK	C169	0.471008949	Q14232	2
TSAPITC*ELLNK		0.470202684	Q14204	2
NFYGGNGIVGAQVPLGAGIALAC*K	C219	0.469291625	P08559 P08559	3
LMSSLPNFC*GIFNHLER	C35	0.468376861	Q96PU8 Q96PU8	4
EKLC*YVALDFEQEMATAASSSSLEK		0.467820552	P60709 Q6S8J3	4
WC*NVQSTQDEFEELTMSQK	C59	0.467163109	D6RCP9 P27707	3
VALEGLRPTIPPGISPHVC*K	C361 C453	0.465887552	Q13418 Q13418	4
ASFENNCEIGC*FAK	C15	0.464733084	P56537	3
THTYEC*R	C1137	0.464057124	C9J4M6 C9J2Y9	2
HLNEIDLFHC*IDPNDSK	C62 C58	0.464021778	A0A087WYT3	3
LGGNPRLALSAC*FLCPPR	C58	0.463898237	H3BTC4	2
AYHEQLTVAEITNAC*FEPANQMVK		0.462243381		4
VEYPIMYSTDPENGHIFNC*IQR	C70	0.46221	Q5VV87 Q5VV89	2
ELEASEELDTIC*PK	C229	0.461476788	O76003	4
NC*NDFQYESK	C112	0.457237891	Q04917	2
SC*GSSTPDEFPTDIPGTK		0.456577017	P41091	3
ASFENNC*EIGCFAK	C11	0.455658144	P56537	2
RQDSDLVQC*GVTSPSSAEATGK		0.455619852	Q9HC52	2
TATAVAHC*K	C25	0.454844588	M0R3H0 M0R210	4
NWYVQPSC*ATSGDGLYEGLTWLTSNY	C155	0.454720452	P62330	4
VAEPELMGTPDGTC*YPPPPVPR	C1889	0.45466	F8VPD4 P27708	2
VFC*VEEEDSESSLQKR	C368	0.453139579	Q14684 Q14684	2
SC*SVTDAVAEQGHLPPPSVAYVHTTP	C341	0.452159266	Q96PU5 Q96PU5	3
NNTQVLINC*R	C46 C36	0.451780843	P62316 P62316	3
C*ALSSPSLAFTPPIK	C120	0.451382117	Q8NFH5 Q8NFH5	4
C*EEETPSLLWGLDPVFLAFAK	C8	0.451063662	Q9H668	3
NVGTGLVGAPAC*GDVMK	C44 C69	0.45086	Q9H1K1 Q9H1K1	2
LC*PLKDEPWPIHPWEPGSFR	C105 C78	0.450523479	E7ETU7 H0Y9G6	2
IIDLEEAEDEIEDIQQEITVLSQC*DSSYV	C77	0.449723492	B4E0Y9 Q9P289	3
EIC*CYSISCK	C158	0.447918315	Q9NVJ2 Q96BM9	3
ILSLIC*NSSSEKPTVQQLQILWK	C584 C111	0.446017607	E5RIM3 Q9Y263	2
SC*SGVEFSTSGSSNTDTGK	C36	0.445910191	A0A0A0MR02	4
VC*LLGDTGVGK	C9 C10	0.445591967	Q13636 Q9UL26	3
LANLAATIC*SWEDDVNHSFAK	C210	0.444789392	Q9NQW6	2
AQAVASTSTVPSPSQTMPSC*TSPSR	C171	0.444666159	E7EV05 E9PFU9	3
FFACAPNYSYAALC*ECLRR		0.443651506	Q96RS6	2
GNFTLPEVAEC*FDEITYVELQKEEAQK	C629	0.443242534	Q00839 Q00839	4
LVHSGSGC*R		0.442815	Q13425	2
AQHIVPC*TISQLLSATLVDEVFR	C57	0.4427938	P15927 P15927	3
ECPSDEC*GAGVFMASHFDR	C126	0.442589343	P62979	3
GGSYSQAASSDSAQGSDVSLTAC*KV	C369 C363	0.44133719	P10316 P30447	2

			P05534 P01891	
NVPHEDIC*EDSDIDGDYR		0.441033314	O00629	2
VLVVGAGGIGC*ELLK	C30	0.440451649	K7EPL2 K7ES38	3
EEQVISLGPQVAEGENVFGVCHIFASFN	C54	0.44043255	P62263 E5RH77	2
QVC*QLPGLFSYAQHIASIDGR		0.440099223	E9PIE4 Q9Y6C9	3
TDC*SPIQFESAWALTNIASGTSEQTK	C133	0.439264105	P52292	4
LTALDYHNPAGFNC*KDETEFR	C19	0.437719087	Q9Y224	4
LILADALC*YAHTFNPK	C376	0.437236195	P28838 P28838	4
VDEFPLC*GHMVSDEYEQLSSEALEAA	C49	0.437157841	X1WI28 P27635	4
LIVGLMRPPAYC*DAK	C64 C96	0.436938538	E5RK63 E5RI05	2
TIGGGDDSFTTFFC*ETGAGK		0.436303436	P68366	4
VCETDGC*SSEAK	C10 C14	0.436094412	D6RF24 H0Y9L0	2
C*LNNLAASQLK	C115 C70	0.435277643	Q14318 Q14318	4
LYYFQYPC*YQEGLR		0.43360393	Q9NRW3	3
SFC*SQFLPEEQAEIDQLFDALSSDKNS	C13	0.432712967	H3BTC5 Q6P9B6	3
GLNPLNAYSDLAEFLETEC*YQTPFNK	C343	0.431331762	O14879	3
SGAAWTC*QQLR	C87	0.430932508	Q9HD33 Q9HD33	3
VVNEINIEDLC*LTK		0.430624169	Q8N5K1	3
YQEAAPNVANNTGPHAASC*FGAK	C618 C517 C564 C295	0.430153311	O60716 O60716	2
TYAIC*GAIR	C56	0.42971921	Q8WVC2 Q9BYK1	3
TLLLC*GYPNVGK	C127	0.429473696	Q9BZE4 Q9BZE4	2
NWYIQATC*ATSGDGLYEGLDWLSNQL		0.429010386	P84077	4
DTGTVHLNELGNTQNFMLLC*PR	C126	0.428580486	Q2NL82 I3L1Q5	2
STMSLPPGLLGNSWGEGAPAWVLLDE	C505 C457	0.428363173	G3V1A6 P57764	2
AAQGPPAPAVPPNTDVMAC*TQTALLQ	C152 C115 C146	0.428184916	H0YEB6 O60232	4
EDLNC*QEEEDPMNK	C139	0.427215	O75821 K7ENA8	2
SAQASVSC*ALEALEPFWEVLVR	C426	0.427119699	Q9UBN7 Q9UBN7	2
SC*PSFSASSEGTR	C9	0.42698	D6RCP9 P27707	2
LLSNMMC*QYR	C136	0.426535361	A0A140T998	4
VTDDLVC*LVYK		0.424965028	P49458	4
IVDAVIQEHQPSVLLELGAYC*GYSAVR	C69	0.423352011	P21964 P21964	4
HVVC*AAETGSGK		0.422563514	Q9NUL7	2
TVLCGTC*GQPADK	C591 C187 C479	0.421047287	P02545 P02545	2
AC*ASPSAQVEGSPVAGSDGSQPAVK		0.42036	Q9UFC0	2
SQSPAASDC*SSSSSSASLPSSGR		0.4197218	O95817	4
QSELEPVVSLVDVLEEDEELENEAC*AV	C35	0.41967322	Q8N806	2
SC*NGPVLVGSPQGGVDIEEVAASNPE	C162	0.419358956	Q96I99 E9PDQ8	3
LC*YVALDFEQEMATVASSSSLEK		0.419163389	A5A3E0	2
QWNNC*AFLESSAK	C141 C99	0.418958253	E7ESV4 P61224	3
CC*LTYCFNKPEDK	C145	0.418395	P62979	2
NLVQC*GDFPHLLVYGPSGAGKK	C32	0.414757125	P40938 P40938	3
THTLC*R	C19	0.414451255	D6RG19 D6R9X9	2
GDSEPTPGC*SGLGPGGVR	C13	0.4144425	Q8WW01	2
VPPAPVPC*PPPSPGPSAVPSSPK		0.413739251	O95817	3
EENVGLHQTLDQTLNELNC*I	C283	0.412386094	P67936 K7EPB9	4
GILLYGPPGC*GK	C259 C170	0.409628664	I3L0N3 P46459	2
MAGIFDVNTC*YGSPQSPQLIR	C428	0.408379379	Q9BTX1 Q9BTX1	2
STGVVNIPAAEC*LDEYEDDEAGQKER	C119	0.406584093	Q96IZ0 H0YI16	4
TGNGPMSVC*GR	C493	0.406172231	O95793 O95793	3
TDICQGALGDC*WLLAAIASLTLNDTLLH	C115	0.405134832	E9PMC6 E9PSA6	4
LEDQATAYVCENQAC*SVPITDPCELR	C726 C770	0.404817088	Q8TB22 Q8TB22	2
LRPLSYPDTDVILMC*FSIDSPDSLENIP	C83	0.402254866	Q5JR08 P61586	2
AIVLFTSDAC*GLSDVAHVESLQEK	C193	0.40148421	P24468 P24468	3
IC*SHSAPEQQAR	C19	0.401091202	O75683	2
KC*SASNR	C17	0.401027922	Q8WVC2 Q9BYK1	3
ENVNVEEMFNC*ITELVLR	C163	0.400213348	F5H157 Q15286	4
SMVSPVPSPTGTISVPNSC*PASPR		0.39806605	P85037 P85037	4
ISEVFDC*WFESGSMPYAQVHYPFENK		0.397886667	J3KR24	2
QALVEFEDVLGAC*NAVNYAADNQIYIAGHPAFVNYSTSQK		0.397627024	M0QXS5 P14866	2

ALADAQIPYSAVDQACVGYVFGDSTC*		0.397555024	P22307	4
AAGELGIAVCNIPSAAVEETADSTIC*HIL	C140 C208	0.39618916	P56545 P56545	3
EGDVAAC*YANPSLAQEELGWTAALGL	C233	0.396025464	Q14376	4
NTVLC*NVVEQFLQADLAR	C70	0.3959133	Q14258	3
TFVPAMTAIHGPPITAPVVC*TR	C594 C549 C660	0.395875491	Q96RN5 Q96RN5	4
C*DLEDERVVGK	C76 C67 C118	0.394315	E7ESV4	2
INEIVYFLPFC*HSELIQLVNK	C513 C371 C572	0.393666523	Q9H078 Q9H078	4
TPSYSISSTLNPQAPEFILGC*TASK	C142	0.393222581	Q14694 H3BQC6	4
EC*PSDECGAGVFMASHFDR	C121	0.39310741	P62979	3
C*AVSDVEMQEHYDEFFEEVFTEMEEK	C67	0.392941621	Q01081 P0DN76	2
ALVGIC*TGHSNPGEDAR	C551	0.392940178	G3XAJ6 Q14699	2
TC*NVLVALEQQSPDIAQGVHLDR		0.3919	P31153	2
LFNC*SASLDWPR	C397	0.39118	Q9Y4W2 Q9Y4W2	2
TC*LLIVFSK	C20	0.390705209	Q5JR08 P61586	4
LIAALSTPSQQVQESVASC*LPPLVPAIK		0.390392569	Q92616	2
NSPLPNC*TYATR		0.389417982	Q5JTD0 Q5JTD0	2
KNEGSC*GPAR	C362	0.38940037	Q9NQZ5	3
EVLEHPWITANSSKPSNC*QNK		0.388901921	O14965	2
IDILINCAAGNFLC*PAGALSFNAFK	C129 C108	0.388441249	Q9NUI1 Q4VXZ8	2
RLDEC*EEAFQGTK	C92 C31 C103	0.385303108	P61289 K7ENH2	3
GGSYSQAAC*SDSAQGSDVSLTA	C349 C228	0.384229645	A0A140T9H3	3
KQC*QQLQTAIAEAEQR	C383	0.383696819	Q5XKE5	4
GHSSDSNPAIC*R	C31	0.383603711	A0A087X1U8	4
C*PARPPPSGSQGLLEEMLAASSSK		0.38314158	Q9C0C2	2
DLNYC*FSGMSDHR	C267	0.381350756	P31943 G8JLB6	3
APPPSLTDC*IGTVDSR	C20	0.38102565	Q9NZZ3 Q9NZZ3	3
DNLTLWTSDSAGEEC*DAAEGAEN	C237	0.380825898	P27348	3
MTGESEC*LNPSTQSR	C1212	0.379894659	Q9H2G2 Q9H2G2	2
MDILDVLTLAAQELSRPGC*LGR	C628 C102	0.379392532	Q9Y4R8 H3BU45	3
EEQVISLGPQVAEGENVFGVC*HIFASF	C31	0.377972397	P62263 E5RH77	4
AVTVAFC*TLPTR		0.377741645	Q5TA50	2
PMC*VESFSDYPPLGR		0.376714513	P68104	4
SSGEIVYC*GQVFEK		0.375999891	M0R117 Q02543	3
NQASC*GSCYSFASMGMLEAR	C255	0.375747204	P53634	2
AAIGC*GIVESILNWVK	C486 C431	0.374770024	P11388 P11388	4
NWYIQATC*ATSGDGLYEGLDWLANQL		0.372666845	P61204	4
AQQEQLLLQKQLQQQQQQPPSQLC*T	C385	0.370245913	Q9Y2D5 Q9Y2D5	2
STACQMLVC*YAK	C687 C705	0.369634308	H0Y8C6 O00410	2
SSVQEEC*VSTISSSKDEDPLAATR	C78	0.369587837	Q7L0Y3 C9JVB6	3
VMTIPYQPMPASSPVIC*AGGQDR	C194	0.369144732	Q15365	4
LGGEVSC*LVAGTK	C53	0.36858917	P13804 H0YLU7	2
VGLNAQAAC*APR	C157	0.364529943	P48681	2
FALNHPELVEGLVLINVDPC*AK	C71 C157 C154	0.364287357	Q5TH30 Q5TH29	4
VRPSTGNSASTPQSQC*LPSEIEVK	C131	0.363673043	Q9UJX3 Q9UJX3	2
LQILNSIFPGIGC*PVPR		0.363367588	Q9NX47	3
VALALC*LGKPADVYLIDEPSAYLDSEQ		0.361460963	P61221	2
AIC*TEAGLMALR	C399	0.361410686	P62191	3
RGPC*IIYNEDNGIIK	C208	0.360686248	P36578	4
NVC*TEAGMFAIR		0.357714617	A0A087X2I1	3
EHSLIEDLILLLEEC*DANIR	C421 C362	0.357302943	Q9H7B4 Q9H7B4	2
LQGINC*GPDFTPSFANLGR	C575 C466 C662	0.356784286	Q04637 Q04637	3
SVPC*DSNEANEMMPETPTGDSDPQP		0.355008286	Q9NS26	3
GYWASLDASTQTTHELTIPNNLIGC*IIG	C293	0.354175077	Q15365	2
GQFHEYQESTIGAAFLTQTVC*LDDTTV	C64	0.353808064	P51148 K7ERQ8	2
EGGGDSSASSPTEEEQEQGEIGAC*SD	C134	0.349176667	P49006	2
LC*EPEVLNSLEETYSPFFR	C261 C177 C224	0.349131881	H0YJA2 Q6PJT7	3

			Q6PJT7	
GYIWNYGAIPQTWEDPGHNDKHTGC*CGDNDPIDVCEIGSK		0.348633356	Q15181	3
NAIQLLASFLANNPFSC*K	C311	0.34838281	Q15021 E7EN77	3
TASISSSPSEGTPTVGSYGC*TPQSLPK	C787	0.348280184	Q6PKG0 Q6PKG0	3
HIPGAAFFDIDQC*SDR	C65	0.34822	B1AH49 P25325	2
ASAQQENSSTC*IGSAIK	C178	0.347958911	Q9NXV6	2
NC*GC*LGASPNLEQLQEENLK	C34 C32	0.34755042	E5RH09 P54136	4
SC*GHQTSASSLK		0.346725	Q9HB90	2
AVSPAIPSAPLYEEITYSGISDGLSQASC	C406	0.346533809	O60291 O60291	3
FSPNSSNPIIVSC*GWDK	C124	0.346380828	D6RAC2 J3KPE3	2
PVC*GLHSVISPSDGR	C172 C181 C147	0.345531487	Q9UG56 H0Y7P7	3
KLFAPQQILQC*SPAN	C230	0.344963524	P04183 K7ERV3	4
APPTAC*YAGAAPAPSQVK	C225	0.344878307	P17676 P17676	4
WASGLTPAQNC*PR	C115	0.343755674	O15533	3
LLQPGGGPDVGTGAPRPGC*SPR		0.343493579	Q9NXH8	3
AEEDVEPEC*IMEK	C56 C127 C32	0.342665	Q9UJU6 Q9UJU6	2
YVENPSQVLNC*ER	C1344 C1280	0.342457081	O75694 E9PF10	2
FHADSVC*K		0.342431846	Q9BW61	4
SQAAPGSSPC*R	C797	0.342416503	Q8N556 Q8N556	2
EGPAQPGAPLPTFC*WEQIR		0.341991493	E9PS00 Q9Y5Q0	2
VHIPNDDAQFDASHC*DSDKGEFGGFG	C141	0.339273333	Q16576 Q16576	2
SPVPLTPPGC*VALDTR	C173	0.337092521	Q567V2 Q567V2	3
AAC*LESAQEPAGAWGNK	C53	0.335677339	C9JT62 C9JES8	4
YSTGSDSASFPHTTPSMC*LNPDLEGP	C217 C213	0.335248747	Q15366 Q15366	2
IGAFGYMEC*SAK		0.333601905	P61586	4
GGC*PGGEATLSQPPPR		0.332537998	P20290	4
TDLLLDSESQGSGVFLPELDEPEYC*NAQNTALWELHALR		0.332122738	Q8WTT2	3
KTPC*GEGSK	C15 C70	0.328561841	P60866 G3XAN0	2
TTC*SSGSALGPGAGAAQPSASPLEGL	C12	0.328522648	Q96FZ5 F8WDZ3	2
LSEAAC*EDEDSASEGLGELFLDGLSTE	C238	0.327375712	O95801	2
CCLTYC*FNKPEDK	C149	0.326593982	P62979	2
GAEPETGSAVSAAQC*QVGPTR	C90	0.326564955	E7ERK9 Q9UI10	2
FCSFSPC*IEQVQR	C209	0.325132855	Q96FX7	2
TPSQLSDNNC*RQ	C334	0.324300271	Q4G0F5	2
NILGGTVFREPIIC*K	C154	0.323234378	P48735 P48735	3
C*ASQAGMTAYGTR	C127	0.323230888	Q15417 Q15417	4
SC*TDSELLLHPELLSQEFLLLTLEQK	C10 C48	0.32139822	C9J4K0 Q9BVC5	3
LFADAGLVC*ITSFISPFAK	C117	0.321268811	O95340 O95340	3
AATSTLSVC*DFLGEK	C137	0.318381826	G3V583 Q8N128	2
VGLSGAPADAC*STAQK	C394	0.317452073	Q8NFW8	4
VTEAPC*YPGAPSTEASGQTGPQEPTS		0.317225623	P40222	4
VASMAQSAPSEAPSC*SPFGK	C222 C196	0.317006667	Q00013 A8MTH1	2
YAC*GLWGLSPASR		0.314281237	H7C0N4 H7C561	2
TPGAATASASGAAEDGACGC*LPNPGT	C76	0.311443333	O96008	2
VC*ENIPIVLC*GNKVDIK		0.311030984	P62826 J3KQE5	4
IC*DQISDAVLDAHLQQDPDAK		0.310975744	P31153	2
LSEEAEC*PNPSTPSK	C947	0.310956119	O94804	3
GEFYVIEYAAC*DATYNEIVTFER		0.31075	P51114 B4DXZ6	2
GRDDC*GTFEDTGPLLQFDYK	C268	0.309654036	Q14684 Q14684	2
DAPAPAASQPSGC*GK	C22 C13 C30 C23	0.308632942	F8WBU3 F8WCL3	2
HFC*PNVPIILVGNK	C107	0.308199037	Q5JR08 P61586	4
ISLGLPVGAVINC*ADNTGAK	C28	0.306817017	P62829 B9ZVP7	4
VNSDC*DSVLPSNFLLGGNIFDPLNLNS		0.305327951	Q7L2J0	2
TTEDEVHIC*HNQDGYSYPSR	C671	0.304419069	P01130 P01130	2
AHQLVLPPC*DVVIK	C279	0.303114304	Q9NZB2 Q9NZB2	2
EFHQAGKPIGLCC*IAPVLAAK	C93 C91 C188	0.30304607	H7C1F6	4
QALVNC*NWSSFNDETCLMMINMFDK		0.301095	Q9UBV8	2
SNSPPALGPEAC*PVSLPSPPEASTLK	C140	0.300555	Q9H0F6 Q9H0F6	2
AAQDFFSTC*R	C59	0.298032974	H0Y5R6 Q5T446	2

AAQVALLYLQELAEELSTALPAPVSC*P		0.290889492	Q8WUA4 Q8WUA4	4
PSASC*DTLLDDIEDIVSQEDSKPQDR		0.290407408	Q5VV42	2
C*APSAGSPAAAVGR		0.288196182	Q7L2J0	2
AGGGPTLQC*PPPSSPEK	C280	0.284970354	Q96N66 Q96N66	3
C*PGPLAVANGVVK		0.281926512	Q9Y6Y8 Q9Y6Y8	2
VC*VPSSASALGTASK	C508	0.279959558	A0A0U1RQX8	4
LALEQQQLIC*K	C69	0.279867191	J3QK89 Q8IWX8	3
AATEQEPLEGTEQTLDAEEEQEESEEA	C37	0.278707397	Q9ULW3	2
SETEAC*FFIC*GDNLSTKGFTYLTNSLF	C482 C478	0.278611249	Q7Z7G8 Q7Z7G8	2
LLVGNKC*DLTTK	C62 C94	0.277543168	E7END7 P62820	3
TEEDETSEDANC*LALSGHDKTEAK		0.277080154	G3V2A0 P51003	2
QRQEVC*QSYK	C27 C59	0.274773163	E5RK63 E5RI05	2
GSSPTPPC*SPVQPSK	C319 C387 C294 C271	0.274199476	Q9NUL3 F8VPI7	3
VAAASGHC*GAFSGSDSSR	C947	0.272673616	Q9NZB2 Q9NZB2	3
LPCIFIC*ENNR	C229 C260	0.27116	P08559 P08559	2
LEKPNEGYLEFFVDC*SASATPEFEGR	C85	0.269422925	Q15024	4
INQMVC*NSDR		0.267260154	P06400	2
FTTSC*MTGYSPQLQGLSSGGSGSYSP	C158 C157	0.265515	Q96SK2 Q96SK2	2
LANTC*FNEIEK	C88	0.26482024	Q9NP61 H0Y6A0	2
SVPTTQC*LDNSK	C226	0.264652694	A0A087WV66	3
AFDLIEHYFGTEDEDSSIAPQVDLNQQQ	C529	0.262060135	P52294	2
FC*AFGGNPPVTGPR	C150	0.26199	O15446 O15446	2
AFLAAALAQGLC*EVLLVVTK	C126	0.259531896	Q8TAC2 Q8TAC2	2
GISC*MNTTLSESPFK		0.255216313	Q15181	3
C*PEALFQPSFLGMESC*GIHETTFNSIM		0.254137144	P60709 P63261	4
SSGC*DVNLPGVNVK		0.25207395	Q09666	3
HPLTQELKEC*EGIVPVPLAEK		0.251819298	P82932	2
C*ASQVGMTAPGTR	C215 C204 C152	0.250992786	Q99439 B4DDF4	4
GPSGC*VESLEVTCR	C646	0.249432826	P47897 P47897	2
EGTQASEGYFSQSQEEEFAQSEELC*A	C659	0.249059294	Q16643 Q16643	4
C*AAPRPPSSSPEQR	C809 C850	0.247987471	E9PKF6 H0YEN2	2
TAVNVPRQPTVTSVC*SETSQELAEGQ		0.246891732	Q96HC4	2
GSDELFSTC*VTNGPFIMSSNSASAANG	C23	0.246323456	A0A0U1RRM4	3
IPC*DSPQSDPVDTPTSTK	C1250	0.244341944	A0A087WV66	3
VHLPNGSPIPAVLLANKC*DQNK	C145	0.241674345	Q13637	3
SC*LLLQFTDKR		0.238425	Q8WUD1 Q5HYI5	2
AGQC*VIGLQMGTNK	C153 C164 C101	0.237476621	Q99439 B4DDF4	3
VRNC*SSPEFSK	C53 C58	0.237218106	Q5JX44 Q5JX45	3
SC*HPTMTILQAPTPAPSTIPGPR		0.230809258	P46695 Q5ST79	2
TTSFAESC*KPVQQPSAFGSMK	C14	0.229146667	P49841 P49841	2
ADPDC*SNGQPQAAPTPGAPQNR	C275	0.228008974	Q9BW85	2
C*PIPGCDGTGHVTGLYPHHRSLSGC*P	C392 C368	0.226700613	E5RHS3 O60284	2
NQASCGSC*YSFASMGMLEAR	C258	0.226290313	P53634	2
DTEGGAAEINC*NGVIEVINYTQNSNNE	C340 C372	0.223108711	Q5R363 Q96SB4	3
VSADAAPDC*PETSNQTPPGPGAAAGP		0.221918904	Q9NXH9 Q9NXH9	3
GAC*SSSGATSSK	C212	0.217554499	O60870 O60870	3
C*SDNSSYEEPLSPISASSSTSR	C205 C711 C346	0.216969669	Q8IXK0	2
MYSSPLC*LTQDEFHPFIEALLPHVR	C7	0.21530068	P08651 P08651	2
ANDQEPC*GWWLAK		0.21092157	P51114 B4DXZ6	2
TQEDEEEISTSPGVSEFVSDAFDAC*NL	C283	0.209941499	Q96A49	2
LNDDWAYGNDLDARPWDFQAEEC*AL	C674	0.20987448	Q5VSL9 Q5VSL9	2
C*ASQSGMTAYGTR	C164 C175 C112	0.208348597	Q99439 B4DDF4	3
SPAGLQVC*VNVSVSLAGMC*HHKQM		0.206596035	F8WFC9	2
GWSGNSWGGISLGPPDPGPC*GETYE	C211	0.201165875	P82675 P82675	3
VDLAGGPEQGAGGPPEPQQQC*QPGA		0.197439943	Q86YR5	2
LLLCVEC*LVSPEHMSHHELTIENALSH	C93	0.19199	Q6P9F5	2
GAQVNAVNQNGC*TPLHYAASK	C107	0.191271709	B1AJY7 O75832	4
LPSSSTWGQQSNTTAC*QSQATLSLAEI	C959 C932	0.188675544	I1E4Y6 Q6Y7W6	4
LDLC*GENVIEVMSAASYLQMNDVVNF		0.18863461	Q8NAP8 Q8NAP8	2

NNAAASASAAAASAAASAAC*ASPAAT	C38	0.180328424	Q9UKL0 J3KN32	3
RGPEVTSQGVQTSSPAC*K	C892 C627	0.180164153	Q99700 Q99700	2
IGTNLPLKPC*AR	C37	0.163232973	E9PLU1 Q9H019	3
AGPGSLELC*GLPSQK	C565	0.162007529	Q14684 Q14684	3
LIIQSSNGHITTTPTPTQFLC*PK	C99	0.158360065	P05412	2
TPTSGQSVSTC*SSK	C87	0.14807073	Q32NC0 L7N2F3	2
ATSAGSSPSC*SLAGR		0.147647235	Q9BXB5 Q9BXB5	3
LIC*LVTGSPSIR	C590	0.146067417	Q6PI48	3
EC*PSDEC*GAGVFMASHFDR	C121 C126	0.145693124	P62979	2
QAC*IDIDEC*IQNGVLCK	C546 C540	0.13375	P35556 D6RJI3	2
PSYSSFTQGDSWGEGEVDEEEGC*DQ	C48	0.128766406	Q8N6S5	4
MPC*QSLQPEPINTPTHTK	C1006	0.126405023	A0A087WV66	2
GPPLPPPPPLPEC*LTISPPVPSGPPSK	C272	0.123423544	Q93015 Q93015	2
RPSGVVLCLLGACFQMLPAAPSGCPQL		0.11861018	C9JPM9 C9JF97	2
SETSVANGSQSESSVSTPSASFEPNNT		0.116520928	Q92575	3
MGIGLGSENAAGPC*NWDEADIGPWAK	C431 C498	0.109465	Q5H907 Q9UNF1	2
TTSSANNPNLMYQDEC*DR	C505 C586 C507	0.091130588	Q92841 H3BLZ8	3
SGGLQTPEC*LSR		0.0911	P85037 P85037	2
IITIPATQLAQC*QLQTK	C458 C410	0.088386037	Q15723 Q15723	2
GC*TIVKPFNLSQGK	C301	0.081629894	Q9ULW0 Q9ULW0	3
VHPAMATAAGGC*R		0.074776141	H7C0N4	3
VLPMNTGVEAGETAC*K		0.074105708	P04181	3
VLVTQQFPC*QNPLPVNSGQAQR		0.041001751	O14965	3
SSSTGSSSSTGGGGQESQPSPLALLAA		0.039298321	H3BVI2 P08047	2
PGHLQEGFGC*VVTNRFDQLFDDESDP	C11	0.034830943	Q8NC51 Q8NC51	4
VLC*PSNSSQR		0.027967349	O14965	2

References

1. NIH-SEER database. *https://seer.cancer.gov/* Available at: 23470257.
2. Li, Z. & Kang, Y. Emerging therapeutic targets in metastatic progression: A focus on breast cancer. *Pharmacol. Ther.* **161,** 79–96 (2016).
3. Dietze, E. C., Sistrunk, C., Miranda-Carboni, G., O'Regan, R. & Seewaldt, V. L. Triple-negative breast cancer in African-American women: disparities versus biology. *Nat. Rev. Cancer* **15,** 248–254 (2015).
4. Zeichner, S. B., Terawaki, H. & Gogineni, K. A Review of Systemic Treatment in Metastatic Triple-Negative Breast Cancer. *Breast Cancer Basic Clin. Res.* **10,** 25–36 (2016).
5. Polyak, K. & Weinberg, R. A. Transitions between epithelial and mesenchymal states: acquisition of malignant and stem cell traits. *Nat. Rev. Cancer* **9,** 265–273 (2009).
6. DeBerardinis, R. J., Lum, J. J., Hatzivassiliou, G. & Thompson, C. B. The Biology of Cancer: Metabolic Reprogramming Fuels Cell Growth and Proliferation. *Cell Metab.* **7,** 11–20 (2008).
7. Hanahan, D. & Weinberg, R. A. Hallmarks of Cancer: The Next Generation. *Cell* **144,** 646–674 (2011).
8. Heiden, M. G. V., Cantley, L. C. & Thompson, C. B. Understanding the Warburg Effect: The Metabolic Requirements of Cell Proliferation. *Science* **324,** 1029–1033 (2009).
9. Christofk, H. R. *et al.* The M2 splice isoform of pyruvate kinase is important for cancer metabolism and tumour growth. *Nature* **452,** 230–233 (2008).
10. Warburg, O. On respiratory impairment in cancer cells. *Science* **124,** 269–270 (1956).
11. Reitman, Z. J. *et al.* Profiling the effects of isocitrate dehydrogenase 1 and 2 mutations on the cellular metabolome. *Proc. Natl. Acad. Sci.* **108,** 3270–3275 (2011).
12. Wise, D. R. *et al.* Hypoxia promotes isocitrate dehydrogenase-dependent carboxylation of α-ketoglutarate to citrate to support cell growth and viability. *Proc. Natl. Acad. Sci. U. S. A.* **108,** 19611–19616 (2011).
13. Metallo, C. M. *et al.* Reductive glutamine metabolism by IDH1 mediates lipogenesis under hypoxia. *Nature* **481,** 380–384 (2012).
14. Menendez, J. A. & Lupu, R. Fatty acid synthase and the lipogenic phenotype in cancer pathogenesis. *Nat. Rev. Cancer* **7,** 763–777 (2007).
15. Wu, X., Daniels, G., Lee, P. & Monaco, M. E. Lipid metabolism in prostate cancer. *Am. J. Clin. Exp. Urol.* **2,** 111–120 (2014).
16. DeBerardinis, R. J. *et al.* Beyond aerobic glycolysis: Transformed cells can engage in glutamine metabolism that exceeds the requirement for protein and nucleotide synthesis. *Proc. Natl. Acad. Sci.* **104,** 19345–19350 (2007).
17. Zhou, W., Liotta, L. A. & Petricoin, E. F. Cancer metabolism and mass spectrometry-based proteomics. *Cancer Lett.* **356,** 176–183 (2015).
18. Vinayavekhin, N., Homan, E. A. & Saghatelian, A. Exploring Disease through Metabolomics. *ACS Chem. Biol.* **5,** 91–103 (2010).
19. Benjamin, D. I., Cravatt, B. F. & Nomura, D. K. Global profiling strategies for mapping dysregulated metabolic pathways in cancer. *Cell Metab.* **16,** 565–577 (2012).
20. Saghatelian, A. *et al.* Assignment of Endogenous Substrates to Enzymes by Global Metabolite Profiling†. *Biochemistry (Mosc.)* **43,** 14332–14339 (2004).
21. Patterson, S. D. & Aebersold, R. H. Proteomics: the first decade and beyond. *Nat. Genet.* **33,** 311–323 (2003).
22. John R. Yates, I. Mass Spectral Analysis in Proteomics. *Annu. Rev. Biophys. Biomol. Struct.* **33,** 297–316 (2004).
23. Lu, W., Bennett, B. D. & Rabinowitz, J. D. Analytical strategies for LC–MS-based targeted metabolomics. *J. Chromatogr. B* **871,** 236–242 (2008).
24. Nomura, D. K. *et al.* Monoacylglycerol Lipase Regulates a Fatty Acid Network that Promotes Cancer Pathogenesis. *Cell* **140,** 49–61 (2010).
25. Gupta, G. P. *et al.* Mediators of vascular remodelling co-opted for sequential steps in lung metastasis. *Nature* **446,** 765–770 (2007).
26. Mills, G. B. & Moolenaar, W. H. The emerging role of lysophosphatidic acid in cancer. *Nat. Rev. Cancer* **3,** 582–591 (2003).
27. Nomura, D. K. *et al.* Monoacylglycerol Lipase Exerts Dual Control over Endocannabinoid and Fatty Acid Pathways to Support Prostate Cancer. *Chem. Biol.* **18,** 846–856 (2011).
28. Benjamin, D. I. *et al.* Ether lipid generating enzyme AGPS alters the balance of structural and signaling lipids to fuel cancer pathogenicity. *Proc. Natl. Acad. Sci.* **110,** 14912–14917 (2013).

29. Zhu, Y. *et al.* Alkylglyceronephosphate synthase (AGPS) alters lipid signaling pathways and supports chemotherapy resistance of glioma and hepatic carcinoma cell lines. *Asian Pac. J. Cancer Prev. APJCP* **15,** 3219–3226 (2014).
30. Piano, V. *et al.* Discovery of Inhibitors for the Ether Lipid-Generating Enzyme AGPS as Anti-Cancer Agents. *ACS Chem. Biol.* **10,** 2589–2597 (2015).
31. Kim, S. K., Jung, W. H. & Koo, J. S. Differential Expression of Enzymes Associated with Serine/Glycine Metabolism in Different Breast Cancer Subtypes. *PLoS ONE* **9,** e101004 (2014).
32. Noh, S., Kim, D. H., Jung, W. H. & Koo, J. S. Expression levels of serine/glycine metabolism-related proteins in triple negative breast cancer tissues. *Tumor Biol.* **35,** 4457–4468 (2014).
33. Antonov, A. *et al.* Bioinformatics analysis of the serine and glycine pathway in cancer cells. *Oncotarget* **5,** 11004–11013 (2014).
34. Locasale, J. W. *et al.* Phosphoglycerate dehydrogenase diverts glycolytic flux and contributes to oncogenesis. *Nat. Genet.* **43,** 869–874 (2011).
35. Teperino, R., Schoonjans, K. & Auwerx, J. Histone Methyl Transferases and Demethylases; Can They Link Metabolism and Transcription? *Cell Metab.* **12,** 321–327 (2010).
36. Wang, Y.-C. *et al.* Regulation of Folate-Mediated One-Carbon Metabolism by Glycine *N*-Methyltransferase (GNMT) and Methylenetetrahydrofolate Reductase (MTHFR). *J. Nutr. Sci. Vitaminol. (Tokyo)* **61,** S148–S150 (2015).
37. Hara, K. *et al.* Amino Acid Sufficiency and mTOR Regulate p70 S6 Kinase and eIF-4E BP1 through a Common Effector Mechanism. *J. Biol. Chem.* **273,** 14484–14494 (1998).
38. Schafer, Z. T. *et al.* Antioxidant and oncogene rescue of metabolic defects caused by loss of matrix attachment. *Nature* **461,** 109–113 (2009).
39. Mehrmohamadi, M. & Locasale, J. W. Context-dependent utilization of serine in cancer. *Mol. Cell. Oncol.* **2,** e996418 (2015).
40. Vogeser, M. & Parhofer, K. Liquid Chromatography Tandem-mass Spectrometry (LC-MS/MS) - Technique and Applications in Endocrinology. *Exp. Clin. Endocrinol. Amp Diabetes* **115,** 559–570 (2007).
41. Jain, M. *et al.* Metabolite Profiling Identifies a Key Role for Glycine in Rapid Cancer Cell Proliferation. *Science* **336,** 1040–1044 (2012).
42. Labuschagne, C. F., van den Broek, N. J. F., Mackay, G. M., Vousden, K. H. & Maddocks, O. D. K. Serine, but Not Glycine, Supports One-Carbon Metabolism and Proliferation of Cancer Cells. *Cell Rep.* **7,** 1248–1258 (2014).
43. Cheng, T. *et al.* Pyruvate carboxylase is required for glutamine-independent growth of tumor cells. *Proc. Natl. Acad. Sci.* **108,** 8674–8679 (2011).
44. Saghatelian, A. & Cravatt, B. F. Discovery metabolite profiling — forging functional connections between the proteome and metabolome. *Life Sci.* **77,** 1759–1766 (2005).
45. Mardis, E. R. *et al.* Recurring Mutations Found by Sequencing an Acute Myeloid Leukemia Genome. *N. Engl. J. Med.* **361,** 1058–1066 (2009).
46. Parsons, D. W. *et al.* An Integrated Genomic Analysis of Human Glioblastoma Multiforme. *Science* **321,** 1807–1812 (2008).
47. Dang, L. *et al.* Cancer-associated IDH1 mutations produce 2-hydroxyglutarate. *Nature* **465,** 966–966 (2010).
48. Chokkathukalam, A., Kim, D.-H., Barrett, M. P., Breitling, R. & Creek, D. J. Stable isotope-labeling studies in metabolomics: new insights into structure and dynamics of metabolic networks. *Bioanalysis* **6,** 511–524 (2014).
49. Higashi, R. M., Fan, T. W.-M., Lorkiewicz, P. K., Moseley, H. N. B. & Lane, A. N. Stable Isotope Labeled Tracers for Metabolic Pathway Elucidation by GC-MS and FT-MS. *Methods Mol. Biol. Clifton NJ* **1198,** 147–167 (2014).
50. Liu, Y., Patricelli, M. P. & Cravatt, B. F. Activity-based protein profiling: The serine hydrolases. *Proc. Natl. Acad. Sci.* **96,** 14694–14699 (1999).
51. Fonovic, M. & Bogyo, M. Activity Based Probes for Proteases: Applications to Biomarker Discovery,Molecular Imaging and Drug Screening. *Curr. Pharm. Des.* **13,** 253–261 (2007).
52. Cravatt, B. F., Wright, A. T. & Kozarich, J. W. Activity-Based Protein Profiling: From Enzyme Chemistry to Proteomic Chemistry. *Annu. Rev. Biochem.* **77,** 383–414 (2008).
53. Blagg, J. & Workman, P. Chemical biology approaches to target validation in cancer. *Curr. Opin. Pharmacol.* **17,** 87–100 (2014).
54. Greenbaum, D. C. *et al.* Small Molecule Affinity Fingerprinting: a Tool for Enzyme Family Subclassification, Target Identification, and Inhibitor Design. *Chem. Biol.* **9,** 1085–1094 (2002).
55. Leung, D., Hardouin, C., Boger, D. L. & Cravatt, B. F. Discovering potent and selective reversible inhibitors of enzymes in complex proteomes. *Nat. Biotechnol.* **21,** 687–691 (2003).

56. Mulvihill, M. M. *et al.* Metabolic Profiling Reveals PAFAH1B3 as a Critical Driver of Breast Cancer Pathogenicity. *Chem. Biol.* **21,** 831–840 (2014).
57. Shields, D. J. *et al.* RBBP9: A tumor-associated serine hydrolase activity required for pancreatic neoplasia. *Proc. Natl. Acad. Sci.* **107,** 2189–2194 (2010).
58. Kidd, D., Liu, Y. & Cravatt, B. F. Profiling Serine Hydrolase Activities in Complex Proteomes†. *Biochemistry (Mosc.)* **40,** 4005–4015 (2001).
59. Patricelli, M. P., Giang, D. K., Stamp, L. M. & Burbaum, J. J. Direct visualization of serine hydrolase activities in complex proteomes using fluorescent active site-directed probes. *PROTEOMICS* **1,** 1067–1071 (2001).
60. Nomura, D. K., Dix, M. M. & Cravatt, B. F. Activity-based protein profiling for biochemical pathway discovery in cancer. *Nat. Rev. Cancer* **10,** 630–638 (2010).
61. Hunerdosse, D. & Nomura, D. K. Activity-based proteomic and metabolomic approaches for understanding metabolism. *Curr. Opin. Biotechnol.* **28,** 116–126 (2014).
62. Kohnz, R. A. *et al.* Activity-Based Protein Profiling of Oncogene-Driven Changes in Metabolism Reveals Broad Dysregulation of PAFAH1B2 and 1B3 in Cancer. *ACS Chem. Biol.* **10,** 1624–1630 (2015).
63. Jessani, N., Liu, Y., Humphrey, M. & Cravatt, B. F. Enzyme activity profiles of the secreted and membrane proteome that depict cancer cell invasiveness. *Proc. Natl. Acad. Sci.* **99,** 10335–10340 (2002).
64. Chiang, K. P., Niessen, S., Saghatelian, A. & Cravatt, B. F. An Enzyme that Regulates Ether Lipid Signaling Pathways in Cancer Annotated by Multidimensional Profiling. *Chem. Biol.* **13,** 1041–1050 (2006).
65. Chang, J. W., Nomura, D. K. & Cravatt, B. F. A Potent and Selective Inhibitor of KIAA1363/AADACL1 that Impairs Prostate Cancer Pathogenesis. *Chem. Biol.* **18,** 476–484 (2011).
66. Martell, J. & Weerapana, E. Applications of Copper-Catalyzed Click Chemistry in Activity-Based Protein Profiling. *Molecules* **19,** 1378–1393 (2014).
67. Speers, A. E. & Cravatt, B. F. Profiling Enzyme Activities In Vivo Using Click Chemistry Methods. *Chem. Biol.* **11,** 535–546 (2004).
68. Prescher, J. A. & Bertozzi, C. R. Chemistry in living systems. *Nat. Chem. Biol.* **1,** 13–21 (2005).
69. Grammel, M. & Hang, H. C. Chemical reporters for biological discovery. *Nat. Chem. Biol.* **9,** 475–484 (2013).
70. Speers, A. E., Adam, G. C. & Cravatt, B. F. Activity-Based Protein Profiling in Vivo Using a Copper(I)-Catalyzed Azide-Alkyne [3 + 2] Cycloaddition. *J. Am. Chem. Soc.* **125,** 4686–4687 (2003).
71. Roberts, A. M., Ward, C. C. & Nomura, D. K. Activity-based protein profiling for mapping and pharmacologically interrogating proteome-wide ligandable hotspots. *Curr. Opin. Biotechnol.* **43,** 25–33 (2017).
72. Weerapana, E., Speers, A. E. & Cravatt, B. F. Tandem orthogonal proteolysis-activity-based protein profiling (TOP-ABPP)--a general method for mapping sites of probe modification in proteomes. *Nat. Protoc.* **2,** 1414–1425 (2007).
73. Wang, C., Weerapana, E., Blewett, M. M. & Cravatt, B. F. A chemoproteomic platform to quantitatively map targets of lipid-derived electrophiles. *Nat. Methods* **11,** 79–85 (2014).
74. Backus, K. M. *et al.* Proteome-wide covalent ligand discovery in native biological systems. *Nature* **534,** 570–574 (2016).
75. Bateman, L. A. *et al.* Chemoproteomics-enabled covalent ligand screen reveals a cysteine hotspot in reticulon 4 that impairs ER morphology and cancer pathogenicity. *Chem. Commun. Camb. Engl.* (2017). doi:10.1039/c7cc01480e
76. Roberts, A. M. *et al.* Chemoproteomic Screening of Covalent Ligands Reveals UBA5 As a Novel Pancreatic Cancer Target. *ACS Chem. Biol.* (2017). doi:10.1021/acschembio.7b00020
77. Flegal, K. M., Carroll, M. D., Kit, B. K. & Ogden, C. L. Prevalence of obesity and trends in the distribution of body mass index among US adults, 1999-2010. *JAMA* **307,** 491–497 (2012).
78. Finucane, M. M. *et al.* National, regional, and global trends in body-mass index since 1980: systematic analysis of health examination surveys and epidemiological studies with 960 country-years and 9·1 million participants. *Lancet Lond. Engl.* **377,** 557–567 (2011).
79. Calle, E. E. & Kaaks, R. Overweight, obesity and cancer: epidemiological evidence and proposed mechanisms. *Nat. Rev. Cancer* **4,** 579–591 (2004).
80. Renehan, A. G., Tyson, M., Egger, M., Heller, R. F. & Zwahlen, M. Body-mass index and incidence of cancer: a systematic review and meta-analysis of prospective observational studies. *Lancet Lond. Engl.* **371,** 569–578 (2008).
81. Jemal, A. *et al.* Global cancer statistics. *CA. Cancer J. Clin.* **61,** 69–90 (2011).
82. Lichtman, M. A. Obesity and the risk for a hematological malignancy: leukemia, lymphoma, or myeloma. *The Oncologist* **15,** 1083–1101 (2010).

83. Li, D. *et al.* Body mass index and risk, age of onset, and survival in patients with pancreatic cancer. *JAMA* **301,** 2553–2562 (2009).
84. MacInnis, R. J. & English, D. R. Body size and composition and prostate cancer risk: systematic review and meta-regression analysis. *Cancer Causes Control CCC* **17,** 989–1003 (2006).
85. Key, T. J. *et al.* Body mass index, serum sex hormones, and breast cancer risk in postmenopausal women. *J. Natl. Cancer Inst.* **95,** 1218–1226 (2003).
86. Vucenik, I. & Stains, J. P. Obesity and cancer risk: evidence, mechanisms, and recommendations. *Ann. N. Y. Acad. Sci.* **1271,** 37–43 (2012).
87. Rocchini, A. P. Childhood obesity and a diabetes epidemic. *N. Engl. J. Med.* **346,** 854–855 (2002).
88. Biro, F. M. & Wien, M. Childhood obesity and adult morbidities. *Am. J. Clin. Nutr.* **91,** 1499S–1505S (2010).
89. Fantuzzi, G. Adipose tissue, adipokines, and inflammation. *J. Allergy Clin. Immunol.* **115,** 911–919; quiz 920 (2005).
90. Gregor, M. F. & Hotamisligil, G. S. Inflammatory mechanisms in obesity. *Annu. Rev. Immunol.* **29,** 415–445 (2011).
91. Neels, J. G. & Olefsky, J. M. Inflamed fat: what starts the fire? *J. Clin. Invest.* **116,** 33–35 (2006).
92. van Kruijsdijk, R. C. M., van der Wall, E. & Visseren, F. L. J. Obesity and cancer: the role of dysfunctional adipose tissue. *Cancer Epidemiol. Biomark. Prev. Publ. Am. Assoc. Cancer Res. Cosponsored Am. Soc. Prev. Oncol.* **18,** 2569–2578 (2009).
93. Cottam, D. R. *et al.* The chronic inflammatory hypothesis for the morbidity associated with morbid obesity: implications and effects of weight loss. *Obes. Surg.* **14,** 589–600 (2004).
94. Weisberg, S. P. *et al.* Obesity is associated with macrophage accumulation in adipose tissue. *J. Clin. Invest.* **112,** 1796–1808 (2003).
95. Carswell, E. A. *et al.* An endotoxin-induced serum factor that causes necrosis of tumors. *Proc. Natl. Acad. Sci. U. S. A.* **72,** 3666–3670 (1975).
96. Leibovich, S. J. *et al.* Macrophage-induced angiogenesis is mediated by tumour necrosis factor-alpha. *Nature* **329,** 630–632 (1987).
97. Orosz, P. *et al.* Enhancement of experimental metastasis by tumor necrosis factor. *J. Exp. Med.* **177,** 1391–1398 (1993).
98. Liu, Z. G., Hsu, H., Goeddel, D. V. & Karin, M. Dissection of TNF receptor 1 effector functions: JNK activation is not linked to apoptosis while NF-kappaB activation prevents cell death. *Cell* **87,** 565–576 (1996).
99. Duyao, M. P., Buckler, A. J. & Sonenshein, G. E. Interaction of an NF-kappa B-like factor with a site upstream of the c-myc promoter. *Proc. Natl. Acad. Sci. U. S. A.* **87,** 4727–4731 (1990).
100. Guttridge, D. C., Albanese, C., Reuther, J. Y., Pestell, R. G. & Baldwin, A. S. NF-kappaB controls cell growth and differentiation through transcriptional regulation of cyclin D1. *Mol. Cell. Biol.* **19,** 5785–5799 (1999).
101. Calado, D. P. *et al.* Constitutive canonical NF-κB activation cooperates with disruption of BLIMP1 in the pathogenesis of activated B cell-like diffuse large cell lymphoma. *Cancer Cell* **18,** 580–589 (2010).
102. Wang, W. *et al.* The nuclear factor-kappa B RelA transcription factor is constitutively activated in human pancreatic adenocarcinoma cells. *Clin. Cancer Res. Off. J. Am. Assoc. Cancer Res.* **5,** 119–127 (1999).
103. Pikarsky, E. *et al.* NF-kappaB functions as a tumour promoter in inflammation-associated cancer. *Nature* **431,** 461–466 (2004).
104. Bours, V. *et al.* Nuclear factor-kappa B, cancer, and apoptosis. *Biochem. Pharmacol.* **60,** 1085–1089 (2000).
105. Kern, P. A., Ranganathan, S., Li, C., Wood, L. & Ranganathan, G. Adipose tissue tumor necrosis factor and interleukin-6 expression in human obesity and insulin resistance. *Am. J. Physiol. Endocrinol. Metab.* **280,** E745-751 (2001).
106. Yan, S. F. *et al.* Induction of interleukin 6 (IL-6) by hypoxia in vascular cells. Central role of the binding site for nuclear factor-IL-6. *J. Biol. Chem.* **270,** 11463–11471 (1995).
107. Bromberg, J. F. *et al.* Stat3 as an oncogene. *Cell* **98,** 295–303 (1999).
108. Darnell, J. E., Kerr, I. M. & Stark, G. R. Jak-STAT pathways and transcriptional activation in response to IFNs and other extracellular signaling proteins. *Science* **264,** 1415–1421 (1994).
109. Yadav, N. *et al.* Antimalarial activity of newly synthesized chalcone derivatives in vitro. *Chem. Biol. Drug Des.* **80,** 340–347 (2012).
110. Park, E. J. *et al.* Dietary and genetic obesity promote liver inflammation and tumorigenesis by enhancing IL-6 and TNF expression. *Cell* **140,** 197–208 (2010).

111. Park, J., Tadlock, L., Gores, G. J. & Patel, T. Inhibition of interleukin 6-mediated mitogen-activated protein kinase activation attenuates growth of a cholangiocarcinoma cell line. *Hepatol. Baltim. Md* **30,** 1128–1133 (1999).
112. Danø, K. *et al.* Plasminogen activation and cancer. *Thromb. Haemost.* **93,** 676–681 (2005).
113. Foekens, J. A. *et al.* Plasminogen activator inhibitor-1 and prognosis in primary breast cancer. *J. Clin. Oncol. Off. J. Am. Soc. Clin. Oncol.* **12,** 1648–1658 (1994).
114. Isogai, C. *et al.* Plasminogen activator inhibitor-1 promotes angiogenesis by stimulating endothelial cell migration toward fibronectin. *Cancer Res.* **61,** 5587–5594 (2001).
115. Bajou, K. *et al.* Absence of host plasminogen activator inhibitor 1 prevents cancer invasion and vascularization. *Nat. Med.* **4,** 923–928 (1998).
116. Hotamisligil, G. S., Arner, P., Caro, J. F., Atkinson, R. L. & Spiegelman, B. M. Increased adipose tissue expression of tumor necrosis factor-alpha in human obesity and insulin resistance. *J. Clin. Invest.* **95,** 2409–2415 (1995).
117. Uysal, K. T., Wiesbrock, S. M., Marino, M. W. & Hotamisligil, G. S. Protection from obesity-induced insulin resistance in mice lacking TNF-alpha function. *Nature* **389,** 610–614 (1997).
118. Samuel, V. T., Petersen, K. F. & Shulman, G. I. Lipid-induced insulin resistance: unravelling the mechanism. *Lancet Lond. Engl.* **375,** 2267–2277 (2010).
119. Carey, D. G., Jenkins, A. B., Campbell, L. V., Freund, J. & Chisholm, D. J. Abdominal fat and insulin resistance in normal and overweight women: Direct measurements reveal a strong relationship in subjects at both low and high risk of NIDDM. *Diabetes* **45,** 633–638 (1996).
120. Cnop, M. *et al.* The concurrent accumulation of intra-abdominal and subcutaneous fat explains the association between insulin resistance and plasma leptin concentrations : distinct metabolic effects of two fat compartments. *Diabetes* **51,** 1005–1015 (2002).
121. Gan, S. K. *et al.* Insulin action, regional fat, and myocyte lipid: altered relationships with increased adiposity. *Obes. Res.* **11,** 1295–1305 (2003).
122. Mu, N., Zhu, Y., Wang, Y., Zhang, H. & Xue, F. Insulin resistance: a significant risk factor of endometrial cancer. *Gynecol. Oncol.* **125,** 751–757 (2012).
123. Barone, B. B. *et al.* Long-term all-cause mortality in cancer patients with preexisting diabetes mellitus: a systematic review and meta-analysis. *JAMA* **300,** 2754–2764 (2008).
124. Ma, J. *et al.* Prediagnostic body-mass index, plasma C-peptide concentration, and prostate cancer-specific mortality in men with prostate cancer: a long-term survival analysis. *Lancet Oncol.* **9,** 1039–1047 (2008).
125. Harris, L. N. *et al.* Predictors of resistance to preoperative trastuzumab and vinorelbine for HER2-positive early breast cancer. *Clin. Cancer Res. Off. J. Am. Assoc. Cancer Res.* **13,** 1198–1207 (2007).
126. Stansbie, D., Brownsey, R. W., Crettaz, M. & Denton, R. M. Acute effects in vivo of anti-insulin serum on rates of fatty acid synthesis and activities of acetyl-coenzyme A carboxylase and pyruvate dehydrogenase in liver and epididymal adipose tissue of fed rats. *Biochem. J.* **160,** 413–416 (1976).
127. Monaco, M. E., Osborne, C. K. & Lippman, M. E. Insulin stimulation of fatty acid synthesis in human breast cancer cells. *J. Natl. Cancer Inst.* **58,** 1591–1593 (1977).
128. Gross, G. E., Boldt, D. H. & Osborne, C. K. Perturbation by insulin of human breast cancer cell cycle kinetics. *Cancer Res.* **44,** 3570–3575 (1984).
129. Liu, Z. *et al.* Epidermal growth factor induces tumour marker AKR1B10 expression through activator protein-1 signalling in hepatocellular carcinoma cells. *Biochem. J.* **442,** 273–282 (2012).
130. Wang, Y. *et al.* Mitogenic and anti-apoptotic effects of insulin in endometrial cancer are phosphatidylinositol 3-kinase/Akt dependent. *Gynecol. Oncol.* **125,** 734–741 (2012).
131. Pollak, M. Insulin and insulin-like growth factor signalling in neoplasia. *Nat. Rev. Cancer* **8,** 915–928 (2008).
132. Böni-Schnetzler, M., Schmid, C., Meier, P. J. & Froesch, E. R. Insulin regulates insulin-like growth factor I mRNA in rat hepatocytes. *Am. J. Physiol.* **260,** E846-851 (1991).
133. Engelman, J. A. Targeting PI3K signalling in cancer: opportunities, challenges and limitations. *Nat. Rev. Cancer* **9,** 550–562 (2009).
134. Schubbert, S., Shannon, K. & Bollag, G. Hyperactive Ras in developmental disorders and cancer. *Nat. Rev. Cancer* **7,** 295–308 (2007).
135. Cully, M., You, H., Levine, A. J. & Mak, T. W. Beyond PTEN mutations: the PI3K pathway as an integrator of multiple inputs during tumorigenesis. *Nat. Rev. Cancer* **6,** 184–192 (2006).
136. Zoncu, R., Efeyan, A. & Sabatini, D. M. mTOR: from growth signal integration to cancer, diabetes and ageing. *Nat. Rev. Mol. Cell Biol.* **12,** 21–35 (2011).
137. Kalaany, N. Y. & Sabatini, D. M. Tumours with PI3K activation are resistant to dietary restriction. *Nature* **458,** 725–731 (2009).

138. Ma, J. *et al.* IGF-1 mediates PTEN suppression and enhances cell invasion and proliferation via activation of the IGF-1/PI3K/Akt signaling pathway in pancreatic cancer cells. *J. Surg. Res.* **160,** 90–101 (2010).
139. Wrobel, G. *et al.* Microarray-based gene expression profiling of benign, atypical and anaplastic meningiomas identifies novel genes associated with meningioma progression. *Int. J. Cancer* **114,** 249–256 (2005).
140. Hartmann, W. *et al.* Insulin-like growth factor II is involved in the proliferation control of medulloblastoma and its cerebellar precursor cells. *Am. J. Pathol.* **166,** 1153–1162 (2005).
141. Perks, C. M. & Holly, J. M. P. The insulin-like growth factor (IGF) family and breast cancer. *Breast Dis.* **18,** 45–60 (2003).
142. Chan, J. M. *et al.* Plasma insulin-like growth factor-I and prostate cancer risk: a prospective study. *Science* **279,** 563–566 (1998).
143. Barozzi, C. *et al.* Relevance of biologic markers in colorectal carcinoma: a comparative study of a broad panel. *Cancer* **94,** 647–657 (2002).
144. Hakam, A. *et al.* Expression of insulin-like growth factor-1 receptor in human colorectal cancer. *Hum. Pathol.* **30,** 1128–1133 (1999).
145. Sesti, G. *et al.* Plasma concentration of IGF-I is independently associated with insulin sensitivity in subjects with different degrees of glucose tolerance. *Diabetes Care* **28,** 120–125 (2005).
146. Nam, S. Y. *et al.* Effect of obesity on total and free insulin-like growth factor (IGF)-1, and their relationship to IGF-binding protein (BP)-1, IGFBP-2, IGFBP-3, insulin, and growth hormone. *Int. J. Obes. Relat. Metab. Disord. J. Int. Assoc. Study Obes.* **21,** 355–359 (1997).
147. de Ostrovich, K. K. *et al.* Paracrine overexpression of insulin-like growth factor-1 enhances mammary tumorigenesis in vivo. *Am. J. Pathol.* **173,** 824–834 (2008).
148. DiGiovanni, J. *et al.* Deregulated expression of insulin-like growth factor 1 in prostate epithelium leads to neoplasia in transgenic mice. *Proc. Natl. Acad. Sci. U. S. A.* **97,** 3455–3460 (2000).
149. Moorehead, R. A., Sanchez, O. H., Baldwin, R. M. & Khokha, R. Transgenic overexpression of IGF-II induces spontaneous lung tumors: a model for human lung adenocarcinoma. *Oncogene* **22,** 853–857 (2003).
150. Pravtcheva, D. D. & Wise, T. L. Metastasizing mammary carcinomas in H19 enhancers-Igf2 transgenic mice. *J. Exp. Zool.* **281,** 43–57 (1998).
151. Carboni, J. M. *et al.* Tumor development by transgenic expression of a constitutively active insulin-like growth factor I receptor. *Cancer Res.* **65,** 3781–3787 (2005).
152. Lopez, T. & Hanahan, D. Elevated levels of IGF-1 receptor convey invasive and metastatic capability in a mouse model of pancreatic islet tumorigenesis. *Cancer Cell* **1,** 339–353 (2002).
153. Baskin, D. G. *et al.* Insulin and leptin: dual adiposity signals to the brain for the regulation of food intake and body weight. *Brain Res.* **848,** 114–123 (1999).
154. Snoussi, K. *et al.* Leptin and leptin receptor polymorphisms are associated with increased risk and poor prognosis of breast carcinoma. *BMC Cancer* **6,** 38 (2006).
155. Howard, J. M., Pidgeon, G. P. & Reynolds, J. V. Leptin and gastro-intestinal malignancies. *Obes. Rev. Off. J. Int. Assoc. Study Obes.* **11,** 863–874 (2010).
156. Friedman, J. M. & Halaas, J. L. Leptin and the regulation of body weight in mammals. *Nature* **395,** 763–770 (1998).
157. Maffei, M. *et al.* Leptin levels in human and rodent: measurement of plasma leptin and ob RNA in obese and weight-reduced subjects. *Nat. Med.* **1,** 1155–1161 (1995).
158. Cheng, S.-P. *et al.* Differential roles of leptin in regulating cell migration in thyroid cancer cells. *Oncol. Rep.* **23,** 1721–1727 (2010).
159. Ptak, A., Kolaczkowska, E. & Gregoraszczuk, E. L. Leptin stimulation of cell cycle and inhibition of apoptosis gene and protein expression in OVCAR-3 ovarian cancer cells. *Endocrine* **43,** 394–403 (2013).
160. Saxena, N. K., Vertino, P. M., Anania, F. A. & Sharma, D. leptin-induced growth stimulation of breast cancer cells involves recruitment of histone acetyltransferases and mediator complex to CYCLIN D1 promoter via activation of Stat3. *J. Biol. Chem.* **282,** 13316–13325 (2007).
161. Drew, J. E. Molecular mechanisms linking adipokines to obesity-related colon cancer: focus on leptin. *Proc. Nutr. Soc.* **71,** 175–180 (2012).
162. Sharma, D., Saxena, N. K., Vertino, P. M. & Anania, F. A. Leptin promotes the proliferative response and invasiveness in human endometrial cancer cells by activating multiple signal-transduction pathways. *Endocr. Relat. Cancer* **13,** 629–640 (2006).
163. Bates, S. H. *et al.* STAT3 signalling is required for leptin regulation of energy balance but not reproduction. *Nature* **421,** 856–859 (2003).
164. Giordano, C. *et al.* Leptin increases HER2 protein levels through a STAT3-mediated up-regulation of Hsp90 in breast cancer cells. *Mol. Oncol.* **7,** 379–391 (2013).

165. Inagaki-Ohara, K. *et al.* Enhancement of leptin receptor signaling by SOCS3 deficiency induces development of gastric tumors in mice. *Oncogene* **33,** 74–84 (2014).
166. Dieudonne, M.-N. *et al.* Leptin mediates a proliferative response in human MCF7 breast cancer cells. *Biochem. Biophys. Res. Commun.* **293,** 622–628 (2002).
167. Hardwick, J. C., Van Den Brink, G. R., Offerhaus, G. J., Van Deventer, S. J. & Peppelenbosch, M. P. Leptin is a growth factor for colonic epithelial cells. *Gastroenterology* **121,** 79–90 (2001).
168. Catalano, S. *et al.* Leptin induces, via ERK1/ERK2 signal, functional activation of estrogen receptor alpha in MCF-7 cells. *J. Biol. Chem.* **279,** 19908–19915 (2004).
169. Zheng, Q. *et al.* Leptin deficiency suppresses MMTV-Wnt-1 mammary tumor growth in obese mice and abrogates tumor initiating cell survival. *Endocr. Relat. Cancer* **18,** 491–503 (2011).
170. Park, J., Kusminski, C. M., Chua, S. C. & Scherer, P. E. Leptin receptor signaling supports cancer cell metabolism through suppression of mitochondrial respiration in vivo. *Am. J. Pathol.* **177,** 3133–3144 (2010).
171. Paz-Filho, G., Lim, E. L., Wong, M.-L. & Licinio, J. Associations between adipokines and obesity-related cancer. *Front. Biosci. Landmark Ed.* **16,** 1634–1650 (2011).
172. Kelesidis, I., Kelesidis, T. & Mantzoros, C. S. Adiponectin and cancer: a systematic review. *Br. J. Cancer* **94,** 1221–1225 (2006).
173. Yamauchi, T. *et al.* The fat-derived hormone adiponectin reverses insulin resistance associated with both lipoatrophy and obesity. *Nat. Med.* **7,** 941–946 (2001).
174. Ouchi, N. *et al.* Adiponectin, an adipocyte-derived plasma protein, inhibits endothelial NF-kappaB signaling through a cAMP-dependent pathway. *Circulation* **102,** 1296–1301 (2000).
175. An, W. *et al.* Adiponectin levels in patients with colorectal cancer and adenoma: a meta-analysis. *Eur. J. Cancer Prev. Off. J. Eur. Cancer Prev. Organ. ECP* **21,** 126–133 (2012).
176. Petridou, E. *et al.* Plasma adiponectin concentrations in relation to endometrial cancer: a case-control study in Greece. *J. Clin. Endocrinol. Metab.* **88,** 993–997 (2003).
177. Konturek, P. C., Burnat, G., Rau, T., Hahn, E. G. & Konturek, S. Effect of adiponectin and ghrelin on apoptosis of Barrett adenocarcinoma cell line. *Dig. Dis. Sci.* **53,** 597–605 (2008).
178. Goktas, S. *et al.* Prostate cancer and adiponectin. *Urology* **65,** 1168–1172 (2005).
179. Tworoger, S. S. *et al.* Plasma adiponectin concentrations and risk of incident breast cancer. *J. Clin. Endocrinol. Metab.* **92,** 1510–1516 (2007).
180. Bub, J. D., Miyazaki, T. & Iwamoto, Y. Adiponectin as a growth inhibitor in prostate cancer cells. *Biochem. Biophys. Res. Commun.* **340,** 1158–1166 (2006).
181. Kim, A. Y. *et al.* Adiponectin represses colon cancer cell proliferation via AdipoR1- and -R2-mediated AMPK activation. *Mol. Endocrinol. Baltim. Md* **24,** 1441–1452 (2010).
182. Taliaferro-Smith, L. *et al.* LKB1 is required for adiponectin-mediated modulation of AMPK-S6K axis and inhibition of migration and invasion of breast cancer cells. *Oncogene* **28,** 2621–2633 (2009).
183. Lam, J. B. B. *et al.* Adiponectin haploinsufficiency promotes mammary tumor development in MMTV-PyVT mice by modulation of phosphatase and tensin homolog activities. *PloS One* **4,** e4968 (2009).
184. Fogarty, S. & Hardie, D. G. Development of protein kinase activators: AMPK as a target in metabolic disorders and cancer. *Biochim. Biophys. Acta* **1804,** 581–591 (2010).
185. Igata, M. *et al.* Adenosine monophosphate-activated protein kinase suppresses vascular smooth muscle cell proliferation through the inhibition of cell cycle progression. *Circ. Res.* **97,** 837–844 (2005).
186. Inoki, K., Zhu, T. & Guan, K.-L. TSC2 mediates cellular energy response to control cell growth and survival. *Cell* **115,** 577–590 (2003).
187. Villa, N. Y. *et al.* Sphingolipids function as downstream effectors of a fungal PAQR. *Mol. Pharmacol.* **75,** 866–875 (2009).
188. Holland, W. L. & Scherer, P. E. PAQRs: a counteracting force to ceramides? *Mol. Pharmacol.* **75,** 740–743 (2009).
189. Takabe, K., Paugh, S. W., Milstien, S. & Spiegel, S. 'Inside-out' signaling of sphingosine-1-phosphate: therapeutic targets. *Pharmacol. Rev.* **60,** 181–195 (2008).
190. Levine, Y. C., Li, G. K. & Michel, T. Agonist-modulated regulation of AMP-activated protein kinase (AMPK) in endothelial cells. Evidence for an AMPK -> Rac1 -> Akt -> endothelial nitric-oxide synthase pathway. *J. Biol. Chem.* **282,** 20351–20364 (2007).
191. Holland, W. L. *et al.* Receptor-mediated activation of ceramidase activity initiates the pleiotropic actions of adiponectin. *Nat. Med.* **17,** 55–63 (2011).
192. Landskroner-Eiger, S. *et al.* Proangiogenic contribution of adiponectin toward mammary tumor growth in vivo. *Clin. Cancer Res. Off. J. Am. Assoc. Cancer Res.* **15,** 3265–3276 (2009).
193. Trujillo, M. E. & Scherer, P. E. Adiponectin--journey from an adipocyte secretory protein to biomarker of the metabolic syndrome. *J. Intern. Med.* **257,** 167–175 (2005).

194. Grossmann, M. E. *et al.* Role of the adiponectin leptin ratio in prostate cancer. *Oncol. Res.* **18,** 269–277 (2009).
195. Hunt, D. A., Lane, H. M., Zygmont, M. E., Dervan, P. A. & Hennigar, R. A. MRNA stability and overexpression of fatty acid synthase in human breast cancer cell lines. *Anticancer Res.* **27,** 27–34 (2007).
196. Gansler, T. S., Hardman, W., Hunt, D. A., Schaffel, S. & Hennigar, R. A. Increased expression of fatty acid synthase (OA-519) in ovarian neoplasms predicts shorter survival. *Hum. Pathol.* **28,** 686–692 (1997).
197. Nguyen, P. L. *et al.* Fatty acid synthase polymorphisms, tumor expression, body mass index, prostate cancer risk, and survival. *J. Clin. Oncol. Off. J. Am. Soc. Clin. Oncol.* **28,** 3958–3964 (2010).
198. Alli, P. M., Pinn, M. L., Jaffee, E. M., McFadden, J. M. & Kuhajda, F. P. Fatty acid synthase inhibitors are chemopreventive for mammary cancer in neu-N transgenic mice. *Oncogene* **24,** 39–46 (2005).
199. Kridel, S. J., Axelrod, F., Rozenkrantz, N. & Smith, J. W. Orlistat is a novel inhibitor of fatty acid synthase with antitumor activity. *Cancer Res.* **64,** 2070–2075 (2004).
200. Boizard, M. *et al.* Obesity-related overexpression of fatty-acid synthase gene in adipose tissue involves sterol regulatory element-binding protein transcription factors. *J. Biol. Chem.* **273,** 29164–29171 (1998).
201. Das, S. K. *et al.* Adipose triglyceride lipase contributes to cancer-associated cachexia. *Science* **333,** 233–238 (2011).
202. Gercel-Taylor, C., Doering, D. L., Kraemer, F. B. & Taylor, D. D. Aberrations in normal systemic lipid metabolism in ovarian cancer patients. *Gynecol. Oncol.* **60,** 35–41 (1996).
203. Argilés, J. M., Alvarez, B. & López-Soriano, F. J. The metabolic basis of cancer cachexia. *Med. Res. Rev.* **17,** 477–498 (1997).
204. Mulligan, H. D., Beck, S. A. & Tisdale, M. J. Lipid metabolism in cancer cachexia. *Br. J. Cancer* **66,** 57–61 (1992).
205. Nieman, K. M. *et al.* Adipocytes promote ovarian cancer metastasis and provide energy for rapid tumor growth. *Nat. Med.* **17,** 1498–1503 (2011).
206. Zhang, Y. *et al.* Stromal progenitor cells from endogenous adipose tissue contribute to pericytes and adipocytes that populate the tumor microenvironment. *Cancer Res.* **72,** 5198–5208 (2012).
207. Wymann, M. P. & Schneiter, R. Lipid signalling in disease. *Nat. Rev. Mol. Cell Biol.* **9,** 162–176 (2008).
208. Erickson, J. R. *et al.* Lysophosphatidic acid and ovarian cancer: a paradigm for tumorogenesis and patient management. *Prostaglandins Other Lipid Mediat.* **64,** 63–81 (2001).
209. Liu, S. *et al.* Expression of autotaxin and lysophosphatidic acid receptors increases mammary tumorigenesis, invasion, and metastases. *Cancer Cell* **15,** 539–550 (2009).
210. Yang, M. *et al.* G protein-coupled lysophosphatidic acid receptors stimulate proliferation of colon cancer cells through the {beta}-catenin pathway. *Proc. Natl. Acad. Sci. U. S. A.* **102,** 6027–6032 (2005).
211. van Corven, E. J., Groenink, A., Jalink, K., Eichholtz, T. & Moolenaar, W. H. Lysophosphatidate-induced cell proliferation: identification and dissection of signaling pathways mediated by G proteins. *Cell* **59,** 45–54 (1989).
212. Fang, X. *et al.* Lysophosphatidic acid prevents apoptosis in fibroblasts via G(i)-protein-mediated activation of mitogen-activated protein kinase. *Biochem. J.* **352 Pt 1,** 135–143 (2000).
213. Takeda, H. *et al.* PI 3-kinase gamma and protein kinase C-zeta mediate RAS-independent activation of MAP kinase by a Gi protein-coupled receptor. *EMBO J.* **18,** 386–395 (1999).
214. van Corven, E. J., Hordijk, P. L., Medema, R. H., Bos, J. L. & Moolenaar, W. H. Pertussis toxin-sensitive activation of p21ras by G protein-coupled receptor agonists in fibroblasts. *Proc. Natl. Acad. Sci. U. S. A.* **90,** 1257–1261 (1993).
215. Boucharaba, A. *et al.* Bioactive lipids lysophosphatidic acid and sphingosine 1-phosphate mediate breast cancer cell biological functions through distinct mechanisms. *Oncol. Res.* **18,** 173–184 (2009).
216. Marshall, J.-C. A. *et al.* Effect of inhibition of the lysophosphatidic acid receptor 1 on metastasis and metastatic dormancy in breast cancer. *J. Natl. Cancer Inst.* **104,** 1306–1319 (2012).
217. Costa, C. *et al.* Cyclo-oxygenase 2 expression is associated with angiogenesis and lymph node metastasis in human breast cancer. *J. Clin. Pathol.* **55,** 429–434 (2002).
218. Howe, L. R. *et al.* HER2/neu-induced mammary tumorigenesis and angiogenesis are reduced in cyclooxygenase-2 knockout mice. *Cancer Res.* **65,** 10113–10119 (2005).
219. Tsujii, M. & DuBois, R. N. Alterations in cellular adhesion and apoptosis in epithelial cells overexpressing prostaglandin endoperoxide synthase 2. *Cell* **83,** 493–501 (1995).
220. Chang, S.-H. *et al.* Role of prostaglandin E2-dependent angiogenic switch in cyclooxygenase 2-induced breast cancer progression. *Proc. Natl. Acad. Sci. U. S. A.* **101,** 591–596 (2004).
221. Castellone, M. D., Teramoto, H., Williams, B. O., Druey, K. M. & Gutkind, J. S. Prostaglandin E2 promotes colon cancer cell growth through a Gs-axin-beta-catenin signaling axis. *Science* **310,** 1504–1510 (2005).

222. Heasley, L. E. *et al.* Induction of cytosolic phospholipase A2 by oncogenic Ras in human non-small cell lung cancer. *J. Biol. Chem.* **272,** 14501–14504 (1997).
223. Weiser-Evans, M. C. M. *et al.* Depletion of cytosolic phospholipase A2 in bone marrow-derived macrophages protects against lung cancer progression and metastasis. *Cancer Res.* **69,** 1733–1738 (2009).
224. Gómez-Muñoz, A. *et al.* Ceramide-1-phosphate promotes cell survival through activation of the phosphatidylinositol 3-kinase/protein kinase B pathway. *FEBS Lett.* **579,** 3744–3750 (2005).
225. Park, K. S. *et al.* S1P stimulates chemotactic migration and invasion in OVCAR3 ovarian cancer cells. *Biochem. Biophys. Res. Commun.* **356,** 239–244 (2007).
226. Li, W. *et al.* Sphingosine kinase 1 is associated with gastric cancer progression and poor survival of patients. *Clin. Cancer Res. Off. J. Am. Assoc. Cancer Res.* **15,** 1393–1399 (2009).
227. Kawamori, T. *et al.* Role for sphingosine kinase 1 in colon carcinogenesis. *FASEB J. Off. Publ. Fed. Am. Soc. Exp. Biol.* **23,** 405–414 (2009).
228. Bektas, M. *et al.* Sphingosine kinase activity counteracts ceramide-mediated cell death in human melanoma cells: role of Bcl-2 expression. *Oncogene* **24,** 178–187 (2005).
229. Limaye, V. *et al.* Sphingosine kinase-1 enhances endothelial cell survival through a PECAM-1-dependent activation of PI-3K/Akt and regulation of Bcl-2 family members. *Blood* **105,** 3169–3177 (2005).
230. Oskouian, B. *et al.* Sphingosine-1-phosphate lyase potentiates apoptosis via p53- and p38-dependent pathways and is down-regulated in colon cancer. *Proc. Natl. Acad. Sci. U. S. A.* **103,** 17384–17389 (2006).
231. Shindou, H. *et al.* A single enzyme catalyzes both platelet-activating factor production and membrane biogenesis of inflammatory cells. Cloning and characterization of acetyl-CoA:LYSO-PAF acetyltransferase. *J. Biol. Chem.* **282,** 6532–6539 (2007).
232. Denizot, Y. *et al.* Platelet-activating factor and human thyroid cancer. *Eur. J. Endocrinol.* **153,** 31–40 (2005).
233. Bussolati, B. *et al.* PAF produced by human breast cancer cells promotes migration and proliferation of tumor cells and neo-angiogenesis. *Am. J. Pathol.* **157,** 1713–1725 (2000).
234. Melnikova, V. O., Mourad-Zeidan, A. A., Lev, D. C. & Bar-Eli, M. Platelet-activating factor mediates MMP-2 expression and activation via phosphorylation of cAMP-response element-binding protein and contributes to melanoma metastasis. *J. Biol. Chem.* **281,** 2911–2922 (2006).
235. Denley, A., Gymnopoulos, M., Kang, S., Mitchell, C. & Vogt, P. K. Requirement of phosphatidylinositol(3,4,5)trisphosphate in phosphatidylinositol 3-kinase-induced oncogenic transformation. *Mol. Cancer Res. MCR* **7,** 1132–1138 (2009).
236. Hernandez-Aya, L. F. & Gonzalez-Angulo, A. M. Targeting the phosphatidylinositol 3-kinase signaling pathway in breast cancer. *The Oncologist* **16,** 404–414 (2011).
237. Krystal, G. W., Sulanke, G. & Litz, J. Inhibition of phosphatidylinositol 3-kinase-Akt signaling blocks growth, promotes apoptosis, and enhances sensitivity of small cell lung cancer cells to chemotherapy. *Mol. Cancer Ther.* **1,** 913–922 (2002).
238. Currie, C. J., Poole, C. D. & Gale, E. a. M. The influence of glucose-lowering therapies on cancer risk in type 2 diabetes. *Diabetologia* **52,** 1766–1777 (2009).
239. Jonasson, J. M. *et al.* Insulin glargine use and short-term incidence of malignancies-a population-based follow-up study in Sweden. *Diabetologia* **52,** 1745–1754 (2009).
240. Bowker, S. L., Majumdar, S. R., Veugelers, P. & Johnson, J. A. Increased cancer-related mortality for patients with type 2 diabetes who use sulfonylureas or insulin. *Diabetes Care* **29,** 254–258 (2006).
241. Erickson, K. *et al.* Clinically defined type 2 diabetes mellitus and prognosis in early-stage breast cancer. *J. Clin. Oncol. Off. J. Am. Soc. Clin. Oncol.* **29,** 54–60 (2011).
242. Govindarajan, R. *et al.* Thiazolidinediones and the risk of lung, prostate, and colon cancer in patients with diabetes. *J. Clin. Oncol. Off. J. Am. Soc. Clin. Oncol.* **25,** 1476–1481 (2007).
243. Kim, S. *et al.* Aspirin may be more effective in preventing colorectal adenomas in patients with higher BMI (United States). *Cancer Causes Control CCC* **17,** 1299–1304 (2006).
244. Ookhtens, M., Kannan, R., Lyon, I. & Baker, N. Liver and adipose tissue contributions to newly formed fatty acids in an ascites tumor. *Am. J. Physiol.* **247,** R146-153 (1984).
245. Cordenonsi, M. *et al.* The Hippo transducer TAZ confers cancer stem cell-related traits on breast cancer cells. *Cell* **147,** 759–772 (2011).
246. Medina-Cleghorn, D. & Nomura, D. K. Chemical approaches to study metabolic networks. *Pflugers Arch.* **465,** 427–440 (2013).
247. Tautenhahn, R., Patti, G. J., Rinehart, D. & Siuzdak, G. XCMS Online: a web-based platform to process untargeted metabolomic data. *Anal. Chem.* **84,** 5035–5039 (2012).

248. Arana, L., Gangoiti, P., Ouro, A., Trueba, M. & Gómez-Muñoz, A. Ceramide and ceramide 1-phosphate in health and disease. *Lipids Health Dis.* **9,** 15 (2010).
249. Tsoupras, A. B., Iatrou, C., Frangia, C. & Demopoulos, C. A. The implication of platelet activating factor in cancer growth and metastasis: potent beneficial role of PAF-inhibitors and antioxidants. *Infect. Disord. Drug Targets* **9,** 390–399 (2009).
250. Ogata, H., Goto, S., Fujibuchi, W. & Kanehisa, M. Computation with the KEGG pathway database. *Biosystems* **47,** 119–128 (1998).
251. Zaugg, K. *et al.* Carnitine palmitoyltransferase 1C promotes cell survival and tumor growth under conditions of metabolic stress. *Genes Dev.* **25,** 1041–1051 (2011).
252. Liu, L., Wang, Y.-D., Wu, J., Cui, J. & Chen, T. Carnitine palmitoyltransferase 1A (CPT1A): a transcriptional target of PAX3-FKHR and mediates PAX3-FKHR-dependent motility in alveolar rhabdomyosarcoma cells. *BMC Cancer* **12,** 154 (2012).
253. Fallani, A. *et al.* Platelet-activating factor (PAF) is the effector of IFN gamma-stimulated invasiveness and motility in a B16 melanoma line. *Prostaglandins Other Lipid Mediat.* **81,** 171–177 (2006).
254. Snyder, F. & Wood, R. Alkyl and alk-1-enyl ethers of glycerol in lipids from normal and neoplastic human tissues. *Cancer Res.* **29,** 251–257 (1969).
255. Kuemmerle, N. B. *et al.* Lipoprotein lipase links dietary fat to solid tumor cell proliferation. *Mol. Cancer Ther.* **10,** 427–436 (2011).
256. Liu, R.-Z. *et al.* Association of FABP5 expression with poor survival in triple-negative breast cancer: implication for retinoic acid therapy. *Am. J. Pathol.* **178,** 997–1008 (2011).
257. Kamphorst, J. J. *et al.* Hypoxic and Ras-transformed cells support growth by scavenging unsaturated fatty acids from lysophospholipids. *Proc. Natl. Acad. Sci. U. S. A.* **110,** 8882–8887 (2013).
258. Louie, S. M., Roberts, L. S. & Nomura, D. K. Mechanisms linking obesity and cancer. *Biochim. Biophys. Acta* **1831,** 1499–1508 (2013).
259. Nomura, D. K. *et al.* Endocannabinoid hydrolysis generates brain prostaglandins that promote neuroinflammation. *Science* **334,** 809–813 (2011).
260. Piro, J. R. *et al.* A dysregulated endocannabinoid-eicosanoid network supports pathogenesis in a mouse model of Alzheimer's disease. *Cell Rep.* **1,** 617–623 (2012).
261. Smith, C. A. *et al.* METLIN: a metabolite mass spectral database. *Ther. Drug Monit.* **27,** 747–751 (2005).
262. Long, J. Z. & Cravatt, B. F. The metabolic serine hydrolases and their functions in mammalian physiology and disease. *Chem. Rev.* **111,** 6022–6063 (2011).
263. Büll, C., Stoel, M. A., Brok, M. H. den & Adema, G. J. Sialic Acids Sweeten a Tumor's Life. *Cancer Res.* **74,** 3199–3204 (2014).
264. Pearce, O. M. T. & Läubli, H. Sialic acids in cancer biology and immunity. *Glycobiology* **26,** 111–128 (2016).
265. Varki, A. & Schauer, R. in *Essentials of Glycobiology* (eds. Varki, A. et al.) (Cold Spring Harbor Laboratory Press, 2009).
266. Kohnz, R. A. *et al.* Protein Sialylation Regulates a Gene Expression Signature that Promotes Breast Cancer Cell Pathogenicity. *ACS Chem. Biol.* **11,** 2131–2139 (2016).
267. Laughlin, S. T. & Bertozzi, C. R. Metabolic labeling of glycans with azido sugars and subsequent glycan-profiling and visualization via Staudinger ligation. *Nat. Protoc.* **2,** 2930–2944 (2007).
268. Khedri, Z. *et al.* A Chemical Biology Solution to Problems with Studying Biologically Important but Unstable 9-O-Acetyl Sialic Acids. *ACS Chem. Biol.* **12,** 214–224 (2017).
269. Louie, S. M. *et al.* GSTP1 Is a Driver of Triple-Negative Breast Cancer Cell Metabolism and Pathogenicity. *Cell Chem. Biol.* **23,** 567–578 (2016).
270. Breast Cancer Treatment, Natl Cancer Inst. PDQ Cancer Info Summary. Available at: https://www.cancer.gov/types/breast/patient/breast-treatment.pdq.
271. Bianchini, G., Balko, J. M., Mayer, I. A., Sanders, M. E. & Gianni, L. Triple-negative breast cancer: challenges and opportunities of a heterogeneous disease. *Nat. Rev. Clin. Oncol.* **13,** 674–690 (2016).
272. Dar, A. A., Goff, L. W., Majid, S., Berlin, J. & El-Rifai, W. Aurora kinase inhibitors--rising stars in cancer therapeutics? *Mol. Cancer Ther.* **9,** 268–278 (2010).
273. Singh, J. *et al.* Phase 2 trial of everolimus and carboplatin combination in patients with triple negative metastatic breast cancer. *Breast Cancer Res. BCR* **16,** R32 (2014).
274. Gomez, H. L. *et al.* Phase I dose-escalation and pharmacokinetic study of ispinesib, a kinesin spindle protein inhibitor, administered on days 1 and 15 of a 28-day schedule in patients with no prior treatment for advanced breast cancer. *Anticancer. Drugs* **23,** 335–341 (2012).
275. Trinh, X. B. *et al.* A phase II study of the combination of endocrine treatment and bortezomib in patients with endocrine-resistant metastatic breast cancer. *Oncol. Rep.* **27,** 657–663 (2012).

276. Garland, L. L., Taylor, C., Pilkington, D. L., Cohen, J. L. & Von Hoff, D. D. A phase I pharmacokinetic study of HMN-214, a novel oral stilbene derivative with polo-like kinase-1-interacting properties, in patients with advanced solid tumors. *Clin. Cancer Res. Off. J. Am. Assoc. Cancer Res.* **12,** 5182–5189 (2006).
277. Claude-Taupin, A., Boyer-Guittaut, M., Delage-Mourroux, R. & Hervouet, E. Use of epigenetic modulators as a powerful adjuvant for breast cancer therapies. *Methods Mol. Biol. Clifton NJ* **1238,** 487–509 (2015).
278. Xiao, Z., Zhang, P. & Ma, L. The role of deubiquitinases in breast cancer. *Cancer Metastasis Rev.* **35,** 589–600 (2016).
279. Alasmael, N., Mohan, R., Meira, L. B., Swales, K. E. & Plant, N. J. Activation of the Farnesoid X-receptor in breast cancer cell lines results in cytotoxicity but not increased migration potential. *Cancer Lett.* **370,** 250–259 (2016).
280. Rafi, M. M. *et al.* Modulation of bcl-2 and cytotoxicity by licochalcone-A, a novel estrogenic flavonoid. *Anticancer Res.* **20,** 2653–2658 (2000).
281. Almahariq, M. *et al.* Pharmacological inhibition and genetic knockdown of exchange protein directly activated by cAMP 1 reduce pancreatic cancer metastasis in vivo. *Mol. Pharmacol.* **87,** 142–149 (2015).
282. Chen, L. C. *et al.* First-in-human study with ARQ 621, a novel inhibitor of Eg5: Final results from the solid tumors cohort. *J. Clin. Oncol.* **29,** 3076
283. Bortolotto, L. F. B. *et al.* Cytotoxicity of trans-chalcone and licochalcone A against breast cancer cells is due to apoptosis induction and cell cycle arrest. *Biomed. Pharmacother. Biomedecine Pharmacother.* **85,** 425–433 (2017).
284. Hu, J. & Liu, J. Licochalcone A Attenuates Lipopolysaccharide-Induced Acute Kidney Injury by Inhibiting NF-κB Activation. *Inflammation* **39,** 569–574 (2016).
285. Tsai, J.-P. *et al.* Licochalcone A induces autophagy through PI3K/Akt/mTOR inactivation and autophagy suppression enhances Licochalcone A-induced apoptosis of human cervical cancer cells. *Oncotarget* **6,** 28851–28866 (2015).
286. Yang, X., Jiang, J., Yang, X., Han, J. & Zheng, Q. Licochalcone A induces T24 bladder cancer cell apoptosis by increasing intracellular calcium levels. *Mol. Med. Rep.* **14,** 911–919 (2016).
287. Chularojanamontri, L., Tuchinda, P., Kulthanan, K., Varothai, S. & Winayanuwattikun, W. A double-blinded, randomized, vehicle-controlled study to access skin tolerability and efficacy of an anti-inflammatory moisturizer in treatment of acne with 0.1% adapalene gel. *J. Dermatol. Treat.* **27,** 140–145 (2016).
288. Liu, J. & Lin, A. Role of JNK activation in apoptosis: a double-edged sword. *Cell Res.* **15,** 36–42 (2005).
289. Shannon, D. A. & Weerapana, E. Covalent protein modification: the current landscape of residue-specific electrophiles. *Curr. Opin. Chem. Biol.* **24,** 18–26 (2015).
290. Weerapana, E. *et al.* Quantitative reactivity profiling predicts functional cysteines in proteomes. *Nature* **468,** 790–795 (2010).
291. Mesa, J. *et al.* Human prostaglandin reductase 1 (PGR1): Substrate specificity, inhibitor analysis and site-directed mutagenesis. *Chem. Biol. Interact.* **234,** 105–113 (2015).
292. Huang, X., Zhou, W., Zhang, Y. & Liu, Y. High Expression of PTGR1 Promotes NSCLC Cell Growth via Positive Regulation of Cyclin-Dependent Protein Kinase Complex. *BioMed Res. Int.* **2016,** 5230642 (2016).
293. Xue, L. *et al.* Knockdown of prostaglandin reductase 1 (PTGR1) suppresses prostate cancer cell proliferation by inducing cell cycle arrest and apoptosis. *Biosci. Trends* **10,** 133–139 (2016).
294. Jeon, W.-K. *et al.* The proinflammatory LTB4/BLT1 signal axis confers resistance to TGF-β1-induced growth inhibition by targeting Smad3 linker region. *Oncotarget* **6,** 41650–41666 (2015).
295. Yue, W. W. *et al.* crystal structure of human leukotriene b4 12-hydroxydehydrogenase in complex with NADP and raloxifene. *RCS Protein Data Bank 2Y05* doi:10.2210/pdb2y05/pdb
296. Rasmussen, B. B. & Wolfe, R. R. Regulation of fatty acid oxidation in skeletal muscle. *Annu. Rev. Nutr.* **19,** 463–484 (1999).
297. Yamada, K. A. *et al.* Cellular uncoupling induced by accumulation of long-chain acylcarnitine during ischemia. *Circ. Res.* **74,** 83–95 (1994).
298. Wajner, M. & Amaral, A. U. Mitochondrial dysfunction in fatty acid oxidation disorders: insights from human and animal studies. *Biosci. Rep.* **36,** e00281 (2015).
299. Yamada, K. A., Kanter, E. M. & Newatia, A. Long-chain acylcarnitine induces Ca2+ efflux from the sarcoplasmic reticulum. *J. Cardiovasc. Pharmacol.* **36,** 14–21 (2000).
300. Xu, T. *et al.* ProLuCID: An improved SEQUEST-like algorithm with enhanced sensitivity and specificity. *J. Proteomics* **129,** 16–24 (2015).
301. Medina-Cleghorn, D. *et al.* Mapping Proteome-Wide Targets of Environmental Chemicals Using Reactivity-Based Chemoproteomic Platforms. *Chem. Biol.* **22,** 1394–1405 (2015).